

Dissertation zur Erlangung des Doktorgrades
der Fakultät für Chemie und Pharmazie
der Ludwig-Maximilians-Universität München

**Lipid-based depots:
manufacturing, administration and
interactions of protein drugs with
lipid formulations**

Michaela Maria Breitsamer

aus

Starnberg, Deutschland

2019

ERKLÄRUNG

Diese Dissertation wurde im Sinne von § 7 der Promotionsordnung vom 28. November 2011 von Herrn Prof. Dr. Gerhard Winter betreut.

EIDESSTATTLICHE VERSICHERUNG

Diese Dissertation wurde eigenständig und ohne unerlaubte Hilfe erarbeitet.

Wolfratshausen, den 20.05.2019

(Michaela Breitsamer)

Dissertation eingereicht am: 20.05.2019
1. Gutachter: Prof. Dr. Gerhard Winter
2. Gutachter: Prof. Dr. Wolfgang Frieß
Mündliche Prüfung am: 25.06.2019

FOR MY FAMILY

“The way to get started is to quit talking and begin doing”

Walt Disney (1901 – 1966)

ACKNOWLEDGEMENTS

The present thesis was prepared between March 2015 and December 2018 at the Department of Pharmacy, Pharmaceutical Technology and Biopharmaceutics at the Ludwig-Maximilians Universität (LMU) in Munich under the supervision of Prof. Dr. Gerhard Winter.

First of all, I would like to express my deepest gratitude to my supervisor Prof. Dr. Gerhard Winter for giving me the opportunity to join his research group and to work on this extremely interesting and interdisciplinary project. I really appreciated his scientific input throughout all phases of this work, his elaborate advice and his guidance, which also contributed to my personal development over the last years. Furthermore, I would like to thank him for the outstanding working and team atmosphere, which he created at the chair, for supporting my participation in scientific conferences and for initiating and motivating me to the numerous collaborations which contributed to a successful thesis.

I would also like to thank Prof. Dr. Wolfgang Frieß for all the helpful and interesting discussion in the past years, as well as for being the co-referee of this thesis. Thank you for creating the pleasant working conditions together with Prof. Dr. Gerhard Winter.

Many thanks also go to Prof. Dr. Olivia Merkel, Dr. Gerhard Simon and Sabine Kohler.

This interdisciplinary work would not have been possible without the support of many cooperation partners, who contributed enthusiastically to this thesis. I would like to thank the group of Prof. Dr. Mathias Ritzmann and especially Dr. Christine Weiß from the Clinic for Swine at the LMU (Oberschleißheim) for their continuous support with pigs and pig skin throughout the course of this thesis. I highly appreciate the collaboration with Dr. Heiko Spilgies and Dr. Karsten Heuser from LTS Lohmann Therapie-Systeme AG.

Furthermore, I would like to express my gratitude to Prof. Dr. Heiko Heerklotz and Anja Stulz from the Albert-Ludwigs-Universität in Freiburg, for the nice discussions and fruitful cooperation. I would also like to thank NanoTemper Technologies GmbH and especially Dr. Nuska Tschammer for helping me with the MST measurements and interpretation thereof.

The groups of Dr. Mathias Schmidt and Prof. Dr. Felix Hausch at the Max-Planck-Institute for Psychiatry in Munich are thanked for the opportunity to collaborate to these successful in vivo studies. Particularly I would like to thank Max Pöhlmann, Dr. Georgia Balsevich and

Dr. Karla-Gerlinde Schraut for the great work together. The same thanks go out to Dr. Sandrine Geranton and Dr. Maria Maiarù from the University College London (UCL) for this fruitful partnership.

I would also like to thank the group of Prof. Dr. Jörg Breitzkreutz and especially Bastian Hahn from the Heinrich Heine Universität in Düsseldorf for hosting me for some days and helping me with the extrusion experiments.

Further I would like to express my gratitude Dr. Jilong Wang and Prof. XiaoJiao Du from the Institutes for Life Sciences and School of Medicine at South China University of Technology for their help with the calculation of PK parameters.

Many thanks are expressed to my students Nadine Hasreiter and Anna Fuchs, who did their “Wahlpflichtpraktikum” on my project and Natalie Deiringer, who conducted her master thesis under my supervision. Thank you, you did a great job! In this context, I would also like to thank Katharina Kopp who continues the preparation of VPGs for our collaboration partners.

A big “Thank you” goes to my former colleagues from the LMU from the Winter, Frieß and Merkel labs for welcoming me so heartily to the group and creating a comfortable and funny atmosphere. All our skiing, hiking and other social events and get togethers were great fun and made the time unforgettable for me.

A special thanks goes to my (extended) lab mates Dr. Moritz Vollrath, Weiwei Liu, Carolin Berner, Dennis Krieg, Markus Zang, Dr. Katharina Geh and Dr. Leticia Rodrigues Neibecker for welcoming me to the lab and the great time we had together in B1.029/B1.028 with all the funny craziness and fruitful discussions.

As a former head of “Disperse” practical course I would also like to express my deep gratitude to the whole Disperse-Team – working with you was always fun and easy!

I am most grateful to Dr. Randy Wanner, Dr. Matthias Lucke, Dr. Kay Strüver, Dr. Benjamin Werner, Dr. Kerstin Hoffmann, Dr. Corinna Dürr and Dr. Ilona Vollrath for welcoming me so warmly to the group in my first few months and to Simon Eisele, Ruth Rieser, Ivonne Seifert and Andreas Stelzl, who made the last years unforgettable. You were not only great colleagues but also became excellent friends and never failed to bring a smile to my face! Special thanks further go to my lunch and coffee gang, Alice Hirschmann, Dr. Laura Engelke and last but not least Andreas Tosstorff, for your friendship and the welcome distraction every day.

I would also like to express my gratitude to Paula, Rita, Flo, Luca, Anna, Jasper, Lina, Leon, Lucas, Jacob and Mira, for all the fun we had together in the last few years besides my work at the university – you are the best friends I could wish for.

My deepest and immense gratitude goes to my parents, Petra and Michael, as well as to my sister, Vroni with Thomas, Flocke and Marini who gave me roots and always supported me. Thank you for making things possible for me, for being there when I needed you and for your infinite and unconditional love!

Last but not least I would like to thank Felix for his continuous encouragement, his endless support, his patience and his love. Thank you for being who you are. You were my dead sea when I was threatened to sink!

TABLE OF CONTENTS

ACKNOWLEDGEMENTS.....	VII
TABLE OF CONTENTS.....	XI
CHAPTER I VESICULAR PHOSPHOLIPID GELS AS DRUG DELIVERY SYSTEMS FOR SMALL MOLECULAR WEIGHT DRUGS, PEPTIDES AND PROTEINS: STATE OF THE ART REVIEW	1
I.1 Abstract	2
I.2 Introduction	4
I.2.1 Liposomes for sustained release of protein drugs.....	4
I.2.2 DepoFoam technology.....	6
I.2.3 Phospholipid-based phase separation gel (PPSG)	7
I.3 Vesicular phospholipid gels (VPGs)	8
I.3.1 Definition and structural features	8
I.3.2 Preparation of VPGs and drug encapsulation techniques	9
I.3.2.1 High-pressure homogenization (HPH)	10
I.3.2.2 Magnetic stirring	11
I.3.2.3 Dual centrifugation (DC)	12
I.3.2.4 Encapsulation techniques for drugs.....	13
I.3.2.5 Sterile manufacturing of VPGs	14
I.3.3 Sustained release of encapsulated drugs from VPGs	15
I.3.4 Applications of VPGs.....	17
I.3.4.1 Application as storage form of liposomes.....	18
I.3.4.2 Application as drug delivery device for the sustained release of small molecular drugs and peptides	19
I.3.4.3 Application as drug delivery devices for the sustained release of proteins.....	20
I.4 Summary.....	22
I.5 References	23
CHAPTER II OBJECTIVES AND OUTLINE OF THE THESIS.....	29

II.1 References	31
------------------------------	-----------

CHAPTER III NEEDLE-FREE INJECTION OF VESICULAR PHOSPHOLIPID GELS.. 33

III.1 Needle-free injection of vesicular phospholipid gels – a novel approach to overcome an administration hurdle for semisolid depot systems	34
---	-----------

III.1.1 Abstract.....	34
III.1.2 Introduction	34
III.1.3 Materials and Methods.....	36
III.1.3.1 Materials	36
III.1.3.2 Preparation of VPGs	36
III.1.3.3 Preparation of gelatin blocks	36
III.1.3.4 Injections into in vitro models.....	37
III.1.3.5 In vitro release of EPO from VPGs after shearing	37
III.1.3.6 Quantification of EPO with RP-HPLC.....	38
III.1.4 Results.....	38
III.1.4.1 Needle-free injection	38
III.1.4.2 In vitro release after shearing	41
III.1.5 Discussion	42
III.1.6 Conclusion.....	43
III.1.7 Supporting information	44

III.2 Further studies.....	46
-----------------------------------	-----------

III.2.1 Material and Methods	46
III.2.1.1 Viscosity measurement	46
III.2.1.2 Determination of the density.....	46
III.2.1.3 Texture analysis.....	46
III.2.1.4 Determination of injection force with needle and syringe	46
III.2.1.5 Needle-free injection of VPGs with Biojector 2000	47
III.2.1.6 Jet force upon ejection with Biojector 2000	48
III.2.2 Results and Discussion	49
III.2.2.1 Viscosity and gel strength of VPGs.....	49
III.2.2.2 Injection force with conventional needles.....	50
III.2.2.3 Further post mortem studies on needle-free injection of VPGs.....	52
III.2.2.3.1 Comparison of different single use syringes in post mortem studies	52
III.2.2.3.2 Injection depth	54
III.2.2.3.3 Injections with large injection volume	55
III.2.2.4 Jet force upon ejection with Biojector 2000	56
III.2.2.4.1 Influence of the phospholipid concentration.....	58

III.2.2.4.2 Influence of ejection temperature	60
III.2.2.4.3 Influence of ejection volume	60
III.3 Conclusion.....	62
III.4 References	63
CHAPTER IV PREPARATION OF VESICULAR PHOSPHOLIPID GELS BY TWIN- SCREW EXTRUSION	65
IV.1 Introduction.....	66
IV.1.1 High pressure homogenization.....	66
IV.1.2 Dual asymmetric centrifugation and dual centrifugation	66
IV.1.3 Magnetic stirring	67
IV.1.4 Twin-screw extrusion	68
IV.2 Material and Methods	70
IV.2.1 Materials.....	70
IV.2.1.1 Phospholipids.....	70
IV.2.1.2 Proteins for release studies and stability.....	70
IV.2.1.3 Other chemicals and salts	70
IV.2.2 Preparation of VPGs	71
IV.2.2.1 Preparation of VPGs by DAC	71
IV.2.2.2 Preparation of VPGs by magnetic stirring.....	72
IV.2.2.3 Preparation of VPGs by TSC extrusion	72
IV.2.2.3.1 ZE-5 Mini-Extruder	72
IV.2.2.3.2 HAAKE MiniLab® Micro Rheology Compounder	73
IV.2.2.3.3 Leistritz Micro 27 GL - 28D	73
IV.2.3 Methods for VPG characterization	74
IV.2.3.1 Rheology	74
IV.2.3.2 Dynamic light scattering	74
IV.2.3.3 Microscopy	75
IV.2.4 Encapsulation of proteins into VPGs	75
IV.2.5 <i>In vitro</i> release studies.....	76
IV.2.5.1 Quantification of FITC-Dextran	76
IV.2.5.2 Quantification of mAb	76
IV.2.5.3 Phospholipid assay.....	77
IV.2.5.4 Optical density	78
IV.2.5.5 Dynamic light scattering	78

IV.2.5.6 Thermogravimetric determination of water loss during VPG preparation.....	78
IV.2.5.7 Determination of the product temperature	79
IV.2.6 Protein stability during extrusion and storage	79
IV.2.6.1 Capillary gel-electrophoresis	79
IV.2.6.2 Sodium dodecyl sulfate-polyacrylamide gel electrophoresis (SDS-PAGE)	79
IV.2.6.3 Fourier transform infrared spectroscopy (FTIR)	80
IV.3 Results and Discussion	81
IV.3.1 Preparation of VPGs by extrusion with repeated circulation	81
IV.3.2 Preparation of VPGs by a continuous extrusion process	86
IV.3.2.1 HAAKE MiniLab® Rheology Compounder	86
IV.3.2.2 ThreeTec ZE-5 Mini-Extruder	90
IV.3.2.3 Leistritz Micro 27 GL – 28D	93
IV.3.3 <i>In vitro</i> release of FITC-Dextran from VPG.....	96
IV.3.4 Stability of proteins in VPG after encapsulation and storage	97
IV.3.4.1 Determination of structural changes by FTIR spectroscopy	97
IV.3.4.2 Evaluation of capillary gel electrophoresis to characterize protein aggregation and fragmentation in VPG.....	98
IV.3.4.3 Characterization of protein aggregation by SDS-PAGE.....	99
IV.3.5 <i>In vitro</i> release of a monoclonal antibody from VPG.....	102
IV.3.6 Storage stability of VPG prepared by different manufacturing processes	105
IV.4 Conclusion	113
IV.5 References.....	115
CHAPTER V INTERACTIONS BETWEEN PROTEINS AND PHOSPHOLIPIDS	119
V.1 DO INTERACTIONS BETWEEN PROTEIN AND PHOSPHOLIPIDS INFLUENCE THE RELEASE BEHAVIOR FROM LIPID-BASED EXENATIDE DEPOT SYSTEMS?	120
V.1.1 Abstract	120
V.1.2 Introduction.....	122
V.1.3 Material and Methods	124
V.1.3.1 Material.....	124
V.1.3.2 Exenatide characterization	124
V.1.3.3 Preparation of vesicular phospholipid gel	124
V.1.3.4 VPG characterization	125
V.1.3.5 <i>In vitro</i> release of exenatide from VPG	125
V.1.3.6 Characterization of VPG erosion during <i>in vitro</i> release.....	125

V.1.3.7 Liposome preparation.....	126
V.1.3.8 Microscale Thermophoresis	127
V.1.4 Results	128
V.1.4.1 Exenatide characterization and encapsulation in VPGs.....	128
V.1.4.2 <i>In vitro</i> release of exenatide from VPG.....	129
V.1.4.3 Erosion behavior of VPGs during exenatide release.....	131
V.1.4.4 Interactions studies	132
V.1.5 Discussion	137
V.1.5.1 <i>In vitro</i> release behavior of exenatide from VPG.....	137
V.1.5.2 Interactions between exenatide and phospholipids	137
V.1.5.3 Erosion-driven, fast release from POPG containing gels	138
V.1.5.4 Barrier based retention in gels of POPC	139
V.1.6 Conclusions.....	141
V.1.7 Acknowledgements	142
V.1.8 Supplement	142
V.2 Further studies.....	143
V.2.1 Material and Methods.....	143
V.2.1.1 Preparation of liposomes.....	143
V.2.1.2 Isothermal titration calorimetry	143
V.2.1.3 Isothermal steady-state Fluorescence.....	144
V.2.1.4 Langmuir trough measurements	145
V.2.1.4.1 Compression isotherms of lipid-monolayers	145
V.2.1.4.2 Surface activity of exenatide.....	145
V.2.1.4.3 Intercalation of exenatide into lipid monolayers.....	145
V.2.2 Results and Discussion.....	147
V.2.2.1 Characterization of interactions by isothermal titration calorimetry.....	147
V.2.2.2 Isothermal steady state fluorescence.....	150
V.2.2.3 Comparison of binding events detected by ITC, fluorescence measurements and MST	153
V.2.2.4 Insertion of exenatide into phospholipid monolayers.....	157
V.3 Conclusion	160
V.4 References	162
CHAPTER VI APPLICATION OF VESICULAR PHOSPHOLIPID GELS AS DEPOT SYSTEM FOR SMALL HYDROPHOBIC DRUGS.....	167
VI.1 Introduction.....	168

VI.1.1 SAFit2	168
VI.1.2 Novel drug candidate #41.....	170
VI.2 Material and Methods	171
VI.2.1 Material	171
VI.2.2 Methods.....	171
VI.2.2.1 Preparation of VPG encapsulating SAFit2 or #41.....	171
VI.2.2.2 Preparation of a SAFit2-solution as control for <i>in vivo</i> study	172
VI.2.2.3 <i>In vitro</i> release studies	172
VI.2.2.3.1 Quantification of SAFit2 by RP-HPLC.....	172
VI.2.2.3.2 Quantification of #41	173
VI.2.2.3.3 Quantification of phosphatidylcholine.....	173
VI.2.2.4 <i>In vivo</i> release studies	173
VI.2.2.4.1 SAFit2-VPG	173
VI.2.2.4.2 #41-VPG	173
VI.3 Development of SAFit2-VPG	175
VI.3.1.1 <i>In vitro</i> release behavior of SAFit2 from VPG	175
VI.3.1.2 Pharmacokinetic study of SAFit2-VPG	176
VI.4 <i>In vivo</i> applications of SAFit2-VPG	179
VI.4.1 Balsevich et al., Stress-responsive FKBP51 regulates AKT2-AS160 signaling and metabolic function, <i>Nature Communications</i> (2017)	179
VI.4.2 Maiarù et al., The stress regulator FKBP51: a novel and promising druggable target for the treatment of persistent pain states across sexes, <i>Pain</i> (2018)	180
VI.4.3 Pöhlmann et al., Pharmacological Modulation of the Psychiatric Risk Factor FKBP51 Alters Efficiency of Common Antidepressant Drugs, <i>Frontiers in Behavioral Neurosciences</i> (2018)	182
VI.5 Development of a VPG formulation for the delivery of #41	184
VI.5.1 <i>In vitro</i> release behavior of #41 from VPG	185
VI.5.2 <i>In vivo</i> performance of #41-VPG.....	186
VI.6 Conclusion	187
VI.7 References.....	189
CHAPTER VII SUMMARY AND OUTLOOK.....	191
CHAPTER VIII APPENDIX.....	197

VIII.1 List of Figures	197
VIII.2 List of Tables	205
VIII.3 List of Abbreviations	207
VIII.4 Publications arising from this thesis.....	211
VIII.5 Patent	213
VIII.6 Poster presentations.....	214

CHAPTER I

VESICULAR PHOSPHOLIPID GELS AS DRUG DELIVERY SYSTEMS FOR SMALL MOLECULAR WEIGHT DRUGS, PEPTIDES AND PROTEINS: STATE OF THE ART REVIEW

This chapter is published as Mini-Review in the International Journal of Pharmaceutics as M. Breitsamer, G. Winter; *Vesicular phospholipid gels as drug delivery systems for small molecular weight drugs, peptides and proteins: state of the art review*; (2018).

I.1 Abstract

Lipid-based drug delivery has been investigated for a long time when it comes to liposomes and solid-lipid implants or solid-lipid nanoparticles. The promising, characteristic properties of these systems have led to the development of newer lipid-based drug delivery systems for the sustained release of drugs like liposomes for sustained delivery of substances, DepoFoam™ technology, phospholipid-based phase separation gels and vesicular phospholipid gels. Vesicular phospholipid gels (VPGs) are highly concentrated, viscous dispersions of high amounts of phospholipids in aqueous drug solution. The easy, solvent-free manufacturing process, high biocompatibility and various applications, as depot formulation for the sustained delivery of drugs and as a storage form of small unilamellar vesicles make VPGs highly attractive as drug carriers. Over the last years, the solvent free preparation process has advanced from high pressure homogenization to dual centrifugation (DC). Thereby a very simple one step process has been established for the preparation of VPGs. The semisolid VPG was first described in 1997 by Brandl et al.. Since then, many formulations have been developed, encapsulating small molecular weight drugs like 5-FU (2003), cetorelix (2005), cytarabine (2012) and exenatide (2015). In 2010, the first pharmaceutical protein, erythropoietin, was encapsulated in VPGs and sustained release of the substance was shown *in vitro*. In 2015, G-CSF was encapsulated in VPGs and tested *in vivo* for rotator cuff repair in a rat model and for PEGylated IFN- β -1b sustained release from vesicular phospholipid gels was demonstrated *in vitro*. Further, a very elegant administration technique for VPGs via needle-free injection was established. However, this promising drug delivery system does still leave space for improvement and optimization.

This review summarizes information about lipid-based depot systems in general and focuses on the historical development of VPGs. It emphasizes the advantages and drawbacks of VPGs as drug delivery device. Additionally, novel preparation methods and applications of VPGs will be discussed. A focus will be set on delivery of pharmaceutical proteins and peptides.

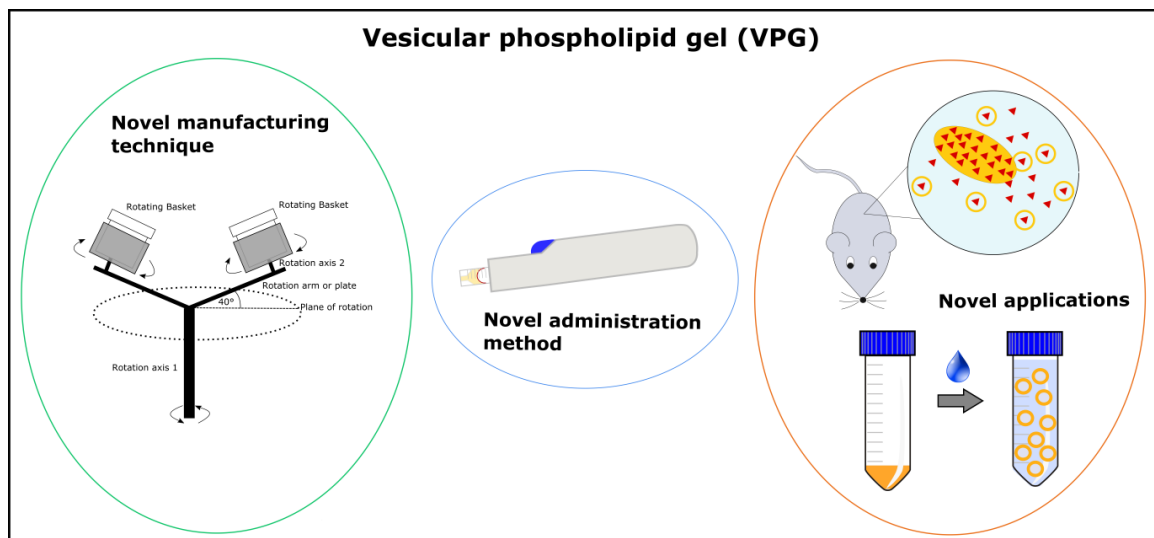


Figure I-1: Graphical abstract.

I.2 Introduction

Controlled drug delivery systems deliver the drug at a predetermined rate, locally or systemically for a specified period of time [1]. Besides, drug delivery devices based on synthetic polymers like PLGA and PLA, many lipid-based drug formulations, e.g. solid lipid implants and liposomes have been investigated for the sustained release of therapeutically relevant substances.

Lipid-based drug delivery systems are composed of physiologically occurring lipids like phospholipids, triglycerides, cholesterol and cholesterolesters [2]. This composition of the carrier material offers a great number of advantages over other drug vehicles [2]. Naturally occurring lipids like phospholipids are the major component of cell-membranes in humans, animals and plants and therefore tolerated well after administration in comparison to synthetic polymers [3]. An additional advantage of lipids as matrix material of drug carriers is the often simple and cheap manufacturing process of lipid-based vehicles as well as the possibilities to adapt the release kinetics by modification of the composition. Besides liposome-based carriers, on which we will focus, many other lipid-based drug delivery devices are available which have been summarized elsewhere [2]–[5]. Thus, in the following we will only give a brief overview on liposomal drug delivery systems for the sustained release of drugs. After that, the published data on vesicular phospholipid gels, a novel and very promising liposomal depot system is summarized.

Our review includes the historical development of the formulation, description of the preparation process, proposed release mechanism for VPGs and the applications for the sustained release of proteins and peptides as well as other drugs. Special focus will be on the last decade of research in this particular field.

I.2.1 Liposomes for sustained release of protein drugs

Liposomes are the most extensively investigated among drug carriers based on phospholipids [1], [6]. First described by Bangham et al. in 1964, the simple phospholipid vesicles, made to overcome toxicities or prevent drug degradation in the blood stream, developed over the years to an easy to manufacture drug carrier with high biocompatibility and the ability for controlled, triggered and sustained release of drugs [7]. From 1990 to 2012 thirteen liposomal formulations have been approved by the FDA

and many more are in clinical trials [3], [4]. However, most of the approved liposomal drug formulations are used for systemic i.v. applications, sometimes protecting the drug from elimination and thereby prolonging the plasma half-life. Liposomes composed of the classical phospholipids are rapidly removed from the blood by the cells of the reticulo-endothelial system (RES) after i.v. systemic application which is the biggest drawbacks of these systems [6]. Surface modifications, e.g. PEGylation, of liposomes increases circulation time of the carriers in the blood by forming a protective layer on the surface, but nevertheless availability of the drug was only prolonged up to a few hours to days [8]. Over the last two decades, especially the incorporation of proteins and peptides into liposomal formulations has increased. Liposomally encapsulated proteins and peptides display improved therapeutic activity, decreased side effects and modulated immune response [6]. Their capability to induce both humoral and cellular immune response at the same time may be a disadvantage in some applications but is also the cause for their use as immunological adjuvants for protein and peptide vaccines.

Size, structure and lipid composition of liposomes contribute to the release of drugs, when used as depot drug delivery systems [9]. The larger size of e.g. multivesicular liposomes (MVL) or multilamellar vesicles (MLV) is preferable for non-vascular routes of administration used for depots e.g. subcutaneous, intrathecal, epidural etc. [10].

Multivesicular liposomes (MVL) have been first described by Kim et al. in 1983 [11]. MVL are unordered structures, consisting of numerous discontinuous internal aqueous compartments which are separated by lipid bilayers [11], [12]. They have to be distinguished from liposome aggregates, where aqueous compartments are separated by two bilayers in close contact. MVL are prepared by a two-step, water-in-oil-in-water, double emulsification process [13]. Due to the high aqueous-volume-to-lipid ratio, high encapsulation efficiencies for water-soluble drugs can be achieved. As a result of the large size of these liposomes, they remain at the injection site and degrade slowly over time [12], [13]. Additionally, they have a prolonged clearance, giving them the ability for the sustained release of drugs and therefore to act as a depot system for few days. To this effect, Mu et al. showed sustained release of Bevacizumab from MVL *in vitro* and *in vivo* over several weeks [12].

Crommelin et al. reported that liposomes can be used as a sustained delivery device over several days after s.c. or i.m. injection [14]. It has also been shown, that subcutaneously

injected stealth liposomes showed prolonged half-lives in comparison to i.v. or i.p. administration [15].

Another approach to manufacture liposomal depots has just been reported recently. This technique uses negatively charged phospholipids in large unilamellar liposomes, which are in situ mixed with divalent cations e.g. calcium or magnesium to induce controlled aggregation of the liposomes [16]. First characterizations of these liposomes show promising results. However, *in vitro* and *in vivo* release behavior has not been investigated so far.

I.2.2 DepoFoam technology

In 2000, a special case of MVL for the controlled delivery of protein and peptide drugs, the DepoFoam™ technology, was first described by Ye et al. [17]. DepoFoam™ is composed of multiple non-concentric compartments with an aqueous core, bound by a continuous network of lipid membranes. This rather structured geometry distinguishes them from the unordered MVL described above. Several mechanisms have been proposed for the release of drugs from DepoFoam™. Breakdown of the lipid membrane, reorganization of the vesicles e.g. internal coalescence and permeation are possible ways, contributing to drug release [18], [19]. Further, lipid phase composition, osmolarity of the aqueous phase, interactions between the encapsulated drug and the lipid and the type of acid used for manufacturing contribute to the release rate from MVL [18].

Ye et al. showed that DepoFoam™ can be an ideal vehicle for controlled drug release [17]. It was possible to modulate the release rate of specific therapeutic proteins and peptides by changes in the formulation e.g. lipid composition or composition of the aqueous phase and to achieve a high encapsulation efficiency and biocompatibility. This new technology was marketed as DepoCyt™ (cytarabine) and as DepoDur™ (morphine) [18], [19].

Vyas et al. observed a sustained release profile of IFN- α -2a from DepoFoam™ *in vitro* over a period of one week [20]. A high percentage of protein encapsulation could be achieved with this DepoFoam™ technique, but the complex manufacturing process by water-in-oil-in-water double emulsification with organic solvent involved is a big disadvantage of this system.

I.2.3 Phospholipid-based phase separation gel (PPSG)

In the last years, phospholipid-based phase separation gels (PPSG) have been developed and evaluated for the sustained release of proteins and peptides [21]–[23]. PPSG are injectable in-situ forming depot formulations containing large quantities of phospholipid (up to 70%), oil and ethanol [21]. Phospholipids are solved in ethanol by stirring and a formulation with relatively low viscosity and acceptable injectability is produced. After administration of the PPSG into the body, solvent exchange leads to a sol to gel transition. Ethanol is replaced by surrounding aqueous medium following a concentration gradient and as a result phospholipids solidify due to their insolubility in aqueous solutions. Due to its composition, the newly formed gel is biodegradable and biocompatible. However, local irritation effects of ethanol at the injection site have been reported [21].

Wu et al. reported that both hydrophobic and hydrophilic chemotherapeutic agents can be easily encapsulated into these PPSG [22]. It was shown, that doxorubicin was released from the depot formulation for more than 14 days after one single injection.

Zhang et al. reported of PPSG for the delivery of octreotide acetate [21]. The addition of medium chain triglycerides (MCT) and significant decrease of ethanol content in the formulation reduced local irritation after administration. Octreotide acetate was released from the PPSG over several weeks and release was found to be slowest for high phospholipid concentrations. A similar system was later used for the release of leuprolide acetate [24].

In 2016 the sustained delivery of antigens and adjuvants from PPSG was shown [23]. It was found, that PPSG not only delivers the drug over a prolonged time but also supports the humoral immune response in synergy with the adjuvant without causing local irritation or systemic toxicity.

I.3 Vesicular phospholipid gels (VPGs)

VPGs are semisolid depot formulations composed of phospholipid vesicles and lamellar structures and have shown many desirable properties in recent research. They were first described by Brandl et al. in 1997 and ten years later, in 2007, he prepared a comprehensive summary of the literature existing on VPGs until then [25], [26].

Since then, new insights concerning the development of VPGs, like the design of a new manufacturing process and novel applications of VPGs have been achieved. In the present review the actual state of the art, summarizing the almost 20 years of research and development on VPGs, will be presented.

I.3.1 Definition and structural features

VPGs are highly concentrated, semisolid dispersions of phospholipids in an aqueous medium e.g. buffer or drug solution [25]–[27]. Unlike other lipid-based depot systems, VPGs consist of phospholipids as major lipidic component of the system. Other lipids, like cholesterol may be added if desired [28]–[30]. The morphology of VPGs has been extensively studied by freeze fracture transmission electron microscopy (FF-TEM) and it was shown that they are mainly composed of closely packed vesicles with compartments containing aqueous medium in the core of the vesicles [25]. Brandl et al. observed that VPGs composed of 35 to 45% (m/m) phosphatidylcholine display a very homogenous structure based on small and uniform vesicles, while higher concentrations of phospholipids result in a more heterogeneous structure with larger vesicles and planar lamellar stacks in between the small vesicles. The vesicles are so tightly packed that the aqueous areas between the vesicles are reduced to a minimum and steric interactions between the hydrophilic head-groups of the phospholipids lead to the rheological behavior which is comparable to other hydrogels incorporating macromolecular viscosity enhancers [26]. This inner structure does not only facilitate the encapsulation of hydrophilic substances in the core of the vesicles but also in between, in the lamellar structure of the gel, and therefore high encapsulation efficiency is obtained in comparison to liposome dispersions.

Another big advantage over other lipid-based systems is the fact that no concentration gradient exists between the core of the vesicles and the surrounding buffer phase (as

there is no such surrounding phase), which is the main cause of low encapsulation efficiency and drug loss during storage of classical liposome dispersions [26], [31]. Additionally, it has been shown that VPGs release their hydrophilic content in a sustained manner [31]. These unique features make VPGs a very promising drug delivery device suitable for the sustained release of drugs with high encapsulation efficiency for hydrophilic and lipophilic drugs. Their excellent tolerability due to their main components, phospholipids, supports their cause essentially.

Next to their application as depot system VPGs can also be used as storage form for small unilamellar liposomes (SUVs). By dilution of VPGs with excess aqueous medium and mixing with the help of ceramic beads in a ball mill, the semisolid gel can be transferred into a dispersion of SUVs [26], [32]. Massing et al. described the production of small liposomes by first preparing VPGs and subsequent dilution of the VPG to liposomal dispersions [33]. Additionally, their use as model membranes comparable to or even better than PAMPA-model has been described [34].

However, one drawback of the system is the rather high viscosity of the formulation, which is influenced by the amount of phospholipids incorporated into the formulation and further by the encapsulated drug [35]. In some *in vivo* studies, VPG was administered directly during surgery or had to be diluted to liposomes before administration [28], [30], [36]–[38]. The high viscosity compromises the administration of the VPGs with thin s.c. needles, so low patient compliance and eventually inaccurate dosing have to be considered. To overcome this drawback, needle-free injection (NFI) technology was investigated for the administration of the highly viscous VPG system [39]. It was shown, that by NFI VPG formulations with up to 45% (m/m) phospholipid content were easily injectable into pig skin with a Biojector 2000.

NFI of VPGs is a major breakthrough in the development of VPG which facilitates future applications of the depot system.

I.3.2 Preparation of VPGs and drug encapsulation techniques

In comparison to other phospholipid-based systems like liposomes and DepoFoam™, the manufacturing process is very simple, does not involve organic solvents like chloroform,

is extremely elegant and cheap and facilitates the preparation of large amounts as well as lab-scale size. Aseptic manufacturing is also feasible.

Next to the preparation of VPGs, consisting only of one phospholipid, in a one-step technique, the manufacturing of VPGs from lipid blends is of course also possible. To achieve a homogeneous distribution of the lipids over the entire lipid phase, solid lipid blends can be prepared by freeze drying from organic solutions [26], [32]. In order to prepare the lipid blends, lipids are dissolved in organic solvents e.g. tert-Butanol or Chloroform or mixtures of both, before the solution is shock-frozen and organic solvents are carefully removed by freeze-drying (e.g. shelf temperature: -55 °C, condenser temperature: -70 °C, vacuum: 20 hPa) as described in detail by Brandl [32]. Alternatively, lipid mixtures can be achieved by extrusion methods as e.g. described by Haas et al. [40]. Further, the film-method, often used for the preparation of liposomes, has also been used for the preparation of lipid mixtures but is less suited due to the high amount of lipids needed for VPGs [28].

Three different preparation techniques for VPGs have been described in the literature.

1.3.2.1 High-pressure homogenization (HPH)

The preparation of VPGs was first described by Brandl et al. in 1997 [25]. For the preparation of the highly viscous VPGs the dry powdered lipids are mixed with buffer or the drug solution respectively. Then the mixture is allowed to swell for a few hours and fed into a high-pressure homogenizer e.g. APV Gaulin Micron Lab 40 as used in the work of Brandl et al. or Microfluidizer 110. Homogenization can be done with up to 150 MPa, usually with 70 MPa in ten cycles to prevent heating of the material and high encapsulation efficiencies are achieved [25], [27], [32]. The described process facilitates the preparation of large amounts of VPGs. However, the originally used high pressure homogenizer (APV Gaulin Micron Lab 40) is not available anymore and it is questionable if similar encapsulation efficiency and homogeneity can be reached with devices by other manufacturers.

HPH is a technology that has been widely studied for food processing and for the preparation of emulsions [41]–[43]. It enables the preparation of very fine dispersions by application of high shearing forces on the formulation.

Freeze fracture microscopy studies revealed that the formulations prepared by HPH could be separated into two groups. Low phospholipid contents resulted in high homogeneity and small, densely packed vesicles, while a more heterogeneous morphology for the higher phospholipid concentrations was observed [25].

Although HPH is a commonly used technique, it is responsible for degradation of DNA or proteins, therefore only short mixing intervals should be used to prevent degradation of the encapsulated substance [2]. HPH is especially useful for the preparation of high amounts of VPG. In research and development small batches are needed and HPH has limitations regarding downscaling to smaller amounts than 40 ml [33].

1.3.2.2 Magnetic stirring

In the same publication in which Brandl et al. described HPH as preparation method, the magnetic stirring method has already been mentioned [25]. VPGs were prepared by first adding dry powdered phospholipids to buffer. Afterwards the mixtures were allowed to swell for two hours under magnetic stirring. Freeze-fracture microscopic examination of the obtained VPGs showed a different size and morphology in comparison to the result obtained by high-pressure homogenization. Low mechanical energy input by magnetic stirring of the mixtures resulted in heterogeneous vesicles with large diameters and uni- to multi-lamellar walls.

In spite of the questionable quality of the VPGs, in 2013 Zhong et al. described the magnetic stirring method for the preparation of VPGs with encapsulated thymopentin [44]. He prepared VPGs with phospholipid concentrations of 300 mg/g to 400 mg/g encapsulating thymopentin by magnetic stirring of the drug solution with egg phosphatidylcholine for 90 minutes. By this method particle sizes of 400 to 500 nm were achieved. Further, Zhang et al. used the magnetic stirring method for the preparation of VPGs encapsulating exenatide [45]. In this work phospholipid contents were between 200 to 400 mg/g which resulted in large average vesicle sizes of about 15 μm after dilution. In this case the VPGs were prepared by addition of exenatide-solution to the accurately weighted phospholipids and subsequent magnetic stirring for 30 minutes at room temperature.

Although magnetic stirring is a very simple and easy to scale up technique, it is questionable if reproducible homogeneity and sufficient stability of the VPGs is obtained

by this method. It is further questionable whether the dispersion after magnetic stirring fulfills the defined criteria for VPGs at all. Zhang et al. reported stratification of formulations with low phospholipid amounts [45]. Nevertheless, first release studies showed that VPGs with sustained release of small substances could be obtained by this preparation method [44], [45].

I.3.2.3 Dual centrifugation (DC)

Massing was the first to describe a new, elegant and straight forward technique for the preparation of VPGs, Liposomes and lipid-based Nanoparticles [33], [46].

DAC is a special centrifugation technique in which a container is not only rotated around the main rotation axis of a conventional centrifuge but also around a second axis in the middle of the container [33]. The two counter-rotating, superposed movements result in a simultaneous inward and outward movement of the material and therefore high shearing forces on the material in the container and an efficient homogenization of the mixture. DAC is well suited for the rapid mixing of two viscous components, which makes it an excellent candidate for the preparation of VPGs as well as for liposomes and fat-emulsions [33], [47]–[51]. Homogeneous mixtures of the substances can be reached in a short time.

Massing et al. investigated several parameters with an influence on the obtained liposomes and VPG [33]. They found that increasing lipid amounts led to decreasing mean liposome size after dilution of the VPG. Further, the homogenization time, choice of beads as dispersion aid to improve the quality and mixing speed have great influence on liposome size. Still, expectantly, the temperature of the formulation increases in the course of longer centrifugations. To this end, a multi-step preparation protocol has to be used with cooling steps in between the centrifugation or a cooled DAC system is required to prevent degradation of the drug during preparation, especially when mixing aids (e.g. glass balls) are used [52].

Over the last years, the DAC method has been improved to dual centrifugation (DC) [51]. In DC the principles of DAC, i.e. two counter-rotating movements for rapid and homogenous mixing of components, are used but the centrifuge has two or more rotating baskets, thus not needing a counterweight in the setup of the centrifuge. Further, DC systems like the ZentriMix 380R centrifuge by Hettrich AG may be equipped with a cooling

system like conventional centrifuges and therefore facilitate also processing of sensitive compounds without applying a multi-step protocol which is needed when using a DAC. A schematic drawing of a DAC in comparison to the novel DC setup is shown in Figure I-2.

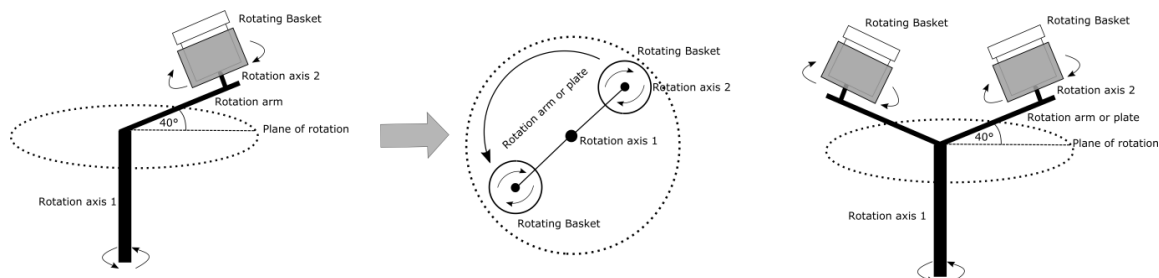


Figure I-2: Schematic drawing of a dual asymmetric centrifuge (left) from the side in comparison to a dual centrifuge from the top (middle) and from the side (right).

The fact that components are mixed in a closed plastic or glass container in a DC makes this method simple in comparison to HPH. DC facilitates also lab scale production of VPGs and is suited for aseptic manufacturing. In contrast to that, during HPH the VPG has direct contact with the metal surface of the instrument, as well as the moving parts needed for homogenization. This may result in metal abrasion into the product. Additionally, if higher energy input is needed to achieve a better mixing quality, centrifugation speed and duration can be easily adapted in a DC. In a HPH the pressure can be increased within certain limits and the material can be recycled several times to achieve better homogeneity. However, the need to remove the material from the HPH and re-introduce it again for multiple cycles, makes the process more susceptible for contamination and other problems.

I.3.2.4 Encapsulation techniques for drugs

In literature three loading techniques are described for VPGs [32]. Hydrophilic drugs are encapsulated into VPGs by direct loading. Here the drug solution is directly added to the phospholipids previous to the preparation via HPH, DC or magnetic stirring and thereby substances are truly entrapped within the vesicles of the gel and in the aqueous phases between the vesicles. This method has often been used in the past, also for the encapsulation of proteins or peptides into VPGs [29], [37], [48].

Further, substances can also be passively loaded into the pre-formed VPG e.g. in a hospital pharmacy setting. Therefore, an appropriate, small volume of drug solution is added to

the drug-free VPG, pre-mixing is done with a sterile spatula and the mixture is incubated until the drug is equally distributed throughout the formulation by diffusion following a concentration gradient [32]. In this case, the phase transition temperature T_m of the phospholipids plays an important role, regarding the encapsulation efficiency. Moog et al. used the described method for the entrapment of gemcitabine into VPGs by diffusion of the drug into the VPG supported by elevated temperature [28]. Further, Kaiser et al. compared this loading method with direct entrapment of 5-fluorouracil and found that the passive loading technique was not suited for encapsulation of the drug [30].

Lipophilic or amphiphilic substances can be incorporated in the lipid-phase. Therefore a homogeneous lipid-drug mixture is formed, e.g. by freeze drying the phospholipid and the drug from organic solutions, which is then hydrated with an appropriate amount of buffer. Balsevich et al., Maiarù et al. and Pöhlmann et al. used this method for the preparation of VPGs encapsulating the selective FKBP51 antagonist SAFit2 [53]–[55].

I.3.2.5 Sterile manufacturing of VPGs

Steam sterilization in the final container is the preferred method for sterilization of parenteral drug formulations. One of the drawbacks of liposomal formulations is a loss of encapsulation efficiency following steam sterilization. This is for example caused by vesicle fusion, leakage of the drug and chemical degradation of the phospholipids [56]. Tardi et al. investigated steam sterilization of VPGs in the terminal container [57]. Autoclaving of VPGs under standard conditions (121 °C, 15 minutes) caused fusion of the vesicles which did influence the release behavior of the gel in respect to slower erosion of the matrix but no hydrolysis of phospholipids was observed. Sterilization stability of cytarabine loaded VPGs has been investigated by Qi et al. [58]. It was found that although changes in characteristic properties of the VPG e.g. viscosity and slower drug release were observed, essential properties of VPGs, like the tightly packed vesicular structure, sustained release and the possibility of redispersion were still preserved [58]. Hence, steam sterilization is the method of choice for sterilization of the end product if the encapsulated drug does allow it.

If steam sterilization is not applicable e.g. due to the sensitivity of the drug against high temperatures, alternatively the VPG can be prepared under aseptic working conditions in a closed container or vial.

I.3.3 Sustained release of encapsulated drugs from VPGs

Tardi et al. were the first to investigate the release behavior of encapsulated calcein from VPGs [31]. A custom made flow through cell as shown in Figure I-3 was used for the examination of the release behavior. For release testing, the VPG was filled in the donor compartment on the downside of the flow-through cell and release medium was pumped through the acceptor compartment with a flow rate of 10 ml/h which is comparable to a clearance time of 180 s.

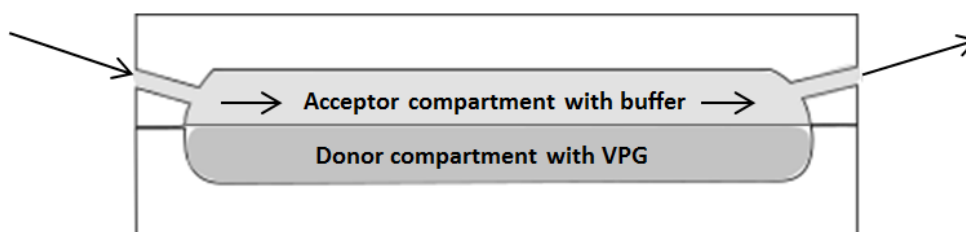


Figure I-3: Schematic drawing of the flow through release cell described by Tardi et al. (1998).

The release of hydrophilic markers from VPGs occurred for time periods of hours up to days and the encapsulated compound was released by two competing mechanisms occurring at the same time: erosion of the phospholipid matrix and diffusion of the drug out of the gel following a concentration gradient. It was observed that VPGs with a phospholipid amount of up to 30% (m/m) disintegrate spontaneously with rather fast release of the encapsulated drug. Release from gels with a phospholipid concentration of up to 40% (m/m) is stated to be erosion controlled, while the release from gels with a phospholipid amount of up to 50% (m/m) seems to be diffusion controlled [31]. Many authors came to the same, not surprising conclusion: a high amount of phospholipids leads to a slower release of drugs from the formulation [29], [45]. Neuhofer also observed that gels with a low phospholipid concentration are washed out of the release cell very fast [35]. He observed that a certain threshold of phospholipids in the formulation is needed to provide high enough viscosity of the gel and therefore a slower release by erosion of the gel. A correlation between viscosity and protein release was found when only the lipid amount of the gel was changed, leaving all other formulation parameters the same.

But not only does the phospholipid content strongly influence the release behavior of drugs from VPGs. The type of phospholipid (e.g. charged phospholipids) and the formulation buffer influence the release kinetics [31], [35], [48], [59]. Additionally, the drug load affects the release behavior significantly. To this end, Grohganz et al. observed differences in release of cetorelix acetate when different concentrations of the peptide were encapsulated into the VPG [29]. The absolute released amount increased up to a certain concentration, above which further increase of the concentration led to a reduced absolute release. Tian et al. showed that by adjustment of the lipid charge the release behavior of EPO from VPGs could be modulated [48]. She found that lipid charge and lipid amount both were the dominant parameters influencing the protein release from VPGs which was mainly due to erosion of the gel. Further, Tian was able to show that an increase of protein load led to a decreased release rate [59]. Additionally to the choice of a suited lipid species and charge, the phase transition temperature (T_m) has to be taken into account when VPG formulations are developed. At temperatures near the T_m of a phospholipid, the drug uptake into the empty liposomes is superior to other temperatures. Thus, higher encapsulation efficiencies may be reached around the T_m of the phospholipid especially when passive loading is used.

Next to the above mentioned factors which influence the release behavior, it is crucial to know if the encapsulated drug is actually encapsulated in the vesicles of the VPG. True encapsulation into the vesicles results in longer release rates, since in this case the drug has to diffuse out of the vesicles, pass one or more membranes and regions with different hydrophobicity. Brandl et al. found a encapsulation efficiency of 30 to 70% for the model compounds calcein and carboxyfluorecein [27]. Kaiser et al. investigated if 5-fluorouracil is encapsulated in the vesicles which were obtained after dilution of a VPG [30]. He could show an effect of lipid composition and pH on the encapsulation efficiency. Further, Grohganz et al. demonstrated an encapsulation efficiency of cetorelix acetate into vesicles of the VPG above 65% [29]. However, the VPG was diluted before determination of the encapsulated drug in the vesicles, thus a leakage of the drug out from the vesicles during dilution steps cannot be ruled out and has to be taken into account.

In recent literature, other methods for the investigation of the release behavior have been described. Even et al. used a micro-centrifugation cap release model for the release of TRP2, a small peptide [60]. The VPG was filled in the round bottom of a micro-

centrifugation cap, buffer was carefully added and samples were taken by complete buffer exchange. Advantages of this model are the simplicity, easy handling and low sample dilution. Another testing method was used by Zhang et al. for the release of exenatide from VPGs [45]. VPGs were filled into dialysis bags with defined molecular weight cut-off and placed in release medium. Again, samples were taken by replacing the release medium.

All currently used release models do still have drawbacks like high dilution of the samples, turbidity of the released fractions and lack of homogeneity of the exposed surface of the depot, therefore further optimization of the release models is needed. Additionally, a decent *in vitro* – *in vivo* – correlation is still not possible, since only few PK data of VPGs in their function as depot system is available.

I.3.4 Applications of VPGs

VPGs have been used in the past for different types of applications which are illustrated in Figure I-4.

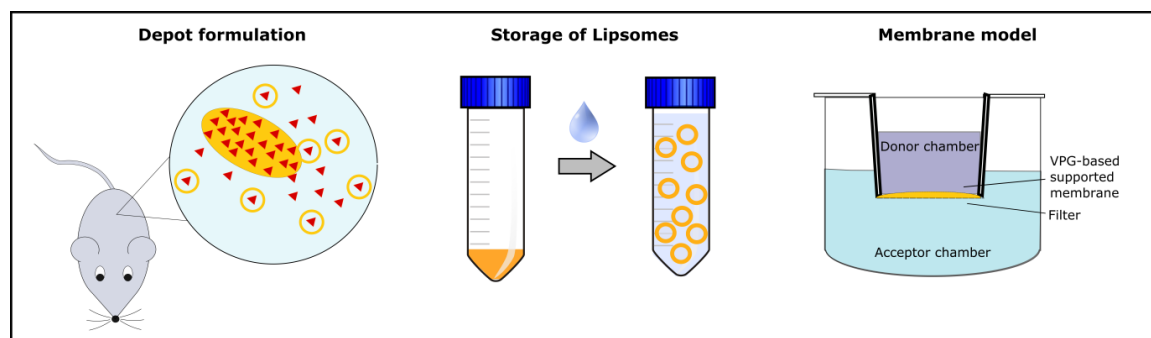


Figure I-4: Overview of applications for VPGs.

Table I-1 summarizes all investigated VPG formulations with different pharmaceutical relevant substances. Especially since 2010, VPGs have been mainly used as depot formulations for the sustained release of drugs.

Table I-1: Chronologic summary of VPG formulations with encapsulated drugs which were investigated over the last years.

Encapsulated drug	Production procedure	Investigated administration type	Year	References
Vincristine	HPH, passive loading	Diluted VPG (i.v. injection)	2002	[38]
Gemcitabine	HPH, passive loading	Diluted VPG (i.v. injection)	2002	[28]
5-fluorouracil	HPH, direct loading	Diluted VPG (<i>in vitro</i>) and depot system (<i>in vitro</i>)	2003	[30]
Cetorelix	HPH, direct loading	Depot system (<i>in vitro</i>)	2005	[29]
Erythropoietin	DAC, direct loading	Depot system (<i>in vitro</i>)	2010	[48], [59]
Cytarabine	HPH or DAC, direct loading	Depot system (implantation during surgery)	2012, 2014	[36], [58]
Thymopentin	Magnetic stirring, direct loading	Depot system (s.c. injection)	2013	[44]
G-CSF	DAC, direct loading	Depot system (implantation during surgery)	2015	[37]
IFN- β -1b	DAC, direct loading	Depot system (<i>in vitro</i>)	2015	[35]
PEG-IFN- β -1b				
TRP2	DAC, direct loading	Depot system (<i>in vitro</i> and <i>in vivo</i>)	2015	[60]
Exenatide	Magnetic stirring	Depot system (s.c. injection, <i>in vivo</i>)	2015	[45]
SAFit2	DAC, direct incorporation technique	Depot system (s.c. injection, <i>in vivo</i>)	2017, 2018	[53]–[55]

I.3.4.1 Application as storage form of liposomes

In the first years, VPGs were mainly used as storage form of liposomes with high encapsulation efficiency for hydrophilic drugs. Liposomal formulations do have the drawback of a low encapsulation efficiency of substances in the core of the vesicles. To remove the free, not liposomal encapsulated drug from the solution an extraction step has to be included in the preparation protocol. However, over longer storage time drugs diffuse out of the vesicles following a concentration gradient.

VPGs are well suited concentrated storage forms of liposomes. By one-step or multi-step dilution of the gel and vigorous mixing, e.g. by shaking of the dispersions with a ball mill, a homogeneous liposome dispersion with small unilamellar liposomes can be obtained

[32]. By this technique liposomes with high encapsulation efficiency can be prepared [27]. This described method has already been successfully used for the preparation of liposomes with encapsulated vincristine, 5-fluorouracil and gemcitabine for anti-cancer treatment and encapsulation efficiencies of up to 54% liposomally entrapped drug were reached [28], [30], [38]. The technique enables the bedside preparation of liposomal dispersions in the oncology clinical setup.

Just recently, Chen et al. described the preparation of a thermoreversible hydrogel with insulin-loaded liposomes [61]. VPG was prepared to encapsulate insulin into the liposomes, before the VPG was diluted to liposomes and insulin-loaded liposomes were incorporated in the hydrogel.

I.3.4.2 Application as drug delivery device for the sustained release of small molecular drugs and peptides

Most publications of the last years on the applications of VPGs have dealt with the sustained release of small molecular weight drugs (MW < 1000 Da) and peptides (< 100 amino acids). Grohganz et al. were the first to encapsulate cetorelix, a small peptide, into VPGs and to use this system for the sustained release of the substance [29]. From short-term release studies (7 days), they predicted that 80% of cetorelix was released over 3 months, depending on the lipid amount and the drug content of the VPG.

In another study thymopentin was incorporated into various VPG formulations with low phospholipid content and sustained release was investigated *in vivo* [44]. Therapeutic efficacy of thymopentin entrapped in VPGs and administered s.c. once weekly was shown to be comparable to a thymopentin solution injected once daily for 7 days. Not only was this result interesting regarding the investigated low phospholipid concentrations, but also in terms of the small size of the entrapped drugs and the preparation process by magnetic stirring. However, similar results were observed for a second small peptide. Exenatide was encapsulated into VPGs by a similar preparation method and showed sustained release over three weeks *in vitro* [45]. *In vivo* results showed that by a single injection of exenatide loaded VPG, a sustained hypoglycemic effect was achieved over 10 days and was comparable to twice daily injections of a drug solution over the same time. However, in both cases VPG encapsulating thymopentin or exenatide were prepared by magnetic stirring and Zhang et al. observed stratification of VPGs with low phospholipid

amount [44], [45]. It is unknown if the preparation process, resulting in VPG with low physical chemical stability, is itself responsible for the sustained release of the drugs. Interactions between the drug and the phospholipids could be an explanation for the sustained release behavior of the small molecules. However, this has not been shown yet. In 2014, Qi et al. described the development of a VPG formulation incorporating cytarabine for the treatment of xenografted glioma [36]. VPGs were prepared by DAC and cytarabine was directly encapsulated into the VPG during preparation. *In vitro* cytarabine was released over 16 days from the VPG. For *in vivo* tests cytarabine loaded VPG was implanted into the brain of mice and therapeutic concentrations were achieved over 28 days in up to 5 mm distance of the implantation site.

Even compared the release of a small peptide, TRP2, from solid lipid implants to the release from VPGs [60]. She found that TRP2 release from VPGs was incomplete and slow *in vitro* and suspected interactions between the peptide and the phospholipids behind this phenomenon. Further, TRP2 was released significantly slower from VPGs in comparison to ovalbumin, a much bigger molecule.

Balsevich et al. encapsulated SAFit2, a selective FKBP51 antagonist, into VPGs (50%, (m/m)) and showed an effect of the drug on metabolic parameters several days after injection of the VPG [53]. Maiarù et al. used SAFit2-VPG (50%, (m/m)) to improve mechanical pain hypersensitivity [54]. It was shown, that SAFit2 released from VPG reduced mechanical hypersensitivity for at least 7 days after application, compared to 24 hours when injected subcutaneously as a solution. After a second application of SAFit2-VPG, hypersensitivity was reduced for at least 16 days. Pöhlmann et al. used SAFit2-VPG together with a commonly prescribed selective serotonin reuptake inhibitor (SSRI) and showed *in vivo* that co-application of both substances lowered the effect of the SSRI on anxiety but improved stress coping behavior [55].

I.3.4.3 Application as drug delivery devices for the sustained release of proteins

In 2010, Tian et al. were the first to report of VPGs as depot systems for the sustained release of a therapeutic relevant protein [48]. It was shown that VPGs were suitable as sustained release systems for erythropoietin (EPO), since EPO was stable during manufacturing and the protein was released over two weeks from VPGs with a

phospholipid content of 55% (m/m) based on 100% egg lecithin (Lipoid E80). Release occurred in a linear manner without any burst effect. With decreasing lecithin content the release rate was increased and by incorporation of charged phospholipids in the formulation, release could be further modulated.

Later it was shown, that the sustained release behavior of EPO was maintained after ejection of the EPO-VPG using a needle-free injection device (Biojector 2000) [39].

Buchmann et al. published *in vitro* and *in vivo* data of the entrapment and sustained release of granulocyte-colony stimulating factor (G-CSF) from VPGs [37]. By the use of VPGs a continuous G-CSF release following zero-order kinetics was achieved *in vitro* and it was shown that the VPG was tolerated well *in vivo* and had no negative influence on wound healing after administration during surgery. However, systemic concentration of G-CSF did not show significant differences between Placebo-group and G-CSF-VPG group and therefore no conclusion could be drawn about the actual local release rate *in vivo*.

Further, the release of interferon- β -1b (IFN- β -1b) and PEGylated IFN- β -1b was investigated *in vitro* [35]. It was observed that the release of native IFN- β -1b from VPGs was not possible and strong protein-lipid interactions were assumed to be responsible for this. PEGylation of IFN- β -1b facilitated the release from the depot system with a very low release rate which indicates that by PEGylation interactions between the protein and the phospholipid were reduced but not completely avoided. However, even after intensive investigation of the mechanism behind the interactions by Neuhofer with several methods, no prediction regarding the influence of interactions between the encapsulated protein and the phospholipids on the release behavior was possible [35].

I.4 Summary

VPGs are a modern depot system for the sustained release of small molecules, peptides and proteins and a stable system for the long-term storage of liposomes, which can be diluted directly before usage. The manufacturing process by DAC facilitates fast and simple preparation of this system and enables production in a broad range of batch sizes. At the same time, DAC is gentle to the encapsulated drug and therefore suitable for the entrapment of sensitive compounds like proteins and peptides.

Over the years, VPGs developed from a storage formulation for liposomes to a lipid-based depot system for subcutaneous injection. Next to the work of several groups in Europe, especially Chinese groups focus on VPGs and their further development as drug delivery system. Several formulations have been developed in the last few years, which are directly administered as depot systems. *In vitro* results show strong evidence that proteins as well as small molecules and peptides are released in a sustained manner from the depot formulation. First *in vivo* results support the benefits of this system for the delivery of those substances, showing sustained release of different drugs and excellent biocompatibility. Still, additional *in vivo* results especially on protein and peptide release from VPGs and a correlation of the PK data to the *in vitro* situation is needed to further develop the depot system and bring it to clinical use.

The application of needle-free injection technology has been evaluated and proven to be suitable for the administration of the depot system, thereby overcoming the challenging administration problems caused by the high viscosity of the system.

I.5 References

- [1] F. Bassyouni, N. Elhalwany, M. Abdel Rehim, and M. Neyfeh, "Advances and new technologies applied in controlled drug delivery system," *Res. Chem. Intermed.*, vol. 41, no. 4, pp. 2165–2200, 2015.
- [2] M. Rawat, D. Singh, S. Saraf, and S. Saraf, "Lipid carriers: a versatile delivery vehicle for proteins and peptides.," *J. Pharm. Soc. Japan*, vol. 128, no. 2, pp. 269–280, 2008.
- [3] J. Li *et al.*, "A review on phospholipids and their main applications in drug delivery systems," *Asian J. Pharm. Sci.*, vol. 10, no. 2, pp. 81–98, 2014.
- [4] T. M. Allen and P. R. Cullis, "Liposomal drug delivery systems: from concept to clinical applications.," *Adv. Drug Deliv. Rev.*, vol. 65, no. 1, pp. 36–48, 2013.
- [5] S. A. Wissing, O. Kayser, and R. H. Müller, "Solid lipid nanoparticles for parenteral drug delivery," *Adv. Drug Deliv. Rev.*, vol. 56, no. 9, pp. 1257–1272, 2004.
- [6] V. P. Torchilin, "Recent advances with liposomes as pharmaceutical carriers.," *Nat. Rev. Drug Discov.*, vol. 4, no. 2, pp. 145–160, 2005.
- [7] A. D. Bangham and R. W. Horne, "Negative staining of phospholipids and their structural modification by surface-active agents as observed in the electron microscope," *J. Mol. Biol.*, vol. 8, no. 5, pp. 660–668, 1964.
- [8] G. Blume and G. Cevc, "Liposomes for the sustained drug release in vivo.," *Biochim. Biophys. Acta*, vol. 1029, no. 1, pp. 91–97, 1990.
- [9] C. Oussoren, J. Zuidema, D. J. A. Crommelin, and G. Storm, "Lymphatic uptake and biodistribution of liposomes after subcutaneous injection. II. Influence of liposomal size, lipid composition and lipid dose," *Biochim. Biophys. Acta - Biomembr.*, vol. 1328, no. 2, pp. 261–272, 1997.
- [10] N. V. Katre, "Liposome-based depot injection technologies: How versatile are they?," *Am. J. Drug Deliv.*, vol. 2, no. 4, pp. 213–227, 2004.
- [11] S. Kim, M. S. Turker, E. Y. Chi, S. Sela, and G. M. Martin, "Preparation of Multivesicular Liposomes," *Biochim. Biophys. Acta*, vol. 728, pp. 339–348, 1983.
- [12] H. Mu *et al.*, "Multivesicular liposomes for sustained release of bevacizumab in treating laser-induced choroidal neovascularization.," *Drug Deliv.*, vol. 25, no. 1, pp. 1372–1383, 2018.
- [13] N. V. Katre, "Lipid-Based Multivesicular Carriers for Sustained Delivery of Therapeutic Proteins and Peptides," *BioPharm*, vol. 14, no. 3, pp. 8–10, 2001.
- [14] D. J. A. Crommelin *et al.*, "Liposomes and immunoliposomes for controlled release or site specific delivery of anti-parasitic drugs and cytostatics," *J. Control. Release*, vol. 16, no. 1–2, pp. 147–154, 1991.
- [15] T. M. Allen, C. B. Hansen, and L. S. S. Guo, "Subcutaneous administration of liposomes: a comparison with the intravenous and intraperitoneal routes of injection," *Biochim. Biophys. Acta - Biomembr.*, vol. 1150, no. 1, pp. 9–16, 1993.
- [16] L. Rahnfeld, J. Thamm, F. Steiniger, P. van Hoogevest, and P. Luciani, "Study on the in situ aggregation of liposomes with negatively charged phospholipids for use as

- injectable depot formulation," *Colloids Surfaces B Biointerfaces*, vol. 168, pp. 10–17, 2018.
- [17] Q. Ye, J. Asherman, M. Stevenson, E. Brownson, and N. V. Katre, "DepoFoam(TM) technology: A vehicle for controlled delivery of protein and peptide drugs," *J. Control. Release*, vol. 64, no. 1–3, pp. 155–166, 2000.
- [18] M. S. Angst and D. R. Drover, "Pharmacology of drugs formulated with DepoFoam™: A sustained release drug delivery system for parenteral administration using multivesicular liposome technology," *Clin. Pharmacokinet.*, vol. 45, no. 12, pp. 1153–1176, 2006.
- [19] S. Mantripragada, "A lipid based depot (DepoFoam technology) for sustained release drug delivery," *Prog. Lipid Res.*, vol. 41, no. 5, pp. 392–406, 2002.
- [20] S. P. Vyas, M. Rawat, A. Rawat, S. Mahor, and P. N. Gupta, "Pegylated protein encapsulated multivesicular liposomes: A novel approach for sustained release of interferon alpha," *Drug Dev. Ind. Pharm.*, vol. 32, no. 6, pp. 699–707, 2006.
- [21] T. Zhang *et al.*, "A high-efficiency, low-toxicity, phospholipids-based phase separation gel for long-term delivery of peptides," *Biomaterials*, vol. 45, pp. 1–9, 2015.
- [22] W. Wu *et al.*, "A Novel Doxorubicin-Loaded in Situ Forming Gel Based High Concentration of Phospholipid for Intratumoral Drug Delivery," *Mol. Pharm.*, vol. 11, no. 10, pp. 3378–3385, 2014.
- [23] L. Han *et al.*, "An injectable, low-toxicity phospholipid-based phase separation gel that induces strong and persistent immune responses in mice," *Biomaterials*, vol. 105, pp. 185–194, 2016.
- [24] D. Long, T. Gong, Z. Zhang, R. Ding, and Y. Fu, "Preparation and evaluation of a phospholipid-based injectable gel for the long term delivery of leuprolide acetate," *Acta Pharm. Sin. B*, vol. 6, no. 4, pp. 329–335, 2016.
- [25] M. Brandl, M. Drechsler, D. Bachmann, and K. H. Bauer, "Morphology of semisolid aqueous phosphatidylcholine dispersions, a freeze fracture electron microscopy study," *Chem. Phys. Lipids*, vol. 87, pp. 65–72, 1997.
- [26] M. Brandl, "Vesicular Phospholipid Gels: A Technology Platform," *J. Liposome Res.*, vol. 17, no. 1, pp. 15–26, 2007.
- [27] M. Brandl, M. Drechsler, D. Bachmann, C. Tardi, M. Schmidtgen, and K. H. Bauer, "Preparation and characterization of semi-solid phospholipid dispersions and dilutions thereof," *Int. J. Pharm.*, vol. 170, pp. 187–199, 1998.
- [28] R. Moog *et al.*, "Change in pharmacokinetic and pharmacodynamic behavior of gemcitabine in human tumor xenografts upon entrapment in vesicular phospholipid gels," *Cancer Chemother. Pharmacol.*, vol. 49, pp. 356–366, 2002.
- [29] H. Grohgan, I. Tho, and M. Brandl, "Development and in vitro evaluation of a liposome based implant formulation for the decapeptide cetorelix," *Eur. J. Pharm. Biopharm.*, vol. 59, no. 3, pp. 439–448, 2005.
- [30] N. Kaiser *et al.*, "5-Fluorouracil in vesicular phospholipid gels for anticancer

- treatment: Entrapment and release properties," *Int. J. Pharm.*, vol. 256, no. 1–2, pp. 123–131, 2003.
- [31] C. Tardi, M. Brandl, and R. Schubert, "Erosion and controlled release properties of semisolid vesicular phospholipid dispersions," *J. Control. Release*, vol. 55, no. 2–3, pp. 261–270, 1998.
- [32] M. Brandl, "Vesicular phospholipid gels," in *Liposomes - Methods and Protocols*, vol. 1, V. Weissing, Ed. New York: Humana Press, 2003, pp. 205–212.
- [33] U. Massing, S. Cicko, and V. Ziroli, "Dual asymmetric centrifugation (DAC)-A new technique for liposome preparation," *J. Control. Release*, vol. 125, no. 1, pp. 16–24, 2008.
- [34] G. E. Flaten, A. B. Dhanikula, K. Luthman, and M. Brandl, "Drug permeability across a phospholipid vesicle based barrier: A novel approach for studying passive diffusion," *Eur. J. Pharm. Sci.*, vol. 27, no. 1, pp. 80–90, 2006.
- [35] C. Neuhofer, "Development of lipid based depot formulations using interferon-beta-1b as a model protein," Dissertation, Ludwig-Maximilians-Universität München, 2015.
- [36] N. Qi *et al.*, "Sustained delivery of cytarabine-loaded vesicular phospholipid gels for treatment of xenografted glioma," *Int. J. Pharm.*, vol. 472, no. 1–2, pp. 48–55, 2014.
- [37] S. Buchmann *et al.*, "Growth factor release by vesicular phospholipid gels: in-vitro results and application for rotator cuff repair in a rat model," *BMC Musculoskelet. Disord.*, vol. 16:82, no. 1, pp. 1–10, 2015.
- [38] F. Güthlein *et al.*, "Pharmacokinetics and antitumor activity of vincristine entrapped in vesicular phospholipid gels," *Anticancer. Drugs*, vol. 13, no. 8, pp. 797–805, 2002.
- [39] M. Breitsamer and G. Winter, "Needle-Free Injection of Vesicular Phospholipid Gels - A Novel Approach to Overcome an Administration Hurdle for Semisolid Depot Systems," *J. Pharm. Sci.*, vol. 106, no. 4, pp. 968–972, 2017.
- [40] H. Haas, S. Waibler, and G. Winter, "Method for Producing Colloidal Nanoparticles with a Compounder," US20070148196A1, 2007.
- [41] J. Flourey, A. Desrumaux, and J. Lardières, "Effect of high-pressure homogenization on droplet size distributions and rheological properties of model oil-in-water emulsions," *Innov. Food Sci. Emerg. Technol.*, vol. 1, no. 2, pp. 127–134, 2000.
- [42] P. E. D. Augusto, A. Ibarz, and M. Cristianini, "Effect of high pressure homogenization (HPH) on the rheological properties of a fruit juice serum model," *J. Food Eng.*, vol. 111, no. 2, pp. 474–477, 2012.
- [43] P. Paquin, "Technological properties of high pressure homogenizers: The effect of fat globules, milk proteins, and polysaccharides," *Int. Dairy J.*, vol. 9, no. 3–6, pp. 329–335, 1999.
- [44] Y. Zhong *et al.*, "Vesicular phospholipid gels using low concentrations of phospholipids for the sustained release of thymopentin : pharmacokinetics and pharmacodynamics," *Pharmazie*, vol. 68, pp. 811–815, 2013.

- [45] Y. Zhang *et al.*, "In vitro and in vivo sustained release of exenatide from vesicular phospholipid gels for type II diabetes," *Drug Dev. Ind. Pharm.*, vol. 42, no. 7, pp. 1042–1049, 2015.
- [46] U. Massing, "Verwendung einer dualen asymmetrischen Zentrifuge (DAZ) zur Herstellung von lipidbasierten Nanopartikeln.," EP2263653B1, Jul-2013.
- [47] S. G. Ingebrigtsen, N. Škalko-Basnet, and A. M. Holsæter, "Development and optimization of a new processing approach for manufacturing topical liposomes-in-hydrogel drug formulations by dual asymmetric centrifugation," *Drug Dev. Ind. Pharm.*, pp. 1–33, 2015.
- [48] W. Tian, S. Schulze, M. Brandl, and G. Winter, "Vesicular phospholipid gel-based depot formulations for pharmaceutical proteins: Development and in vitro evaluation," *J. Control. Release*, vol. 142, no. 3, pp. 319–325, 2010.
- [49] F. Tenambergen, C. H. Maruiama, and K. Mäder, "Dual asymmetric centrifugation as an alternative preparation method for parenteral fat emulsions in preformulation development," *Int. J. Pharm.*, vol. 447, no. 1–2, pp. 31–37, 2013.
- [50] S. G. Ingebrigtsen, N. Škalko-Basnet, C. de Albuquerque Cavalcanti Jacobsen, and A. M. Holsaeter, "Successful co-encapsulation of benzoyl peroxide and chloramphenicol in liposomes by a novel manufacturing method - dual asymmetric centrifugation," *Eur. J. Pharm. Sci.*, vol. 97, pp. 192–199, 2017.
- [51] U. Massing, S. G. Ingebrigtsen, N. Škalko-Basnet, and A. M. Holsæter, "Dual Centrifugation - A Novel 'In Vial' Liposome Processing Technique," in *Liposomes*, A. Catala, Ed. IntechOpen, 2017, pp. 3–28.
- [52] G. Winter, M. Brandl, S. Schulze, and W. Tian, "Vesicular phospholipid gels comprising proteinaceous substances," EP 2 601 934 A1, 2013.
- [53] G. Balsevich *et al.*, "Stress-responsive FKBP51 regulates AKT2-AS160 signaling and metabolic function," *Nat. Commun.*, vol. 8:1725, pp. 1–12, 2017.
- [54] M. Maiarù *et al.*, "The Stress Regulator Fkbp51: A Novel and Promising Druggable Target for the Treatment of Persistent Pain States Across Sexes," *Pain*, vol. 159, pp. 1224–1234, 2018.
- [55] M. L. Pöhlmann *et al.*, "Pharmacological Modulation of the Psychiatric Risk Factor FKBP51 Alters Efficiency of Common Antidepressant Drugs," *Front. Behav. Neurosci.*, vol. 12:262, pp. 1–8, 2018.
- [56] M. Toh and G. N. C. Chiu, "Liposomes as sterile preparations and limitations of sterilisation techniques in liposomal manufacturing," *Asian J. Pharm. Sci.*, vol. 8, no. 2, pp. 88–95, 2013.
- [57] C. Tardi, M. Drechsler, K. H. Bauer, and M. Brandl, "Steam sterilisation of vesicular phospholipid gels," *Int. J. Pharm.*, vol. 217, no. 1–2, pp. 161–172, 2001.
- [58] N. Qi *et al.*, "Sterilization stability of vesicular phospholipid gels loaded with cytarabine for brain implant," *Int. J. Pharm.*, vol. 427, pp. 234–241, 2012.
- [59] W. Tian, "The Development of Sustained Release Formulation for Pharmaceutical Proteins based on Vesicular Phospholipid Gels," Dissertation, Ludwig-Maximilians-

Universität München, 2010.

- [60] M.-P. Even, "Twin-Screw Extruded Lipid Implants for Vaccine Delivery.," Dissertation, Ludwig-Maximilians-Universität München, 2015.
- [61] X. Chen *et al.*, "Long-lasting Insulin Treatment Via a Single Subcutaneous Administration of Liposomes in Thermoreversible Pluronic® F127 Based Hydrogel," *Curr. Pharm. Des.*, vol. 23, no. 39, pp. 6079–6085, Feb. 2018.

Chapter II

OBJECTIVES AND OUTLINE OF THE THESIS

This thesis is based on years of successful research and development on vesicular phospholipid gels and aimed to further develop this drug delivery system, by designing more sophisticated administration and manufacturing techniques for VPGs and contributing to a better understanding of the mechanisms behind drug release from lipid-based depots.

Consequently, the present work was aimed to address the following objectives:

- i. In many studies VPGs were administered either after dilution of the highly viscous phospholipid dispersion or during surgery [1]–[4]. Administration with a conventional s.c. needle and syringe is only possible with excessive injection force due to the high concentration of phospholipids in the formulation and the resulting high viscosity.

As a first objective, a novel administration technique is established. In **Chapter 3**, needle-free injection is used to overcome administration difficulties for VPGs, which are caused by the high viscosity of the formulation arising from large phospholipid concentrations. The aim is to show the robustness of needle-free injection technology against changes in injection volume and phospholipid concentration of the formulation. Further different single-use syringes, which can be used with the Biojector 2000, are evaluated.

- ii. Further the established preparation processes, i.e. high pressure homogenization, dual asymmetric centrifugation and magnetic stirring, do have several limitations like difficulties in temperature control, high shearing forces, long production duration and batch mode production only with restrictions on up- and down-scaling [5], [6].

In **Chapter 4** twin-screw extrusion, a gentle, easily controllable and continuous method is investigated for its applicability as manufacturing technique for VPGs. Three differently sized extruders were evaluated and extrusion parameters like temperature, screw speed and the size of the nozzle are varied to investigate their influence on physical-chemical parameters of the VPGs. Long-term *in vitro* release studies with FITC-Dextran and a monoclonal antibody from the produced VPGs are conducted to investigate the effect of different preparation processes on release behavior and the stability of encapsulated proteins was tested. Moreover, storage stability of the VPGs is evaluated.

- iii. It is known that phospholipid concentration, the encapsulated protein or peptide and the type of phospholipids each contribute to the release behavior from VPGs [7]–[10]. However, the exact mechanisms behind the release of drugs from VPGs have not been investigated so far. It is assumed that protein-lipid-interactions may play an important role regarding the release kinetics.

Chapter 5 focuses on the effect of interactions between encapsulated proteins and peptides and the phospholipids on the release behavior from VPGs. Different analytical methods e.g. isothermal titration calorimetry (ITC) and microscale thermophoresis (MST) are tested for their applicability to investigate the interactions between liposomes and a peptide. The interactions between exenatide and different phospholipids are characterized to contribute to a better understanding of the release behavior of peptides and proteins from lipid-based depots, especially VPGs. The focus is set on the effect of differently charged phospholipids and the pH of the formulation on interactions.

- iv. In **Chapter 6** VPGs are used as novel drug delivery systems for two small molecular drugs, SAFit2 and #41, in different applications. A preparation process for the encapsulation of the two non-water-soluble drugs into VPGs is developed and the release behavior was characterized *in vitro* and *in vivo*. In pharmacological studies the effects of the two substances after release from VPGs on metabolic function, pain sensation and depression are investigated.

II.1 References

- [1] N. Kaiser *et al.*, "5-Fluorouracil in vesicular phospholipid gels for anticancer treatment: Entrapment and release properties," *Int. J. Pharm.*, vol. 256, no. 1–2, pp. 123–131, 2003.
- [2] S. Buchmann *et al.*, "Growth factor release by vesicular phospholipid gels: in-vitro results and application for rotator cuff repair in a rat model," *BMC Musculoskelet. Disord.*, vol. 16:82, no. 1, pp. 1–10, 2015.
- [3] R. Moog *et al.*, "Change in pharmacokinetic and pharmacodynamic behavior of gemcitabine in human tumor xenografts upon entrapment in vesicular phospholipid gels," *Cancer Chemother. Pharmacol.*, vol. 49, pp. 356–366, 2002.
- [4] F. G uthlein *et al.*, "Pharmacokinetics and antitumor activity of vincristine entrapped in vesicular phospholipid gels," *Anticancer. Drugs*, vol. 13, no. 8, pp. 797–805, 2002.
- [5] U. Massing, S. Cicko, and V. Ziroli, "Dual asymmetric centrifugation (DAC)-A new technique for liposome preparation," *J. Control. Release*, vol. 125, no. 1, pp. 16–24, 2008.
- [6] M. Brandl, M. Drechsler, D. Bachmann, and K. H. Bauer, "Morphology of semisolid aqueous phosphatidylcholine dispersions, a freeze fracture electron microscopy study," *Chem. Phys. Lipids*, vol. 87, pp. 65–72, 1997.
- [7] C. Tardi, M. Brandl, and R. Schubert, "Erosion and controlled release properties of semisolid vesicular phospholipid dispersions," *J. Control. Release*, vol. 55, no. 2–3, pp. 261–270, 1998.
- [8] W. Tian, S. Schulze, M. Brandl, and G. Winter, "Vesicular phospholipid gel-based depot formulations for pharmaceutical proteins: Development and in vitro evaluation," *J. Control. Release*, vol. 142, no. 3, pp. 319–325, 2010.
- [9] M.-P. Even, "Twin-Screw Extruded Lipid Implants for Vaccine Delivery.," Dissertation, Ludwig-Maximilians-Universit at M unchen, 2015.
- [10] C. Neuhofer, "Development of lipid based depot formulations using interferon-beta-1b as a model protein," Dissertation, Ludwig-Maximilians-Universit at M unchen, 2015.

Chapter III

NEEDLE-FREE INJECTION OF VESICULAR PHOSPHOLIPID GELS

Section III.1 of this chapter has been published in the Journal of Pharmaceutical Sciences as: M. Breitsamer, G. Winter; *Needle-free injection of vesicular phospholipid gels - a novel approach to overcome an administration hurdle for semisolid depot systems*; (2017).

To maintain the train of reading throughout the chapter, references of the published manuscript (section III.1) and all further studies (section III.2) are combined in section III.4 .

III.1 Needle-free injection of vesicular phospholipid gels – a novel approach to overcome an administration hurdle for semisolid depot systems

III.1.1 Abstract

Vesicular phospholipid gels (VPGs) are depot formulations for the sustained release of drugs which are characterized by a high amount of phospholipids in the formulation. They consist of physiological excipients only and therefore display high biocompatibility. Their manufacture is simple, cheap, solvent free and ideal for the processing of proteins and peptides because of the low stress on the molecule e.g. by elevated temperatures. One major hurdle of VPGs is their high viscosity which makes them hard to almost impossible to inject with conventional, thin needles used for subcutaneous administration. However, so far no data is published to overcome this administration challenge. In the present study, needle-free injection (NFI) was investigated and successfully applied as a technology for the easy and elegant administration of VPGs. VPGs with different phospholipid content were injected with a Biojector 2000 into gelatin blocks and full thickness pig skin post mortem as in vitro models and the injection depth was determined after injection. The release behavior was tested after shearing the VPG with the device to evaluate the effect of shearing on the drug release from the formulation. No differences were observed when compared to an ejection with needle and syringe.

III.1.2 Introduction

Vesicular phospholipid gels are semisolid dispersions of large amounts of phospholipids in an aqueous phase [1]. They have been used in the past as depot formulations for the sustained release of proteins, peptides and other small molecular weight drugs [2]–[4]. VPGs are prepared by high pressure homogenization (HPH) or dual asymmetric centrifugation (DAC) [1], [5]. The preparation of VPGs is easy to scale-up and free of organic solvent. Further, gentle manufacturing with low temperatures facilitates the processing of proteins and peptides in the formulations. Due to the fact that VPGs are

only composed of buffer, the drug itself and phospholipids which are the main component of cell-membranes, the system is tolerated well after injection. Furthermore, high encapsulation efficiencies can be achieved in comparison to liposomal formulations, since hydrophilic drugs are not only encapsulated in the vesicles but localized in-between the vesicular structures of the phospholipid matrix. All these advantages taken together, VPGs are perfectly suited as a depot formulation for the sustained release of pharmaceutical relevant substances.

Tian et al. showed that the sustained release of substances from VPGs correlates to the phospholipid amount of the formulation[4]. High phospholipid content results in slow release of the substance from the depot, which makes these formulations highly attractive but also causes difficulties in application due to the high viscosity of the formulation. Large needle sizes, which facilitate the subcutaneous injection, are not tolerated well by the patient as well as very slow injection rates. Reduction of the phospholipid content of the formulation decreases the viscosity, but it was shown before that this results in rapid release of the drug and therefore in a loss of the desired function of the depot [6]. By variation of the manufacturing process like it was described by Zhong et al., a lower viscosity and therefore injectability of the formulation could be achieved [7], [8]. However, the described preparation method produces rather highly concentrated dispersions of crude multi-lamellar liposomes than VPGs.

The injection force with needle and syringe is highly influenced by the viscosity of the formulation [9], [10].

Therefore, to overcome the administration challenge, needle-free injection (NFI) is a promising technique. NFI devices work by forcing a liquid with high velocity through a tiny nozzle which is pressed against the skin [11]. The Bernoulli equation is used for the description of the injection force with NFI [10]. In this equation the only formulation property influencing the injection force is the density of the formulation and therefore injection of formulations with a NFI device is largely independent of the viscosity. Several review articles summarize the methodology, different injectors and applications of NFI technology [11]–[13].

To our knowledge, the administration of semisolid depot systems like VPGs by using NFI technology has not been demonstrated before.

III.1.3 Materials and Methods

III.1.3.1 Materials

Egg lecithin (Lipoid E80) was a kind gift of Lipoid GmbH (Ludwigshafen, Germany). Methylene blue (MB), Sulforhodamine B (SRB), gelatin (Bloom 175, from porcine skin) and Trifluoroacetic acid (TFA) were purchased from Sigma-Aldrich (Steinheim, Germany). Chloroform was obtained from Merck (Darmstadt, Germany). High performance liquid chromatography (HPLC) grade acetonitrile was purchased from Fisher Scientific (Schwerte, Germany). For preparation of buffers highly purified water (HPW, Purelab Plus, USF Elga, Germany) was used.

Human erythropoietin (EPO) solution in phosphate buffer pH 7.2 was concentrated with Vivaspin[®] 20 Tubes (MWCO 5 kDa; Sartorius AG, Germany).

III.1.3.2 Preparation of VPGs

The preparation of VPGs was based on the preparation method first described by Massing et al. [5]. VPGs with a phospholipid amount between 25 and 55% (m/m) were prepared by dual asymmetric centrifugation (Speedmixer[™] DAC 150 FVZ, Hauschild GmbH & Co KG, Germany). In short, the accurately weighted phospholipids were mixed with either 20 mM PBS buffer pH 7.4, MB- or SRB-solution in 20 mM PBS buffer pH 7.4 or EPO solution in phosphate buffer pH 7.2. The formulations with EPO contained a total protein load of 10 mg/g. For homogenization of the mixtures with the Speedmixer[™] a process speed of 3500 rpm was utilized and centrifugation time was 45 minutes. The used DAC was equipped with a custom-made cooling system keeping the temperature below 28 °C to avoid potential heat stability problems of the protein.

III.1.3.3 Preparation of gelatin blocks

Gelatin blocks were prepared as soft models for in vitro evaluation of injectability of VPGs by NFI. They were composed of gelatin (6%), glycerin (16%) and HPW. Each block was cylindrical in shape, with a height and diameter of 45mm. Gelatin was used because of its transparency, controllable mechanical properties, controllable dimensions and easy and cheap preparation.

After preparation the bloom value of a random sample of gelatin blocks was determined using a Texture Analyzer (TA.XT plus, Stable Micro Systems, UK) and Young's moduli were calculated with (see equation (III-1)) [14].

$$E = \frac{\sigma(\varepsilon)}{\varepsilon} = \frac{F/A_0}{\Delta L/L_0} \quad (\text{III-1})$$

E: Young's modulus (modulus of elasticity)

ε : strain

$\sigma(\varepsilon)$: stress

F: force exerted on object under tension

A_0 : cross-sectional area of the probe by which the force is applied

ΔL : length change

L_0 : original length of the object

III.1.3.4 Injections into in vitro models

0.25 ml of the formulation was filled in single-use syringes suitable for the Biojector 2000 (Bioject™ No2 with Biojector 2000, Bioject Inc., USA). For better visualization of the injected depot, the used formulations were either dyed with MB or SRB.

The full thickness skin of a shortly before sacrificed 8 to 9 month old pig (provided by Veterinary Clinic for Swine, LMU Munich, Oberschleißheim, Germany) was used. During the experiment the skin was unharmed on the cadaver to retain the elasticity and consistency of the skin in real life. Injections into the pig skin were accomplished in the lower abdominal area of the pig. After injecting into the gelatin blocks or the pig skin, penetration depth was measured with a scale after cutting through the injection site.

III.1.3.5 In vitro release of EPO from VPGs after shearing

The model for the release of EPO from VPGs was based on the eppendorf cap model described by Even [15]. Release of EPO from VPGs was tested after ejection of 0.2 g VPG with the Biojector 2000 or with a conventional syringe and cannula (Sterican® Size 1 [Ø 0.90 mm x 40 mm], B. Braun Melsungen AG, Germany).

Briefly, 0.2 g VPG were filled into 2 ml eppendorf caps and 1 ml of 20 mM PBS buffer pH 7.4 was carefully added to the VPG on the bottom of the tube without causing turbidity of the sample. Release experiments were carried out in triplicates by complete buffer exchange in a Certomat Incubation Shaker (Sartorius AG, Göttingen, Germany) at 37 °C and 30 rpm.

For the extraction of EPO from the obtained liposomal released fraction chloroform (1:1) was added to the released fraction and the samples were centrifuged for 30 minutes at 15 °C with 5000 rpm before taking the clear supernatant for quantification of the samples with reverse phase high performance liquid chromatography (RP-HPLC) [4].

III.1.3.6 Quantification of EPO with RP-HPLC

For quantification of EPO a Dionex Ultimate 3000 (Thermo Fisher Scientific, USA) with a FLD3100 fluorescent detector (Excitation: 280 nm; Emission: 343 nm) and a Phenomenex Jupiter 5 μ C18 column (300 A, 250 x 4.6 mm) was used. Mobile phase A was composed of 10% acetonitrile, HPW and 0.1% TFA and mobile phase B was composed of acetonitrile with 0.1% TFA. A flow of 0.5 ml/min was used and elution was done with a linear ramp. Good linearity of the calibration curve was obtained between 0.5 μ g and 20 μ g EPO which was injected into the HPLC system. 50 μ l of the sample was injected for each run and the retention time of EPO was 22.3 minutes.

III.1.4 Results

III.1.4.1 Needle-free injection

Gelatin blocks

Baxter et al. reported that the Young's modulus of human skin is 0.3 MPa \pm 0.09 MPa, while Young's moduli for pig skin highly depend on the anatomical location of the skin and the age of the pig and ranges between 0.5 MPa and 1.0 MPa [14]. We prepared gelatin blocks as soft skin models for the in vitro needle-free injection of VPGs. All prepared gelatin blocks had a Young's modulus of 0.35 MPa \pm 0.02 MPa which is comparable to human skin.

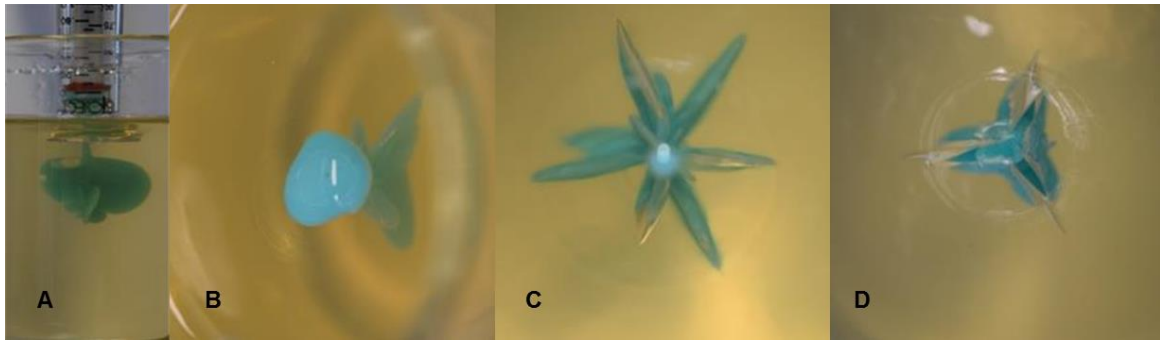


Figure III-1: (A) Visual appearance of the injected depot from the side (MB-VPG 35% (m/m)); (B), (C) and (D) injection site from above after the injection of formulations with (B) 25% (m/m), (C) 35% (m/m) and (D) 55% (m/m) phospholipid content.

All formulations up to a phospholipid concentration of 50% (m/m) were easily injectable with the Biojector 2000 into gelatin blocks. When VPGs with phospholipid contents of 25% (m/m) and 30% (m/m) were injected wet-shots occurred, meaning that residues of the VPG were visible on the surface of the gelatin after injection. The injection of VPGs with a phospholipid amount of 55% (m/m) caused the formation of large jet channels and ruptures in the gelatin blocks from the surface.

In conclusion, NFI of VPGs into gelatin block was successful for formulations with a phospholipid content in the range between 35 and 50% (m/m).

Pig skin post mortem

Since the gelatin blocks lack the characteristic skin structure with different skin layers, elasticity and consistency further injections into pig skin were done, using the cadaver of a recently killed pig.

VPGs with a phospholipid content from 25 to 45% (m/m) could be successfully injected into the pig skin. The formulations penetrated into the subcutaneous tissue and in rare cases into the muscle tissue below the skin and no residues of the VPG were observed on the surface of the skin after injection. A longish appearance of the injected depot, which was situated parallel to the skin surface, was observed after cutting out the injected VPG without harming the depot. This observation was especially apparent when VPGs with low phospholipid amount were injected and penetrated into the muscle layer.

VPG with a phospholipid content of 50% (m/m) was successfully injected into the dermis of the skin and only partially into the fat tissue. Intradermal administered VPG formed a palpable bleb at the injection site which was slightly raised and brightly colored.

Sometimes wet-shots occurred when these high phospholipid amounts were injected and residues of the formulation were observed on the nozzle or the skin after injection.



Figure III-2: NFI into pig skin post mortem. (1A) Injection site from above after injection of a formulation containing 40% (m/m) phospholipids. (1B) Cut through the injection site for the visualization of the penetration depth. (2A) Intradermal injection (SRB-VPG 50% (m/m)) without residues of the VPG on the surface. Pink color of the dyed VPG is visible through the upper skin layers. (2B) Cut through the injection site.

In conclusion, formulations with a phospholipid amount between 25 and 45% (m/m) were injectable into pig skin using the Biojector 2000. VPGs with a phospholipid content of 50% (m/m) were injectable but results were not reliable due to the variable injection depth into different skin layers and the occasional incidence of wet-shots.

Penetration depth

Injection depth was measured with a scale after cutting through the injection site. For each phospholipid concentration at least two measurements were done and the mean was calculated.

The VPGs penetrate about 2.5 fold deeper into the gelatin blocks in comparison to the penetration depth into pig skin after NFI. This is due to the different layers of the skin which display different texture and resistance to the jet stream of VPG into the tissue. In

both models the injection depth decreases with increasing phospholipid content which is due to the decrease of fluidity of the samples with increasing phospholipid amount.

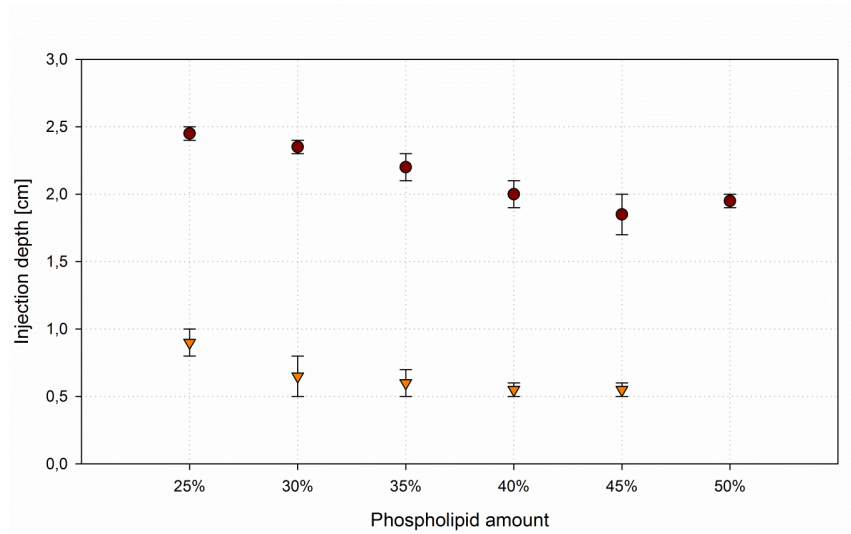


Figure III-3: Injection depth of VPG formulations into (●) gelatin blocks and (▼) pig skin post mortem with increasing phospholipid amount. Data is plotted as mean \pm SD (n=2 or 3).

III.1.4.2 In vitro release after shearing

We successfully injected VPG formulations into gelatin blocks and into pig skin. Still, the question if this administration technique with its high shearing forces does influence the release behavior of VPGs e.g. by destruction of the gel inner structure, has to be answered. Therefore, we tested the release of EPO from VPG with a phospholipid content of 45% (m/m) and a final EPO concentration of 10 mg/g. Before release testing the VPG was either ejected with a conventional needle and syringe or the Biojector 2000 was used. When ejecting with needle and syringe cannulas with large diameter of 0.90mm were chosen to facilitate the ejection of the formulation, since ejection with a conventional subcutaneous needle with a diameter between 0.45 and 0.30mm was not possible.

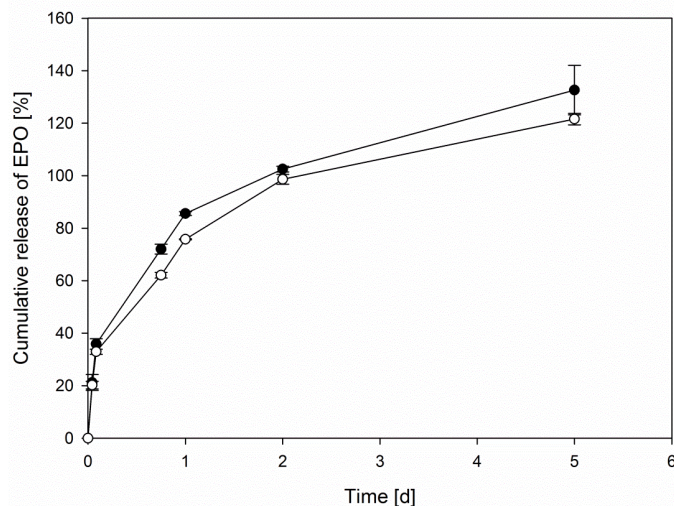


Figure III-4: Cumulative release of EPO from VPG with a phospholipid content of 45% (m/m). EPO-VPG was either filled into the eppendorf tubes with a conventional needle and syringe \bullet or ejected with the Biojector 2000 \circ previous to release testing. Data is plotted as mean \pm SD (n=3).

Sustained release of EPO was observed over five testing days. The curves of the formulations ejected with needle and syringe and with the Biojector 2000 are similar in shape and total amount of released drug.

III.1.5 Discussion

The present study shows that NFI technology is a promising method to overcome the s.c. administration hurdle for VPGs. All formulations up to phospholipid content of 55% (m/m) were easily injectable with the Biojector 2000 into gelatin blocks. The wet-shots occurring at lower phospholipid contents are due to the limited inner elasticity of the gelatin blocks and the relatively low viscosity of the formulations. These factors lead to the back flow of the fluid through the injection channel.

VPGs with phospholipid content up to 45% (m/m) were injectable into pig skin and penetrated into the subcutaneous tissue. Previous publications describe a spherical or cylindrical shape of the injected liquid after administration with a needle-free injector [13], [16]. The shape of the obtained depot in our study highly depended on the phospholipid content and penetration depth of the sample. For VPGs with lower phospholipid content ($\leq 45\%$ (m/m)) the propulsion of the semisolid material is not sufficient to infiltrate deeper layers and therefore stagnation pressure leads to the distribution of the gel in the subcutaneous tissue and rarely the upper muscle layers into two directions following the muscle macro-structure. A longish shape of the depot which

is parallel to the skin surface is the result. A spherical shape in the intradermal and subcutaneous layers occurs when higher phospholipid contents (50% (m/m)) are injected. However, in our NFI study with pig skin the chosen injection site as well as elasticity and consistency of the skin does have great influence on the outcome. Baxter et al. already found that the texture of pig skin is highly dependent on the anatomical location of the skin [14]. They described that abdominal porcine skin is highly similar to human skin. We found that NFI is best feasible when injecting into the lower abdomen of the pig, while injections into the hind leg or breast skin often resulted in wet-shots. Further, when VPGs with a low phospholipid content of 25% (m/m) were injected, in some cases we observed intra muscular injections due to the high propulsion of the material with relatively low viscosity. Since these i.m. injections were not the intention of this study, we propose that for the administration of these formulations with low viscosity an adjustment of the jet force of the injector is needed. Further, we conclude that VPGs with 30 to 45% (m/m) ideally combine best suitability for NFI with a Biojector 2000 and superior applicability as depot systems because of their slow release rates.

Another important factor is the quality of the VPG after shearing with the Biojector 2000. It has been reported, that VPGs release their contents by diffusion and matrix erosion [4], [6], [17]. In our study we could show that shearing of the gel with the Biojector 2000 does not influence the release behavior of EPO.

III.1.6 Conclusion

NFI is not only beneficial for the administration of semisolid systems but additionally prevents needle stick injuries, reduces the risk of infections and overcomes patient aversion towards needles [12]. We succeeded in NFI of VPGs with different phospholipid content and therefore could show that it is possible to administer this promising depot system via a very simple and elegant method. The in vitro release behavior of EPO was not affected by shearing of the VPG with the Biojector 2000.

In conclusion the injection of VPGs with a Biojector 2000 is feasible and this excellent depot system is now ready for future applications in clinical trials.

III.1.7 Supporting information

This article contains supplementary material.

Supplement 1 – Equations for calculation of injection forces

Rearranged Bernoulli equation for the calculation of the injection force for NFI-devices.

$$F = 2 \rho A \left(\frac{4 Q}{C_f \pi D^2} \right)^2 \quad \text{(III-2)}$$

F = syringe plunger force

Q = volumetric flow rate

ρ = fluid density

C_f = orifice flow coefficient (0.95 for a practical, round edged orifice)

D = orifice diameter

A = cross-sectional area of syringe plunger

Hagen-Poiseuille equation for the calculation of injection force with needle and syringe of Newtonian fluids.

$$F = \frac{8 Q \mu L A}{\pi D^4} \quad \text{(III-3)}$$

F = syringe plunger force

Q = volumetric flow rate

μ = dynamic viscosity

L = needle length

D = needle inner diameter

A = cross-sectional area of syringe plunger

Supplement 2 – Physical properties of VPGs

Table III-1: Summary of the physical properties of VPGs. Viscosity was determined with a rotational rheometer (PP25 with Physica MCR 100, Anton Paar, Ostfildern, Germany) with a plate/plate geometry. Gel strength and injection forces were determined with a Texture Analyzer (TA.XT plus, Stable Micro Systems, UK) in compression mode.

Phospholipid amount [%]	Viscosity [Pa*s]	Gel strength [g]	Injection force [N]			
			0.1 ml/sec; RT; 27G	17.5 µl/sec; RT; 27G	0.1 ml/sec; 45°C; 27G	0.1 ml/sec; RT; 23G
25	0.13 ± 0.02	0.23 ± 0.05	10.81 ± 0.21	3.22 ± 0.23	7.28 ± 0.14	3.03 ± 0.09
30	0.28 ± 0.02	0.17 ± 0.09	21.92 ± 1.70	5.85 ± 0.07	14.32 ± 0.07	4.30 ± 0.09
35	0.81 ± 0.11	0.23 ± 0.05	40.44 ± 1.86	11.02 ± 0.14	32.24 ± 0.41	8.09 ± 0.15
40	2.28 ± 1.01	0.57 ± 0.05	47.12 ± 3.54	21.91 ± 1.59	> 50	19.40 ± 0.52
45	8.41 ± 0.45	3.03 ± 0.09	> 50	38.83 ± 4.68	> 50	34.00 ± 0.27
50	41.74 ± 7.15	22.53 ± 0.25	> 50	48.56 ± 2.42	>50	> 50
55	84.70 ± 11.95	31.57 ± 0.65	> 50	> 50	> 50	> 50

III.2 Further studies

Additionally to the above described study, which was finally published in January 2017 in Journal of Pharmaceutical Sciences, deepening research on the topic was conducted, which is described in the following. To maintain the train of reading, references of both sections are summarized at the end of the chapter.

III.2.1 Material and Methods

For detailed information on the used materials see III.1.3.1 .

VPGs were prepared as described in III.1.3.2 .

III.2.1.1 Viscosity measurement

Viscosity of the prepared formulations was determined using a rotational rheometer with a plate-plate geometry (MCR 100 with PP25, Anton Paar, Ostfildern, Germany). The shearing rate was set to 10 – 100 s⁻¹ and approximately 0.2 g VPG was used for one measurement. For comparison the viscosity at a shearing rate of 32.9 s⁻¹ was used.

III.2.1.2 Determination of the density

To determine the density of the VPGs a glass pycnometer (volume: 1 ml) was used. For each measurement VPG was filled into the pycnometer and the mass of the VPG was determined by weighing. Density was calculated ($\rho = m/V$) from the determined mass (m) and volume (V).

III.2.1.3 Texture analysis

Gel strength of the VPGs was measured using a Texture Analyzer (TA.XT Plus, Stable Micro Systems, UK). For each measurement about 1 g of VPG was carefully filled in a 2 ml centrifugation tube. A micro probe with a diameter of 4 mm was pushed into the gel with a speed of 0.5 mm/sec to a final penetration depth of 5 mm. The gel strength was determined as the maximum force needed.

III.2.1.4 Determination of injection force with needle and syringe

Injection forces into air and into the skin of a piglet were measured using the Texture Analyzer. 0.5 ml VPGs with different phospholipid concentration (between 25% (m/m) and 55% (m/m)) were filled into BD 1 ml syringes with Luer-Lok TM Tip (BD Franklin Lakes,

New Jersey, USA). Sterican[®] Size 20 cannulas with a diameter of 0.4 mm and a length of 20 mm (27G x 3/4 ") (B. Braun, Melsungen, Germany) which are often used for the subcutaneous injection of liquids were used for measurement of injectability of VPGs into air.

All injections into pig skin were done following the protocol of the National Institutes of Health (NIH Clinical Center Patient Education Materials). In short, the skin was pinched up with two fingers and the needle was injected into the skin in a 90-degree angle. Injection force measurements into pig skin were performed at different conditions:

- Variation of the injection rate: 0.1 ml/sec and 17.5 μ l/sec
- Variation of the formulation temperature: room temperature (ca. 20 °C) and 45 °C
- Variation of needle diameter:
 - Sterican[®] Size 20 cannulas; 27G; diameter 0.4 mm
 - Sterican[®] Size 16 cannulas; 23G; diameter 0.6 mm

The average force of at least two measurements was calculated. The experimental setup for the measurement of the injection force is shown in Figure III-5.

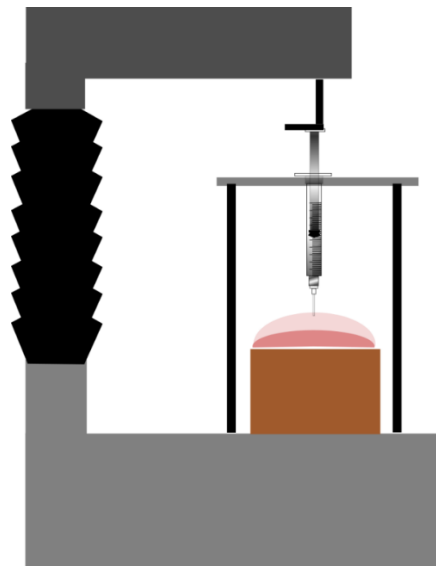


Figure III-5: Schematic drawing of the Texture Analyzer for measurement of injection force.

III.2.1.5 Needle-free injection of VPGs with Biojector 2000

A detailed description of needle-free injection of VPGs using a Biojector 2000 is given in section III.1.3.4 .

Two different single use syringes were used for further evaluation of the needle-free injection process: No2 (32G; 0.004 inches; Bioject Inc., USA) and No3 (30G, 0.006 inches; Bioject Inc., USA).

III.2.1.6 Jet force upon ejection with Biojector 2000

The impact force after ejection of a VPG-stream by the Biojector 2000 on a piezo-sensor (Kistler 9215) was measured. The generated tension is increased by a charge amplifier (Kistler 5011) and visualized with an oscilloscope (FLUKE 123 Scopemeter). Since it was not possible to collect digital data, photos of the displayed graphs were taken and the data was digitalized using a commercially available plot to data digitalizer (WebPlotDigitizer). During the ejection of the jet, the Biojector was set in a custom made coupler and fixed with a stand to minimize vibrations of the injector itself and to guarantee an exact position of the injector above the sensor. The gap width between the orifice and the force plate was 2.5 mm. The experimental setup of the jet force measurements is shown in Figure III-6. The sensor is calibrated so the force can be directly taken from the oscilloscope (1 V = 1 N). The influence of phospholipid concentration (25%, 30%, 35%, 40%, 45% and 50% (m/m)), composition of the lipid phase (S100, POPC, POPC/POPG, E80+MCT (35% + 5% (m/m)), E80+MCT (40% + 5% (m/m))), injection volume (0.25 ml, 0.5 ml, 1.0 ml) and the temperature (25 °C, 30 °C, 35 °C, 40 °C, 45 °C) of the formulation on the jet force was investigated with the two single use syringes also used for post mortem injections (No2 and No3). For all measurements with increased temperature during injection, samples were pre-warmed for at least 30 minutes at the respective temperature and ejection onto the pressure sensor was done directly after taking the sample out from the incubator. Triplicate measurements were conducted for each sample.



Figure III-6: Experimental setup of the jet force measurement.

All pressure calculations were based on the inner area of the nozzle of the syringe. Pressures were calculated with the following equation:

$$P = \frac{F}{A} \quad (\text{III-4})$$

with F as the measured force (initial peak force or drop-off force), A as the area calculated from the inner diameter of the nozzle and P as the pressure of the ejected jet-stream.

III.2.2 Results and Discussion

III.2.2.1 Viscosity and gel strength of VPGs

As it has already been shown before, the viscosity and gel strength of the formulations increase with increasing concentration of phospholipids in the formulation [4]. Viscosity of VPGs composed of different contents of Lipoid E80 and 20 mM PBS pH 7.4 was compared at a shearing rate of 32.9 s^{-1} . VPG-formulations with a phospholipid content of 25% (m/m) display a viscosity of only $0.13 \text{ Pa}\cdot\text{s} \pm 0.02 \text{ Pa}\cdot\text{s}$, while VPGs with a phospholipid content of 55% (m/m) display a huge viscosity of up to $90 \text{ Pa}\cdot\text{s}$.

The viscosity and gel strength of VPGs with an increasing concentration of Lipoid E80 are shown in Figure III-7.

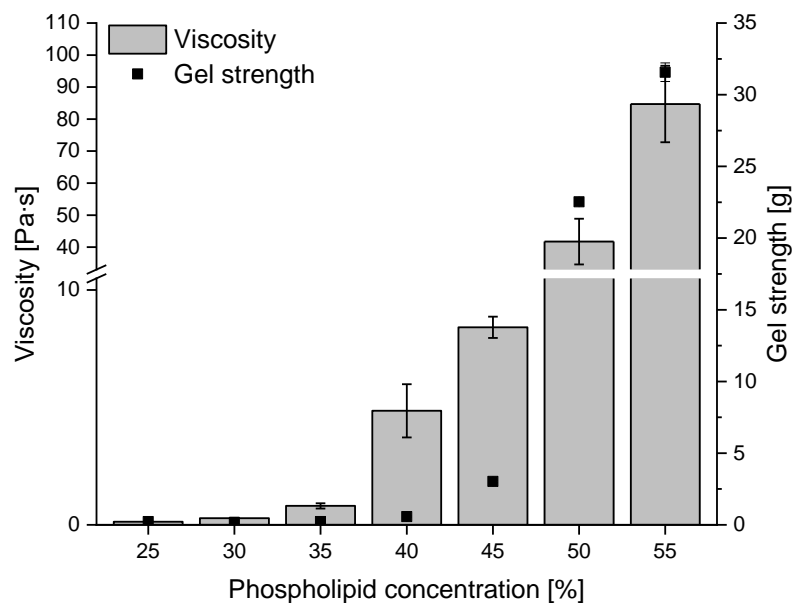


Figure III-7: Viscosity (at shearing rate 32.9 s^{-1}) and gel strength of VPGs with increasing phospholipid concentration in % (m/m). VPGs were composed of Lipoid E80 and 20 mM PBS pH 7.4. (n=3, Mean \pm SD)

III.2.2.2 Injection force with conventional needles

Injection force during an injection with needle and syringe can be split in three phases. First the resistance of the plunger has to be overcome, before kinetic energy is passed on to the liquid and the liquid is finally forced through the needle [18]. Additional force is needed to overcome the tissue resistance at the needle tip when injecting into subcutaneous tissue [19]. The addition of all these processes results in the total injection force, used here to characterize syringeability and injectability.

All formulations (25, 30, 35, 40, 45, 50 and 55% (m/m)) were injected subcutaneously into pig skin with an injection rate of 0.1 ml/sec commonly used for testing, which is appropriate for the end-user [9], [20]. However, not all formulations could be injected with this injection rate due to the exceptional high forces needed. Subsequently all formulations were tested with a rather slow injection speed of $17.5 \mu\text{l}/\text{sec}$. The moderation of the injection force by using slower injection rates is a common technique to facilitate for example the injection of highly viscous formulations or injection of liquids by handicapped patients e.g. rheumatoid arthritis patients [20]. In general, as expected the injection force needed increases significantly with increasing phospholipid concentration. The complete range of VPG-formulations could be injected into pig skin at a very slow injection rate of $17.5 \mu\text{l}/\text{sec}$. At the higher injection rate of 0.1 ml/sec injection

was only possible up to a maximum phospholipid concentration of 40% (m/m) in the formulation. There are no generally accepted limits for injection force and injection time [21]. Still, several authors give clues on the feasibility of an injection by the patient. Rungseevijitprapa et al. stated that liquids can be injected easily up to an injection force of 25 N [22]. Sheikhzadeh et al. found that patients with rheumatoid arthritis are able to apply average injection forces of 22.5 N with conventional syringes and maximum forces of up to 33 N were measured [20].

However, not only the injection speed is contributing to the injection force. Many parameters, including device components (e.g. syringe size, needle diameter and length) and drug formulation properties (e.g. dynamic viscosity), have great influence on the injection force [19], [21]. This relationship is described by the Hagen-Poiseuille-Equation:

$$F = \frac{8 \cdot Q \cdot \mu \cdot L \cdot A}{\pi \cdot D^4} \quad \text{(III-5)}$$

Additionally to these physical parameters, human factors (e.g. strength, flexibility and coordination) contribute to the injectability of liquids. The syringe plunger force needed for injection (F) directly correlates to the volumetric flow rate (Q), the dynamic viscosity (μ), the length of the needle (L) and the cross-sectional area of the syringe plunger (A). An indirect correlation exists to the inner diameter of the needle (D).

There are several parameters according to this equation which can be adapted in certain limits to achieve better syringeability and injectability. Next to injection with lower injection speed, another method to facilitate the injection of highly viscous formulations is the injection at higher temperatures (with certain limitations regarding the drug compound). Dynamic viscosity of formulations greatly depends on the temperature of the formulation. This aspect was investigated for VPGs by pre-warming of the formulations to the desired temperature of 45 °C for at least 45 minutes and direct testing of the injection force thereafter. Further, the inner diameter of the needle can be increased to a certain limit by using thicker needles or thin wall needle to reach lower injection forces. However, this is often associated with higher sensation of pain

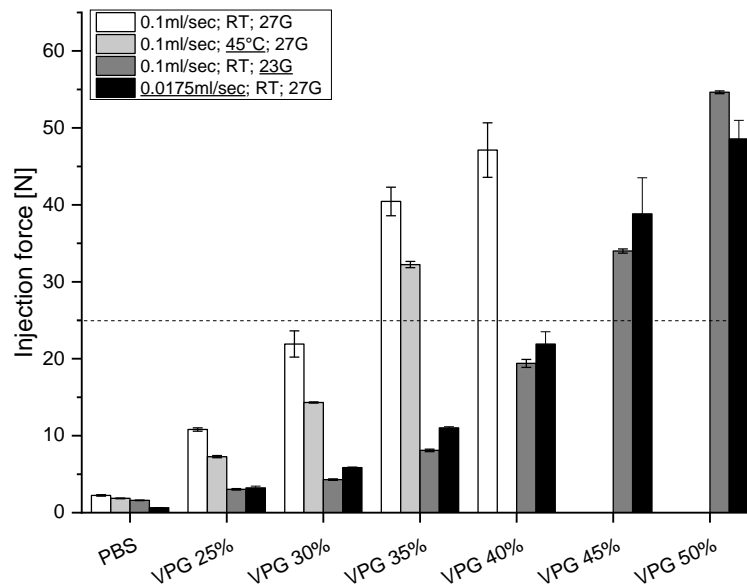


Figure III-8: Injection force of VPGs with different phospholipid concentration during injection with needle and syringe - comparison of different injection conditions. Dashed line shows injection force of 25 N.

As shown in Figure III-8 the injection force at 45 °C is slightly lower in comparison to the injection force at room temperature. However, a higher injection temperature did not lead to satisfying results regarding the needed force for injection since VPG formulations with a phospholipid concentration above 30 to 35% (m/m) still were not easily injectable. Further, a second needle with larger inner diameter was tested. As it was also observed for the very slow injection rate of 17.5 $\mu\text{l}/\text{sec}$, the injection force could be lowered significantly by using larger needles. In conclusion, it is in theory possible to inject VPG formulations with high phospholipid concentration by lowering the injection speed to very slow rates or using large needles. Still, the injection forces needed for VPGs with a high phospholipid concentration exceed the force which can be managed by humans at far and less patient compliance is to be expected for both techniques due to the long and painful administration duration.

III.2.2.3 Further post mortem studies on needle-free injection of VPGs

III.2.2.3.1 Comparison of different single use syringes in post mortem studies

To complement our already published data on needle-free injection of VPGs using No2 single use syringes, injections into pig skin post mortem were performed with a second

single use syringe, No3 [23]. No3 syringes do have a larger inner diameter of the orifice in comparison to No2 syringes. According to the manufacturer information, both, No2 and No3, syringes can be used for subcutaneous injections of liquids into skin [24].

VPGs with a phospholipid concentration from 30 to 50% (m/m) were easily injectable into pig skin with a volume of 0.25 ml per injection using a No3 syringe.

Formulations mainly penetrated into the subcutaneous tissue without leaving residues on the surface of the skin. Sometimes partial intradermal injection (see Figure III-9A), which could be identified by a bright, easily visible color of the SRB-VPG (Sulforhodamine B-VPG) below the skin directly at the injection site, occurred. In other cases, the VPG penetrated into muscle tissue of the skin, which is shown in Figure III-9D for a 50% (m/m) VPG. The occurrence of intramuscular injections, which was rare in general, was more likely when No3 syringes were used in comparison to No2 syringes, leading to the conclusion that the propulsion of an ejected stream from a No3 syringes is higher in comparison to No2 syringes. This was to be expected, since depth of penetration tests for liquids showed deeper injections and a higher probability for i.m. injections for the No3 syringes [24].

As described before also for liquid injections, the shape of the injected VPG was spherical or longish [13], [16].

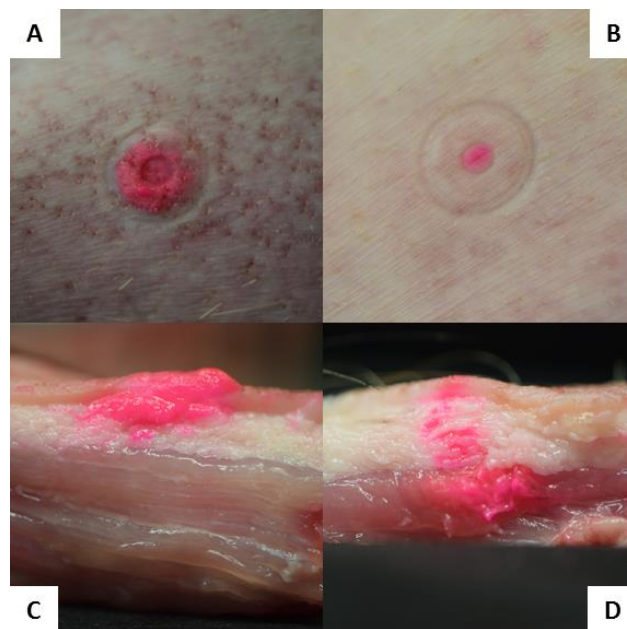


Figure III-9: NFI into pig skin post mortem. Injection site from above after injection of SRB-VPGs containing 40% (m/m) (A) or 50% (m/m) (B) phospholipids using a No3 single use syringe for injection. Lower row shows cuts through the injection site: 40% (m/m) SRB-VPG (C) and 50% (m/m) SRB-VPG (D).

III.2.2.3.2 Injection depth

In a next step the injection depth of VPG-formulations was determined after cutting through the injection site

Injection depth into pig skin after NFI was between 0.4 and 1.2 cm (Figure III-10). This difference is caused by the different layers of the skin, which display different texture and resistance to the jet stream of VPG into the tissue. Further, the muscle tissue below the subcutaneous tissue acts like a barrier due to the completely different structure and prohibits that the jet stream of VPG penetrates deeper. Since the subcutaneous tissue of the pigs had a thickness of about 1.0 cm, the shots from No3 syringes sometimes resulted in partial intramuscular injections as also observed in trans-sectional cuts through the injection site.

For both single-use syringes the injection depth decreases slightly with increasing phospholipid concentration, which is due to the decrease of fluidity of the samples with increasing phospholipid concentration. The velocity of the jet stream decreases during its path through the outer skin and different skin layers until finally the jet stream is stopped in the subcutaneous tissue. This process is faster for VPGs with high viscosity in comparison to VPGs with low viscosity, resulting in low injection depth.

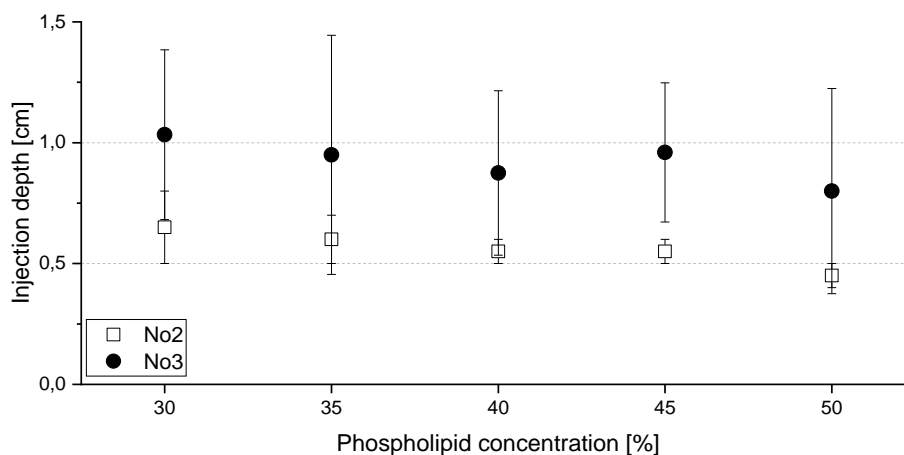


Figure III-10: Injection depth of VPG formulations composed of E80 as phospholipid and 20mM PBS pH 7.4 as aqueous phase. VPGs with phospholipid concentrations between 30 and 50% (m/m) were injected into pig skin post mortem with No2 (white squares) and No3 (black dots) single use syringes.

Additionally, the variability between the injection depths in a triplicate was higher for the No3 syringes in comparison to No2 syringes, since standard deviations are significantly higher for No3 syringes. This is a result of the i.m. injections which occurred sometimes for these syringes, resulting in higher values for the injection depth, while sometimes the

same formulations stayed in the subcutaneous tissue resulting in lower values for the injection depth.

Further, it is notable that the amount of phospholipid in the formulation only has a minor impact or none at all on the injection depth.

III.2.2.3.3 Injections with large injection volume

In all previous studies, a VPG volume of 0.25 ml was used to show injectability with NFI of the highly viscous system. Although these small volumes are perfectly suited for the application in a study with small animals and drugs which can be encapsulated in VPGs with a high drug load, higher administration volumes might be necessary for treatment of humans or larger animals and drugs which cannot be encapsulated in highly concentrated formulations. To this end, we tested the administration of 0.5 ml and 1.0 ml VPG by needle-free injection using No2 and No3 syringes. The Biojector 2000 has the ability to deliver a maximum volume of 1.0 ml solution and volumes between 0.5 ml and 1.0 ml are commonly used in its application [25].

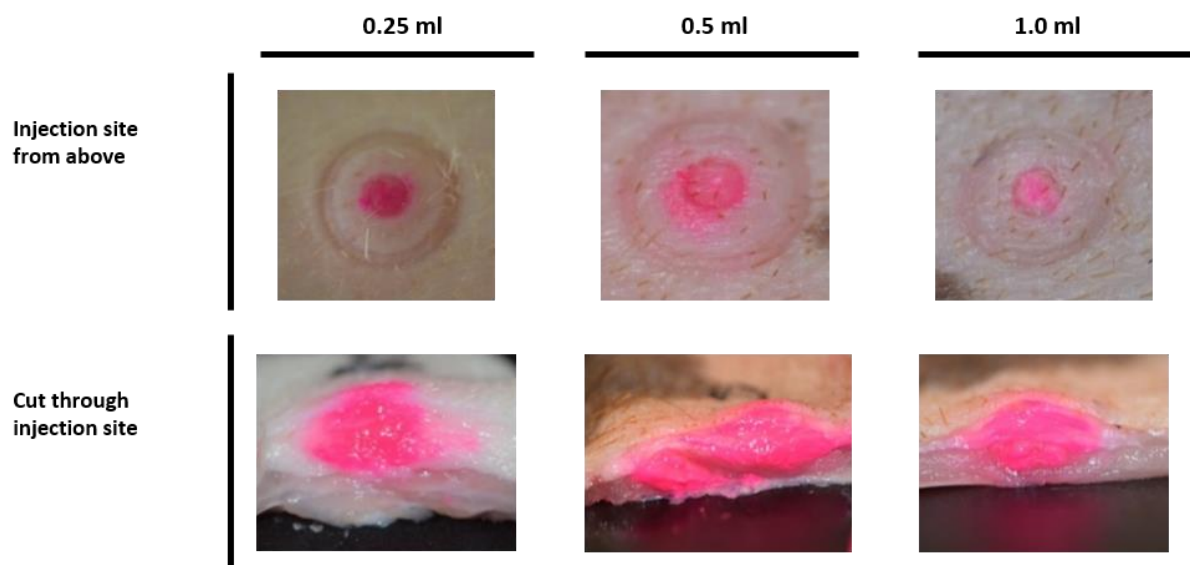


Figure III-11: Needle-free injection of 0.25 ml, 0.5 ml and 1.0 ml (from left to right) of VPGs (composed of 45% (m/m) Lipoid E80 and Sulforhodamin B solution in 20 mM PBS pH 7.4) using the Biojector 2000 device with No2 syringes. Top row shows injection site from above directly after administration. Bottom row shows trans-sectional cuts through the injection site.

Using No2 syringes, all formulations with a phospholipid concentration between 25 and 45% (m/m) were injectable with larger volumes up to 1.0 ml. When VPGs with 45% (m/m) phospholipid were used, sometimes wet shots occurred with a volume of 1.0 ml and tiny

residues of the formulation on the skin surface or on the orifice were observed, leading to the conclusion that 45% (m/m) phospholipid concentration is the limit of injectability for this syringe type. With No3 syringes only injections with 45% (m/m) and 50% (m/m) were tested with larger volumes, since it is to expect that lower phospholipid concentration results in superior injectability in comparison. 45% (m/m) and 50% (m/m) VPGs were easily injectable up to a volume of 1.0 ml using the No3 syringes. When 1.0 ml of the 50% (m/m) formulation was injected, tiny residues of the formulation on the skin surface were observed sometimes. These wet shots occurred more often when large volumes were injected. Again, it is assumed, that the limit of injectability is reached with 50% (m/m) phospholipid concentration and 1.0 ml injection volume.

III.2.2.4 Jet force upon ejection with Biojector 2000

Jet force measurements were performed using an experimental setup comparable to the one described by Shergold et al. [26]. The injector was placed above a piezoelectric sensor to measure the force of an ejected jet stream. Different parameters like phospholipid concentration, VPG temperature, ejected volume and the VPG composition was varied to test the robustness of the injector against changes.

According to Chase et al., there are three stages of injection with a needle-free device [27]. During peak pressure phase, the optimal pressure to penetrate the skin is reached, followed by delivery phase, during which the formulation is delivered to the injection site and pressure decreases slowly. Finally, during drop-off phase at the end of the injection the pressure drops instantaneously down to almost zero after the formulation is completely delivered. A similar profile with all three phases was observed for the ejection of VPG using the Biojector 2000 (see Figure III-12). After a sharp increase of the force on the sensor at the beginning of the injection, force slowly decreases during the ejection of the VPG and drops down to a minimum when the formulation is completely ejected. It is well known, that a drop-off pressure below 1200 psi (~ 8 MPa) can lead to a leak-back of the injectant through the injection channel after injection [28].

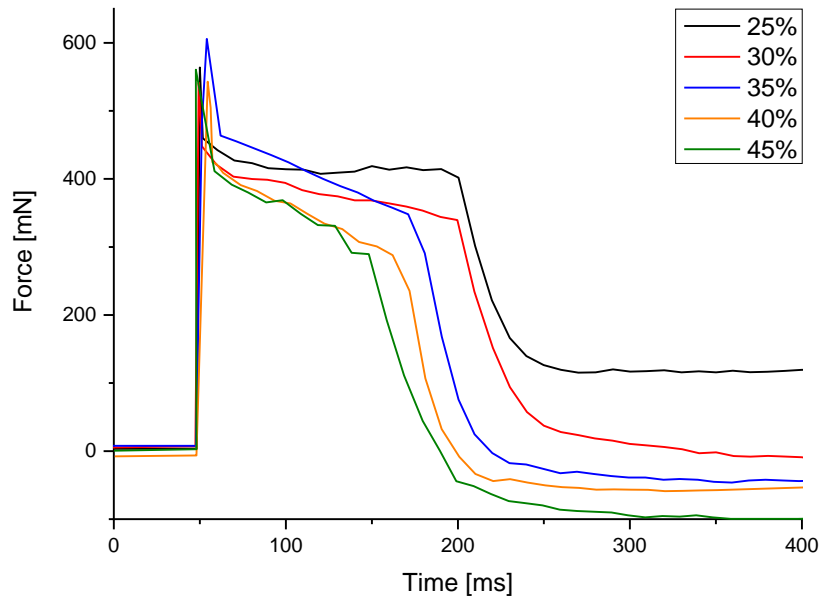


Figure III-12: Exemplary force profiles of VPGs after ejection of 0.25 ml with a Biojector 2000 and No2 syringe. Phospholipid concentration was increased from 25% (m/m) to 45% (m/m).

The two previously used single use syringes were used to investigate the influence of the orifice diameter on the injection force. Differences caused by the ratio of calculated jet area and measured orifice area, like it was described by Shergold et al., were not taken into account by a correction factor [26].

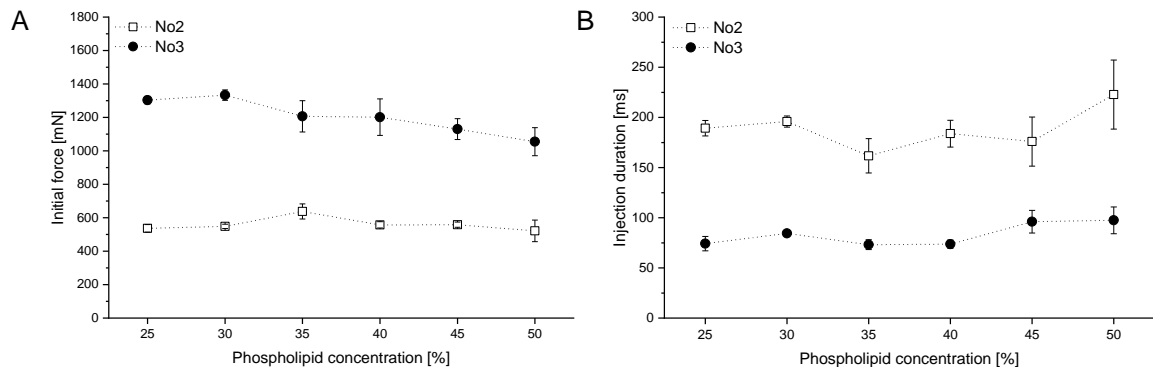


Figure III-13: Initial force (A) and injection duration (B) of the ejection of VPGs with increasing phospholipid concentration with different single-use syringes (No2 and No3). VPGs were composed of Lipoid E80 (25 -50% (m/m)) and 20mM PBS pH 7.4. Graphs show mean ($n=3$) \pm SD.

The two different orifice sizes resulted in differences in the measured force and ejection duration. The initial force of the jet stream ejected from the Biojector 2000 was higher when No3 syringes were used, independently of the phospholipid concentration in the VPG (see Figure III-13A). However, when the jet stream pressure was calculated from the

measured force using equation (III-4), both single-use syringes resulted in similar initial pressure values due to the differences in the orifice area (see Figure III-15A). Ejection was faster when using the No3 syringes with a larger inner diameter of the orifice (see Figure III-13B), since the amount of VPG passing the orifice per time is larger leading to a faster emptying of the syringe.

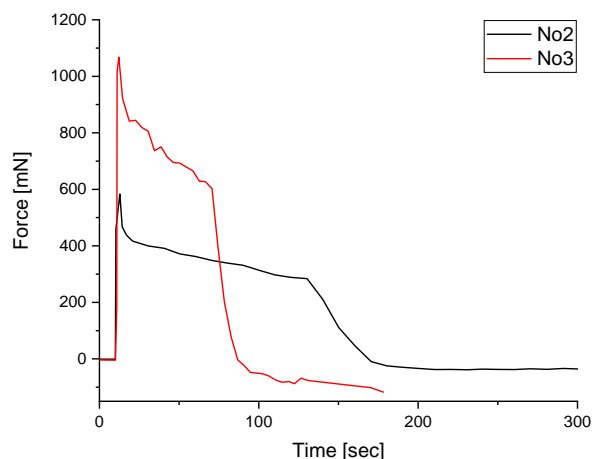


Figure III-14: Exemplary force profiles of the ejection of 0.25 ml of 40% (m/m) VPGs composed of Lipoid E80 and 20mM PBS pH 7.4 with No2 (black curve) and No3 (red curve) syringe.

The faster decrease of maintenance pressure during delivery phase is an additional result of the larger orifice. Injections with No2 syringe showed a mean injection duration of $188.23 \text{ ms} \pm 20.62 \text{ ms}$ ($n=3$) for VPG containing 40% (m/m) phospholipids, while injections of the same formulation with No3 syringes were significantly faster ($83.14 \text{ ms} \pm 11.36 \text{ ms}$; $n=3$). Two exemplary force profiles of these injections are shown in Figure III-14.

III.2.2.4.1 Influence of the phospholipid concentration

The viscosity of the VPG increases rapidly with increasing concentration of phospholipid in the formulation. This increase is especially pronounced for high phospholipid concentrations from 40% (m/m) and above (see Figure III-15B red bars). Since the injection with needle and syringe is strongly influenced by the viscosity of the formulation, leading to unacceptable high injection forces, it was to be expected that needle-free injection may have limitations regarding formulation viscosity.

With increasing phospholipid concentration, initial pressure and drop-off pressure decrease slightly for injections with a volume of 0.25 ml (see Figure III-15A and Figure III-15B). Still, all values were above 30 MPa. Injection duration was similar for all

phospholipid concentrations but depended on the syringe type which was used (see Figure III-13B).

During delivery phase, maintenance force decreased faster when VPGs with a higher phospholipid concentration were ejected (see Figure III-12).

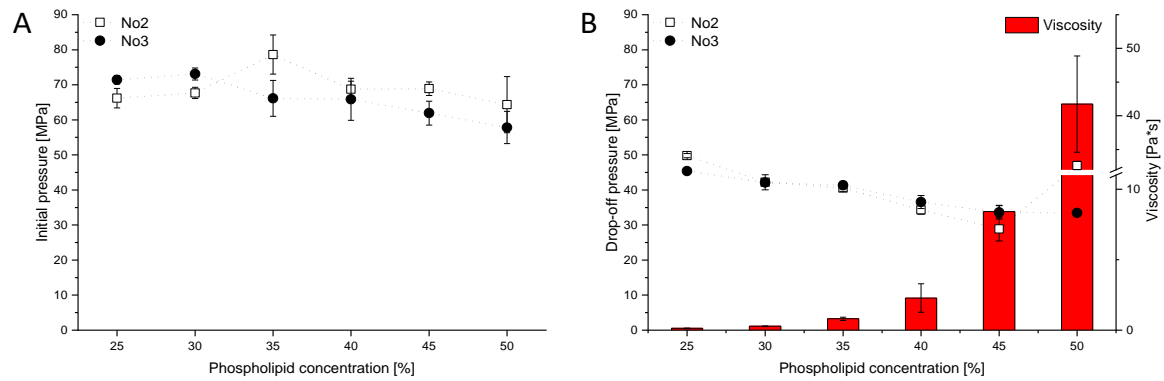


Figure III-15: Initial pressure (A) and drop-off pressure (B) of the jet stream of VPGs with increasing phospholipid concentration. Red bars in (B) show viscosity of the formulation. Viscosity was compared at a shearing rate of 32.9 s^{-1} . VPGs were composed of Lipoid E80 (25 - 50% (m/m)) and 20mM PBS pH 7.4. Graphs show mean ($n=3$) \pm SD.

Following the Bernoulli equation, injection with a needle-free injector is largely independent of the viscosity [10]. It has to be pointed out that the application of the Bernoulli equation is limited to cases of steady, laminar flow, which is to a good approximation true for single-use syringes which are used for needle-free injection devices.

$$F = 2 \cdot \rho \cdot A \left(\frac{4 \cdot Q}{c_f \cdot \pi \cdot D^2} \right)^2 \quad (\text{III-6})$$

with F as the plunger force, Q as volumetric flow rate, ρ as fluid density, c_f as orifice fluid coefficient, D as orifice diameter and A as syringe plunger area.

To this end, viscosity of the formulation should not be a limiting factor in needle-free injection technology. The pressure measurements support this assumption. Differences in initial pressure and drop-off pressure are small, while viscosity increases massively with increasing phospholipid concentration. An explanation for this observation might render from changes in density of the formulation. In liquid formulations a density similar to the one of water (around 1 g/cm^3) is to be expected. However, the density of VPGs is higher (i.e. phospholipid concentration of 30% (m/m): $1.1023 \pm 0.0005 \text{ g/cm}^3$ ($n=3$)) in comparison to water due to the high phospholipid concentration. This results in higher

force needed for administration of VPGs according to the Bernoulli equation (equation (III-6)). During injection a higher amount of energy from the NFI device is consumed for propulsion of the VPG in comparison to liquids, thus the pressure of the VPG jet decreases faster while energy is used up and in the following lower drop-off pressure is observed for higher phospholipid concentration.

III.2.2.4.2 Influence of ejection temperature

Another factor influencing the injectability and syringeability of formulations is the temperature of the injected formulation. Higher temperatures facilitate the injection of highly viscous formulations with needle and syringe, due to its effect on viscosity of the formulation. In this part we investigated the effect of higher temperatures on the viscosity and pressures during needle-free injection of VPGs.

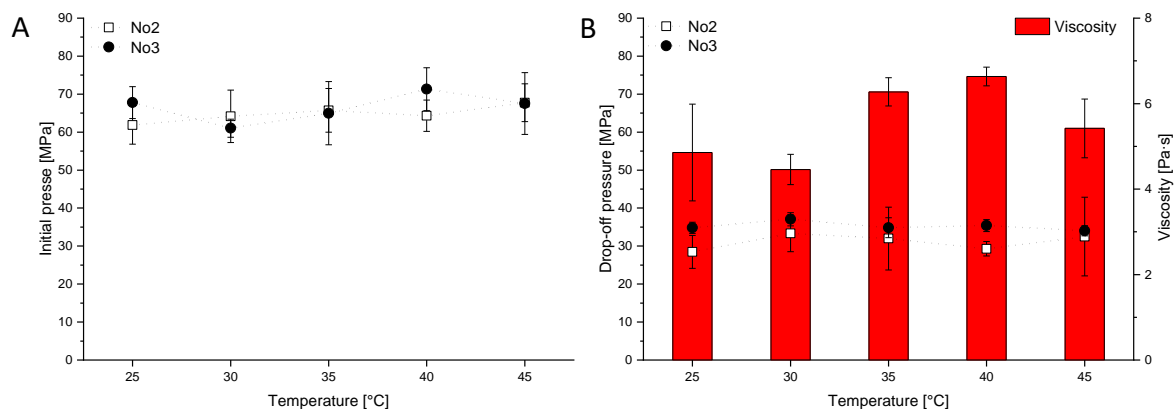


Figure III-16: Initial pressure (A) and drop-off pressure (B) of 40% (m/m) VPG composed of Lipoid E80 and 20 mM PBS pH 7.4 after injection of 0.25 ml. Red bars in (B) show viscosity of the formulation at different temperatures. Viscosity was compared at a shearing rate of 32.9 s^{-1} . Graphs show mean ($n=3$) \pm SD.

Surprisingly, increasing the temperature of VPG formulations to $45 \text{ }^\circ\text{C}$ does not necessarily also influence the viscosity of the formulation. No differences in initial pressure or drop-off pressure were observed for increasing temperatures for both syringes.

III.2.2.4.3 Influence of ejection volume

Three different volumes were tested to show differences between the initial injection pressures, injection time and drop-off pressure. No differences were observed between the initial injection pressures for all three volumes. Higher injection volumes resulted in longer injection durations for both syringe types. A two-fold increase of the volume led to a two-fold increase of the injection time (Figure III-17B). As pointed out before, injection

duration was shorter for No3 syringes in comparison to the No2 syringes. This is a result of the larger orifice, allowing a higher volume per time flow.

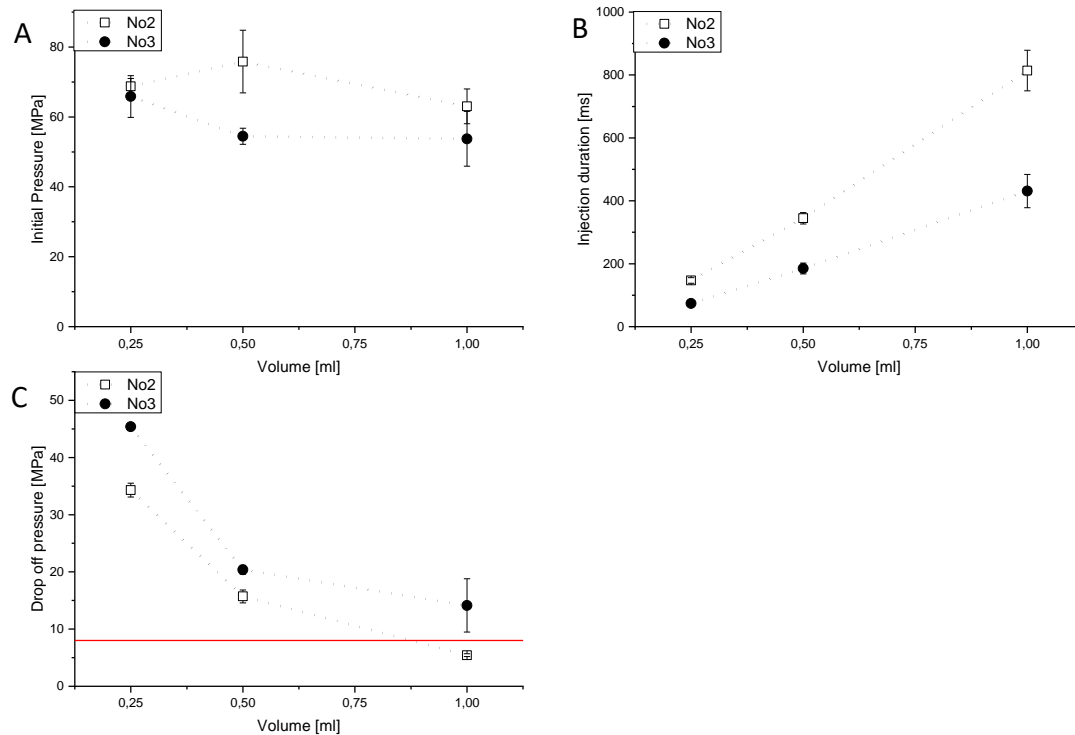


Figure III-17: Initial pressure (A), injection duration (B) and drop-off pressure (C) of VPG composed of 40% (m/m) Lipoid E80 and 20 mM PBS pH 7.4 for different injection volumes (0.25 ml, 0.5 ml and 1.0 ml). Graphs show mean ($n=3$) \pm SD. Red line indicates critical drop-off pressure at 8 MPa.

With increasing volume of the VPG, decreasing drop-off pressure was observed for both syringe types. A drop-off pressure of 5.5 MPa for an ejected volume of 1.0 ml was measured for the No2 syringe. This value is below the critical limit of 8 MPa, leading to the conclusion that these high injection volumes might lead to wet shots more often. Limits of injectability are reached for the No2 syringe. These findings are also in accordance with the observations for the needle-free injections into pig skin post mortem, where wet shots occurred more often for these larger volumes.

For the No3 syringe, the critical value is not reached for a 40% (m/m) VPG formulation. However, the results of the post mortem experiments indicate that the injection of VPGs with higher phospholipid concentration also may lead to critical drop-off pressures.

III.3 Conclusion

The administration of VPG, a semisolid drug formulation with high viscosity, is one of the challenges, which has to be overcome before clinical studies with the drug delivery system can be started.

In this study, the injectability and syringeability of VPGs were investigated and it was shown that exceptional high injection forces are reached for VPGs when conventional syringes and needles for s.c. injections are used. These difficulties could only to some extent be overcome by using needles with larger inner needle diameter or by very slow injection rates. However, both of these measures are correlated to low patient compliance, due to longer duration and their association with higher sensation of pain. Due to these restrictions and difficulties arising from injection of VPGs with conventional needles and syringe, a more convenient and patient friendly method is urgently needed. Needle-free injection of VPGs with different phospholipid concentration, composition of the lipid component, injection volumes and two different single use syringes was successfully demonstrated up to 50% (m/m) phospholipid. Injection of VPGs into the subcutaneous tissue of pig skin post mortem was possible. Furthermore, the applied administration technology shows a high robustness against changes in viscosity and temperature, while limitations were visible when larger volumes were injected. Pressure measurements confirmed the conclusions gained from post mortem injections, that high injection volumes may result in wet shots more often due to the low drop-off pressure reached at 1.0 ml injections. Beyond the fact that needle-free injection technology facilitates the elegant and simple administration of VPGs, this technique also prevents needle-stick injuries, thereby reducing the risk of infections, and overcomes patients aversions against needles [12].

Additionally, it was ensured that an encapsulated protein (EPO) was still released with the favorable sustained release kinetics, which makes VPGs such an interesting depot formulation. Shearing of VPGs by the Biojector 2000 does neither destroy the inner structure of the VPGs, responsible for the sustained release behavior, nor do shearing forces lead to degradation of the encapsulated protein.

III.4 References

- [1] M. Brandl, M. Drechsler, D. Bachmann, and K. H. Bauer, "Morphology of semisolid aqueous phosphatidylcholine dispersions, a freeze fracture electron microscopy study," *Chem. Phys. Lipids*, vol. 87, pp. 65–72, 1997.
- [2] H. Grohganz, I. Tho, and M. Brandl, "Development and in vitro evaluation of a liposome based implant formulation for the decapeptide cetorelix," *Eur. J. Pharm. Biopharm.*, vol. 59, no. 3, pp. 439–448, 2005.
- [3] S. Buchmann *et al.*, "Growth factor release by vesicular phospholipid gels: in-vitro results and application for rotator cuff repair in a rat model," *BMC Musculoskelet. Disord.*, vol. 16:82, no. 1, pp. 1–10, 2015.
- [4] W. Tian, S. Schulze, M. Brandl, and G. Winter, "Vesicular phospholipid gel-based depot formulations for pharmaceutical proteins: Development and in vitro evaluation," *J. Control. Release*, vol. 142, no. 3, pp. 319–325, 2010.
- [5] U. Massing, S. Cicko, and V. Ziroli, "Dual asymmetric centrifugation (DAC)-A new technique for liposome preparation," *J. Control. Release*, vol. 125, no. 1, pp. 16–24, 2008.
- [6] C. Tardi, M. Brandl, and R. Schubert, "Erosion and controlled release properties of semisolid vesicular phospholipid dispersions," *J. Control. Release*, vol. 55, no. 2–3, pp. 261–270, 1998.
- [7] Y. Zhong *et al.*, "Vesicular phospholipid gels using low concentrations of phospholipids for the sustained release of thymopentin : pharmacokinetics and pharmacodynamics," *Pharmazie*, vol. 68, pp. 811–815, 2013.
- [8] Y. Zhang *et al.*, "In vitro and in vivo sustained release of exenatide from vesicular phospholipid gels for type II diabetes," *Drug Dev. Ind. Pharm.*, vol. 42, no. 7, pp. 1042–1049, 2015.
- [9] A. Allmendinger *et al.*, "Rheological characterization and injection forces of concentrated protein formulations: An alternative predictive model for non-Newtonian solutions," *Eur. J. Pharm. Biopharm.*, vol. 87, no. 2, pp. 318–328, 2014.
- [10] A. Fry, "Injecting Highly Viscous Drugs," *Pharm. Technol.*, vol. 38, no. 11, pp. 8–10, 2014.
- [11] R. B. Kumar, "Needle-free injection system," US6676630, 2004.
- [12] S. L. Patwekar, S. G. Gattani, and M. M. Pande, "Needle free injection system: A review," *Int. J. Pharm. Pharm. Sci.*, vol. 5, no. 4, pp. 14–19, 2013.
- [13] T. R. Kale and M. Momin, "Needle Free Injection Technology," *PharmaTutor*, vol. 5, no. 1, pp. 1–8, 2014.
- [14] J. Baxter and S. Mitragotri, "Jet-induced skin puncture and its impact on needle-free jet injections: Experimental studies and a predictive model," *J. Control. Release*, vol. 106, no. 3, pp. 361–373, 2005.
- [15] M.-P. Even, "Twin-Screw Extruded Lipid Implants for Vaccine Delivery.," Dissertation, Ludwig-Maximilians-Universität München, 2015.

- [16] J. Seok *et al.*, "Investigating skin penetration depth and shape following needle-free injection at different pressures: A cadaveric study," *Lasers Surg. Med.*, March, pp. 1–5, 2016.
- [17] M. Brandl, "Vesicular Phospholipid Gels: A Technology Platform," *J. Liposome Res.*, vol. 17, no. 1, pp. 15–26, 2007.
- [18] F. Cilurzo *et al.*, "Injectability evaluation: an open issue," *AAPS PharmSciTech*, vol. 12, no. 2, pp. 604–609, 2011.
- [19] A. Allmendinger *et al.*, "Measuring Tissue Back-Pressure - In Vivo Injection Forces During Subcutaneous Injection," *Pharm. Res.*, no. 32, pp. 2229–2240, 2014.
- [20] A. Sheikhzadeh, J. Yoon, D. Formosa, B. Domanska, D. Morgan, and M. Schiff, "The effect of a new syringe design on the ability of rheumatoid arthritis patients to inject a biological medication.," *Appl. Ergon.*, vol. 43, no. 2, pp. 368–75, Mar. 2012.
- [21] M. Adler, "Challenges in the Development of Pre-filled Syringes for Biologics from a Formulation Scientist ' s Point of View Syringeability," *Am. Pharm. Rev.*, vol. 15, pp. 1–7, 2012.
- [22] W. Rungseevijitprapa and R. Bodmeier, "Injectability of biodegradable in situ forming microparticle systems (ISM)," *Eur. J. Pharm. Sci.*, vol. 36, no. 4–5, pp. 524–531, 2009.
- [23] M. Breitsamer and G. Winter, "Needle-Free Injection of Vesicular Phospholipid Gels - A Novel Approach to Overcome an Administration Hurdle for Semisolid Depot Systems," *J. Pharm. Sci.*, vol. 106, no. 4, pp. 968–972, 2017.
- [24] Bioject Inc., "Guide to Selection and Use of Biojector Syringes," Tigard, OR, USA.
- [25] J. Bennett, F. Nichols, M. Rosenblum, and J. Condry, "Subcutaneous administration of midazolam: a comparison of the Bioject jet injector with the conventional syringe and needle.," *J. oral Maxillofac. Surg. Off. J. Am. Assoc. Oral Maxillofac. Surg.*, vol. 56, no. 11, pp. 1249–1254, 1998.
- [26] O. A. Shergold, N. A. Fleck, and T. S. King, "The penetration of a soft solid by a liquid jet, with application to the administration of a needle-free injection," *J. Biomech.*, vol. 39, no. 14, pp. 2593–2602, 2006.
- [27] C. Chase, C. Daniels, and R. Garcia, "Needle-free injection technology in swine: Progress toward vaccine efficacy and pork quality," *J. Swine Heal. Prod.*, no. October, pp. 254–261, 2008.
- [28] S. F. Peterson, C. N. J. McKinnon, P. E. Smith, T. Nakagawa, and V. L. Bartholomew, "Needleless Hypodermic Injection Methods and Device," US005399163A, 1995.

Chapter IV

PREPARATION OF VESICULAR PHOSPHOLIPID GELS BY TWIN-SCREW EXTRUSION

Parts of this chapter have been submitted as patent to “Deutsches Patent- und Markenamt” with the title “Herstellung von VPG mittels Schnecken-Extrusion” (application number: DE 10 2018 010 063.5). The publication as a patent application by the DPMA is pending.

Furthermore, parts of this work have been performed by Natalie Deiringer throughout the course of her Master Thesis from May 2017 to October 2017 under my supervision. The following figures are adapted and partially edited from her work: Figure IV-6, Figure IV-7, Figure IV-8, Figure IV-9, Figure IV-10, Figure IV-13, Figure IV-14, Figure IV-15, Figure IV-16.

IV.1 Introduction

One of the advantages of VPGs as drug delivery systems over others is their easy and cheap manufacturing. Three different processes have been used in the past for the preparation of VPGs.

IV.1.1 High pressure homogenization

Originally developed for the preparation of liposomes, to avoid the film method, high pressure homogenization (HPH) is the first described method used for the preparation of VPGs [1]–[3]. By HPH, small and unique vesicle sizes below 100 nm can be prepared without the involvement of organic solvents by forced lecithin hydration [4]. The method allows the preparation of batch sizes up to tens to hundreds of grams of VPG and is especially suited for large scale production [5]. A pre-dispersion of dry phospholipids or a blend of lipids and buffer or drug solution are fed into the high-pressure homogenizer, where ultra-fine lipid particles are formed, which then evolve to vesicles after swelling [3]. The lipid dispersion is forced through a narrow gap with high pressure, resulting in homogenization by cavitation and shearing. In some cases repeated cycles are necessary to reach satisfying vesicle sizes [1]. Size distribution of the obtained vesicles depends on the applied pressure during the process, the number of cycles as well as lipid type and concentration. However, HPH has drawbacks in the production of VPGs in small lab scale, the one-step approach is not suited for lipid-mixtures and temperature control may be a challenge. Additionally, only short mixing intervals can be used to prevent degradation of the encapsulated drug or phospholipids as a result of the high shearing forces and thus heat development [6].

IV.1.2 Dual asymmetric centrifugation and dual centrifugation

Dual asymmetric centrifugation (DAC) is a technique, suited for the preparation of fat emulsions, liposomes, nanoparticles and VPGs [5], [7]–[9]. Massing et al. showed that preparation of VPGs by DAC is possible in a broad range of phospholipid concentrations and, with the addition of glass beads as homogenization aid, even the preparation of liposomes smaller than 100 nm is possible [5]. In a dual asymmetric centrifuge, the

container is rotated around a central axis like in a commonly used centrifuge, while a counter rotation around the containers center is taking place at the same time. Thereby the sample is pushed to the outer side of the container, due to centrifugal forces, and on the other hand is pushed in the opposite direction as a result of adhesive forces between the sample and the container by the rotation around its own center. By a defined angle of the main rotation axis, the content of the vial is forced into the corner between the bottom and the vial wall [5].

A further development of dual asymmetric centrifugation (DAC) is dual centrifugation (DC) [10]. It is based on the same principle as DAC i.e. two counter-rotating movements result in rapid and homogenous mixing of components, however in the instrumental setup of a DC two rotating baskets are used instead of one. No counterweight as in an asymmetric centrifuge is needed. Further, these novel DC systems may be equipped with a cooling system as applied with conventional centrifuges, thereby facilitating the encapsulation of sensitive compounds into VPGs.

DAC or DC are fast and easy options to produce VPGs with high encapsulation efficiency in small lab scale up to hundreds of grams (depending on the size of the centrifuge). Additionally, aseptic production in a closed container is possible. However, the process is only possible in batch-to-batch mode production and does not facilitate continuous manufacturing.

IV.1.3 Magnetic stirring

Next to HPH and DAC, which both apply high shearing forces during manufacturing, magnetic stirring has been described for the preparation of VPGs [11], [12]. The dry lipid powder is added to buffer and the mixture is allowed to swell, before homogenization is conducted by magnetic stirring. However, freeze-fracture microscopic examination showed larger vesicle sizes and different morphology for the obtained VPG in comparison to VPG prepared by HPH or DAC [2]. Due to significantly lower mechanical energy input during the process, dispersity and homogeneity of the VPGs is expected to be lower in comparison the HPH or DAC.

Although magnetic stirring is straight forward and easy to scale up, homogeneity and stability of the obtained VPGs is questionable.

IV.1.4 Twin-screw extrusion

The main advantages of extrusion technology over other preparation techniques are a continuous operation and manufacturing, high flexibility in batch sizes, high process variability by temperature control, screw design and screw speed and excellent mixing ability. A twin-screw (TSC) extruder consists of two co- or counter-rotating screws embedded in a barrel, which is equipped with temperature control and a feeding system (see Figure IV-1). This conveying system transports the material following the action of Archimedes' infinite screws, to the die, which then forms the material [13], [14]. The rotation of the two screws leads to homogenization and transportation of the introduced material. Heating of the barrel may contribute to this process. Depending on the screw design, co- and counter-rotating screws have different mixing abilities. While co-rotating screws can be equipped with conveying and kneading elements and result in an excellent mixing, counter-rotating screws only convey the material without interchange of the material between the screws [15], [16].

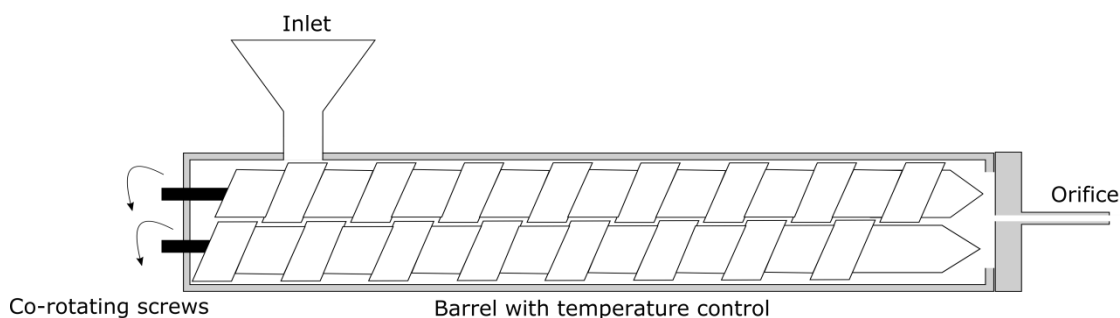


Figure IV-1: Schematic drawing of the barrel of a twin-screw extruder with co-rotating screws.

Extrusion was many years ago introduced to pharmaceutical industry as a novel manufacturing technique for polymeric, fat or starch matrices. Especially hot melt extrusion (HME) has become a well-established manufacturing method in this field, due to its many advantages like the chance to work solvent-free, low costs and the ability for fast and continuous manufacturing [13]. Until today, lipid-based implants containing sensitive compounds like proteins were developed and sustained release of the protein from these depot systems was shown [17]–[20]. Stability of the protein was shown during manufacturing and release.

By using TSC extrusion for the preparation of the semisolid VPGs, several advantages like continuous manufacturing and the possibility to encapsulate sensitive compounds, as well

as a fast and solvent-free preparation are used to improve the manufacturing process for VPGs. Additionally, Haas et al. achieved a homogeneous mixture of two compounds using a TSC extruder [21]. This may facilitate the homogenous mixing of two or more phospholipids or even the encapsulation of lipophilic drugs by a simple one-step process, without the need for preparation of the mixtures, e.g. by freeze-drying, prior to homogenization with the aqueous phase.

In this chapter, we evaluate TSC extrusion as a novel method for the continuous manufacturing of VPGs.

IV.2 Material and Methods

IV.2.1 Materials

IV.2.1.1 Phospholipids

Egg lecithin (Lipoid E80, Lipoid GmbH, Ludwigshafen am Rhein, Germany) containing 80 - 85% phosphatidylcholine (PC), 7 – 9.5% phosphatidylethanolamine, a maximum of 3% lysophosphatidylcholine and 2 – 3% sphingomyelin was used for the preparation of all VPG formulations.

IV.2.1.2 Proteins for release studies and stability

Erythropoietin (EPO), Interferon β (IFN β) and a monoclonal antibody of IgG-class was used for stability and *in vitro* release studies.

EPO is a glycoprotein with a single-chain of 165 amino acids and a molecular weight of 30.4 kDa [22], [23]. The protein is primarily produced in the kidney and regulates the erythropoiesis by inducing proliferation and differentiation of erythroid progenitor cells [23]. In therapy EPO was used for the treatment of kidney diseases and hematological disorders. EPO is formulated at a concentration of 2.38 mg/ml in 10 mM phosphate buffer, containing 100 mM sodium chloride at a pH of 7.5.

Interferon β (IFN β) is a non-glycosylated cytokine, produced by eukaryotic cells in response to viral infections and other biological inducers [24]. In general, IFNs act antiviral, antiproliferative and immunomodulatory. IFN β -1b was the first disease-modifying therapy, approved for the treatment of multiple sclerosis [25]. The protein was formulated at a concentration of 2 mg/ml in acetate buffer, containing 0.1% (m/v) SDS and EDTA at a pH of 5 to 6.

Further, a monoclonal antibody of the IgG-type was used. The antibody was formulated in histidine buffer, containing polysorbate 20 and trehalose with a concentration of 120 mg/ml.

IV.2.1.3 Other chemicals and salts

All reagents and chemicals used within this work were of analytical grade and are listed in Table IV-1.

Table IV-1: List of chemicals and salts, which were used.

Substance	Abbreviation	Supplier
di-Sodium hydrogen phosphate dihydrate	Na ₂ HPO ₄ *2H ₂ O	Bernd Kraft GmbH, Duisburg, Germany
Fluorescein Isothiocyanate-Dextran (70 kDa)	FITC-Dextran	Sigma-Aldrich Chemie GmbH, Steinheim, Germany
Potassium chloride	KCl	AppliChem GmbH & Co. KG, Darmstadt, Germany
Potassium dihydrogen phosphate	KH ₂ PO ₄	Merck KGaA, Darmstadt, Germany
Sodium chloride	NaCl	Bernd Kraft GmbH, Duisburg, Germany

IV.2.2 Preparation of VPGs

VPGs with phospholipid concentrations between 35 and 50% (m/m) were prepared by different methods. 20 mM PBS pH 7.4 was used as aqueous phase if not stated otherwise. Lipoid E80 was accurately weighted and the desired amount of buffer or drug solution was added. Then the mixture was homogenized using one of the methods described in the following. Batch sizes were 2 g for magnetic stirring (MAG) and DAC, 3 g for the ThreeTec extruder (TTE), 5 to 8 g for the HAAKE extruder (HE) and 300 g for the Leistritz extruder (LEI).

IV.2.2.1 Preparation of VPGs by DAC

VPGs were homogenized following the method, first described by Massing et al. [5]. The weighted components were homogenized using a Speedmixer™ DAC 150 FVZ (Hauschild GmbH & Co KG, Hamm, Germany) in a 25 ml cylindrical container (PP15-25ml Hauschild GmbH & Ca KG, Hamm, Germany)) at a speed of 3500 rpm for 45 minutes. A custom-made cooling system, using compressed air, was used to keep the product temperature below 30 °C.

IV.2.2.2 Preparation of VPGs by magnetic stirring

The mixture of phospholipid and aqueous phase was homogenized using a magnetic stirrer (Variomag Telesystem HP 6, VWR International GmbH, Darmstadt, Germany) in combination with an agitator (3.0 cm x 0.5 cm) which covered the whole bottom of the container (25 ml PP). Speed was set to 300 rpm.

IV.2.2.3 Preparation of VPGs by TSC extrusion

Except otherwise stated, phospholipid and aqueous phase were shortly premixed by three minutes of magnetic stirring at 300 rpm. These pre-mixtures were then manually introduced to the extruder barrel using a syringe. The effect of different extrusion parameters, e.g. rotation speed of the screws, die diameter and length, barrel temperature, the usage of a cycling function, lipid concentration and preparation method, on the product quality was evaluated.

Three different extruders were used to prepare VPGs by TSC extrusion.

IV.2.2.3.1 ZE-5 Mini-Extruder

The ZE-5 Mini-Extruder (ThreeTec GmbH, Seon, Switzerland) was used for the production of small quantities of VPGs. The barrel (L/D ratio 15:1) of the extruder is equipped with three heating zones which can be controlled separately and an outlet in 180° angle to the screws. The parallel, closely intermeshing, conveying screws (length: 75 mm, diameter: 5 mm) have a pitch of 5 mm. Dies with different diameter (0.4 mm, 0.8 mm, 1.5 mm, 1.7 mm and 2.0 mm) and length (2 mm or 20 mm) are used with this extruder.

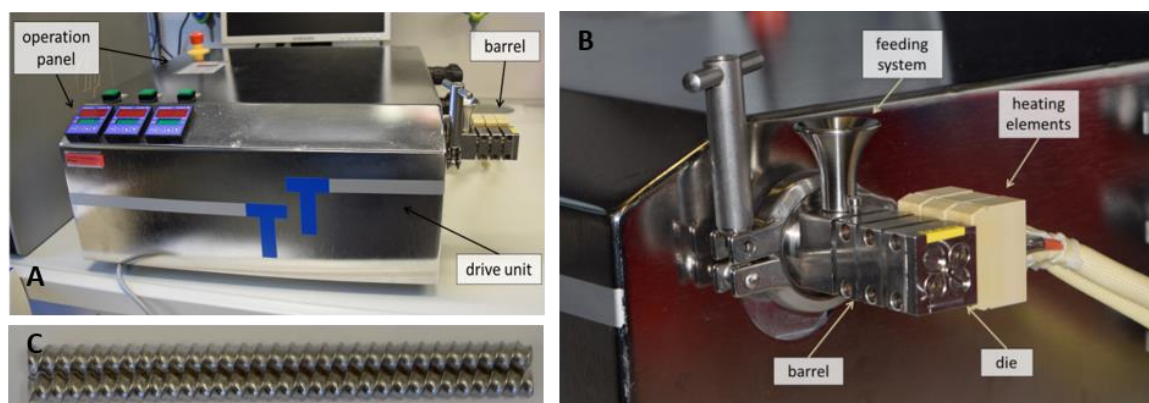


Figure IV-2: A) ZE-5 Mini-Extruder with barrel and drive unit. B) Detailed image of the barrel with three heating elements and the die. C) Parallel, conveying screws used during extrusion with the ZE-5 Mini-Extruder.

IV.2.2.3.2 HAAKE MiniLab® Micro Rheology Compounder

The HAAKE MiniLab® Micro Rheology Compounder (ThermoFisher Scientific, Karlsruhe, Germany) was used for a minimum amount of 5 g. The barrel of this twin-screw extruder can be heated electrically or cooled using air or water and has a bypass function for circulation of the material through the barrel several times. It is equipped with conical, co-rotating screws (length: 110 mm; diameter: 10 to 4 mm) and different die diameters (0.5 mm, 1.0 mm, 1.5 mm and 2.0 mm) were used. The extruder has a rectangular setup of the die to the screws.

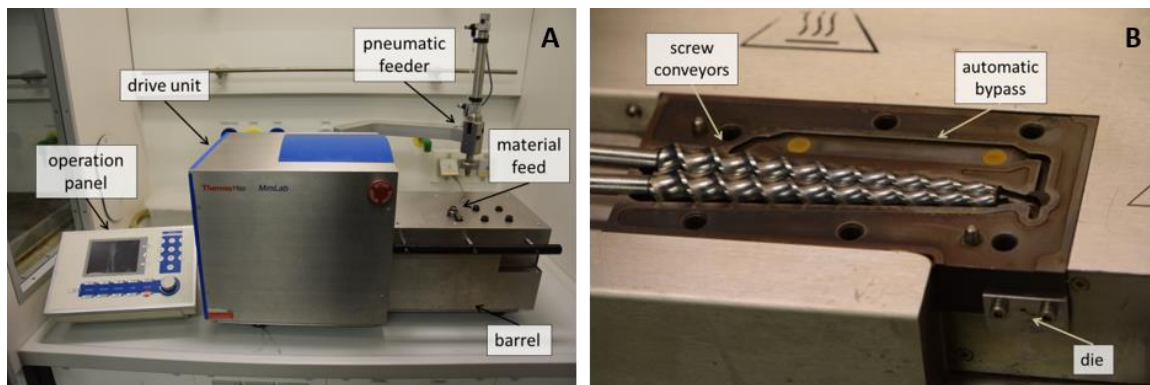


Figure IV-3: A) MiniLab® Micro Rheology Compounder. B) Detailed view of the open barrel with the two conical, conveying screws and the automatic bypass.

IV.2.2.3.3 Leistritz Micro 27 GL - 28D

The Leistritz Micro 27GL - 28D (Leistritz Extrusionstechnik GmbH, Nürnberg, Germany) is a large-scale extruder suitable for research-scale and small-scale production. A minimum amount of 300 g is needed for this extruder.

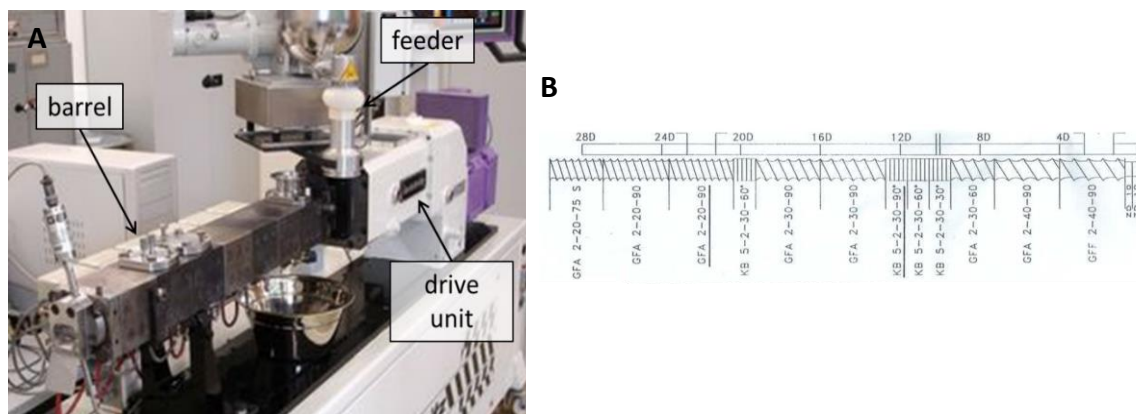


Figure IV-4: A) Leistritz Micro 27GL extruder. B) Schematic drawing of the screw design used for the mixing screw.

The extruder is equipped with a heatable barrel (L/D ratio 28:1) with separately controllable sections. The parallel, co-rotating screws (length: 1100 mm, diameter:

27 mm) are made of sections which can be modulated to the desired design using conveying and mixing elements. Two different screw designs were used. Screw A is geared to the design often used for hot-melt extrusion (see Figure IV-4B), while screw B is solely equipped with conveying elements. A die with an inner diameter of 1.0 mm was used for all experiments.

IV.2.3 Methods for VPG characterization

All VPGs were characterized with a series of methods including rheological measurements, particle size analysis, microscopy, thermogravimetric analysis and visual inspection. Each experiment was performed in triplicates.

IV.2.3.1 Rheology

Viscosity was determined with a rotational rheometer (Physica MCR 100, Anton Paar GmbH, Ostfildern, Germany) using a plate-plate geometry (PP-25, Anton Paar GmbH, Ostfildern, Germany). For each measurement approximately 0.2 g of VPG was used. Viscosity was measured with a logarithmic ramp of the shearing rate between 10 and 100 s⁻¹ and a temperature of 25 °C. For comparison of the different formulation viscosity at 32.9 s⁻¹ was taken.

Further, oscillatory measurements were conducted to evaluate stability of the VPGs. To this end a PP-08 was used and an amplitude sweep test was performed. Frequency was kept constant at 1 Hz and storage modulus (G') and loss modulus (G'') was determined at a shear stress of 5 to 750 Pa (logarithmic ramp) at a constant temperature of 25 °C.

IV.2.3.2 Dynamic light scattering

10 mg of VPG was accurately weighted and dispersed in 1 ml HPW. After vigorous mixing for 20 s, using a CapMix™ (3M Deutschland GmbH, Neuss, Germany), the solution was further diluted (1:10) and mixed again. Z-Average and PDI of the obtained vesicles were determined using a Zetasizer Nano ZS (Malvern Instruments, Worcestershire, UK) at a temperature of 25 °C.

IV.2.3.3 Microscopy

Microscopic images of VPGs were taken, using a Biozero BZ 8100 microscope (Keyence, Osaka, Japan) equipped with a Nikon Plan Apo λ (Mag 10x/NA 0.45, Nikon, Tokyo, Japan) objective.

IV.2.4 Encapsulation of proteins into VPGs

EPO and INF β -1b were prepared for encapsulation by dialysis (Spectra/Por Dialysis Membrane, Spectrum Laboratories, Rancho Dominguez, USA) for purification. Additionally, up-concentration was necessary using 20 ml Vivaspin tubes (Sartorius Stedim Biotech GmbH, Goettingen, Germany). For up-concentration, Vivaspins were centrifuged at 8000 rpm at 6 °C until the desired concentration was reached. Protein concentration was determined by UV-spectroscopy at 280 nm. Protein preparation steps for these two proteins are summarized in Table IV-2.

Table IV-2: Summary of protein preparation prior to encapsulation into VPGs.

Protein	Original formulation	Dialysis buffer	Vivaspin membrane MWCO	Final concentration
EPO	2.38 mg/ml in 10 mM Phosphate buffer, containing 100 mM sodium chloride pH 7.5	5 mM phosphate buffer pH 7.0	10 kDa	4.8 mg/ml
IFN β-1b	1.67 mg/ml in acetate buffer pH 5-6 containing 0.1% SDS and EDTA	10 mM sodium acetate buffer pH 5.3	5 kDa	4.3 mg/ml

Further, mAb was used in its original formulation (120 mg/ml), which was composed of a histidine buffer, containing polysorbate 20 and trehalose.

For VPG preparation a direct encapsulation process was chosen. Phospholipids were accurately weighted and the desired amount of protein in buffer was added to the lipids before homogenization with one of the above described methods. VPGs containing EPO (3 mg/g) or IFN β -1b (2 mg/g) were prepared by DAC, magnetic stirring and extrusion, using the ZE-5 Mini-Extruder or the MiniLab[®] Extruder. VPGs containing mAb (10 mg/g)

were prepared by DAC, magnetic stirring and extrusion, using the ZE-5 Mini-Extruder or the Leistritz Micro 27GL.

Additionally, Ovalbumin (40mg/ml in 20mM PBS pH 7.4) was encapsulated into VPGs (20mg/g) by DAC using the same protocol as described above.

IV.2.5 *In vitro* release studies

For *in vitro* release studies VPGs (45% (m/m) phospholipids) containing 2 mg/g FITC-Dextran (70 kDa) were prepared, using the direct encapsulation process described before for proteins. Aqueous phase was composed of 20 mM PBS pH 7.4.

Additionally, mAb-VPGs (45% (m/m) phospholipids) with a protein-load of 10 mg/g were used for release studies.

Custom-made flow through cells (FTC), made of Teflon, were used for release testing following previously described release experiments [26]. Approximately 0.5 g VPG was accurately weighted into the donor compartment of the release cells, before cells were closed tightly. 20 mM PBS pH 7.4 was pumped through the acceptor compartment using a multi-syringe pump and a flow-rate of 0.5 ml/h was used. Temperature was kept constant at 37 °C using a water bath (JULABO GmbH, Seelbach, Germany). Samples were taken at predetermined time points and quantified as follows.

IV.2.5.1 Quantification of FITC-Dextran

FITC-Dextran was quantified using a Cary Eclipse Fluorescence Spectrophotometer 50 (Agilent Technologies, Santa Clara, CA, USA). Released fractions were centrifuged at 4000 rpm to remove phospholipids. The clear supernatant was used for quantification. 492 nm was used as excitation wavelength and emission was determined at 518 nm.

IV.2.5.2 Quantification of mAb

Released mAb was quantified by RP-HPLC using a Dionex UltiMate™ 3000 (Thermo Fisher Scientific, Waltham, USA) equipped with an autosampler (UltiMate™ WPS-3000SL) and a fluorescence detector (UltiMate™ FLD 3400RS). Before sample measurement extraction had to be performed. Therefore, all samples were diluted with pure ethanol (1:1) and mixed accurately. Then phospholipids were removed by centrifugation and the clear supernatant was used for quantification.

The same extraction protocol was performed with a mAb solution in buffer (100 µg/ml) as well as with mAb-VPG with known mAb-concentration in the sample. An extraction efficiency of $104.1\% \pm 7.0\%$ was reached and no effects of the extraction process on the mAb was observed.

Mobile phase A was composed of 10% (m/m) acetonitrile, 0.1% (m/m) trifluoroacetic acid (TFA) and highly purified water (HPW) and mobile phase B was composed of 0.1% (m/m) TFA in acetonitrile. A Phenomenex Jupiter C4, 5 µm column (Phenomenex Inc. Torrance, USA) was used as solid phase and the oven temperature was set to 50°C. In a simple one step gradient 100% mobile phase A was changed to 100% mobile phase B in 20 minutes. mAb was detected at a retention time of 15.2 minutes using fluorescence ($\lambda_{\text{exc.}} = 280 \text{ nm}$; $\lambda_{\text{em.}} = 350 \text{ nm}$). The method was qualified with samples containing defined concentrations of mAb, phospholipids and mixtures after extraction. The mAb concentration in each sample was calculated using a calibration curve ($R^2 = 0.9998$).

IV.2.5.3 Phospholipid assay

Further, erosion of the lipid matrix was determined by quantification of PC in the released fractions. To this end, a LabAssay™ Phospholipid (FUJIFILM Wako Chemicals Europe GmbH, Neuss, Germany) was used as described before by Weiwei Tian [27]. Further qualification of the method was performed separately by Weiwei Liu (Pharm. Technology and Biopharmaceutics, LMU Munich).

Samples were prepared following the supplier's instructions and measured at a wavelength of 600 nm using a FLUOstar Omega plate reader (BMG LABTECH, Ortenberg, Germany). In this assay, phospholipids are hydrolyzed by phospholipase D and the liberated choline is then oxidized by choline oxidase to betaine [28]. Simultaneously hydrogen peroxide is produced which initiates the coupling of 4-aminoantipyrine and DAOS (N-Ethyl-N-(2-hydroxy-3-sulfopropyl)-3,5-dimethoxyaniline, sodium salt) to a blue chromophore by oxidation.

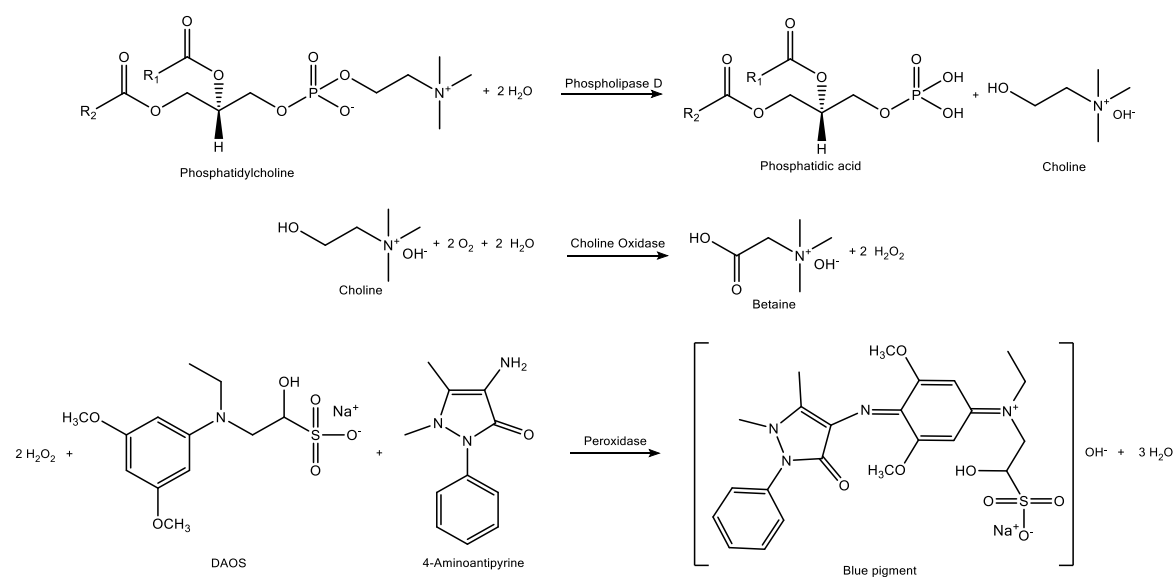


Figure IV-5: Schematic reaction of the phosphatidylcholine quantification [29].

IV.2.5.4 Optical density

Optical density (OD) of the released fractions was determined to further characterize the erosion behavior. The absorbance for each fraction was measured at 600 nm, using a microplate reader (FLUOstar Omega, BMG LABTECH, Ortenberg, Germany).

IV.2.5.5 Dynamic light scattering

Dynamic light scattering (DLS) was used to determine the vesicle size of VPGs after dilution with buffer. 10 mg VPG was accurately weighed and dispersed in 1 ml highly purified water by vigorous mixing using a CapMix™ (3M Espe AG, Seefeld, Germany). The obtained dispersion was further diluted (1:10) before measurement with a Zetasizer Nano ZS (Malvern Instruments, UK). Z-Average and PDI of the lipid dispersion were determined.

IV.2.5.6 Thermogravimetric determination of water loss during VPG preparation

To determine if water evaporates during preparation, especially at higher temperatures, thermogravimetric analysis was carried out on a Hi-Res TGA 2950 (TA Instruments, New Castle, USA). Samples of approximately 20 mg were weighed into aluminum pans and placed on a microbalance. Then samples were heated from 27 °C to 250 °C, using a linear ramp (10 °C/min) under nitrogen atmosphere. Each measurement was performed twice.

IV.2.5.7 Determination of the product temperature

Product temperature was determined directly at the outlet of the extruder with a data logger thermometer HH147U (OMEGA, Deckenpfronn, Germany). The sensor was inserted directly into the VPG.

IV.2.6 Protein stability during extrusion and storage

IV.2.6.1 Capillary gel-electrophoresis

300 mg VPG containing EPO or IFN- β was diluted in 1 ml formulation buffer and dispersed by vigorous mixing with a CapMix™. Then samples were centrifuged for 10 minutes at 10 000 min⁻¹ at 6 °C to remove the lipids. The two proteins were analyzed under non-reducing conditions using a Protein 230 Kit (Agilent, Santa Clara, CA, USA). Following the manufacturers protocol, 4 μ l of sample and 2 μ l of sample buffer were mixed and incubated at 95 °C for 5 minutes for protein denaturation. 84 μ l HPW were added and 6 μ l of this mixture were then pipetted into the sample wells of the protein chip. Further, the chip was prepared by loading the gel-dye mix, destaining solution and molecular weight marker on the chip. Capillary gel electrophoresis was performed applying an Agilent 2100 Bioanalyzer system (Agilent, Santa Clara, CA, USA).

IV.2.6.2 Sodium dodecyl sulfate-polyacrylamide gel electrophoresis (SDS-PAGE)

Aggregation and fragmentation of proteins was monitored by non-reducing denaturing SDS-PAGE. Protein containing VPGs were therefore diluted to a final protein concentration of 0.05 mg/ml with formulation buffer. Tris-buffer pH 6.8 containing 2% SDS and 2% glycerin was added to the samples before denaturation at 90 °C for 10 minutes.

Different gels were used for separation and resolution of the proteins. EPO and IFN- β were analyzed using NuPAGE® 4-12% Bis-Tris Gels (Novex high performance pre-cast gels, Invitrogen, Karlsruhe, Germany) with NuPAGE® MES SDS running buffer (Invitrogen, Karlsruhe, Germany). Separation was accomplished with a XCell SureLock™ Mini-Cell Electrophoresis System (Novex by Life Technologies, Carlsbad, CA, USA) at a constant voltage of 200 V for approximately 25 minutes using a BioRad PowerPac 2000 (Bio-Rad

Laboratories, Hercules, CA, USA). Mark12™ Unstained Standard (Invitrogen, Karlsruhe, Germany) was used as molecular weight marker.

mAb was analyzed using a NuPAGE® 3-8% Tris Acetate Gel (Novex high performance pre-cast gels, Invitrogen, Karlsruhe, Germany) in combination with NuPAGE® Tris-Acetate SDS running buffer (Invitrogen, Karlsruhe, Germany). Again, separation was performed at a constant voltage of 200 V for approximately 45 minutes. HiMark™ Pre-stained Protein Standard (Invitrogen, Karlsruhe, Germany) was used as molecular weight marker.

SilverXPRESS® Silver Staining Kit (Invitrogen, Karlsruhe, Germany) or SimplyBlue™ SafeStain (Invitrogen, Karlsruhe, Germany) was used to visualize the results, following the manufacturers' protocols.

IV.2.6.3 Fourier transform infrared spectroscopy (FTIR)

Changes in secondary structure of proteins and peptides may be identified by FTIR measurements. To evaluate if this method is applicable for characterization of proteins extracted from VPGs, ovalbumin was selected as a cheap model protein. FTIR spectra were recorded using a Tensor 27 FTIR Spectrometer (Bruker Optics, Ettlingen, Germany) equipped with a BioATR II cell. Prior to measurements the detector was cooled down with liquid nitrogen for one hour.

For analysis an ovalbumin solution in HPW (1 mg/ml), VPG with 45% (m/m) Lipoid E80 and VPG with 45% (m/m) Lipoid E80, containing 10 mg/g ovalbumin were chosen. Protein was extracted from VPGs prior to measurement with chloroform. To this end, 200 mg VPG was diluted with 200 µl HPW and mixed properly. Then 500 µl chloroform was added and the mixture was centrifuged for 10 minutes at 6 °C and 15 000 rpm. The supernatant was taken and the chloroform extraction was repeated two more times before the supernatant was clear and could be used for analysis. As control, ovalbumin solution was treated similarly. Spectra were collected from 4 000 to 850 cm⁻¹ wavenumbers and were processed by buffer spectra subtraction, followed by vector normalization and subsequent determination of the second derivative using the Opus software (Version 6.8, Bruker Optics, Ettlingen, Germany).

IV.3 Results and Discussion

TSC extruders are often used in pharmaceutical manufacturing due to their excellent mixing ability and process variability. The typical setup with two intermeshing screws results in a high degree of conveying with short residence times [13], [15], [16]. During development of a suitable process for the preparation of pharmaceutical products like VPGs, barrel temperature, screw configuration and speed, feeding system and die design are the most crucial parameters and all contribute to the residence time of the material in the extruder [13], [30]. In this chapter, the different parameters influencing the product quality during extrusion of VPGs were addressed, further *in vitro* release of the obtained VPGs was evaluated and protein stability after extrusion and during storage was investigated.

IV.3.1 Preparation of VPGs by extrusion with repeated circulation

VPGs are characterized by a high inner homogeneity and small vesicular structures. To achieve this appearance, shearing forces have to be high enough. On the other side, shearing forces should not be too high to prevent drug degradation, especially if proteins or peptides are encapsulated into the VPGs.

Method development for preparation of VPGs by extrusion was started with a batch process, using the re-cycling function of the MiniLab[®] Extruder by HAAKE. The MiniLab[®] Micro Rheology Compounder by HAAKE is an extruder for lab scale up to small industrial scale production with conically shaped screws. The option to use a bypass for repeated re-cycling of the material through the conveying screws facilitates efficient mixing. At the same time operating the extruder in this mode allows only batch production of VPGs up to several grams. Still, this setup was used for first extrusion runs to gain first basic experience.

Different parameters like the screw rotation speed, the cycling duration using the bypass function, the temperature as well as the die diameter were varied to evaluate the effect of these parameters on the mixing quality and homogeneity of the VPGs. Additionally, a pneumatic feeder was available for this extruder to introduce the material into the barrel. Table IV-3 summarizes the different settings which were used.

Table IV-3: Overview of settings changed during method development using the re-cycling function. (Varied parameters are emphasized for each experiment in bold letters.)

	Screw rotation speed [rpm]	Cycling duration [min]	Temp. [°C]	Die diameter [mm]	Pre-mixing method	Lipid concentration [% (m/m)]
A	40; 100; 200; 300	10	30	2.0	3min magnetic stirring	45
B	300	0; 5; 10; 20	30	2.0	3min magnetic stirring	45
C	300	10	10; 20; 30; 60	2.0	3min magnetic stirring	45
D	300	10	30	0.5; 1.5; 2.0	3min magnetic stirring	45
E	300	10	30	2.0	3min magnetic stirring; unstirred, feeder	45
F	300	10	30	0.5	3min magnetic stirring	35; 40; 45; 50

In vitro drug release from VPGs and homogeneity, satisfying pharmaceutical requirements, are the two most important factors, when the depot systems are characterized. In this study, homogeneity is evaluated based on viscosity measurements, since viscosity is linked to (i) volume fraction and (ii) particle size distribution. High viscosity for the same formulation is often related to small particle sizes with a narrow particle size distribution and increased packing density of the vesicles [31]. As a consequence of the increased packing density the fluidity of the bilayer membranes in the VPG decreases and increased viscosity is observed [31], [32].

It was shown before, that particle size is influenced by screw speed during hot melt extrusion [33]. When the rotation speed of the extruder screws was varied, an increase in VPG viscosity was observed with increasing speed (Figure IV-6A). While VPGs prepared with a rotation speed of 40 rpm displayed a viscosity comparable to that of VPGs prepared

by magnetic stirring, higher viscosity values (10.3 Pa·s), which are comparable to the VPGs prepared by DAC (10.7 Pa·s), were reached with the fastest rotation speed of 300 rpm. As explained above, high viscosity is correlated to smaller vesicles and a higher packing density, thus a high rotation speed results in smaller vesicles, which was confirmed by DLS measurements.

Next, different cycling durations were evaluated. Without cycling of the VPG through the bypass and thereby only one single shearing process, a rather low viscosity of the VPG (4.4 Pa·s) and thus larger vesicle sizes were achieved (see Figure IV-6B). When the re-cycling function was used, viscosity increased to 10 to 12 Pa·s and only a slight increase in viscosity was observed with increasing cycling duration. Thus, cycling duration has only a minor effect on viscosity and vesicle size, but cycling itself strongly affects the VPG quality. It is known, that increasing the temperature from 10 to 30 °C leads to a softening of the phospholipids and thus better processability although at the same time, residence time in the barrel may decrease slightly [14], [30]. Using the water and compressed air-cooling system of the extruder, even low barrel temperatures can be reached. Low temperatures of 10 °C result in VPG with rather low viscosity despite of the re-cycling of ten minutes, while high temperatures of 60 °C result in exceptional high viscosity (see Figure IV-6C). It is important to note that the temperature of the VPG itself only has little or no effect on the viscosity of the final formulation (as described in Chapter III). In conclusion, higher temperatures influence the manufacturing process by affecting the phospholipids consistency. Thus, at rather low temperatures the mixing is not as efficient and VPGs with larger vesicles and therefore low viscosity are produced. On the other hand, high temperatures e.g. 60 °C may lead to water loss by evaporation especially when the material is re-cycled several times through the heated barrel. At 60 °C water evaporation led to a liquid loss of $16.1 \pm 1.5\%$ (m/m), which resulted in the exceptional high viscosity of 41.7 Pa·s. Further optimization of the process temperature between 30 and 60 °C is needed, to reach good VPG quality without significant water evaporation.

Another factor which should not be neglected is the preparation of the mixture and the feeding into the extruder. In this study, lipids and aqueous phase were accurately weighted and either injected into the extruder without further preparation, using a syringe (manual injection), or samples were stirred after weighing for a few minutes until a pre-mixture was achieved which was then injected into the extruder manually or with a

pneumatic feeder (feed rate: 25 min⁻¹). Results show a rather high viscosity for the sample introduced without any preparation by manual injection (see Figure IV-6D). A pre-swelling of the mixture is urgently needed to achieve a homogenous mixture of the phospholipids with the aqueous phase. When both components are introduced to the extruder without previous stirring, only partial homogenization is achieved by extrusion and a crude VPG-mixture with separate water is the result. The obtained VPG has a lower water content in the gel and thus higher viscosity is the result (water amount in the VPG determined by gravimetric analysis: 33.9% (m/m) instead of 55% (m/m)).

Preparation of the VPG by stirring, gives the lipid time to swell in presence of the buffer. Introduction of this pre-mixture by manual injection or the pneumatic feeder results in viscosity comparable or slightly higher than the viscosity reached by the sample prepared with DAC. In both cases, water loss was below 4% (m/m) which is considered acceptable and may also be the case in VPG prepared by other methods (water loss not determined) as a result of weighing and other process steps. Manual injection is not the desired strategy for introduction of semisolid mixtures into an extruder. Feeders like the pneumatic feeder are more accurate in injection speed and less dead volume occurs. The slightly increased viscosity of the sample which was introduced with the pneumatic feeder, indicates a better mixing quality with smaller vesicles. Two main types of feeders are generally used in industrial scale extrusion: Volumetric feeders with an auger or screw conveyor, which discharges material from a hopper with constant volume per time and gravimetric feeders using a volumetric feeder associated with a weighing system to control the powder supply [13]. Both may be applicable in future scale up.

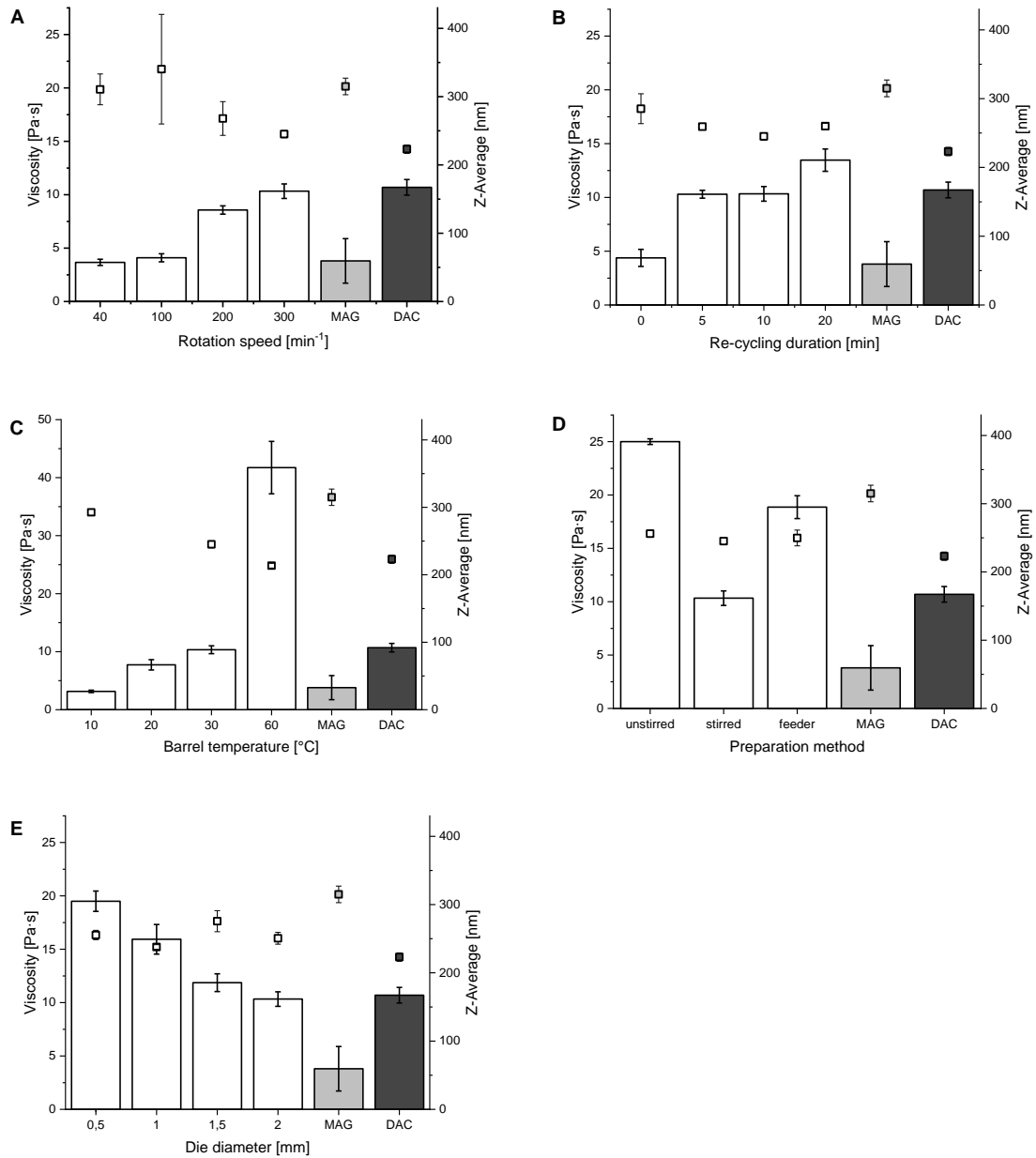


Figure IV-6: Effects of different parameters during extrusion on viscosity (bar plot) and vesicle size (scatter plot) after dilution of the VPG. A) Variation of the screw rotation speed. B) Variation of re-cycling duration. C) Variation of the barrel temperature. D) Comparison of different preparation methods. E) Variation of the die diameter. White symbols or bars represent samples prepared by extrusion, grey symbols or bars represent samples prepared by magnetic stirring and black symbols or bars represent samples prepared by dual asymmetric centrifugation. (Mean \pm SD; n=3)

Further, dies with different inner diameters were used. A decrease in die diameter led to increasing viscosity (Figure IV-6E). By using smaller dies, the pressure in the barrel and residence time of the material in the barrel is increased during the phase when the material is flushed from the barrel after re-cycling. Thus, better mixing may be achieved. However, due to the high amount of aqueous phase present in the mixture in comparison

to e.g. solid lipid implants, the residence time in the barrel could not be prolonged enough by the die only to achieve smaller vesicles.

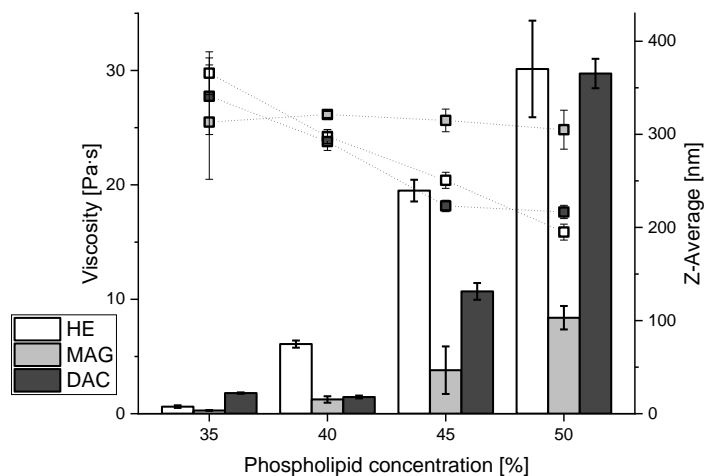


Figure IV-7: Effect of increasing phospholipid concentration on viscosity (bar plot) and vesicle size (scatter plot) after dilution of the VPG after preparation by different methods. White symbols or bars represent samples prepared by extrusion, grey symbols or bars represent samples prepared by magnetic stirring and black symbols or bars represent samples prepared by dual asymmetric centrifugation. (Mean ± SD; n=3)

Increasing phospholipid concentration of the VPG in general results in increasing viscosity. The same effect was observed here for different manufacturing techniques (bar plot in Figure IV-7). While viscosity increase was less pronounced for VPG prepared by magnetic stirring (from 0.3 ± 0.04 Pa·s for 35% (m/m) VPG to 8.4 ± 1.0 Pa·s for 50% (m/m) VPG), a stronger increase was observed for samples prepared by DAC (from 1.8 ± 0.06 Pa·s for 35% (m/m) VPG to 29.7 ± 1.3 Pa·s for 50% (m/m) VPG) or extrusion (from 0.6 ± 0.1 Pa·s for 35% (m/m) VPG to 30.1 ± 4.2 Pa·s for 50% (m/m) VPG). At the same time, smaller vesicles were achieved with increasing concentration of phospholipid when samples were prepared by extrusion or DAC, while no difference was observed in vesicle size when samples were prepared by magnetic stirring (scatter plot in Figure IV-7).

IV.3.2 Preparation of VPGs by a continuous extrusion process

IV.3.2.1 HAAKE MiniLab® Rheology Compounder

On the basis of the re-cycling run, a continuous run was developed. For this again, different parameters were changed i.e. screw rotation speed, temperature, die diameter

and the preparation method. An overview of the different runs which were conducted can be found in Table IV-4.

Table IV-4: Overview of settings changed during method development with the HAAKE MiniLab® extruder. (Varied parameters are emphasized for each experiment in bold letters.)

	Screw rotation speed [rpm]	Temp. [°C]	Die diameter [mm]	Pre-mixing method	Lipid concentration [% (m/m)]
A	40; 100; 200; 300	30	2.0	3min magnetic stirring	45
B	300	10; 20; 30; 60	2.0	3min magnetic stirring	45
C	300	30	0.5; 1.5; 2.0	3min magnetic stirring	45
D	300	30	2.0	3min magnetic stirring; feeder	45
E	300	30	0.5	3min magnetic stirring	35; 40; 45; 50

In the continuous run, rotation speed does not affect the viscosity of the VPGs (Figure IV-8A). Viscosity was for all four tested settings similar to the viscosity of the VPG prepared by magnetic stirring and is significantly lower in comparison to the viscosity of the VPG prepared by DAC. A trend to smaller vesicles with increasing rotation speed was observed. However, the residence time of the mixture in the barrel is not sufficient to achieve small vesicles and thus a high viscosity, even when shearing stress is increased by increasing the screw speed.

Table IV-5: Comparison of product temperature of the VPGs after extrusion and the set barrel temperature during continuous run. (n = 3; Mean ± SD)

Set barrel temperature [°C]	Product temperature [°C]
10	13.3 ± 0.2
20	20.5 ± 0.2
30	29.7 ± 0.2
60	54.3 ± 0.2

Additionally, the effect of different barrel temperatures on viscosity and vesicle size is determined. To evaluate if the efficiency of heat transfer from the barrel to the VPG during

extrusion, product temperature was determined directly at the die when the VPGs were flushed from the system.

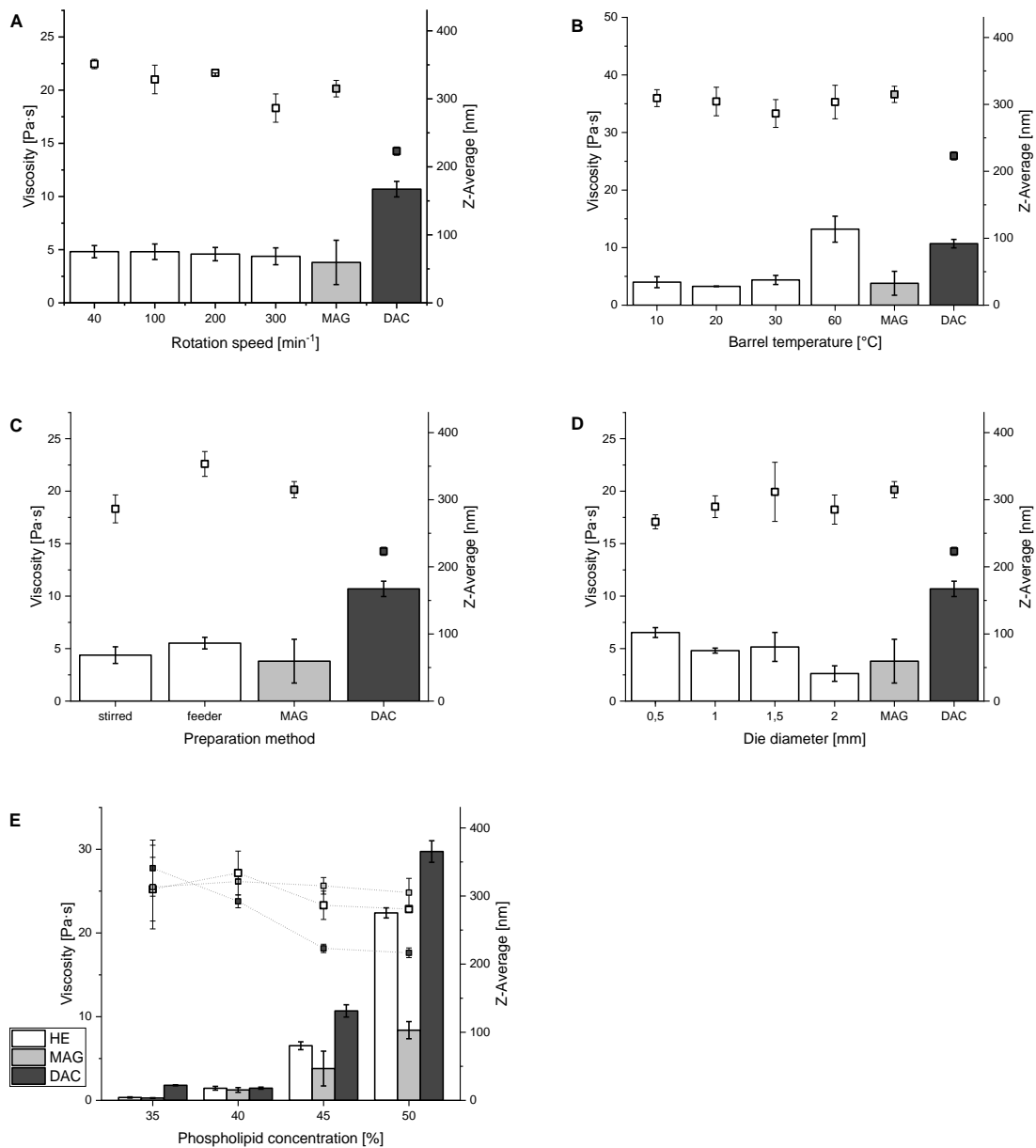


Figure IV-8: Effects of different parameters during extrusion on viscosity (bar plot) and vesicle size (scatter plot) after dilution of the VPG. A) Variation of the screw rotation speed. B) Variation of the barrel temperature. C) Comparison of different preparation methods. D) Variation of the die diameter. E) Comparison of different phospholipid concentrations. White symbols or bars represent samples prepared by extrusion, grey symbols or bars represent samples prepared by magnetic stirring and black symbols or bars represent samples prepared by dual asymmetric centrifugation. (Mean \pm SD; n=3)

Only a high temperature of 60 °C affected the viscosity (Figure IV-8B). For this sample water loss was determined by gravimetric analysis and only 1.5% (m/m) water was lost during extrusion. In this case, the high temperature above the melting temperature of the

phospholipid leads to softening of the material and thus better homogenization of the buffer phase with the soft phospholipids. However, a product temperature of 54.3 °C is too high for sensitive compounds and thus not suitable for the encapsulation of proteins and peptides. As already stated before, further optimization of the process temperature between 30 °C and 60 °C is needed.

Feeding the pre-mixed material into the extruder with the pneumatic feeder (feeding rate: 25 min⁻¹) led to a slight increase in viscosity of the VPGs in comparison to manual feeding with a syringe (Figure IV-8C). However, this trend is not significant and the viscosity of the DAC sample is not reached.

Similarly, the effect of the die diameter is minor. Decreasing the die diameter does not increase the viscosity statistically significant (Figure IV-8D). However, a trend to higher viscosities with decreasing size of the die is observed. Decreasing the size of the die, results in longer residence time in the barrel and thus mixing quality is improved. In a continuous extrusion run this effect should be even more pronounced in comparison to the re-cycling run, since residence time in the barrel can only be increased by smaller dies or slower rotation speed of the barrel. However, in the case of VPGs, the effect of the die diameter is minor. The buffer-phospholipid mixture shows better flowability in comparison to solid lipids or PLGA, used for implant preparation and thus further decrease of the die diameter may be needed to observe a stronger effect on residence time and mixing quality. The residence time is only prolonged for few seconds and the pressure in the barrel does not rise enough to obtain an improvement of homogenization during VPG preparation.

Increasing phospholipid concentration results in increasing viscosity for the samples prepared by extrusion and the other methods as well. Viscosity of the sample prepared by extrusion is between the viscosity of the samples prepared by magnetic stirring or DAC (Figure IV-8E). Determination of the vesicle size of these samples, confirms again, that increasing viscosity is correlated to smaller vesicles. In general, higher lipid concentration results in smaller vesicles and lower PDI values for samples prepared by extrusion or DAC. Thus, DAC and extrusion, both are able to prepare homogeneous mixtures of phospholipids with small vesicle sizes and small PDI, especially for high phospholipid concentration.

IV.3.2.2 ThreeTec ZE-5 Mini-Extruder

The ThreeTec extruder can be used for small lab scale production. In this study it was used as a smaller alternative to the above described HAAKE MiniLab®. In contrast to the MiniLab®, which is equipped with conical screws and has a rectangular setup of the screws to the die, the ZE-5 extruder is equipped with parallel screws and a linearly arranged die. During method development different settings of the extruder like screw speed, temperature and die diameter were varied and the obtained product was characterized. Table IV-6 summarizes the parameters which were varied in the different experiments.

Table IV-6: Overview of settings changed during method development with the ThreeTec ZE-5. (Varied parameters are emphasized for each experiment in bold letters.)

	Screw rotation speed [rpm]	Temp. [°C]	Die diameter [mm]	Die length [mm]	Pre-mixing method	Lipid concentration [% (m/m)]
A	40; 100; 200; 300	30	2.0	0.2	3min magnetic stirring	45
B	300	30; 60	2.0	0.2	3min magnetic stirring	45
C	300	30	0.4; 0.8; 1.5; 1.7; 2.0	0.2	3min magnetic stirring	45
D	300	30	0.4	0.2	3min magnetic stirring or vortexing	45
E	300	30	0.4; 0.8; 1.7; 2.0	0.2; 2.0	3min magnetic stirring	45
F	300	30	2.0	0.2	3min magnetic stirring	35; 40; 45; 50

An increase of rotation speed does not influence the viscosity significantly (Figure IV-9A). The viscosity of the obtained VPGs was comparable to the viscosity of VPGs prepared by magnetic stirring. In comparison to VPG prepared by DAC, both, magnetic stirring and extrusion, produced VPG with significantly lower values.

In contrast to these findings, a higher barrel temperature during extrusion of 60 °C (resulting product temperature: 61.1 ± 0.5 °C), results in slightly increased viscosity of the VPG (Figure IV-9B). Still, the viscosity values of VPG prepared by DAC are not reached and a decrease of the vesicle size is observed with increasing viscosity but still the values ranges in the area of the sample prepared by magnetic stirring. Additionally, higher temperatures may lead to degradation of the encapsulated drugs, especially when sensitive compounds like proteins are used. Hence, further optimization of the process temperature between barrel temperatures of 30 °C (product temperature 29.7 ± 0.2 °C) and 60 °C is urgently needed.

A short pre-mixing step of few minutes was found to be beneficial regarding the mixing quality. Different preparation techniques were tested before the material was introduced into the extruder. No differences were observed when the sample was vortexed before extrusion in comparison to the sample which was introduced into the extruder after simple magnetic stirring (Figure IV-9C). Thus, magnetic stirring was found adequate, since high shearing forces during vortexing could potentially result in instabilities of the encapsulated drug.

With decreasing inner diameter of the die, the viscosity increases slightly, however the homogeneity of the VPG, i.e. vesicle sizes and PDI, does not improve (Figure IV-9D). Again, this may arise from the comparably high flowability of the buffer-phospholipid mixture, resulting in less back-pressure from the die and shorter residence time in the barrel in comparison to the extrusion of solids, where the effect of the die is more pronounced. The length of the die does not affect the viscosity or vesicle size of the VPG significantly (Figure IV-9F).

An increase in phospholipid concentration of the VPG led to an increase of viscosity (Figure IV-9E). However, this increase was less pronounced for VPG prepared by magnetic stirring or extrusion in comparison to the sample prepared by DAC. Additionally, the deviation of the viscosity of the VPG prepared by magnetic stirring or extrusion of the viscosity of the VPG prepared by DAC was more explicit for VPGs with higher phospholipid concentration ($\geq 45\%$ (m/m)).

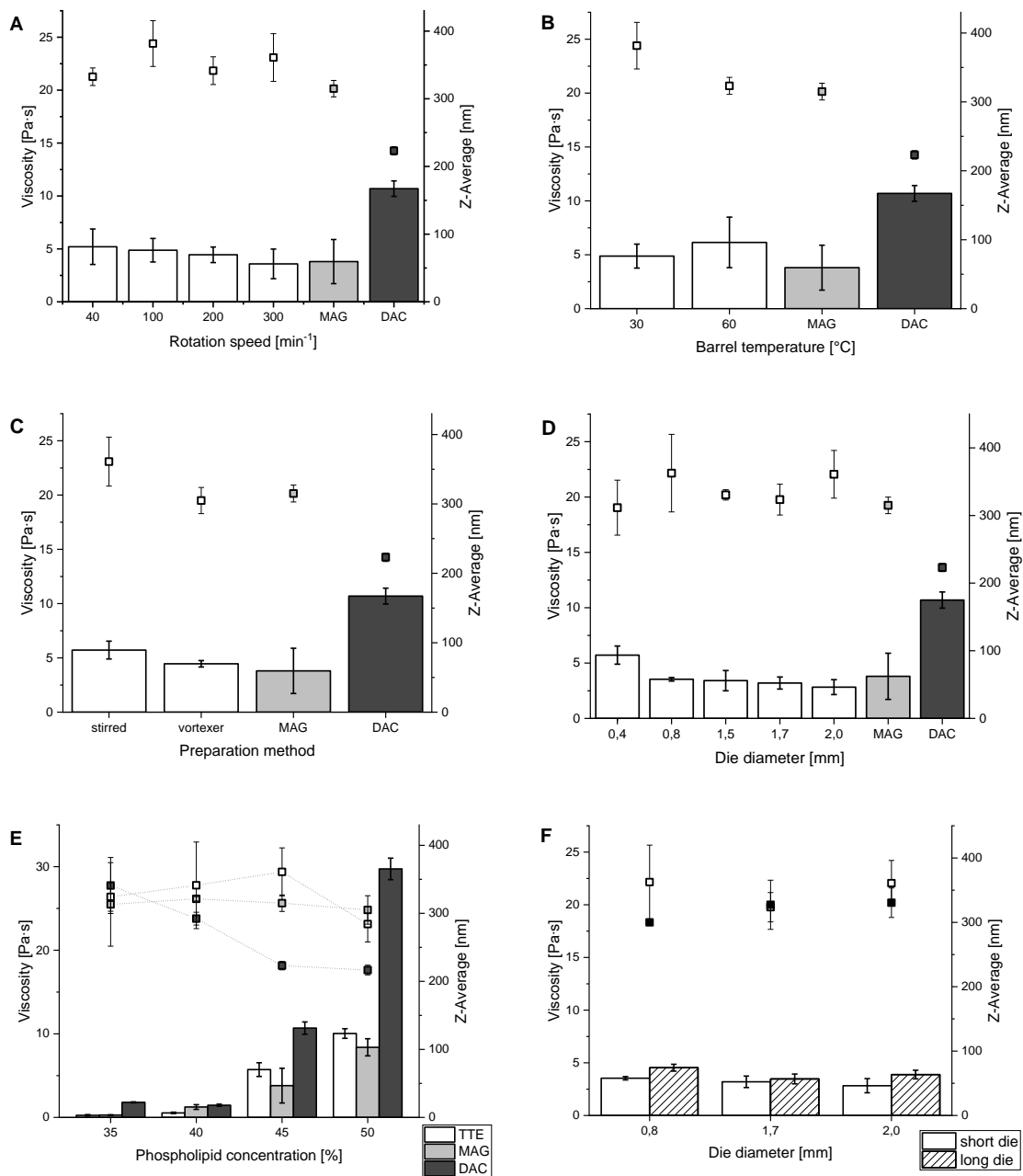


Figure IV-9: Effects of different parameters during extrusion on viscosity (bar plot) and vesicle size (scatter plot) after dilution of the VPG. A) Variation of the screw rotation speed. B) Variation of the barrel temperature. C) Comparison of different preparation methods. D) Variation of the die diameter. E) Comparison of different phospholipid concentrations. F) Comparison of the effect of different die lengths (short: 0.2 mm, long: 2.0 mm). White symbols or bars represent samples prepared by extrusion, grey symbols or bars represent samples prepared by magnetic stirring and black symbols or bars represent samples prepared by dual asymmetric centrifugation. (Mean \pm SD; n=3)

Characterization of the VPG with DLS showed particle sizes of approximately 300 nm for all VPGs with low phospholipid concentration (< 45% (m/m)) regardless of the preparation method. However, when the phospholipid concentration was increased (\geq 45% (m/m)) differences in particle size were observed between the different preparation methods.

VPG prepared by DAC showed smaller particles (approx. 200 nm) after dilution with corresponding lower PDI values (< 0.4), while VPG prepared by extrusion or magnetic stirring showed vesicle sizes of about 300 nm and a PDI value above 0.5. These findings are in good accordance with the above discussed assumption that smaller vesicles, result in a higher packing density and thus higher viscosity, while large vesicles result in lower viscosity.

By extrusion and magnetic stirring larger vesicles are produced which results in beneficial viscosity regarding the injectability of the VPG. Still, the release behavior has to be tested, to confirm if this most important feature of the VPG is maintained despite of the differences in particle size and viscosity.

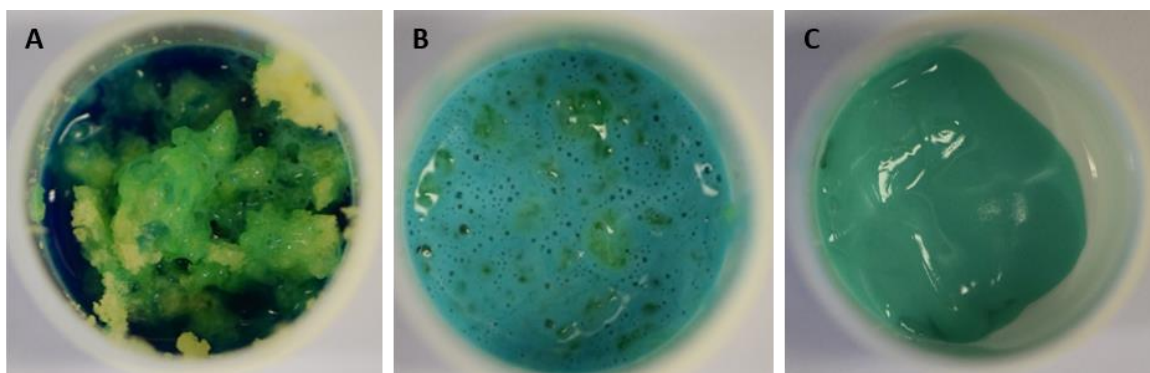


Figure IV-10: Macroscopic appearance of the VPG during preparation process by extrusion. A) Untreated phospholipids with methylene blue solution. B) Pre-mixture of phospholipids and methylene blue solution after 3 minutes of magnetic stirring. C) VPG after a single extrusion process of the pre-mixture.

Macroscopically, the VPG prepared by a single extrusion process using the Mini-Extruder ZE-5 was homogenous without any visible phospholipid particles or separation of the aqueous phase from the lipids (Figure IV-10).

IV.3.2.3 Leistritz Micro 27 GL – 28D

The Leistritz Micro 27 GL-28D extruder is an instrument used for large-scale production. A minimum amount of 300 g of material is needed to process it with this extruder. Similarly to the ZE-5 extruder, it is equipped with parallel screws and a linearly arranged die. The extruder is equipped with a gravimetric feeder with integrated conveyance screws to transport the material to the inlet. The liquid phase is pumped into the extruder separately. However, this feeding system could not be used due to poor flowability and stickiness of the phospholipid powder at room temperature. An advantage of the extruder is the modular construction of the screws, which enables the design of different screws

with mixing, kneading and conveying elements as desired. In this study, a conveying screw, composed of only conveying elements, and a mixing screw, composed of mixing and kneading elements as well as conveying elements, were used to investigate the impact of different screws on the product quality.

Viscosity and vesicle size were investigated to compare the two screws with each other. Additionally, the overall performance of the extruder in comparison to DAC and magnetic stirring was evaluated in terms of viscosity and vesicle size.

By the incorporation of mixing and kneading blocks in the screw design, superior mixing quality can be reached [13]. In the present study, the usage of a screw equipped with mixing and kneading elements affected the VPG characteristics. Viscosity is higher when the mixing screws are used, in contrast to the conveying screws. However, this effect is only statistically significant for a phospholipid concentration of 45% (m/m) and no differences were observed for a phospholipid concentration of 40% (m/m) (Figure IV-11A). Just changing the screws from a conveying only design to a mixing design, does not affect size of the vesicles after dilution (Figure IV-11B) and the PDI (Figure IV-11C), regardless of the phospholipid concentration. The rotation speed of the screws has two effects. First, the residence time of the material in the barrel is affected i.e. short residence times for fast rotation speed and second, the high shearing forces can be achieved by fast rotation of the screws. The effect of the rotation speed on the VPG properties was evaluated with the mixing screws, since these were expected to affect the material properties more effectively. When the rotation speed of the screws was decreased, no significant changes in viscosity were observed in comparison to the fast mixing. However, viscosity was significantly increased for both rotation speeds in comparison to the conveying screw. This effect was only statistically significant for a phospholipid concentration of 45% (m/m), not for 40% (m/m). Size of the vesicles obtained after dilution of the VPG significantly increased with decreasing rotation speed when the mixing screws were used. No significant differences regarding PDI were observed for all setups and formulations.

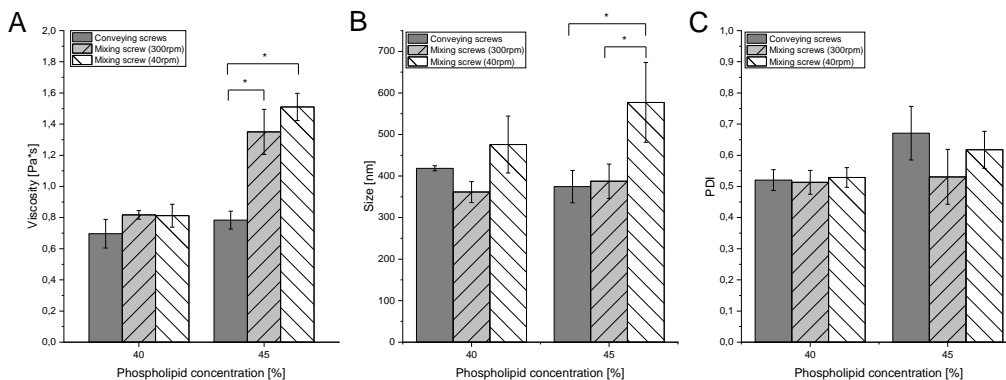


Figure IV-11: Effect of screw design and speed on A) viscosity, B) Size and C) PDI of VPGs after dilution. VPGs with a phospholipid concentration of 40% (m/m) and 45% (m/m) were prepared.

Independent of the differences which could be shown in viscosity and size measurement when using a mixing screw or different rotation speed of the screw, the VPG prepared with the large extruder shows extremely low viscosity in comparison to VPG prepared by DAC or the two other extruders at a phospholipid concentration of 45% (m/m) (see Figure IV-12). The extremely low viscosity is advantageous regarding the injectability of the depot system. However, it is questionable if the viscosity and differences in vesicle size also influences the release behavior of drug substances from VPG and if the dispersion quality and stability meet pharmaceutical standards.

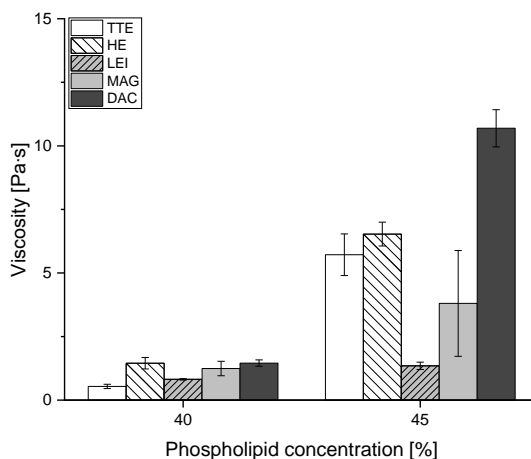


Figure IV-12: Comparison of viscosity of VPGs prepared by different methods, with increasing phospholipid concentration.

IV.3.3 *In vitro* release of FITC-Dextran from VPG

VPG with a phospholipid concentration of 45% (m/m), containing 2 mg/g FITC-dextran (70 kDa) was prepared with the above described manufacturing methods. For preparation by extrusion, the following settings were used: screw rotation speed 300 rpm, barrel temperature 30 °C, die diameter depending on the extruder (0.4 mm ThreeTec ZE-5; 0.5 mm HAAKE MiniLab®). All samples were prepared by a single continuous run.

Release from VPG is mainly dominated by erosion and matrix-controlled diffusion [34]. When looking at the physical parameters of VPGs, release rates depend on viscosity, since a high viscosity results in higher resistance of the material to the flow. Thus, a slow release was expected for VPGs with high viscosity i.e. the samples prepared by DAC. The viscosity of all 45% (m/m) VPG formulations used for FITC-dextran release is shown in Figure IV-13A.

Surprisingly, all samples showed sustained release of FITC-Dextran over 52 days with a zero-order like release behavior, independently of the manufacturing method (see Figure IV-13B). Still, slight differences were observed for the differently prepared samples. VPG prepared by DAC showed the fastest FITC-dextran release, followed by the VPG prepared with the ThreeTec ZE-5 and the VPG prepared by magnetic stirring. Slowest release was observed for the VPG prepared with the HAAKE MiniLab® extruder.

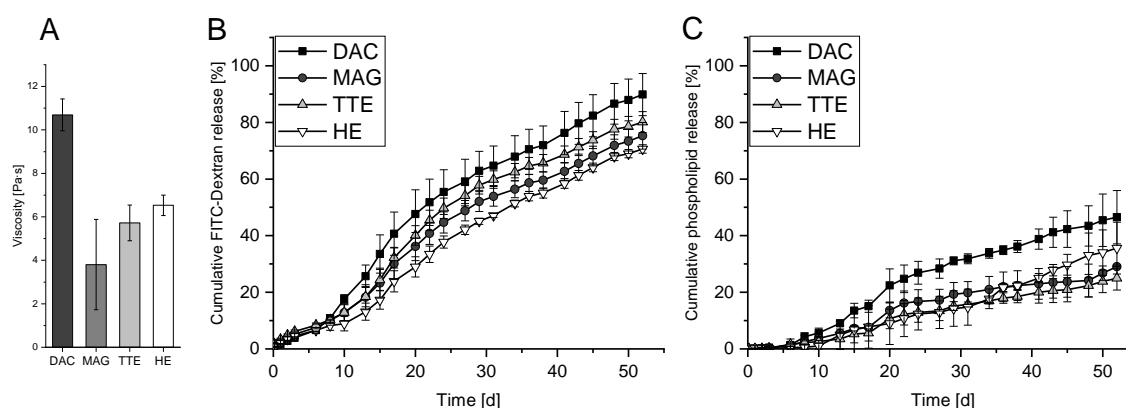


Figure IV-13: Characterization of *in vitro* release behavior of the model compound FITC-Dextran (70 kDa) from 45% (m/m) VPG. VPG were prepared by dual asymmetric centrifugation (DAC), magnetic stirring (MAG) or extrusion using the ThreeTec ZE-5 Mini-Extruder (TTE) or the HAAKE MiniLab® Rheology Compounder (HE). A) Viscosity at shearing rate of 32.9 s⁻¹. B) Cumulative release of FITC-Dextran (70 kDa). C) Cumulative release of phosphatidylcholine for characterization of the erosion process. (Mean ± SD, n=3)

To characterize the erosion behavior of the differently prepared VPGs, phosphatidylcholine concentration was determined in the released fractions and optical

density was measured. The released amount of PC is shown in Figure IV-13C. Both release profiles together indicate a mixture of diffusion and erosion as the dominating release mechanisms. This impression is supported by optical density measurements (data not shown). The smaller vesicles sizes obtained in the VPG prepared by DAC may result in higher viscosity, however, it also leads to a faster erosion of the VPG matrix and thus faster FITC-dextran release. At the same time the larger vesicles obtained after preparation of the VPG by extrusion or magnetic stirring, results in slower release rates and thus slower FITC-dextran release.

Further, released fractions were characterized by measuring the vesicle size in the sample by DLS. Results show the smallest vesicles for the sample prepared by DAC (≤ 500 nm), while larger vesicles (≥ 500 nm) were found in the released fractions of all other samples (Figure IV-14A). Additionally, PDI was comparably low for the released fractions from the sample prepared by DAC (Figure IV-14B).

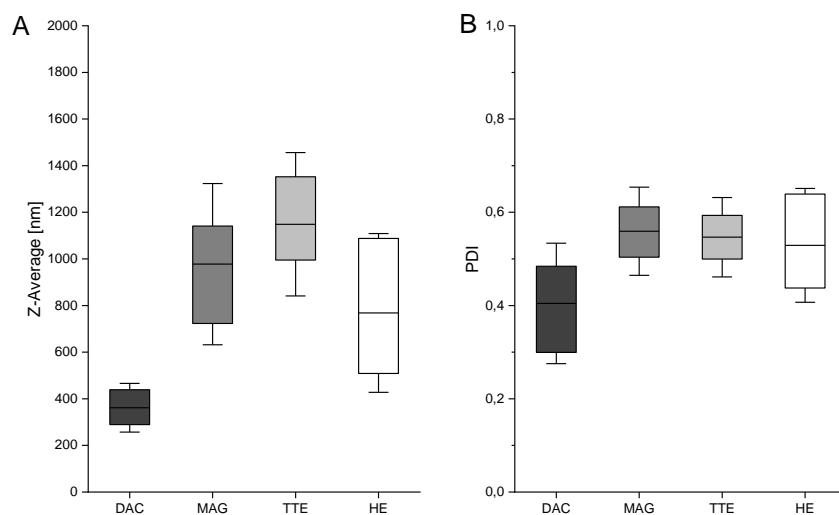


Figure IV-14: Characterization of the released fractions. A) Vesicle sizes determined in the released fractions. B) PDI of the released fractions. Black lines show mean, boxes show 25-75% range and error bars show standard deviation. All values were calculated from measured data of all released fractions (n = 25 in triplicates).

IV.3.4 Stability of proteins in VPG after encapsulation and storage

IV.3.4.1 Determination of structural changes by FTIR spectroscopy

Conformational changes of the protein are commonly determined by FTIR spectroscopy. In general, FTIR spectroscopy is a commonly used technique for the characterization of

proteins directly in the matrix in which they are embedded e.g. in PLGA microspheres [35]–[37]. The applicability of the system was evaluated using ovalbumin (OVA) as high amounts of protein are needed in the VPG to obtain FTIR spectra from the diluted samples and OVA is cheap and easily acquired in large quantities.

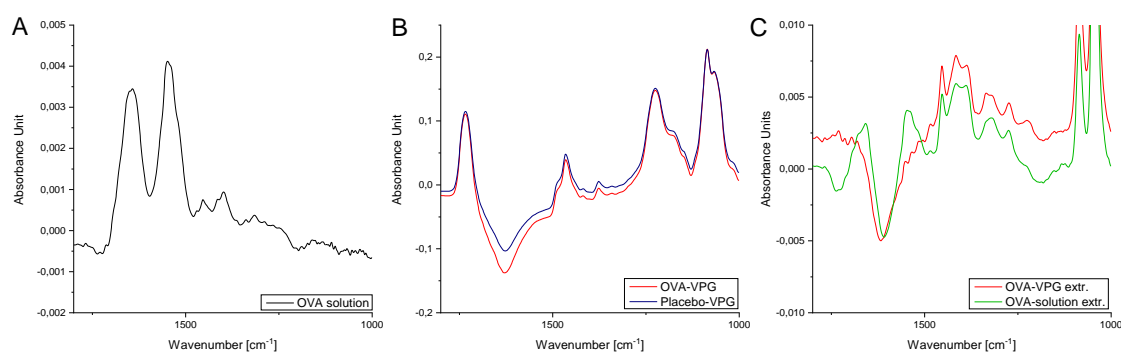


Figure IV-15: FTIR spectra of OVA. A) OVA-solution; B) OVA-VPG (red) and placebo VPG (blue) directly on the ATR-crystal; C) OVA-VPG after dilution and chloroform extraction (red) and OVA-solution after extraction treatment (green).

The spectrum of a native OVA solution is illustrated in Figure IV-15A and shows two defined amid bands (amid I $\approx 1650\text{ cm}^{-1}$ and amid II $\approx 1550\text{ cm}^{-1}$) as it was expected. As already described by Weiwei Tian for G-CSF, it was not possible to detect OVA in the VPG itself (Figure IV-15B), after dilution of the OVA-VPG or extraction of the protein from the VPG (Figure IV-15C) [27]. The baseline in the range of the two amid bands is not flat when OVA is encapsulated into VPG or extracted from VPG and thus background subtraction is not possible [35]. Hence, it is not possible to investigate the secondary structure of the protein in the VPG without a suitable extraction method which does not interfere with the spectrum of the protein solution. The development of such an extraction method is beyond the scope of this thesis and thus not further investigated.

IV.3.4.2 Evaluation of capillary gel electrophoresis to characterize protein aggregation and fragmentation in VPG

On-chip capillary gel electrophoresis, using an Agilent 2100 Bioanalyzer is a method to characterize aggregates or fragments in protein samples. Since the system offers fast and reliable separation, as well as sizing and quantification of proteins of a molecular weight between 14 kDa and 230 kDa, it is a convenient and preferred analysis method in comparison to others. Capillary gel electrophoresis has been successfully used before to

investigate protein integrity after encapsulation and during release from solid lipid implants [18]. However, in the case of VPGs a complete extraction of the protein from the phospholipids is not possible.

First, EPO-VPG was used for analysis. However, the glycosylated protein did not show any signal on the chip. Thus, non-glycosylated IFN β -1b was used to test the system for its applicability. IFN β -1b showed reproducible signals in the stock solution and a heat-stress control revealed protein aggregation linked to a decrease in the monomeric peak.

However, when samples from VPGs were analyzed (Figure IV-16), the signal of the internal standard protein ladder was disturbed and a broadly tailing peak was found in the area of the expected molecular weight of the protein (ca. 20 kDa). To remove some of the lipid from the sample, samples were centrifuged and the clear supernatant was reanalyzed. However, this procedure resulted in massive protein loss and insufficient lipid removal. Still, the signal of the on-chip gel electrophoresis was disturbed by the remaining phospholipids (dashed line in Figure IV-16). Thus, it was concluded that on-chip gel electrophoresis is not suited for samples from VPGs until a method for complete extraction of the phospholipids from the samples is found.

Additionally, the method is not applicable for large molecules like monoclonal antibodies and therefore could not be used to investigate the stability of mAb, since aggregates of the antibodies (ca. 150 kDa) are already outside of the detectable range.

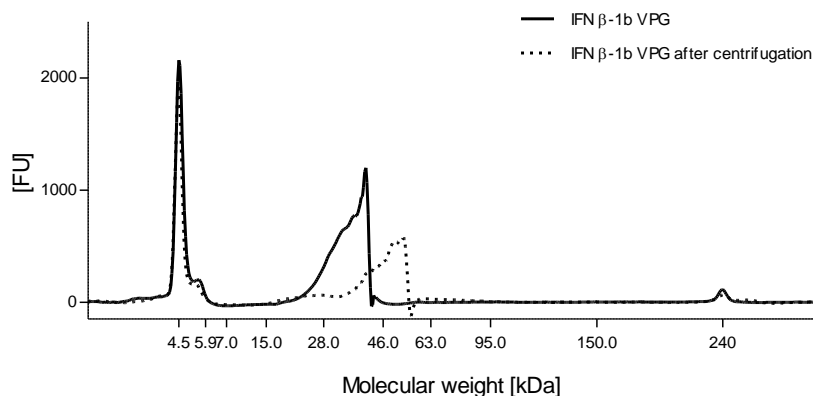


Figure IV-16: Chromatograph of IFN β -1b incorporated in VPG directly after dilution (solid line) or after centrifugation (dotted line).

IV.3.4.3 Characterization of protein aggregation by SDS-PAGE

In order to determine if the extrusion process induces protein destabilization e.g. aggregation, the VPG was diluted to a final protein concentration of 0.05 mg/ml with

buffer directly after preparation and used as sample for SDS-PAGE. VPG containing EPO or mAb as model proteins were analyzed by non-reducing SDS-PAGE with subsequent silver staining.

EPO-stock solution showed only a single band arising from monomeric EPO (line 2 in Figure IV-17A). Lines 3 to 6 in Figure IV-17A show the signal of EPO encapsulated in VPG prepared by the different methods: DAC, magnetic stirring and extrusion with either the ThreeTec extruder or HAAKE-extruder. All samples show primarily the single band from monomeric EPO, leading to the conclusion that EPO is encapsulated into VPGs mainly in its monomeric form. After one month (Figure IV-17B) or three months (Figure IV-17C) of storage of the EPO-VPG at 2 to 4 °C, again primarily monomeric EPO was found after analyzing the samples by SDS-PAGE.

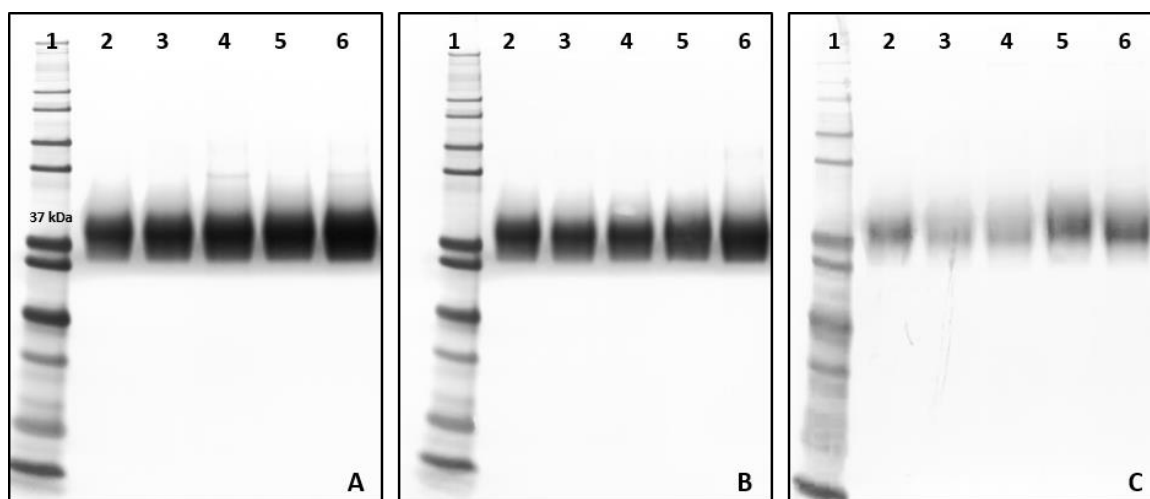


Figure IV-17: Investigation of EPO stability in VPG evaluated by SDS-PAGE. A) Directly after preparation of the VPG by the different techniques. B) After one month storage of the VPG prepared by different techniques. C) After three months storage of the VPG. Line 1: Molecular weight standard; Line 2: EPO-stock solution; Line 3: EPO-VPG prepared by DAC; Line 4: EPO-VPG prepared by magnetic stirring; Line 5: EPO-VPG prepared with ThreeTec extruder; Line 6: EPO-VPG prepared by HAAKE-extruder.

VPGs prepared with different manufacturing techniques, containing a monoclonal antibody of the IgG-type were investigated. As described above, samples were used for SDS-PAGE directly after dilution from the VPG with buffer (final protein concentration 0.05 mg/ml) without further extraction of the phospholipids.

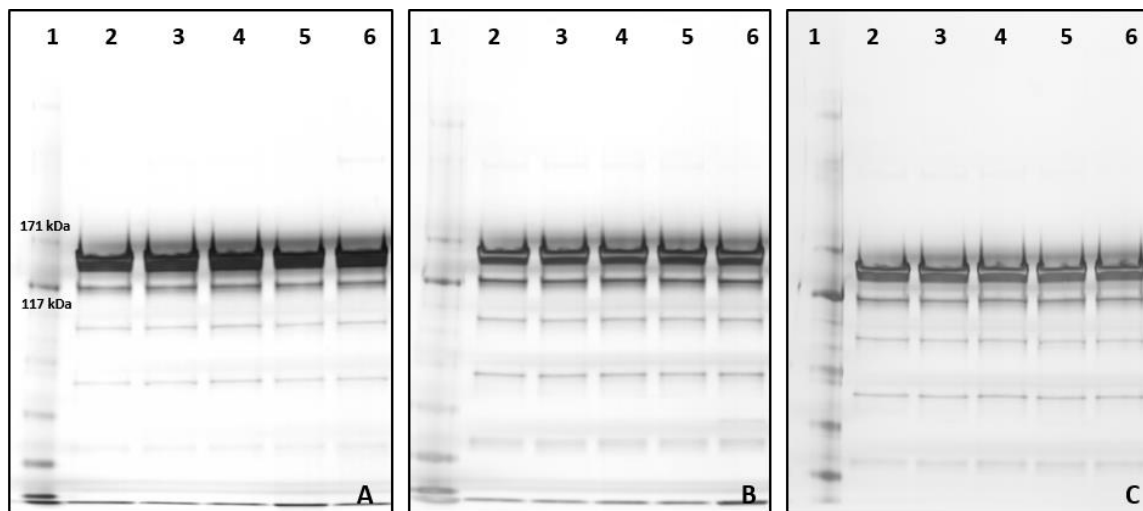


Figure IV-18: Investigation of mAb stability in VPG evaluated by SDS-PAGE. A) Directly after preparation of the VPG by the different techniques. B) After one month storage of the VPG prepared by different techniques. C) After three months storage of the VPG. Line 1: Molecular weight standard; Line 2: mAb-VPG prepared by DAC; Line 3: mAb-VPG prepared by magnetic stirring; Line 4: mAb-VPG prepared with ThreeTec extruder; Line 5: mAb-VPG prepared by Leistritz-extruder; Line 6: mAb-stock solution.

Next to the band arising from monomeric mAb at approximately 145 kDa, a few, paler bands with lower molecular weight, i.e. representing fragments of the antibody, are visible (Figure IV-18A). These fragments are already present in the mAb-bulk material (line 6) and no further aggregates were found. After all the antibody is stable over one (Figure IV-18B) and three months (Figure IV-18C) of storage in the VPG and no new bands for aggregates or fragments are found.

TSC extrusion has been used before to manufacture protein or peptide loaded depot formulations e.g. solid lipid implants and its applicability for these sensitive compounds has been shown [18], [38]. In 2009, Schulze et al. showed that the manufacturing process by TSC extrusion does not induce protein destabilization for interferon α (IFN- α) [17]. In the present study the applicability of TSC extrusion for sensitive compound like proteins is confirmed. SDS-PAGE shows that encapsulation of EPO or a monoclonal antibody into VPG does not lead to significant protein aggregation or fragmentation and the protein is stable in the VPG for up to three months after preparation at a storage temperature of 2 to 4 °C. However, in the present study SDS-PAGE was not qualified with a sample showing aggregation or degradation of the two proteins. Thus, even though the method has been a standard method for determining protein aggregation and fragmentation over many

years, results have to be seen critically and further experiments are needed for a definite statement about stability of the two proteins in VPGs.

IV.3.5 *In vitro* release of a monoclonal antibody from VPG

In order to support the data obtained from the *in vitro* release of FITC-dextran, which was used as a cheap and easy to quantify model compound for proteins, the release behavior of a monoclonal antibody of the IgG-type was determined. Furthermore, simultaneously the release behavior of phosphatidylcholine (PC), which is the major component of Lipoid E80, is investigated to characterize the erosion process of the VPG. VPG was either prepared with the ZE-5 extruder (TTE) or with the Leistritz extruder (LEI) and compared with a sample prepared by the standard method DAC. All three VPG show sustained release of mAb and PC (Figure IV-19).

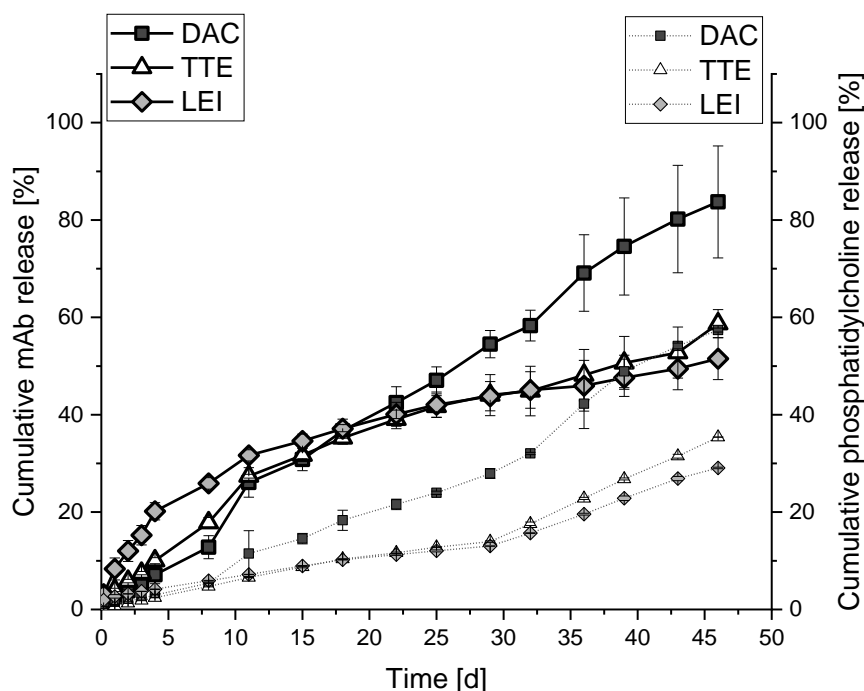


Figure IV-19: Characterization of *in vitro* release behavior of mAb from VPG (large symbols, solid lines, left axis) in comparison to cumulative release of phosphatidylcholine (small symbols, dashed lines, right axis). mAb-VPG (10 mg/g) was prepared by dual asymmetric centrifugation (DAC) or extrusion using the ThreeTec ZE-5 Mini-Extruder (TTE) or the Leistritz Micro 27 GL (LEI). (n=3, Mean \pm SD).

However, differences between the release profiles of mAb are obvious. An almost linear release behavior with a release rate of 0.2 to 1.6% per day was observed for mAb released from VPG prepared by DAC. In contrast to that, the VPG prepared with the Leistritz extruder showed a fast release of mAb (ca. 5% per day) in the first 5 days of the release

period, which then slows down (0.1% per day). The VPG prepared with the ZE-5 extruder, shows similar release behavior to the sample prepared by DAC in the first 20 days of the release period, after which the release rate of the TTE sample decreases and slower release is observed (0.1% per day).

As observed for the mAb release, differences in PC release were observed as well. Almost linear PC release is observed for all three VPG. However, PC is released faster from VPG prepared by DAC. In this case, mAb release and PC release can be linearly correlated and differences between the two curves may be explained by diffusion-controlled release of the antibody next to the erosion process and release of the antibody which is adsorbed to the surface of the VPG and is released faster and easier. In contrast to that, the correlation between erosion of the PC matrix and mAb release is not as obvious for the two samples prepared by extrusion. Especially in the beginning of the release test, the LEI sample shows fast release of the mAb. This may derive from the loosely attached mAb on the surface of the VPG. This fraction is larger in comparison to the TTE and DAC sample. In the second phase of the release experiment, mAb release from the LEI and TTE sample is slower again and can now be correlated to the slow PC release and thus the erosion of the phospholipid matrix.

In general, *in vitro* release tests with FITC-dextran and mAb both show slower erosion when VPG is prepared by extrusion in comparison to VPG prepared by DAC. This effect may derive from the above described differences in vesicle size and homogeneity of the VPG. VPG with larger vesicles disintegrate slower despite of the lower viscosity of the VPG which may falsely be taken as an indicator for release behavior. Larger vesicles result in a higher packing density of the VPG matrix, which may result in slower erosion of the VPG. A certain rate of polydispersity of the system may contribute to the increase in packing density to some extent and thus reinforce this effect. A similar phenomenon has been described before by Tardi et al., who observed a slower release of the hydrophilic marker carboxyfluorescein from VPGs which were previously sterilized by autoclaving [39]. The steam sterilization process led to an increase in vesicle size e.g. by fusion of the primarily small vesicles and as a result of that slower release rates were achieved. Both, the VPG prepared by the ZE-5 extruder and by the Leistritz extruder show slower release of the phospholipids.

In the light of these findings it is still surprising that VPG prepared with the Leistritz extruder, with a tendency to even larger vesicles and increased polydispersity, releases its content faster in the first few days in comparison to the VPG prepared with the ZE-5 extruder. This difference can be explained by differences in the encapsulation of the antibody. True encapsulation of the antibody into the vesicles of the VPG results in longer release times (VPG prepared by ZE-5 extruder and DAC), while loosely adsorbed antibody to the outer surface of the VPG is released faster. A mixture of both encapsulation types may be present in VPG independently of the preparation method. However, the fraction of loosely adsorbed mAb in comparison to truly encapsulated mAb may change, depending on the homogenization quality. VPG prepared by the Leistritz extruder releases the mAb faster in the first few days since it is not truly encapsulated and thus is released with a faster off-rate. This theory is also supported by the data obtained from the phospholipid assay. The difference in encapsulation may be influenced by slight differences in setup of the extruders. Due to its large size, the Leistritz extruder has larger slits between the two intermeshing screws, which may result in lower mixing quality and thus less true mAb encapsulation into the vesicles.

After all, in the context of erosion driven release, one should also take into account the release model which was used. Flow-through cells (which are used here) are the standard release systems for VPG. Their shape and setup allow their application with comparable volumes as they might be used for depot systems like VPG *in vivo*. The defined exposed surface of the VPG to the acceptor medium maintains the same throughout the release test, allowing a good comparability between data. A constant flow models the situation *in vivo* to some extent. Additionally, no membrane is needed to separate the VPG from the acceptor medium, thus membrane influence on the release behavior is out of the question. However, the absence of a membrane also facilitates the erosion of larger VPG fragments and particles which might be restricted in the subcutaneous tissue *in vivo*. This has to be considered when looking at the *in vitro* release. Vollrath et al. showed a sustained release of a mAb over more than 100 days *in vitro* from solid lipid implants (SLI) [18]. Similar *in vitro* release time for another mAb from SLI was observed by Sax [20]. Thus, a sustained release of mAb of more than 50 days but below 100 days from VPG as semi-solid depot system, is within expectations, showing that the release model itself produces data in a realistic range.

IV.3.6 Storage stability of VPG prepared by different manufacturing processes

In order to assess the physical stability of the VPG over three months, VPG with a phospholipid concentration of 40% (m/m) prepared by DAC, magnetic stirring and TSC extrusion with the different extruders were stored at 2 to 4 °C and 25 °C for three months. The process parameters used for preparation of the VPGs by TSC extrusion are summarized in Table IV-7.

Samples were characterized by oscillatory rheologic measurements, DLS, microscopy and macroscopic appearance directly after preparation. Subsequently, samples were taken at predetermined time points and analyzed.

Table IV-7: Overview on process parameters during preparation by extrusion.

Extruder		Rotation speed [rpm]	Temperature [°C]	Screw	Die diameter [mm]
ThreeTec Extruder ZE-5	Mini-	300	30	Conveying, parallel	0.4
HAAKE Micro Compounder	MiniLab® Rheology	300	30	Conveying, conical	0.5
Leistritz Micro 27 GL		300	30	Mixing, parallel	1.0

Oscillatory rheologic measurements can not only be used to characterize multiphase viscoelastic systems and their internal structure, but also to predict the stability of these systems [40]. Typically, storage modulus (G') and loss modulus (G'') are determined directly by the rheometer. While G'' represents the viscous behavior of a sample, G' is a measure for the elastic behavior of the material. At the flow point or cross over point ($G' = G''$) the gel character of a systems turns into liquid character [41]. The flow point correlates to the strength of inter-particle interaction in the three-dimensional network of a semisolid formulation [40]. A high value indicates a higher amount of contact surfaces and more dense packing between the particles. Further, the difference between G' and G'' at the linear viscoelastic (LVE) region can be correlated to stability [42]. In the course of this study, an amplitude sweep was conducted for each sample and the difference between G' and G'' as well as the flow point were determined. Figure IV-20 shows

representative amplitude sweeps for each VPG (40% (m/m) Lipoid E80 in 20mM PBS pH 7.4) prepared by different manufacturing methods.

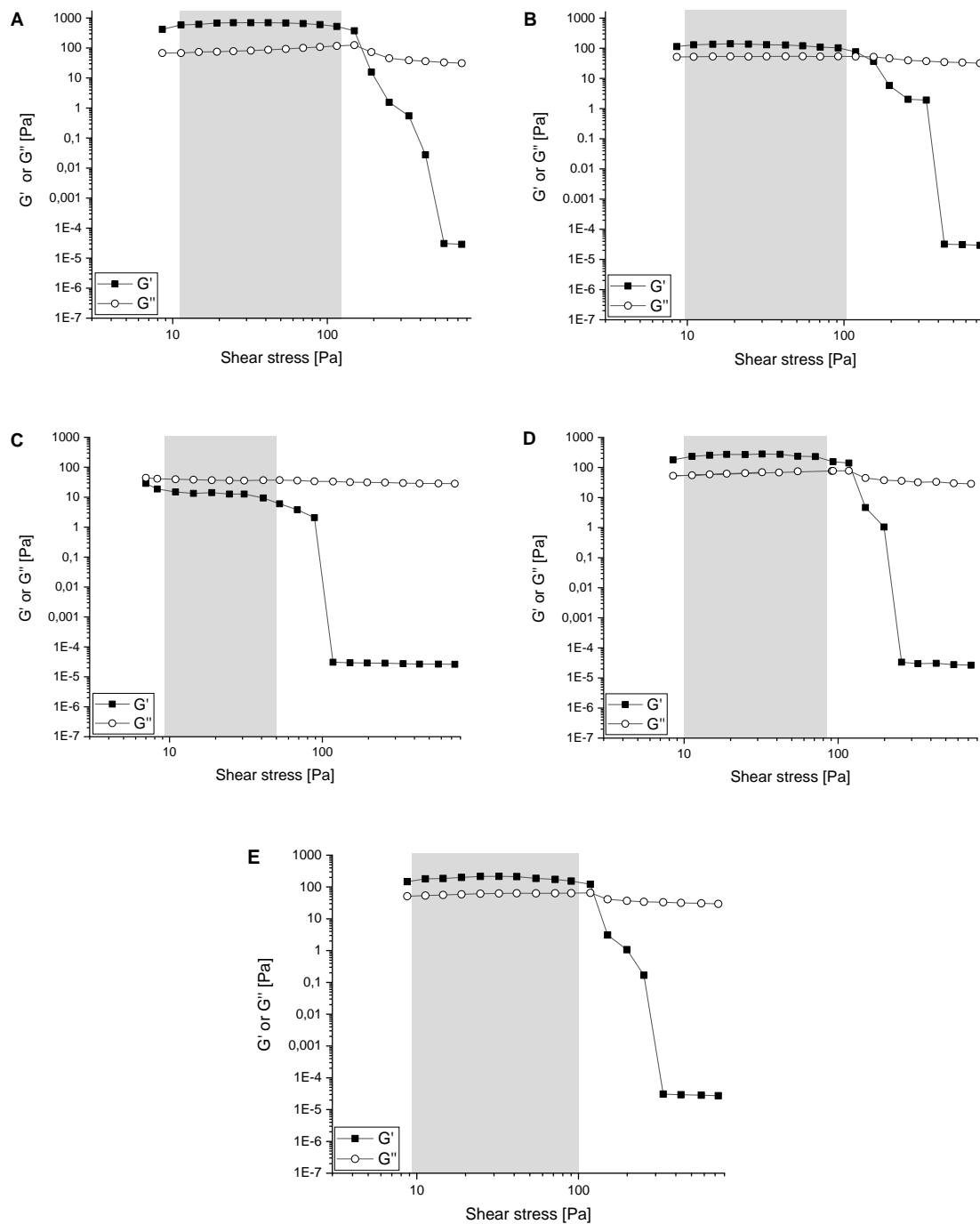


Figure IV-20: Amplitude sweep for VPGs (40% (m/m) Lipoid E80, 20mM PBS pH 7.4) prepared by A) DAC, B) HAAKE MiniLab® extruder (HE), C) Leistriz extruder (LEI), D) ThreeTec ZE-5 Mini-Extruder (TTE) or E) magnetic stirring (MAG). LVE-region is marked in grey.

The samples prepared by DAC, magnetic stirring, the ThreeTec ZE-5 Mini-Extruder or the HAAKE MiniLab® extruder show a larger storage modulus than loss modulus in the

beginning of the measurement. The elastic portion of the viscoelastic behavior is larger in this case. This is caused by a tight inner structure of the gel. Links inside the material, e.g. chemical bonds or physical-chemical interactions lead to inter-particle interactions and a highly ordered structure. Only the sample prepared by the Leistritz extruder shows a larger loss modulus than storage modulus from the beginning. In this case the sample shows the behavior of a liquid rather than a gel. Additionally, the VPG prepared by DAC shows the highest rigidity (high G') from the beginning, thus it has the thickest consistency in comparison to all other samples.

Table IV-8 summarizes the rheologic parameters. The linearity limit of the LVE-region, described by the yield point, indicates the maximum deformation tolerated by the sample [40], [43]. The yield point was estimated based on the graphs in Figure IV-20 as the last τ -value of the LVE-region at which G' is beginning to show a noticeable deviation from the previously constant values. As expected, the sample prepared by DAC exhibits the highest yield point.

Table IV-8: Parameters derived from rheologic measurements.

Sample	Yield point τ_y [Pa]	Flow point τ_f [Pa]	$G'-G''$ in LVE-region [Pa]	Viscosity at $\dot{\gamma} = 32.9 \text{ s}^{-1}$ [Pa·s]
DAC	167.4 ± 28.9	179.2 ± 22.9	459.8 ± 196.2	1.9 ± 0.1
HE	100.1 ± 16.1	111.4 ± 21.1	155.4 ± 108.7	1.2 ± 0.2
LEI	76.0 ± 11.1	-	-15.1 ± 13.5	0.8 ± 0.1
TTE	106.2 ± 14.5	113.3 ± 14.8	261.9 ± 156.8	0.9 ± 0.1
MAG	93.9 ± 24.1	105.1 ± 25.6	119.2 ± 18.2	0.9 ± 0.1

Mechanical stability of the DAC sample is higher in comparison to the others. The LEI sample is characterized by the lowest limit value for the LVE-region. Furthermore, for this sample no flow point could be determined since G' is below G'' from the beginning. For all other samples the flow transition index (τ_f / τ_y) approaches the value 1, indicating a higher tendency of the samples for brittle fracturing [41], [43]. VPGs produced by the ThreeTec ZE-5 and HAAKE MiniLab® show increased stability in comparison to the sample

prepared with the Leistritz extruder. The difference between magnitude of storage modulus and loss modulus in the LVE-region is another stability indicating factor. This difference is the highest for samples prepared by DAC, while the samples prepared either by magnetic stirring or by extrusion using the ThreeTec ZE-5 or HAAKE MiniLab® extruder showed significantly lower values. Thus, the sample prepared by DAC is the most stable system, followed by the samples prepared by the two smaller extruders (TTE and HE) and the sample prepared by magnetic stirring. Preparation of VPG with the Leistritz extruder results in a product with rather liquid properties in comparison. In this case, the mixture of phospholipid and buffer is unstable and phase separation may occur.

In the light of the *in vitro* release study presented above, where sustained release of a mAb was shown from samples prepared with the Leistritz extruder, the phospholipid concentration has to be taken into account. In the release study VPG with 45% (m/m) phospholipids was tested, while storage stability was determined with VPG with a phospholipid concentration of 40% (m/m). A higher concentration of phospholipid may lead to a better mixing quality, VPG with more viscous character and an increased rate of true encapsulation. Additionally, the encapsulation of a protein e.g. a monoclonal antibody may affect the viscoelastic behavior of the VPG. In this context, Neuhofer observed an increase in VPG viscosity when proteins like IFN- β were encapsulated [44]. He observed a change in viscoelastic behavior from plastic to rheopectic behavior after incorporation of the protein. However, the effect of mAb encapsulation on VPG properties and stability of the VPG was not within the scope of this work and should be investigated in the future.

Next to the oscillatory tests performed directly after preparation, rotational experiments were conducted at each predetermined time point. Viscosity of the sample prepared by DAC is the highest followed by the HE, TTE and MAG, while the sample prepared with the Leistritz extruder shows the lowest viscosity (Figure IV-21A and Figure IV-21B). Furthermore, viscosity of the samples increases slightly during storage. This trend is observable for both storage temperatures.

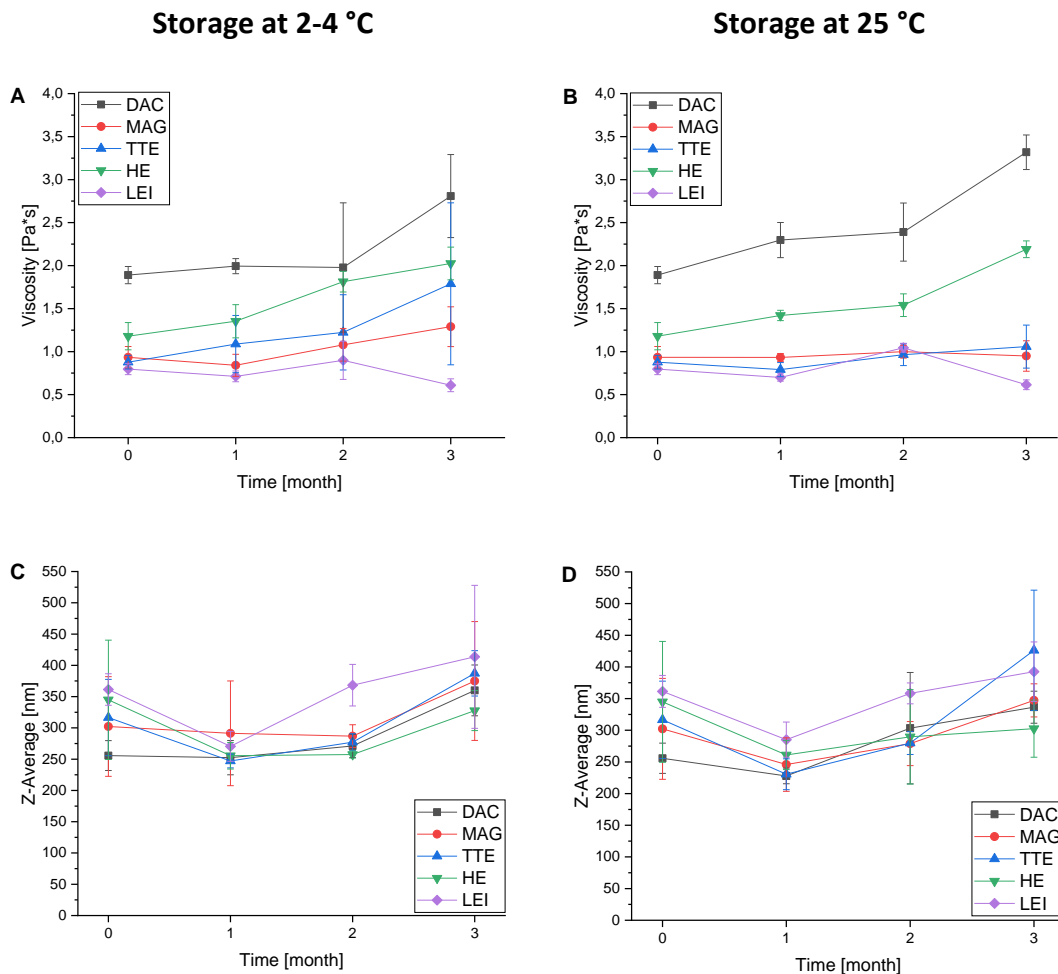


Figure IV-21: Characterization of VPG composed of 40% (m/m) Lipoid E80 and 20mM PBS pH 7.4 over storage time of three months. VPGs are prepared by dual asymmetric centrifugation (DAC), magnetic stirring (MAG), or extrusion with the ThreeTec ZE-5 (TTE), HAAKE MiniLab® (HE) or Leistritz extruder (LEI). Viscosity of the samples stored at A) 4°C or B) 25 °C is compared at 32.9 s^{-1} . Z-Average of the vesicles obtained after dilution of the VPG after storage at C) 4°C or D) 25 °C.

DLS-measurements reveal that neither size (Figure IV-21C and Figure IV-21D) nor PDI (data not shown) of the vesicles obtained after dilution, change significantly over a storage period of three months independently of the storage temperature. Slight differences between the samples prepared by different methods were observed i.e. smaller vesicles for VPG prepared by DAC and large vesicle in the LEI sample.

Macroscopically, the overall appearance of a homogenous VPG structure was maintained over three months, with the exception of the LEI sample which showed starting phase separation (Figure IV-22). Additionally, after the complete storage time some samples (especially when stored at 25 °C) were slightly darker in color and smelled characteristically. Long-term storage of lipid-based systems may lead to chemical degradation of the phospholipids, resulting in characteristic odor and color.

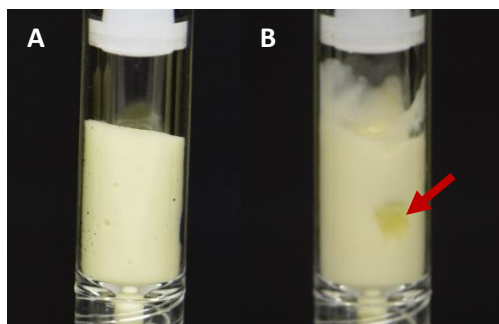


Figure IV-22: Macroscopic appearance of VPG 40% (m/m) prepared with Leistritz extruder. A) VPG directly after preparation is homogenous in appearance without visible phase separation. B) VPG after three months of storage at 25 °C shows phase separation. Red arrow indicates separated aqueous phase in the VPG.

When looking at the microscopic appearance of the VPG, differences between the sample prepared by DAC and the other methods were more pronounced after storage. All samples show a homogeneous appearance with finely dispersed vesicles directly after preparation of the VPG. After three months of storage the sample prepared by DAC still shows small vesicles and a homogenous structure, while in all other samples larger vesicles and inhomogeneity is observed with different extent depending on the preparation method. The sample prepared with the ThreeTec ZE-5 Mini-Extruder and the sample prepared with the HAAKE MiniLab[®], as well as the sample prepared by magnetic stirring show slightly larger vesicles and a minor increase of polydispersity. The sample prepared with the Leistritz extruder shows larger vesicles and a very polydisperse appearance after three months of storage.

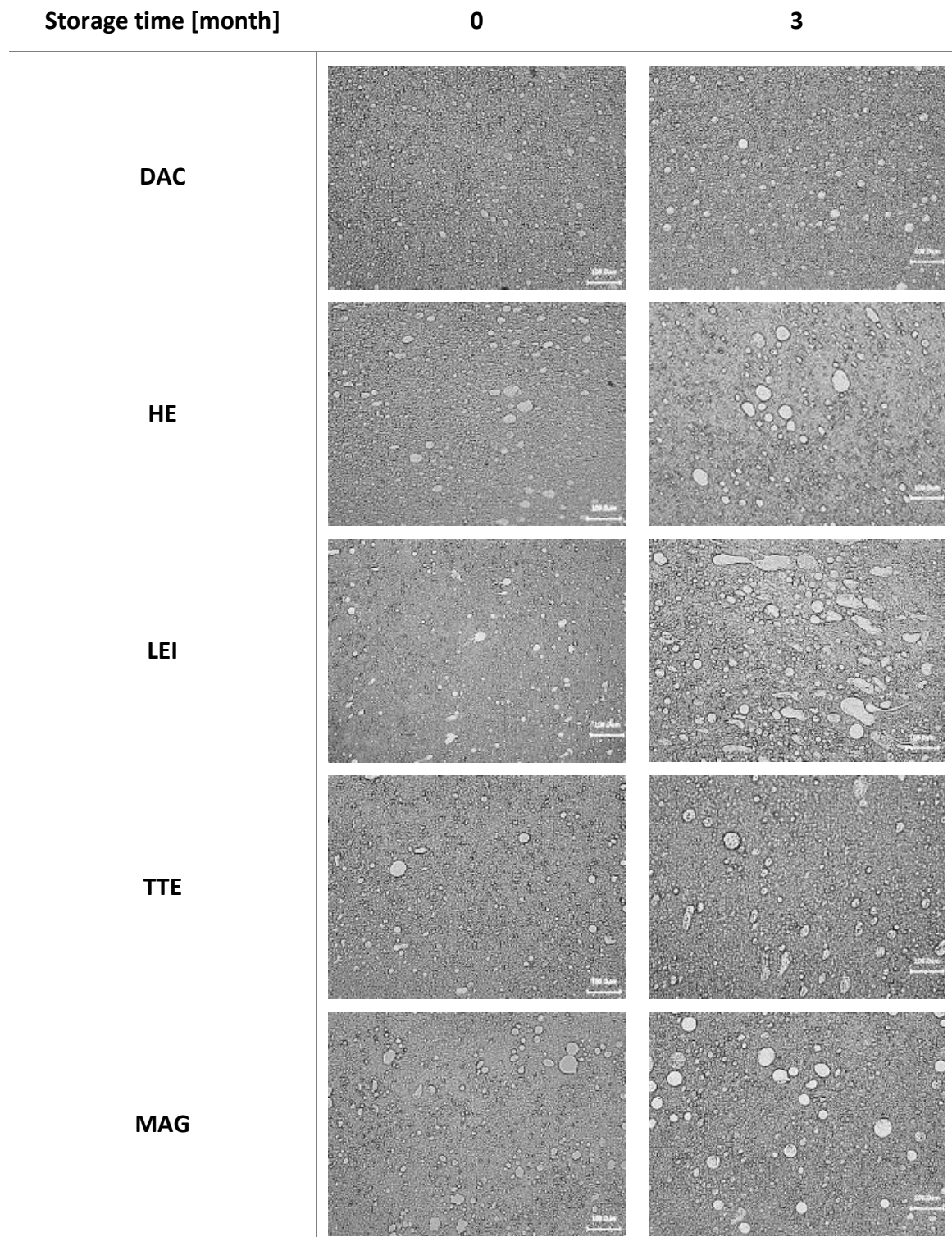


Figure IV-23: Representative microscopic images of the differently prepared VPGs directly after preparation (left) and after three months of storage at 2-4 °C (right). Pictures are taken with 100-fold magnification.

Above described and explained data, shows that VPG prepared with the large Leistritz extruder is not stable enough for long-term storage. So far, this preparation method results in a VPG with a rather liquid appearance, low viscosity and large vesicles. Phase separation of the VPG occurs after storage for few months.

At the same time, both of the smaller extruders produce VPG with smaller vesicle sizes, which are more stable over a longer storage period even if the physical stability of the VPG prepared by DAC cannot be reached. After all, there are different optimization strategies how to address the challenge to achieve a more stable VPG by extrusion even with large extruders. By smaller dies, pressure in the barrel is increased and additionally a slower screw speed results in prolonged residence time of the material in the barrel, thus potentially resulting in an improved mixing quality. Other options would be to optimize the extrusion temperature. By softening the phospholipids at moderate but higher temperatures (30 – 50 °C), homogenization may be improved and the ratio of true encapsulation may be increased. Further, optimization of the screw design may lead to the desired effect. VPG used for stability testing was prepared by screws with conveying elements only. As already seen before (see Figure IV-11A), the incorporation of mixing and kneading elements into the screw design can increase viscosity and thus seems to have an effect on the viscoelastic behavior of the VPG.

As already mentioned above chemical instabilities have to be considered, additional to physical instabilities, which were investigated here. Phospholipids are mainly sensitive to hydrolysis and peroxidation which may both result e.g. in differences in membrane permeability and thus may affect the release from lipid-based drug carriers [45]. Especially the moving metal parts in a TSC extruder i.e. the screws, may cause metal abrasion, which may catalyze chemical reactions. Again, there are different options to overcome these difficulties. For once, antioxidants or metal chelators can be added to the formulation to prevent lipid oxidation. Further, extruders made from ceramic parts or coated surfaces could be used to prevent metal abrasion itself. However, the investigation of metal abrasion during the process and chemical instabilities was not within the scope of the present study.

After all, preparation of VPG by extrusion is a promising new manufacturing technique with many advantages, resulting in VPG with superior sustained release properties but lower viscosity than DAC. Still, the process has to be further optimized and challenges as up-scaling and metal abrasion have to be overcome.

IV.4 Conclusion

The established manufacturing techniques for VPG do have several disadvantages like long manufacturing durations and high and uncontrollable shearing forces. Additionally, DAC and HPH, as well as magnetic stirring, can only be used in batch to batch production and have limitations in up- and down-scaling.

In this chapter a novel manufacturing technique, TSC extrusion of VPGs, was successfully developed and evaluated. Homogenization of phospholipids and aqueous solution by extrusion, resulted in macroscopically homogenous VPGs with low viscosity but larger vesicles compared to VPG prepared by DAC. Low viscosity, resulting in easier injectability, is beneficial for later *in vivo* applications. However, the effect of larger vesicles *in vivo* is difficult to predict but differences in circulation half-life of the vesicles are to be expected [46].

Within our study, the effect of different extruders, screw speed and design, die diameter and length, as well as barrel temperature were evaluated. Die design, screw speed and screw design affect the product quality majorly. Fast rotation speed, results in a better mixing quality with smaller vesicles. Additionally, a screw equipped with kneading elements improved product quality in comparison to a screw with conveying elements only. When a die with smaller diameter was used, smaller vesicle sizes were achieved, whereas the die length did not influence the product quality significantly.

Release experiments showed sustained release of FITC-dextran and a monoclonal antibody from VPG after preparation by extrusion. Despite the low viscosity, release rates of the VPG prepared by extrusion were surprisingly slower in comparison to those of the VPGs prepared by DAC. It was hypothesized that rather vesicle size than viscosity is an indicator for the release behavior of VPG by erosion processes.

Furthermore, it was shown that proteins (mAb and EPO) show similar stability during preparation by extrusion compared to DAC. After 3 months of storage, no aggregation or fragmentation of the protein was observed in SDS-PAGE.

Finally, the physical stability of the VPG itself was evaluated over a storage period of 3 months. Oscillatory rheologic measurements were conducted to predict the gel stability. Amplitude sweeps yielded superior stability of the VPG prepared by DAC, followed by the VPG prepared with the ThreeTec ZE-5 Mini-Extruder and the HAAKE MiniLab® Rheology

Compounder. Despite the lower viscosity and larger vesicles in VPGs prepared by extrusion, the VPG was macroscopically and microscopically stable when prepared with the ThreeTec ZE-5 Mini-Extruder or the HAAKE MiniLab® Rheology Compounder. Vesicles size and viscosity did not change significantly during storage. However, VPG prepared with the large Leistritz Micro 27 GL showed a rather liquid appearance in rheologic measurements and low stability in macroscopic and microscopic analysis.

In conclusion, extrusion is a process which is well suited for the preparation of VPG encapsulating sensible compounds like proteins. However, further optimization of the method is needed. First, up-scalability has to be improved. By applying higher pressure, longer residence times in the barrel and using different screw design, VPG quality may be improved in larger extruders, resulting in a more stable VPG. After all, a compromise between easiness of the method and good up-scalability, quality and storage stability of the VPG, as well as sustained release behavior has to be found.

Furthermore, the method may also be applicable to the direct encapsulation of lipophilic compounds into VPG without the use of organic solvents. It is known that co-extrusion of two lipophilic substances results in a homogenous mixture [21]. The transfer of this technique to the preparation of VPGs encapsulating lipophilic drugs is thinkable and has to be investigated further.

IV.5 References

- [1] M. Brandl, D. Bachmann, M. Drechsler, and K. H. Bauer, "Liposome preparation by a new high pressure homogenizer gaulin micron lab 40," *Drug Dev. Ind. Pharm.*, vol. 16, no. 14, pp. 2167–2191, 1990.
- [2] M. Brandl, M. Drechsler, D. Bachmann, and K. H. Bauer, "Morphology of semisolid aqueous phosphatidylcholine dispersions, a freeze fracture electron microscopy study," *Chem. Phys. Lipids*, vol. 87, pp. 65–72, 1997.
- [3] M. Brandl, "Vesicular Phospholipid Gels: A Technology Platform," *J. Liposome Res.*, vol. 17, no. 1, pp. 15–26, 2007.
- [4] M. Stang, H. Schuchmann, and H. Schubert, "Emulsification in High-Pressure Homogenizers," *Eng. Life Sci.*, vol. 1, no. 4, pp. 151–157, 2001.
- [5] U. Massing, S. Cicko, and V. Ziroli, "Dual asymmetric centrifugation (DAC)-A new technique for liposome preparation," *J. Control. Release*, vol. 125, no. 1, pp. 16–24, 2008.
- [6] M. Rawat, D. Singh, S. Saraf, and S. Saraf, "Lipid carriers: a versatile delivery vehicle for proteins and peptides.," *J. Pharm. Soc. Japan*, vol. 128, no. 2, pp. 269–280, 2008.
- [7] U. Massing, "Verwendung einer dualen asymmetrischen Zentrifuge (DAZ) zur Herstellung von lipidbasierten Nanopartikeln.," EP2263653B1, Jul-2013.
- [8] S. G. Ingebrigtsen, N. Škalko-Basnet, and A. M. Holsæter, "Development and optimization of a new processing approach for manufacturing topical liposomes-in-hydrogel drug formulations by dual asymmetric centrifugation," *Drug Dev. Ind. Pharm.*, pp. 1–33, 2015.
- [9] F. Tenambergen, C. H. Maruiama, and K. Mäder, "Dual asymmetric centrifugation as an alternative preparation method for parenteral fat emulsions in preformulation development," *Int. J. Pharm.*, vol. 447, no. 1–2, pp. 31–37, 2013.
- [10] U. Massing, S. G. Ingebrigtsen, N. Škalko-Basnet, and A. M. Holsæter, "Dual Centrifugation - A Novel 'In Vial' Liposome Processing Technique," in *Liposomes*, A. Catala, Ed. IntechOpen, 2017, pp. 3–28.
- [11] Y. Zhang *et al.*, "In vitro and in vivo sustained release of exenatide from vesicular phospholipid gels for type II diabetes," *Drug Dev. Ind. Pharm.*, vol. 42, no. 7, pp. 1042–1049, 2015.
- [12] Y. Zhong *et al.*, "Vesicular phospholipid gels using low concentrations of phospholipids for the sustained release of thymopentin : pharmacokinetics and pharmacodynamics," *Pharmazie*, vol. 68, pp. 811–815, 2013.
- [13] J. Thiry, F. Krier, and B. Evrard, "A review of pharmaceutical extrusion: Critical process parameters and scaling-up," *Int. J. Pharm.*, vol. 479, no. 1, pp. 227–240, 2015.
- [14] J. Breitenbach, "Melt extrusion: From process to drug delivery technology," *Eur. J. Pharm. Biopharm.*, vol. 54, p. 107, 2002.
- [15] A. Limper, "Mehrschneckenextruder," in *Verfahrenstechnik der*

- Thermoplastextrusion*, Munich: Carl Hanser Verlag GmbH & Co. KG, 2012, pp. 41–108.
- [16] A. Limper, H. Greif, and G. Fattmann, *Technologie der Extrusion - Lern- und Arbeitsbuch für die Aus- und Weiterbildung*, 2nd ed. Munich: Carl Hanser Verlag GmbH & Co. KG, 2017.
- [17] S. Schulze and G. Winter, "Lipid extrudates as novel sustained release systems for pharmaceutical proteins," *J. Control. Release*, vol. 134, no. 3, pp. 177–185, 2009.
- [18] M. Vollrath, J. Engert, and G. Winter, "Long-term release and stability of pharmaceutical proteins delivered from solid lipid implants," *Eur. J. Pharm. Biopharm.*, vol. 117, pp. 244–255, 2017.
- [19] M. Vollrath, "Extruded lipid implants for intravitreal use - protein stability, release kinetics and process design," Dissertation, Ludwig-Maximilians-Universität München, 2017.
- [20] G. L. Sax, "Twin-screw extruded lipid implants for controlled protein drug delivery," Dissertation, Ludwig-Maximilians Universität, 2012.
- [21] H. Haas, S. Waibler, and G. Winter, "Method for Producing Colloidal Nanoparticles with a Compounder," US20070148196A1, 2007.
- [22] R. J. Ho and M. Gibaldi, "Transforming proteins and genes into drugs - The Science and the Art," in *Biotechnology and Biopharmaceuticals*, Hoboken, NJ: John Wiley & Sons, Inc, 2013.
- [23] X.-R. Qi, Y. Maitani, N. Shimoda, K. Sakaguchi, and T. Nagai, "Evaluation of Liposomal Erythropoietin Prepared with Reverse-Phase Evaporation Vesicle Method by Subcutaneous Administration in Rats," *Chem. Pharm. Bull. (Tokyo).*, vol. 43, no. 2, pp. 295–299, 1995.
- [24] A. Basu *et al.*, "Structure-Function Engineering of Interferon-1b for Improving Stability, Solubility, Potency, Immunogenicity, and Pharmacokinetic Properties by Site-Selective Mono-PEGylation," *Bioconjug. Chem.*, vol. 17, no. 3, pp. 618–630, 2006.
- [25] M. Marziniak and S. Meuth, "Current Perspectives on Interferon Beta-1b for the Treatment of Multiple Sclerosis," *Adv. Ther.*, vol. 31, no. 9, pp. 915–931, 2014.
- [26] C. Tardi, M. Brandl, and R. Schubert, "Erosion and controlled release properties of semisolid vesicular phospholipid dispersions," *J. Control. Release*, vol. 55, no. 2–3, pp. 261–270, 1998.
- [27] W. Tian, "The Development of Sustained Release Formulation for Pharmaceutical Proteins based on Vesicular Phospholipid Gels," Dissertation, Ludwig-Maximilians-Universität München, 2010.
- [28] M. Takayama, S. Itoh, I. Nagasaki, and I. Tanimizu, "A new enzymatic method for determination of serum choline-containing phospholipids," *Clin. Chim. Acta*, vol. 79, no. 1, pp. 93–98, 1977.
- [29] FUJIFILM Wako Diagnostics U.S.A Corporation, "Phospholipids Choline oxidase-DAOS method (Brochure)." FUJIFILM Wako Diagnostics U.S.A. Corporation,

- Mountain View, CA, 2018.
- [30] E. Reitz, H. Podhaisky, D. Ely, and M. Thommes, "Residence time modeling of hot melt extrusion processes," *Eur. J. Pharm. Biopharm.*, vol. 85, pp. 1200–1205, 2013.
- [31] C. Parkinson, S. Matsumoto, and P. Sherman, "The influence of particle-size distribution on the apparent viscosity of non-newtonian dispersed systems," *J. Colloid Interface Sci.*, vol. 33, no. 1, pp. 150–160, 1970.
- [32] J. Bender, W. Michaelis, and R. Schubert, "Morphological and thermal properties of vesicular phospholipid gels studied by DSC, rheometry and electron microscopy," *J. Therm. Anal. Calorim.*, vol. 68, no. 2, pp. 603–612, 2002.
- [33] E. Reitz, C. Vervaet, R. H. H. Neubert, and M. Thommes, "Solid crystal suspensions containing griseofulvin - Preparation and bioavailability testing," *Eur. J. Pharm. Biopharm.*, vol. 83, pp. 193–202, 2013.
- [34] M. Brandl *et al.*, "Three-dimensional liposome networks: freeze fracture electron microscopical evaluation of their structure and in vitro analysis of release of hydrophilic markers," *Adv. Drug Deliv. Rev.*, vol. 24, pp. 161–164, 1997.
- [35] T. Yang, A. Dong, J. Meyer, O. L. Johnson, J. L. Cleland, and J. F. Carpenter, "Use of infrared spectroscopy to assess secondary structure of human growth hormone within biodegradable microspheres," *J. Pharm. Sci.*, vol. 88, no. 2, pp. 161–165, 1999.
- [36] M. van de Weert, W. E. Hennink, and W. Jiskoot, "Protein instability in poly(lactico-glycolic acid) microparticles," *Pharm. Res.*, vol. 17, no. 10, pp. 1159–1167, 2000.
- [37] K. Fu, K. Griebenow, L. Hsieh, A. M. Klibanov, and Robert Langer, "FTIR characterization of the secondary structure of proteins encapsulated within PLGA microspheres," *J. Control. Release*, vol. 58, no. 3, pp. 357–366, 1999.
- [38] M. Vollrath, J. Engert, and G. Winter, "New insights into process understanding of solid lipid extrusion (SLE) of extruded lipid implants for sustained protein delivery," *Eur. J. Pharm. Biopharm.*, vol. 130, pp. 11–21, 2018.
- [39] C. Tardi, M. Drechsler, K. H. Bauer, and M. Brandl, "Steam sterilisation of vesicular phospholipid gels," *Int. J. Pharm.*, vol. 217, no. 1–2, pp. 161–172, 2001.
- [40] C. Ibănescu, M. Danu, A. Nanu, M. Lungu, and B. C. Simionescu, "Stability of disperse systems estimated using rheological oscillatory shear tests," *Rev. Roum. Chim.*, vol. 55, no. 11–12, pp. 933–940, 2010.
- [41] Anton Paar GmbH, "Amplitude sweeps: Anton Paar Wiki." [Online]. Available: <https://wiki.anton-paar.com/en/amplitude-sweeps/>. [Accessed: 06-Sep-2018].
- [42] F. Meyer, "Performing Rheological Tests in Oscillation with the HAAKE Viscotester iQ Rheometer." Application Note V-279, Thermo Fisher Scientific, Material Characterization, Karlsruhe, 2014.
- [43] T. G. Mezger, *The Rheology Handbook: For Users of Rotational and Oscillatory Rheometers*, 2nd ed. Hannover: Vincentz Network GmbH & Co KG, 2006.
- [44] C. Neuhofer, "Development of lipid based depot formulations using interferon-beta-1b as a model protein," Dissertation, Ludwig-Maximilians-Universität

München, 2015.

- [45] B. Heurtault, P. Saulnier, B. Pech, J.-E. Proust, and J.-P. Benoit, "Physico-chemical stability of colloidal lipid particles," *Biomaterials*, vol. 24, pp. 4283–4300, 2003.
- [46] A. Akbarzadeh *et al.*, "Liposome: classification, preparation, and applications," *Nanoscale Res. Lett.*, vol. 8:102, pp. 1–9, 2013.

Chapter V

INTERACTIONS BETWEEN PROTEINS AND PHOSPHOLIPIDS

Parts of this chapter have been submitted or are intended for publication:

- Section V.1 : M. Breitsamer, A. Stulz, H. Heerklotz, G. Winter; *Do interactions between Protein and Phospholipids influence the release behavior from lipid-based exenatide depot systems?*

Submitted for publication to European Journal of Pharmaceutics and Biopharmaceutics in January 2019.

- Parts of section V.2 : A. Stulz, M. Breitsamer, G. Winter, H. Heerklotz; *Different aspects of a complex protein-lipid binding equilibrium as seen by ITC, Fluorescence, and MST.*

Manuscript in preparation.

To maintain the train of reading throughout the chapter, references of the published manuscript and further studies are combined in section V.4 .

This work was conducted in close cooperation with Albert-Ludwigs-Universität Freiburg. The personal contribution covers the preparation and characterization of exenatide-VPG, including *in vitro* release behavior, as well as the implementation and evaluation of steady state fluorescence and microscale thermophoresis measurements, including written parts of these experiments. Isothermal titration calorimetric measurements were conducted together with Anja Stulz. Prof. Dr. Heiko Heerklotz and Anja Stulz evaluated and interpreted the ITC data.

V.1 DO INTERACTIONS BETWEEN PROTEIN AND PHOSPHOLIPIDS INFLUENCE THE RELEASE BEHAVIOR FROM LIPID-BASED EXENATIDE DEPOT SYSTEMS?

V.1.1 Abstract

The release mechanism for proteins and peptides from vesicular phospholipid gels (VPGs) is very complex. Drug release proceeds via a combination of erosion of the gel and diffusion of the drug out of it. This diffusion can be retarded by a slow permeation of the drug across the lipid bilayers in the gel as well as by its direct binding or adsorption to the lipid bilayers. Finally, the viscosity and homogeneity of the formulation may affect the release behavior. So far, a direct correlation between one of these parameters and the release kinetics is not possible.

In the present study, we aimed to investigate the contribution of drug-membrane interactions to the release kinetics of exenatide from differently composed VPGs (POPC, POPG and mixtures of both). To this end, *in vitro* release of exenatide as well as *in vitro* release of the phospholipids was monitored. Binding affinities were determined by microscale thermophoresis (MST).

The sustained release behavior of exenatide could not simply be correlated to high viscosity of the VPG formulation. Release of exenatide from VPGs of anionic membranes containing POPG proceeded with a half-life of the order of 5 days and it seems to be controlled by the erosion of the gel. Its rate is unaffected by the initial pH inside the gel, independently of the strong impact of pH on exenatide binding to the membrane. At pH 4.5, exenatide is cationic and binds to membranes containing anionic POPG with a high affinity ($K_d \approx 10\text{-}30 \mu\text{M}$).

No high affinity membrane binding of exenatide is detected in this at pH 7.4, where exenatide is anionic, and to zwitterionic membranes composed of POPC. Exenatide release from the latter has a significantly longer half-life of 30 to 55 days. That means, these VPGs are much more resistant to erosion and show a very slow diffusional release. In this case, diffusion should be slowed down by the barrier function of the membranes rather than membrane affinity.

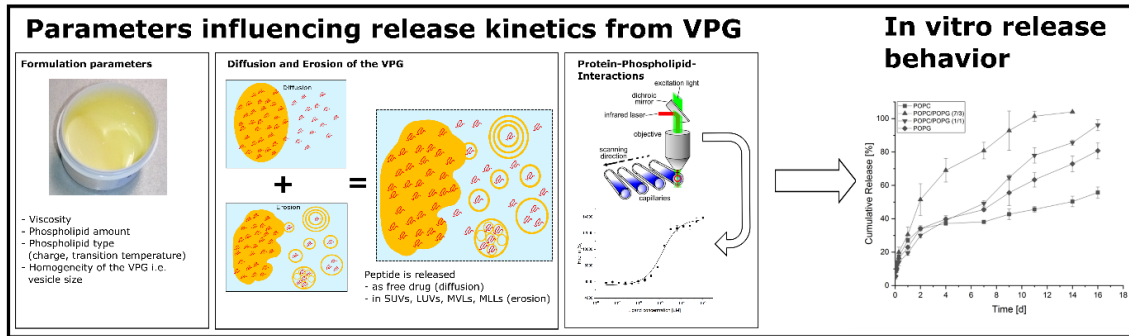


Figure V-1: Graphical abstract.

V.1.2 Introduction

Vesicular phospholipid gels (VPGs) are semisolid drug formulations which are composed of phospholipids and a simple aqueous phase only [1], [2]. They are prepared by elegant one step manufacturing techniques like high pressure homogenization (HPH) or dual asymmetric centrifugation (DAC). Their capability to release drugs and especially proteins and peptides with a slow release rate, combined with their easy and cheap manufacturing and their high biocompatibility makes them very promising drug delivery systems [3]–[6]. Next to their application for large molecules like proteins, they have also been used for the sustained delivery of small molecules [7]–[12]. The administration via needle-free injection facilitates the versatile application of VPGs [13].

The release behavior of VPG is dominated by a combination of an erosion controlled and an diffusion controlled process [5]. Tardi et al. found that these two processes occur at the same time. VPGs with up to 30% (m/m) phospholipids disintegrate fast. VPGs with 35 to 40% (m/m) phospholipids show erosion controlled release behavior and VPGs with a phospholipid concentration above 45% (m/m) show rather diffusion controlled release kinetics. However, there seems to be more behind this release process. Depending on the encapsulated drug substance and the phospholipid composition, changes in release behavior have been observed [14]–[16]. Possible interactions between the encapsulated protein or peptide and the phospholipids may be responsible for the different sustained release profiles.

In this context, Neuhofer et al. addressed the interactions between interferon β -1b and the triglycerides H12 and D118, but also different phospholipids [14]. Additionally, he found that the extraction of native interferon β -1b from VPG was not possible and concluded that interactions were responsible for this phenomenon. PEGylation reduced the interaction effects but could not completely avoid it. He also found that the presence of a protein drug affected the mechanical properties of the VPG matrix and concluded that interactions may be responsible. To this end, he used a Langmuir film balance and a quartz crystal microbalance (QCM) to investigate different models like liposomes or monolayers. But no consistent correlation between the different methods and no prediction of the release behavior could be established.

Even et al. investigated the interactions of peptides with different charge and hydrophobicity with lipids including D114, soy lecithin, and cholesterol by adsorption studies [16]. It was shown that the size, hydrophobicity, or charge of encapsulated proteins or peptides are not alone responsible for the sustained release from VPGs. The release of a small peptide from VPGs was, against all expectations, slow and incomplete, whereas a much bigger protein was released fast in comparison. Additionally, no direct relationship between hydrophobicity of the molecule and release rate could be identified. Further, it was shown that the high dispersity of VPG produced by DAC or HPH, including small vesicles and multi-lamellar structures, is not necessarily needed to obtain a sustained release behavior [17]. Zhang et al. showed *in vitro* and *in vivo* sustained release of exenatide from VPGs after preparation by magnetic stirring.

These indications in literature brought us to the hypothesis that sustained release of proteins or peptides from lipid-based depots could be controlled by interactions between the molecules, more specifically by a binding of the peptides to the phospholipid layers. The possibility to tune the release behavior by using these interactions motivated us to further investigate and characterize the interactions between proteins and phospholipids in this context.

Interactions between proteins and phospholipids have been studied extensively in the past with various methods (SPR, MST, ITC, Flotation assays etc.) [18]. However in such studies, the focus was mainly on interactions of proteins with cellular membranes [18]–[21]. Only few studies on the release behavior of lipid-based depots have been conducted so far and in many cases, the focus was on solid lipid implants (SLI) as drug delivery system and triglycerides as their main components [14], [16], [22].

In this study, we aimed to investigate the interactions between exenatide, a pharmaceutically highly relevant, relatively small peptide with a defined secondary structure and phospholipids with microscale thermophoresis (MST) measurements and correlate our findings to the release behavior from VPGs.

V.1.3 Material and Methods

V.1.3.1 Material

Exenatide acetate was purchased from Chemos GmbH&Co.KG (Regenstauf, Germany) and purified by dialysis (MWCO 5 kDa) into highly purified water (HPW, Purelab Plus, USF Elga, Germany) before freeze-drying of the solution for storage. An exenatide stock solution was freshly prepared in 50 mM sodium acetate buffer pH 4.5 or 20 mM phosphate buffered saline (PBS) pH 7.4 with a concentration of 200 μ M. Dilutions thereof were used for interaction measurements.

All phospholipids (POPC, POPG) were purchased from Lipoid GmbH (Ludwigshafen am Rhein, Germany).

V.1.3.2 Exenatide characterization

A Zetasizer nano ZS (Malvern Instruments, UK) was used for determination of the zeta potential of exenatide. Zeta potential of an exenatide solution with a concentration of 5 mg/ml was measured in HPW after adjustment of the pH value with 1 M hydrochloric acid or 1 M sodium hydroxide.

FTIR measurements were used to investigate the secondary structure of exenatide with changing pH value. A Tensor 27 spectrometer (Bruker Optics, Ettlingen, Germany) using a BioATR cell II (Harrick, New York, USA) was used to record FTIR spectra. For each measurement, 30 μ l sample with an exenatide concentration of 5 mg/ml was pipetted into the cell. Measurements were controlled using OPUS 7.5 and transmission spectra were truncated from 1350 cm^{-1} to 1750 cm^{-1} . Further spectra were edited by vector normalization and second derivatives were calculated using a 17-point smoothing function.

V.1.3.3 Preparation of vesicular phospholipid gel

VPGs with a phospholipid concentration of 40% (m/m) were prepared by dual asymmetric centrifugation (SpeedmixerTM DAC 150 FVZ, Hauschild GmbH & Co KG, Hamm, Germany) as described previously [3], [6], [13]. Four different phospholipid combinations were prepared: POPC and POPG were used as sole phospholipids; additionally, mixtures of POPC and POPG in a ratio of 7:3 and 1:1 were prepared. Phospholipids were accurately

weighed in the required amounts before exenatide solution was added until a final exenatide concentration of 0.5 mg/g was reached in the VPG.

V.1.3.4 VPG characterization

Rheology measurements were performed to characterize the VPG formulations [3]. The viscosity of the VPG at a shearing rate of 32.9 s^{-1} was determined by a rotational rheometer (Physica MCR 100, Anton Paar GmbH, Ostfildern, Germany) with a plate-plate geometry. All measurements were performed at $25 \text{ }^\circ\text{C}$ and the shear rate was set to $10\text{--}100 \text{ s}^{-1}$. Approximately 0.2 g VPG was used per measurement.

V.1.3.5 *In vitro* release of exenatide from VPG

For the *in vitro* release studies, 200 mg of VPG were carefully overlaid with 1 ml 20 mM PBS buffer pH 7.4 in 2 ml centrifugation tubes. Then, all samples were incubated at $37 \text{ }^\circ\text{C}$ and 30 rpm in a vertical incubation shaker (Certomat incubation Shaker, Sartorius AG, Germany) in upright position. Release experiments were carried out by complete buffer exchange [13], [16].

The concentration of exenatide was determined using a reverse phase high pressure liquid chromatography (RP-HPLC). A Jupiter $5 \mu\text{m}$ C18 300A column (Phenomenex, USA) was used for quantification of the peptide. Mobile phase A was composed of 10% (m/m) acetonitrile, HPW and 0.1% (m/m) TFA and mobile phase B was composed of acetonitrile and 0.1% (m/m) TFA. Table V-3 shows the multi-step-gradient which was used for the quantification of exenatide with a flow of 0.5 ml/min. Column temperature was set to $55 \text{ }^\circ\text{C}$ and the retention time of exenatide was 12 minutes. Exenatide was extracted by 1:1 dilution with ethanol, heating for five minutes at $60 \text{ }^\circ\text{C}$, followed by 20 minutes of cooling at $2\text{--}4 \text{ }^\circ\text{C}$ and five minutes centrifugation. The resulting supernatant was taken for quantification.

V.1.3.6 Characterization of VPG erosion during *in vitro* release

The erosion behavior of the differently composed VPGs was characterized in parallel to the *in vitro* release of exenatide. One way of quantifying erosion was in terms of sample turbidity which, in turn, was expressed on the basis of optical density.

All samples were diluted as needed (1:4 or 1:10) with highly purified water and the absorbance at a wavelength of 600 nm was determined using a FLUOstar Omega plate

reader (BMG LABTECH, Ortenberg, Germany). 300 µl of diluted sample were pipetted into U-bottom 96-well-plates (MICROLON® 200, greiner bio-one, Frickenhausen, Germany). Absorbance values after dilution were between 0.1 and 1.5 and optical densities of the undiluted samples were calculated.

Alternatively, erosion of the lipid matrix was determined by quantification of PC in the released fractions. A LabAssay™ Phospholipid (FUJIFILM Wako Chemicals Europe GmbH, Neuss, Germany) was used for this purpose. Samples were prepared following the supplier's instructions and measured at a wavelength of 600 nm using a FLUOstar Omega plate reader (BMG LABTECH, Ortenberg, Germany). In this assay, phospholipids are hydrolyzed by phospholipase D and the liberated choline is then oxidized by choline oxidase to betaine [23]. Thereby, hydrogen peroxide is produced which, in turn, initiates the coupling of 4-aminoantipyrine and N-ethyl-N-(2-hydroxy-3-sulfopropyl)-3,5-dimethoxyaniline sodium salt (DAOS) to a blue chromophore by oxidation, catalyzed by peroxidase.

V.1.3.7 Liposome preparation

Liposomes were prepared by thin film hydration method. The respective phospholipid was solved in chloroform (25 mg/ml), the accurate amount of phospholipid solution was mixed as needed using a vortexer and the solvent was removed under a constant stream of nitrogen while the glass vial was turned producing a thin phospholipid film on the wall of the glass vial. After that, the film was hydrated with 50 mM sodium acetate buffer pH 4.5, 10 mM Tris buffer pH 7.4 (containing 110 mM NaCl and 0.5 mM EDTA), or 20 mM PBS pH 7.4. Liposomes were extruded by a Lipex (Burnaby, Canada) extruder. Five extrusion cycles through a 200 nm polycarbonate membrane were followed by several extrusions through a 100 nm polycarbonate membrane to achieve homogeneous liposome dispersions. Size, PDI, and zeta potential were determined by dynamic light scattering (DLS) using a Zetasizer nano ZS (Malvern Instruments, UK).

The lipid concentration in the liposome dispersion was determined using a gravimetric determination [24].

V.1.3.8 Microscale Thermophoresis

Microscale thermophoresis (MST) measurements were performed using a Monolith NT.LabelFree (NanoTemper Technologies GmbH, Germany) with MO.Control v1.5.3.. Dilution series were prepared for each of the liposome dispersions (1.0 mM to 3.05E-05 mM or 0.5 mM to 1.53E-05 mM) following the instrument's instructions. Then exenatide stock solution was added. During the assay, the exenatide concentration was kept constant at 2.5 or 5 μ M, respectively. All samples were either prepared in 50 mM sodium acetate buffer pH 4.5 containing 0.1% (m/v) Pluronic F-127 or in 20 mM PBS pH 7.4 containing 0.1% (m/v) Pluronic F-127.

Samples were loaded into coated glass capillaries (Monolith NT.LabelFree Capillaries, Zero Background, MST Premium Coated). Then, capillaries were placed on a tray and inserted into the instrument before fluorescent scans were performed to determine the position of the capillaries. After that, 16 subsequent thermophoresis measurements (LED 20%, IR laser: Medium-Power) were performed. Ambient temperature of the instrument was set to 23 °C. For each ligand, a pre-test (with buffer, liposome-dispersion, and exenatide) was performed to qualify the sample for measurement before the binding affinity test, using the parameters determined in the pre-test. Dissociation constants were calculated after the measurement using NanoTemper MO.Affinity Analysis v2.2.7 software.

V.1.4 Results

V.1.4.1 Exenatide characterization and encapsulation in VPGs

Determination of the zeta potential of exenatide over a broad range of pH values showed that exenatide turns from positive to negative between pH 4.5 and pH 5.0 (see Figure V-2). This is in good accordance with the literature value for the isoelectric point of exenatide of 4.86 [25].

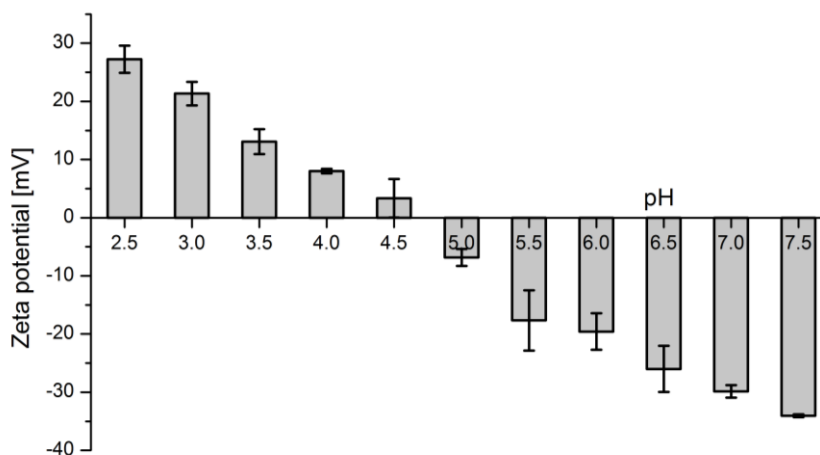


Figure V-2: Zeta potential of exenatide with increasing pH value. (Mean \pm SD, n=3)

With FTIR spectroscopy, the secondary structure of proteins and peptides can be analyzed. In order to get further information about the folding behavior of exenatide at different pH-values, FTIR measurements were conducted.

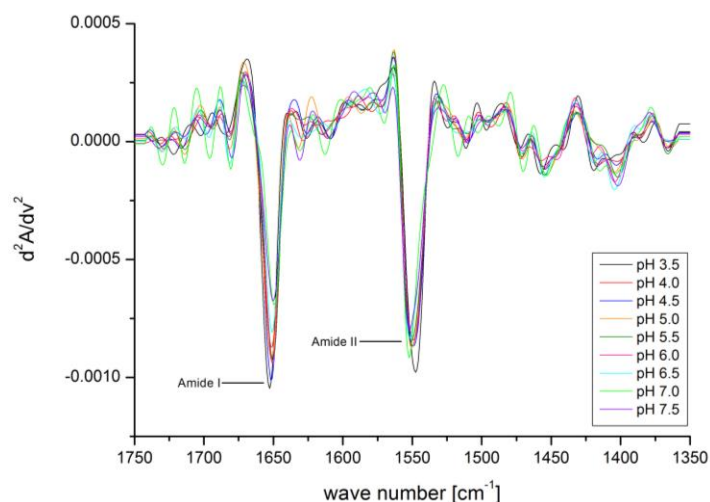


Figure V-3: FTIR spectra of exenatide solution with increasing pH value.

The measurements confirm the alpha-helical structure of exenatide, which is described in literature [26]. This alpha-helical structure is preserved over the complete pH range from

3.5 to 7.5 (see Figure V-3). No changes or shifts in amid I or amid II band were observed, indicating structural integrity of the protein over the complete pH range.

Exenatide was successfully encapsulated into VPG by direct encapsulation process using a DAC as described [6]. In comparison to other preparation methods, this technique is very gentle and has been used for the preparation of protein loaded VPG before [3]. Exenatide loaded VPG were prepared containing 40% (m/m) of phospholipid and characterized by visual inspection and viscosity measurements.

Visual inspection exhibited a homogeneous appearance of the VPG without lipid agglomerates. Rheological behavior of the VPG was studied by rotational rheometry. The viscosity of the VPG was compared at a shearing rate of 32.9 s^{-1} .

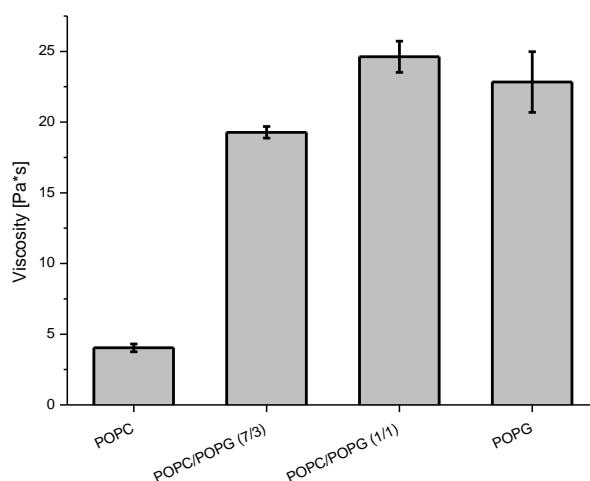


Figure V-4: Viscosity of VPG with a total phospholipid concentration of 40% (m/m) loaded with exenatide (0.5 mg/g). VPG was prepared with different phospholipid compositions. For comparison the viscosity at a shearing rate of 32.9 s^{-1} was taken. (Mean \pm SD, n=3)

All formulations containing POPG showed a high viscosity (above $15 \text{ Pa}\cdot\text{s}$) (see Figure V-4). VPG formulations of POPC displayed lower viscosity (below $5 \text{ Pa}\cdot\text{s}$). The viscosity of the VPG was not influenced by the encapsulation of the peptide, i.e., placebo VPG showed similar values.

V.1.4.2 *In vitro* release of exenatide from VPG

The *in vitro* release of exenatide from VPGs was determined using formulations with pH 4.5 and with pH 7.4. In both cases, exenatide is released very slowly from VPG composed of POPC only, while a faster release is observed from formulations composed of POPC/POPG mixtures or the single POPG formulation. Complete exenatide release

within 16 days was observed for the formulations composed of a mixture of POPC and POPG or the POPG only formulation, while VPG composed of POPC only released a maximum of 40% of the encapsulated drug within this period. No burst effect was observed for all tested formulations and encapsulation pH values.

At the same time, only slight differences between the two encapsulation pH values were observed. At an encapsulation pH 7.4 (see Figure V-5B), exenatide is released faster from the formulation containing POPC only in comparison to encapsulation at pH 4.5 (see Figure V-5A). Otherwise, the previously observed trend, a faster release from formulations containing POPG, was confirmed.

The release kinetics were fitted by a model taking into account the possibility of two fractions A_1 and $1 - A_1$, with different release rates k_1 and k_2 :

$$C_{released} = c_{max} \cdot \left[1 - A_1 \cdot e^{-k_1 t} - (1 - A_1) \cdot e^{-k_2 t} \right] \quad (V-1)$$

The half-life of the drug fraction in its retained state, $t_{1/2}$, is then given by:

$$t_{1/2} = \frac{\ln 2}{k} \quad (V-2)$$

analogously for k_1 and k_2 . The dashed lines in Figure V-5A and Figure V-5B show the fit lines.

A biphasic release behaviour was identified for the formulations containing POPG. One fraction (5 to 20%) being released with a half-life of less than 20 minutes and a second fraction (80 to 95%) being released with a half-life of 5 days. In contrast to that, formulations composed of POPC have a significantly longer half-life of 30 to 50 days (approximately 80%) with a small fraction (20%) being released with a half-life of 1 to 10 days.

V.1.4.3 Erosion behavior of VPGs during exenatide release

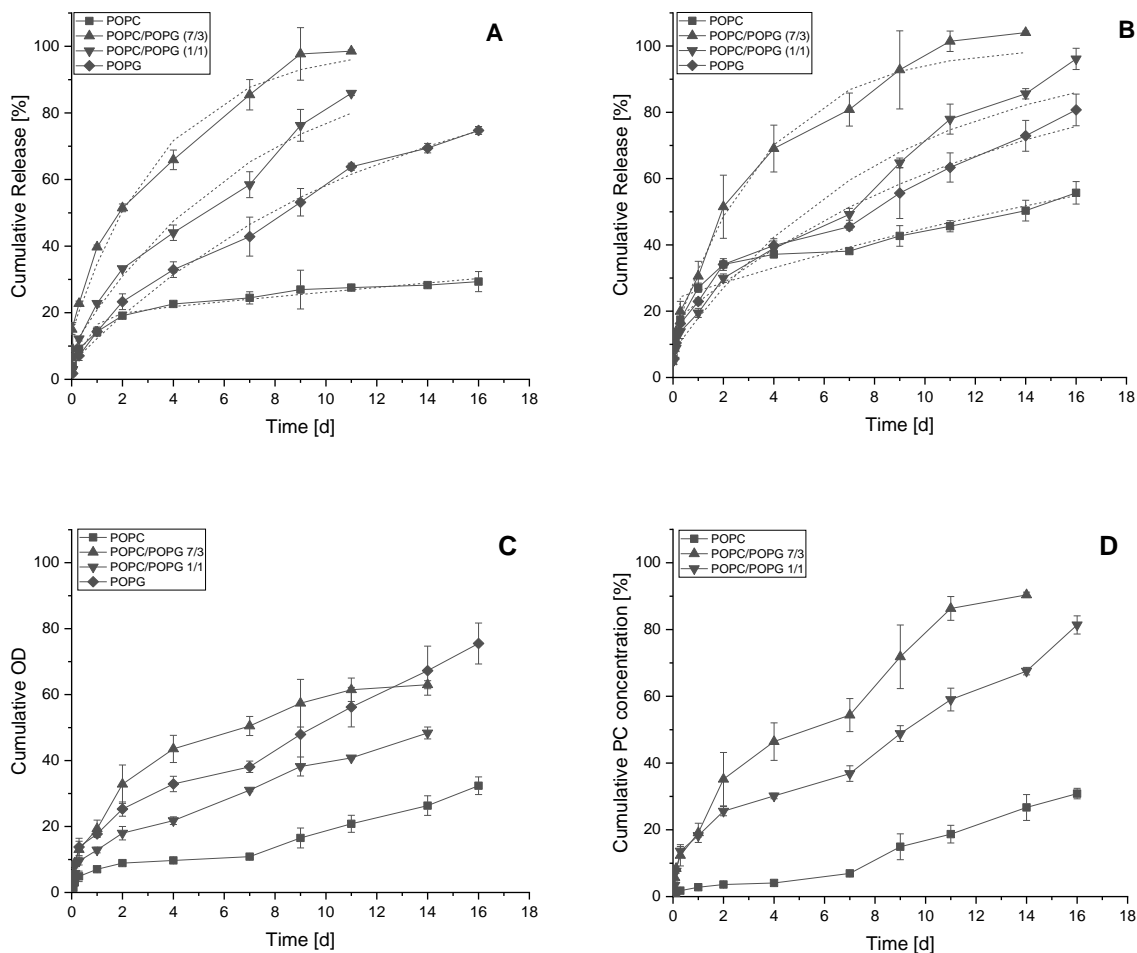


Figure V-5: *In vitro* release of exenatide from VPG and erosion behavior of VPG during release. **A)** Cumulative exenatide release from VPG. Exenatide was encapsulated at pH 4.5 in all formulations. (Release medium: 20 mM PBS pH 7.4). Dashed lines show fit with equation (V-1). **B)** Cumulative exenatide release from VPG. Exenatide was encapsulated at pH 7.4 in all formulations. (Release medium: 20 mM PBS pH 7.4). **C)** Cumulative optical density of the released fractions obtained from *in vitro* release of exenatide. **D)** Cumulative PC concentration obtained from phospholipid assay for all formulations containing POPC is shown in percentage of total PC in the VPG formulation. (Mean \pm SD; n = 3)

One possible mechanism of drug release from VPGs is the erosion of the lipid matrix. Optical density (OD) of the release fractions correlates to the erosion of the lipid matrix. When optical density is plotted cumulatively, erosion profiles for phospholipids are obtained, which are shown in Figure V-5C. Erosion of the VPG composed of POPC is rather slow in comparison to the three formulations containing POPG.

Figure V-5D shows the PC release profiles for the three formulations containing POPC. Slow PC release is observed for POPC-VPG while fast release is observed for the two

mixtures with POPG. These results do correlate rather well with the release profiles found for exenatide. For formulations containing POPG, release of exenatide can be correlated linearly to the erosion of the VPG from the beginning. In contrast to that, for formulations composed of POPC a linear correlation between exenatide release and erosion can be found after a lag-phase of few days. This lag-phase may be a result of the release of loosely bound exenatide in the VPG which is released faster. After the lag-phase, erosion of the VPG composed of POPC sets in and controls the release behavior.

V.1.4.4 Interactions studies

When testing the *in vitro* release behavior of exenatide from VPG, a correlation between viscosity and release kinetics was expected in a way that highly viscous systems should release slowly and vice versa. However, since this expectation was not fulfilled, interactions between the encapsulated peptide and the phospholipids were investigated to see if these are responsible for the slow sustained release from VPG composed of POPC only.

Interaction studies were performed by MST measurements. Since MST has to be performed in free “solution”, unilamellar vesicles were prepared for the interaction studies by thin film hydration. Z-average size and zeta potential (see Table V-1) of the liposomes were determined directly after homogenization of the liposomes by extrusion in the respective buffers. Z-average of all liposomes was ≤ 130 nm and PDI ≤ 0.15 .

Table V-1: Zeta potential of the liposomes used for interaction studies. (Mean \pm SD, n = 3)

Liposome composition	Zeta potential [mV]	
	pH 4.5	pH 7.4
POPC	-0.6 \pm 0.6	-5.6 \pm 2.2
POPC/POPG 7:3	-6.2 \pm 1.2	-17.6 \pm 0.8
POPC/POPG 1:1	-6.5 \pm 1.7	-20.5 \pm 0.8
POPG	-7.2 \pm 1.7	-25.4 \pm 1.7

Microscale thermophoresis

Microscale thermophoresis allows the quantitative investigation of interactions of proteins or peptides in free solution with other molecules e.g. phospholipids at low sample volumes [27], [28]. Label-free measurements have the additional advantages that

no sample preparation is required, that the site of interaction on a molecule is not disturbed or hindered by the attachment of a fluorescent label to the protein or peptide and that mobility is not restricted [28]. Native binding behavior is measured with label-free MST. It has been demonstrated before that even liposomes with a size of several 100 nm can be analyzed with MST [29].

Since label-free MST is not possible if both binding partners show similar tryptophan fluorescence or if background fluorescence by the buffer components leads to increased noise, control experiments have to be performed before measuring. Further, optimal buffer conditions have to be determined before the experiments [30]. To prevent unspecific adsorption to the capillary walls, Pluronic F127 was added to the buffer before measurement. At low liposome concentrations, the unbound exenatide displays a migration towards higher temperatures, corresponding to a negative thermophoretic signal. Upon binding of exenatide to the liposomes, increasing positive thermophoresis was observed (see Figure V-6). Similar behavior has been reported before for RNA-ligand interactions [31].

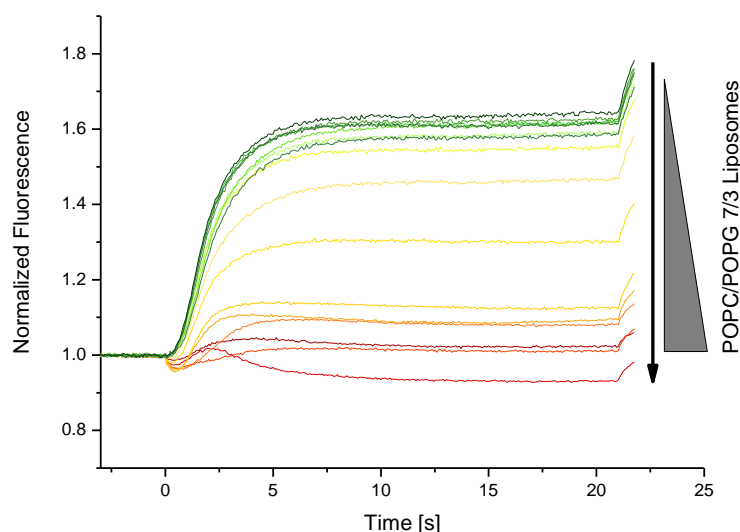


Figure V-6: Raw MST-traces of the titration of exenatide ($5 \mu\text{M}$) with liposomes composed of a mixture of POPC and POPG 7:3 at pH 4.5. Liposome concentration increases from dark green (30.5 nM) over yellow ($7.8 - 31.25 \mu\text{M}$) to dark red (1.0 mM) as arrow indicates.

Different parts of an MST signal can be analyzed [29]. Before the sample is heated, initial intrinsic fluorescence is determined. Usually, the initial fluorescence should be constant for all samples; changes in initial fluorescence occur only if the ligand binds closely to the

fluorophore. Artifacts or adsorption of the peptide to the reaction tubes have to be ruled out to account for this phenomenon.

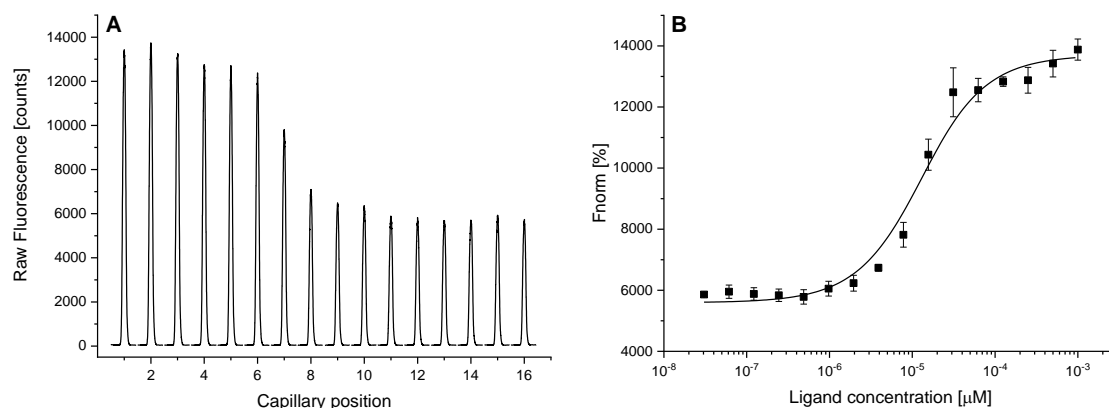


Figure V-7: A) Raw fluorescence spectra: Initial Fluorescence change with increasing amount of POPC/POPG 1:1 liposomes in exenatide solution (pH 4.5). Liposome concentration decreases from capillary position 1 (0.5 mM) to capillary position 16 (15.3 μM). B) Fitting function of the initial fluorescence signal of POPC/POPG 1:1 liposomes to exenatide at pH 4.5. (Mean \pm Kd Confidence, n = 3)

In the present study, initial fluorescence changes occurred, indicating a screening of the tryptophan residue in exenatide from water upon binding to liposomes. In this case, the binding constant K_d may already be calculated from the initial fluorescence changes. Raw fluorescence scans of each capillary for the titration of exenatide with POPC/POPG 1:1 liposomes are illustrated in Figure V-7A. These initial fluorescence changes were not observed for any of the formulations at pH 7.4 or for the pure POPC liposomes at pH 4.5. For POPC/POPG mixtures and pure POPG liposomes, binding constants could be derived from a fit of the normalized, initial fluorescence data to the law of mass action. An exemplary fit for the titration of exenatide with liposomes composed of POPC/POPG 1:1 is shown in Figure V-7B. Primarily, MST-signals describe the fluorescence change at a given position in the sample as a function of time after heating by an IR-laser [27], [29]. The following thermophoretic movement lasts several seconds until the laser is turned off again. Changes in thermophoresis indicate a change in size, charge and the hydration shell of a molecule and are therefore highly specific for binding events.

In our case, initial fluorescence and the MST-signal by 5 seconds was used for data evaluation. K_d -values were determined by a fitting function using the law of mass action [28].

$$K_d = \frac{c_L c_P}{c_{LP}} = \frac{(c_{L0} - c_{LP})(c_{P0} - c_{LP})}{c_{LP}} \quad (\text{V-3})$$

A change of thermophoretic movement was observed for liposomes containing POPG at pH 4.5 (see Figure V-8A), but neither for liposomes of pure POPC nor for formulations at pH 7.4 (see Figure V-8B).

The dissociation constants K_d for all liposomal formulations as obtained by MST are summarized in Table V-2. The fits, derived from the software intern fit-function, resulted in binding constants of $K_d \approx 10\text{-}30 \mu\text{M}$ for the initial fluorescence analysis and analysis of the MST-signal. We may conclude that all POPG containing formulations investigated here show a high affinity binding of exenatide, while no such binding was detectable for pure, zwitterionic POPC membranes.

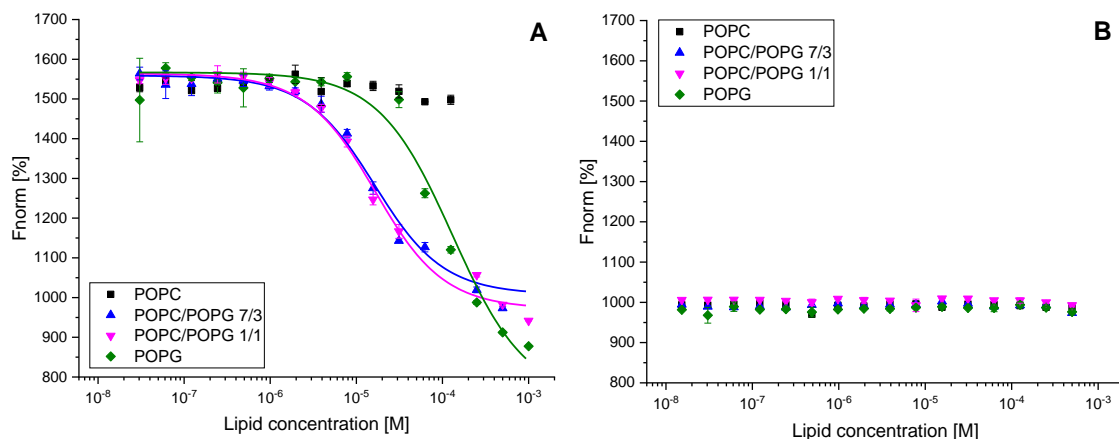


Figure V-8: Comparison of Dose Response determined by MST-Signals of the titration of exenatide (5 μM) with liposomes at A) pH 4.5 and B) pH 7.4 (n=3). Fit functions for the two POPC/POPG mixtures and the pure POPG liposomes are shown for pH 4.5.

Significance and meaning of the apparent differences between the dissociation constants are not important for the current study and would need considerable, additional efforts and methods to be elucidated. In particular, the apparently higher K_d for POPG as obtained repeatedly from the MST signal but not from initial tryptophan fluorescence should not be claimed significant without further validation. Potential sources of enhanced error or biases might be an oversimplification of the binding model, incomplete equilibration, aggregation phenomena, etc.

Table V-2: Summary of K_d -values [μM] derived from the MST measurements. All experiments were performed at pH 4.5 in 50 mM sodium acetate buffer.

Lipid composition	Initial Fluorescence K_d [μM]	MST-Signal K_d [μM]
POPC	-	-
POPC/POPG 7:3	27.3 (\pm 3.2)	13.8 (\pm 2.5)
POPC/POPG 1:1	10.4 (\pm 2.0)	13.9 (\pm 2.0)
POPG	13.7 (\pm 4.0)	128.4 (\pm 35.2)

V.1.5 Discussion

V.1.5.1 *In vitro* release behavior of exenatide from VPG

As discussed above, several previous studies suggested faster, erosion controlled release from low-viscosity gels and slower, diffusion controlled release from more viscous ones [3], [32]. Exenatide release from the formulations studied here showed the opposite behavior. The formulations composed of POPC showed significantly lower viscosity than those containing POPG but, nevertheless, substantially slower release than those with POPG. Obviously, viscosity alone is not always sufficient to understand or predict release characteristics. Instead, a complex combination of release mechanisms with their individual kinetics has to be considered for a more detailed understanding.

There are two principal mechanisms of drug release from VPGs, diffusion of the drug out of the gel and erosion of the gel releasing the embedded drug. According to the Einstein-Stokes equation, a peptide of 5 kDa should have a diffusion coefficient in water of the order of $D = 130 \mu\text{m}^2/\text{s}$. Taking into account that the mean square distance of diffusion, $\text{MSD} = 2Dt$, this D implies that within a time of $t = 1 \text{ h}$, the peptide spreads out over a root mean square distance of $\text{RMSD} \approx 1 \text{ mm}$. Depending on the dimensions, tortuosity, and micro-viscosity of the gel, this should be the order of magnitude of releasing non-entrapped drug from the gel. Our experimental setup was designed to record long-term release and not suited to precisely quantify release on this time scale, but practically all release curves showed a release of the order of 10 – 20% of the drug with a half-life of up to 1 hour.

We found a substantial retardation of release for the majority of the drug in all formulations tested here, by about 2.5 days for POPG containing gels and by several weeks by purely zwitterionic gels of POPC. In the following, we will attempt to interpret this behavior on the basis of additional data.

V.1.5.2 Interactions between exenatide and phospholipids

In order to assess the contributions of exenatide binding to the lipid gel to the retardation of drug release, we have studied exenatide-liposome interactions in dilute systems by microscale thermophoresis. The binding of exenatide to phospholipid membranes strongly depends on the charge of the peptide and phospholipid. Given that strong

binding was observed only for cationic peptide (pH 4.5) to anionic, POPG containing, membranes supports the idea of a largely electrostatic, superficial adsorption with little or no intrusion of hydrophobic side chains into the membrane.

Binding was detected based on changes in tryptophan fluorescence and thermophoretic mobility with MST measurements. Except for one apparent outlier of unclear significance as discussed above, dissociation constants for all liposomes containing POPG are, within error, of the order 10-30 μM . A detailed and rigorous discussion of the subtle differences between the K_d -values is, however, not warranted and outside the scope of this study.

Binding to zwitterionic POPC is significantly weaker and was not measurable in the investigated concentration range. Such a high K_d may still suffice for binding all peptide in a lipid gel with its far higher concentration but the weaker binding energy would still allow for a faster off rate and, hence, release kinetics from the surface to the bulk solution.

V.1.5.3 Erosion-driven, fast release from POPG containing gels

Let us recapitulate the insights obtained for exenatide in POPG containing gels. The retarded release of $\geq 80\%$ of the drug showed half-lives of 2.5 – 8 days and showed a good, linear correlation with lipid erosion into the supernatant ($r > 0.98$, not shown explicitly). At pH 4.5, exenatide binds to POPG-containing liposomes with a high affinity ($K_d \approx 10\text{-}30 \mu\text{M}$). As one should expect, binding to the anionic membrane was not detectable at pH 7.4, where the peptide is negatively charged, too. Nevertheless, release kinetics were virtually unaffected by the initial pH within the gel.

Taken all these points together, we can conclude that the kinetics of exenatide release from POPG containing gels studied here is governed by the kinetics of gel erosion. However, it has to be taken into account that exenatide released in vesicles may contribute significantly to *in vitro* release data, but not necessarily be fully bioavailable *in vivo*.

Note that in contrast to zwitterionic lipids swelling spontaneously, only up to a certain level of hydration, anionic lipids may swell infinitely due to their electrostatic repulsion [33]. An excess of bound peptide at pH 4.5 would overcompensate the charge of the lipid and render the overall charge of the peptide-lipid-particles or layers positive. Again, this might promote erosion of the gel. Interestingly, both the strongly bound exenatide in the pH 4.5 VPGs as well as the non-membrane-interacting exenatide in the pH 7.4 VPGs show

no substantial diffusional release that would detectably add to that by erosion. Of course, a change in diffusion due to binding will not matter to overall release kinetics as long as erosion remains rate limiting. Second, the pH in the VPGs (4.5 or 7.4) approaches the pH of the surrounding buffer (20 mM PBS pH 7.4) during the first days of release by diffusion. Alignment of the pH of the buffer inside of the VPG to the pH of the surrounding release buffer may explain the strong similarities between the release curves at encapsulation pH 4.5 and 7.4. Third, as discussed in the next section, both very strong binding and repulsion will prevent diffusional release from a multilamellar gel, either by attraction or by barrier function, respectively.

V.1.5.4 Barrier based retention in gels of POPC

Gels of the zwitterionic lipid POPC retarded the release of $\approx 80\%$ of the loaded exenatide to rates that suggest half-lives of several weeks and the correlation with lipid erosion was less compelling. An affinity of the peptide to these membranes could not be observed at least in dilute liposomal systems implying that interactions in the gel are repulsive or only weakly attractive.

No matter what finally controls release, both erosion and diffusion of these gels are retarded to half-lives of at least weeks. The lack of high affinity binding of exenatide to these VPGs suggests that it is primarily the barrier function of membranes in the gel that allows for this very slow diffusional release. Note that at least a low affinity of the drug to the phospholipid is vital for the molecule to penetrate into and across the phospholipid bilayer. The partitioning-diffusion model defines membrane permeability P on the basis of partition (here: K) and diffusion coefficient (D):

$$P = \frac{K \cdot D}{d} \quad (\text{V-4})$$

for a given membrane thickness of d . That means, membrane binding/partitioning is a prerequisite for permeation. For sink conditions, the resulting time dependence of the retained concentration becomes:

$$c_{donor}(t) = c_0 \cdot \exp\left\{-\frac{P \cdot A}{V_{donor}} \cdot t\right\} \quad (\text{V-5})$$

with the initial drug concentration on the donor side of c_0 , the membrane area A , and the volume of the donor compartment of V_{donor} . That means, the rate of drug release across a membrane is expected directly proportional to P and hence, to K . The exenatide-liposome system might not obey the partitioning-diffusion model to a good approximation, for example because the peptide might adsorb on the surface rather than partitioning into the membrane. Nevertheless, a higher concentration at the membrane should facilitate permeation compared to the case of a membrane that is not approached by the peptide. In this context, it is also instructive to recall Lipinski's rules that, in the end of the day, describe prerequisites for passive absorption of a drug across a membrane. For fast permeation, it needs intermediate polarity and hydrophobicity values. Too hydrophobic molecules ($\log P > 5$) are little soluble and get stuck in the membrane; too polar molecules (too many H-bond donors and acceptors) prevent the drug from entering the membrane in the first place. Hence, it is very plausible that barrier-controlled release from a lipid membrane based drug delivery system does not increase or decrease monotonically with a certain parameter, such as hydrophobicity.

V.1.6 Conclusions

Release from VPGs is an extremely complex process, resulting of different mechanisms like erosion, interactions, diffusion and permeability of the lipid bilayers, all occurring at the same time and complementing each other. Additional factors influencing drug release may be the inner structure e.g. vesicle size and homogeneity as well as the viscosity of the VPG.

A high viscosity of the VPG was previously connected to slow release and erosion rates of the system. This correlation was not confirmed in the present study. For POPG containing VPGs, the release of exenatide showed half-lives of several days that were, obviously, governed by the erosion of the gel. In spite of the fact that these lipid mixtures bound exenatide with high affinity ($K_d \approx 10\text{-}30 \mu\text{M}$) at pH 4.5 but not detectably at pH 7.4, gels produced at these two pH values shared similar release rates. This can be explained by diffusion not being rate limiting and relatively fast pH matching between VPG and release medium due to diffusion of protons or hydroxide.

VPG of POPC showed much slower release of exenatide, with a half-life of several weeks. The fact that this lipid did not show high affinity binding of exenatide suggests that their very strong retardation of the diffusional release of exenatide is primarily based on its very weak permeability across the lipid membranes in the gel.

Notably, both very high and lacking affinity of the drug to the gel retard diffusion, by attraction or barrier function, respectively.

Thus, a mathematical description of the release from VPGs resulting from this complex mixture of mechanisms, contributing to or influencing the release behavior is not possible at the moment. A rational design of the depot formulation based on mathematical predictions of the release behavior for novel drug candidates is still impossible.

Further investigations on the release behavior and characterization of the fluidity and barrier functionality of the multiple lipid bilayers of the VPG are necessary to resolve all mechanisms behind the release kinetics completely, to be finally able to describe release behavior from VPG mathematically.

V.1.7 Acknowledgements

The authors thank NanoTemper Technologies GmbH and especially Dr. Nuska Tschammer for helping with the development of the MST-method, conduction of the measurements and the interpretation thereof.

A.S. thanks the RTG 2202 “Transport across and into membranes” funded by the Deutsche Forschungsgemeinschaft for financial and other support.

V.1.8 Supplement

Table V-3: Multi-step-gradient elution used during RP-HPLC quantification of exenatide.

Time [min]	Mobile phase A [%]	Mobile phase B [%]
0	100	0
2	70	30
10	20	80
15	20	80
20	70	30
32	100	0

V.2 Further studies

In order to support the data in section V.1 on interactions between exenatide and phospholipids, isothermal titration calorimetry and isothermal steady state fluorescence measurements were additionally conducted. Furthermore, the permeability of the differently composed lipid-membranes for exenatide was tested in monolayer measurements at the air/water interface.

Part of the work in this chapter has been conducted in close cooperation with the Albert-Ludwigs-Universität in Freiburg. ITC measurements were performed together with Anja Stulz or by Anja Stulz alone. Prof. Dr. Heiko Heerklotz and Anja Stulz evaluated and interpreted the results of these measurements as described in section V.2.2.1. All other data was evaluated and interpreted in intensive collaboration. Parts of this section are intended for publication. A manuscript with the working title *“Different aspects of a complex protein-ligand binding equilibrium as seen by ITC, Fluorescence and MST.”* is in preparation.

V.2.1 Material and Methods

V.2.1.1 Preparation of liposomes

Liposomes were prepared using the thin-film method described in section V.1.3.7. Alternatively, to the described method a SpeedVac system (Christ RVC 2-18, Martin Christ Gefriertrocknungsanlagen GmbH, Germany) was used to produce a thin lipid-film on the wall of the glass vial. Subsequently, films were hydrated with 50 mM sodium acetate buffer pH 4.5, 10 mM Tris buffer pH 7.4 (containing 110 mM NaCl and 0.5 mM EDTA), or 20 mM PBS pH 7.4. Liposomes were extruded by a Lipex (Burnaby, Canada) or LiposoFast (Avestin Inc., Canada) extruder.

The lipid concentration in the liposome dispersion was either determined using a Bartlett Assay or by gravimetric determination [24], [34].

V.2.1.2 Isothermal titration calorimetry

Isothermal titration calorimetry (ITC) measurements were carried out on a MicroCal VP-ITC instrument (Malvern Instruments, UK). All runs were performed at 25 °C with a stirring speed of 394 rpm. Typically, 8 µL injections were made every 5-10 minutes. As usual, the

heat of an initial injection of 1 μL was excluded from the analysis to eliminate its higher error. All samples were degassed prior to loading into the calorimeter. In exenatide-into-lipid titrations, aliquots from the syringe containing an exenatide solution (100 μM) were injected to the calorimeter cell ($V_{\text{cell}} = 1.4288 \text{ mL}$) which contained a dispersion of vesicles (typically, 80 μM lipid). In lipid-into-exenatide titrations, the cell was filled with an exenatide solution (typically, 3 μM) and the syringe was loaded with lipid vesicles (800 μM lipid). In parallel to some runs, DLS measurements were conducted to check vesicle size and size distribution during the ITC experiment. To imitate the exenatide-into-lipid ITC run, 8 μL aliquots of an exenatide solution (100 μM) were titrated into a cuvette containing 1.4 mL POPC/POPG 1:1 vesicles (80 μM lipid) every 5 minutes. Vice versa, 8 μL aliquots of POPC/POPG 1:1 vesicles (800 μM lipid) were titrated into 1.4 mL exenatide solution (3 μM) imitating the lipid-into-exenatide ITC. Five minutes after each injection, Z-average size and PDI were measured with a Zetasizer nano ZS (Malvern Instruments, UK). MicroCal PEAQ-ITC analysis software (Malvern Instruments, UK) was used for data evaluation and curve fitting according to the law of mass action.

V.2.1.3 Isothermal steady-state Fluorescence

Steady-state fluorescence was measured using a Cary Eclipse fluorescence spectrometer (Agilent Technologies, USA) and an Optim 1000 instrument (Avacta, USA). Dilution series were prepared with a constant amount of exenatide in the solution (typically, 5 μM) and increasing amount of liposomes. The two components were incubated for 10 minutes before measurement. Samples were prepared either in 50 mM sodium acetate buffer pH 4.5 or in 20 mM PBS pH 7.4. Interactions were assessed by steady-state fluorescence using a Cary Eclipse spectrometer with an excitation wavelength of 280 nm while emission was measured in a range between 300 and 450 nm. Fluorescence was measured using a cuvette at a defined temperature of 20 $^{\circ}\text{C}$ and spectra were corrected for background intensities and scattering of liposomes by background subtraction [35]. Excitation and emission slits with 5 nm bandpass were used for all measurements.

At the Optim 1000 instrument, intrinsic fluorescence mode was used for all measurements ($\lambda_{\text{exc}} = 266 \text{ nm}$, $\lambda_{\text{em}} = 250\text{-}720 \text{ nm}$). Experiments were performed in isothermal mode, at a fixed temperature of 20 $^{\circ}\text{C}$. MCAs with a capillary volume of 9 μl

were used for the measurements. Each MCA was measured five times and background subtraction of the respective blanks was performed for spectra correction.

V.2.1.4 Langmuir trough measurements

Experimental measurements were conducted with a Langmuir-Blodgett Trough (Microtrough XS, Kibron Inc., Helsinki, Finland). The rectangular (59 x 397 mm²) PTFE trough was equipped with a metal alloy dyne probe for surface pressure (π) measurements. The surface area can be adjusted by two mobile PTFE barriers with a maximum area of 234 cm². Prior to each measurement the trough was rinsed with ethanol and then highly purified water. All experiments were conducted at 20 °C.

V.2.1.4.1 Compression isotherms of lipid-monolayers

Separate stock solutions of the individual lipids (POPC, POPG) or lipid mixtures (POPC/POPG 7:3 or POPC/POPG 1:1) were prepared by solving the respective lipids in chloroform (1 mg/ml). Monolayers of the phospholipids were obtained by carefully spreading 20 μ l of the solution on the surface of the 20 mM PBS buffer subphase (pH 7.4) using a Hamilton microsyringe (Hamilton Co., Reno, NV, USA). The film was allowed to equilibrate for at least 15 minutes, before the film was compressed with a compression speed of 56,1 mm/min. Measurements were done in triplicates for each lipid.

V.2.1.4.2 Surface activity of exenatide

Further, the surface activity of exenatide was studied in order to determine the equilibrium spreading pressure of the peptide on buffer surface. To this end, exenatide solutions with different concentrations (0.39063 μ M to 200 μ M) in 20 mM PBS pH 7.4 were prepared and the surface pressure of each solution was determined.

V.2.1.4.3 Intercalation of exenatide into lipid monolayers

The kinetics of peptide insertion into the monolayers (POPC, POPG, POPC/POPG 7:3 and POPC/POPG 1:1) were determined using the same setup as for the compression isotherms. Lipid-solutions were added drop wise to the surface of the subphase (20 mM PBS pH 7.4) and the film was allowed to equilibrate for 5 minutes to ensure complete chloroform evaporation. Then the film was compressed very slowly to a surface pressure of 30 mN/m, which is the monolayer-bilayer equivalence pressure, at which the molecular

area of lipids in a bilayer and in a monolayer are the same or at least similar and thus the lipid packing density of a normal bilayer is mimicked [36]–[38]. Next, 1 ml exenatide solution (375 μ M) (or buffer for controls) was carefully injected in the subphase and surface pressure was recorded for 60 minutes. Since, the monolayer was kept at a constant area without further movement of the barriers, increase in surface pressure was taken as measure for interactions of exenatide with the phospholipid monolayer. Measurements were performed in triplicates for each phospholipid solution.

V.2.2 Results and Discussion

V.2.2.1 Characterization of interactions by isothermal titration calorimetry

Figure V-9 shows the heats produced by the dilution of aliquots of 100 μM exenatide at pH 4.5 injected into the cell filled with matching buffer. The experiment shows small but significant heats that decrease quasi-exponentially with increasing concentration of titrant in the cell. This is the typical behaviour if the molecules of the titrant show substantial interactions in the syringe [39]–[42]. Such interactions include the formation of dimers or oligomers, but may also be very transient and short-lived. For simplicity, it is referred to these interacting molecules as “oligomers” without restriction regarding their size, lifetime, or stability. After an injection of an aliquot of oligomers into the cell, these oligomers are diluted and dissociate. For subsequent interactions, the cell is “filling up” with monomers and the degree of dissociation of the injectant decreases. Integration of the curve yields a value of 60 kJ/mol, representing the product of the maximal mole number of monomers forming in the cell and their enthalpy of dissociation. Such ITC signals have, for example, been used to describe the oligomerization behaviour of doxorubicin in quite some detail [40].

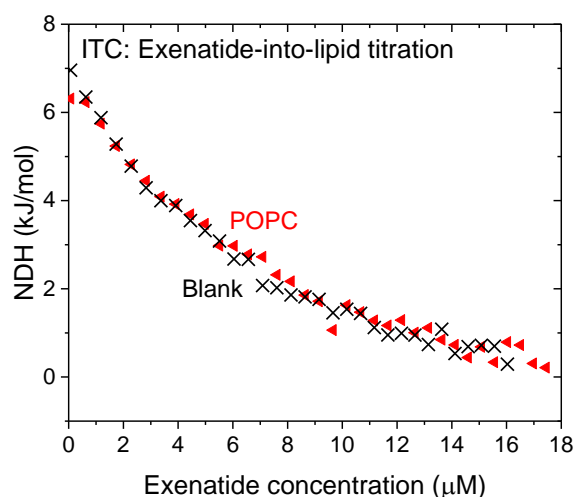


Figure V-9: A dilution experiment (“blank”, black crosses) performed by diluting aliquots of exenatide (100 μM) into matching acetate buffer at pH 4.5 indicates that exenatide assembles at high concentrations. Titration of exenatide aliquots (100 μM) into the cell filled with POPC vesicles (red triangles) (80 μM lipid) yields practically identical heats. Data are shown as a function of exenatide concentration.

Repeating the peptide titration schedule now with liposomes of 80 μM POPC filled into the cell, the heats are practically identical with those in the absence of lipid (orange symbols in Figure V-10A, C). This can be explained with (1) exenatide showing no significant interaction with POPC liposomes at 80 μM or, (2), the interaction being exclusively entropic in nature and hence, isocaloric ($\Delta H = 0$).

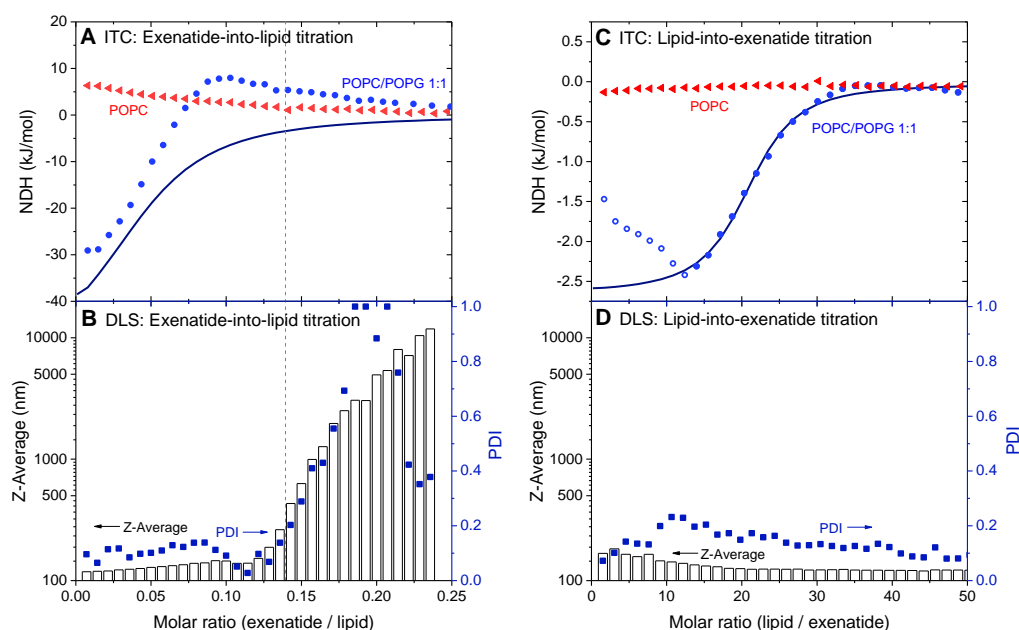


Figure V-10: A) ITC of POPC (red triangles) and POPC/POPG 1:1 (blue dots) vesicles (80 μM lipid) titrated with exenatide (100 μM) at pH 4.5. Data is shown as a function of exenatide/lipid ratio. The solid line represents a simulation with the same fitting parameters found by the fit in panel C. B) DLS measurements of exenatide-into-lipid titration. 8 μL aliquots of an exenatide solution (100 μM) were titrated into a cuvette containing 1.4 mL POPC/POPG 1:1 vesicles (80 μM lipid) every 5 minutes. C) ITC curve of exenatide (3 μM) titrated with lipid vesicles (800 μM) composed of POPC (red triangles) and POPC/POPG 1:1 (blue dots). Data is shown as a function of lipid/exenatide ratio. As in panel A, no interaction of exenatide with pure POPC could be observed under the chosen conditions. The model ‘one set of sites’ was used to fit POPC/POPG 1:1 data (solid line). Injections at the beginning of the titration at low lipid/exenatide ratio were excluded. D) DLS measurements of lipid-into-exenatide titration. 8 μL aliquots of POPC/POPG 1:1 vesicles (800 μM lipid) were titrated into a cuvette containing 1.4 mL exenatide solution (3 μM) every 5 minutes.

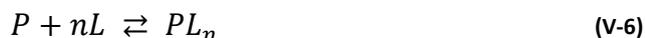
The latter option seems very unlikely in the light of data on similar systems, but cannot be ruled out formally. The lack of any detectable interaction would imply that, if there was a binding of exenatide to POPC, its product of dissociation constant K_d and stoichiometry n (lipids per binding site) would need to be larger than $nK_d = 80 \mu\text{M}$. That means, affinity would be fairly weak if there was some in the first place. The same result is observed at

pH 7.4 with all tested lipid mixtures (POPC, POPG and POPC/POPG mixtures) (data not shown).

Doing the same sequence of injections into the cell pre-loaded with liposomes of POPC/POPG 1:1 (Figure V-10A, blue dots), we obtain a complex curve with a quasi-sigmoidal, exothermic behavior followed by a local, endothermic maximum. This shape has been discussed before for the binding of a self-associating drug, doxorubicin, to polymeric nanoparticles [40]. In the beginning, the peptide oligomers dissociate like in the blank, but there are fewer monomers accumulating in solution since most of the injected peptide molecules bind to the liposomes. We will find below that the contribution from this “primary” binding of peptide monomers to the membrane is approximately represented by the blue, simulated curve. Hence, the heats in the beginning of the titration are simply up-shifted from the black, primary binding curve by about 7 kJ/mol, the “blank” heat of dissociating injected oligomers (Figure V-9). Primary binding saturates centered at 0.05 peptides per lipid, implying the existence of defined “binding sites” for the peptide on the membrane. In the current example, the average number of lipid molecules per site is $1/0.05 = 20$. Note that this does not mean that all these lipids really take part in peptide binding. Beyond 0.05 peptide/lipid, it is not only that further exothermic, primary binding comes to a halt gradually and injected oligomers keep on dissociating. The endothermic offset increases to values larger than the blank and the liposomes start to grow gradually while maintaining a PDI < 0.2 (see Figure V-10B). These phenomena can be assigned to a secondary, super-saturating binding of peptide to the liposomes. At even higher peptide concentration of about 0.13 peptide/lipid, a dramatic increase in size and PDI implies aggregation of the peptide-supersaturated liposomes.

Figure V-10C illustrates the reverse experiment, titrating liposomes into a 3 μM peptide solution. Up to $1/0.13 \approx 7$ lipids/peptide, the peptide to lipid ratio is in the secondary binding range but the absolute liposome concentrations are considerably lower than in Figure V-10A. As a result, aggregation is quite limited but there is an endothermic deviation from the blue, primary binding curve (identical parameters as the one in Figure V-10A). Continuing the titration beyond 7 lipids/peptide, possible small aggregates may be disintegrated and peptide oligomers in solution are dissociated (endothermic) as more and more peptide is adsorbed by added liposomes. At about 15 lipids/peptide, these processes seem to be finished. The only significant process left is the binding of the

peptide monomers remaining in solution to primary sites on the injected liposomes. These data define the blue, primary binding curves in Figure V-10C and, re-calculated, Figure V-10A, according to the law of mass action for the generalized reaction:



yielding a dissociation constant, K_d :

$$K_d = \frac{(nc_L^0 - c_P^b)(c_P^0 - c_P^b)}{c_P^b} \quad (\text{V-7})$$

where c_L^0 stands for the total lipid concentration and c_P^0 for the total peptide. c_P^b denotes the concentration of membrane bound peptide and, in other words, the concentration of occupied sites, and nc_L^0 represents the total concentration of membrane binding sites with the average number of lipids per binding site, n . The binding site is a pre-assembled membrane patch (so, n does not appear in the exponent) and n may include contributions from inactive lipids, e.g. in an inaccessible interior of the liposome, or of a non-binding lipid species.

Fit and simulation were done using Malvern-MicroCal software for ITC. It should be emphasized that the approach to exclude the beginning of the experiment, where secondary binding occurs, from the fit means that the fit parameters obtained here should refer to primary binding only.

Qualitatively similar curves and consistent fits were obtained repeating the lipid-into-exenatide titrations at different exenatide concentrations (not shown in detail). For the other lipid systems studied, the respective results are compiled in Table V-4 on page 154. Summarizing this section, we find no binding of exenatide to POPC in the lower μM concentration range. In the presence of POPG, we find rather strong primary binding saturating at about 9 -26 lipids per peptide depending on the specific PC-PG ratio. Upon saturation of the primary sites, further, secondary binding proceeds as an endothermic process. We have not been able to obtain a quantitative description of this secondary binding from ITC data.

V.2.2.2 Isothermal steady state fluorescence

The sensitivity of the initial tryptophan fluorescence of exenatide to exenatide-liposome interactions seen in the MST system (see section V.1.4.4), motivated a more detailed inspection in a fluorescence spectrometer [43]. Contact of tryptophan and many other

fluorophores with water causes fluorescence quenching and dipolar relaxation phenomena to lower energies, indicated by a red shift of the spectrum. Hence, binding processes shielding previously superficial tryptophan residues from water and rendering their environment less polar can be detected in terms of an increase in intensity as well as a spectral shift to lower wavelengths [43]–[47].

A significant shift of the fluorescence spectral maximum of exenatide to smaller wavelengths (blue-shift) was, indeed, observed in the presence of liposomes composed of POPC/POPG mixtures or liposomes composed of 100% POPG at pH 4.5 (see Figure V-11A). The fluorescence maximum shifts from approximately 347 nm to 334 nm after the addition of POPG liposomes to a 5 μ M exenatide solution at pH 4.5.

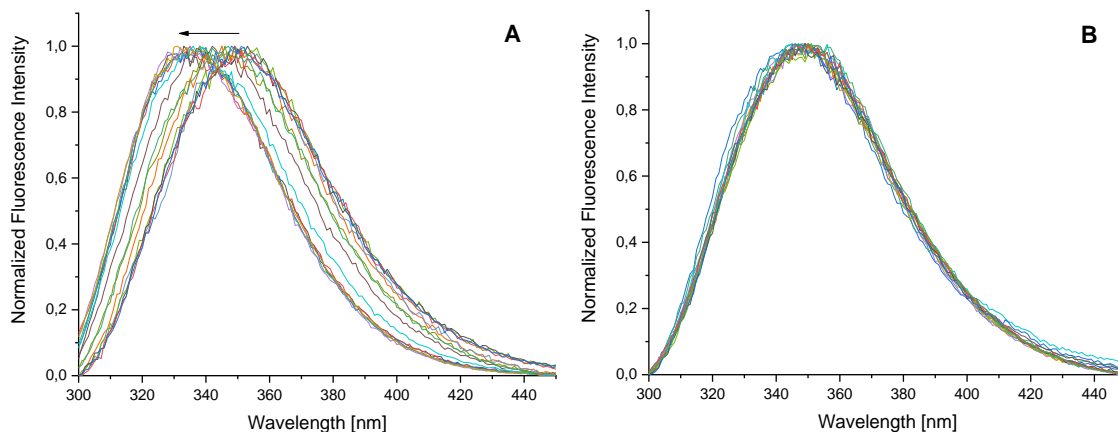


Figure V-11: Normalized fluorescence spectra of the titration of exenatide (5 μ M) with A) POPG-liposomes (0.5 mM - 1.5×10^{-5} mM) and B) POPC-liposomes (0.5 mM - 1.5×10^{-5} mM).

No changes in fluorescence maximum were observed for the addition of liposomes composed of 100% POPC (see Figure V-11B) and for all formulations at pH 7.4.

To fit these data, we have assumed a two-state system with tryptophan showing the properties of the “free” or “bound” states. We may, then, write for the intensity, F , at a given wavelength, λ , as a function of the degree of binding, x_b :

$$F_{\lambda}(x_b) = x_b F_{\lambda}(1) + (1 - x_b) F_{\lambda}(0) \quad (\text{V-8})$$

with x_b defined as:

$$x_b = \frac{C_p^b}{C_p^0} \quad (\text{V-9})$$

and $F(0)$ and $F(1)$ representing the intensity expected if all peptide is free or all peptide is bound, respectively; these values should not depend on x_b and be conserved in a binding experiment if the peptide concentration is held constant.

To compute x_b for a given parameter set, we have to calculate the concentration of bound peptide, c_P^b , by solving equation (V-7):

$$c_P^b = \frac{K_d}{2} \cdot \left[\frac{nc_L^0 + c_P^0}{K_d} + 1 - \sqrt{\left(\frac{nc_L^0 - c_P^0}{K_d} \right)^2 + 2 \cdot \frac{nc_L^0 + c_P^0}{K_d} + 1} \right] \quad (\text{V-10})$$

Equation (V-8) with (V-9) and (V-10) was used to fit K_d and n along with $F_{330}(0)$, $F_{330}(1)$, $F_{350}(0)$, and $F_{350}(1)$ to the intensity changes at both 330 and 350 nm simultaneously as a function of lipid concentration (see Figure V-12A). Data was fitted in Excel by nonlinear least-square fitting as shown by Kemmer et al. [48]. Our fit was fairly robust, which was tested by manually fixing K_d and n values to values slightly different from the optimal ones and observing how the sum of squared residuals is affected by changes of each of the parameters separately.

Alternatively, we may fit the spectral shift, independently of intensity changes. Given that the maximum of the very broad spectrum is not well defined, we rather express spectral shifts in terms of the ratio

$$R_{350/330} = \frac{F_{350}}{F_{330}} \quad (\text{V-11})$$

which decreases upon a blue-shift of the spectrum. Equation (V-8) applies to F_{330} and F_{350} independently with shared x_b . For $R_{350/330}$, equations (V-8) and (V-11) yield:

$$R_{350/330}(x_b) = \frac{x_b F_{350}(1) + (1 - x_b) F_{350}(0)}{x_b F_{330}(1) + (1 - x_b) F_{330}(0)} \quad (\text{V-12})$$

In contrast to F_λ , $R_{350/330}$, is not simply an x_b -weighted average of the values for all-free and all-bound peptide but additionally spectral shifts are taken into account. This fit is illustrated by Figure V-12B. The parameters, also included in Table V-4, agree with those from the intensity fit within experimental error.

Again, both F and $R_{350/330}$ of exenatide are found unaffected by the addition of POPC liposomes at pH 4.5 as well as any lipid tested at pH 7.4.

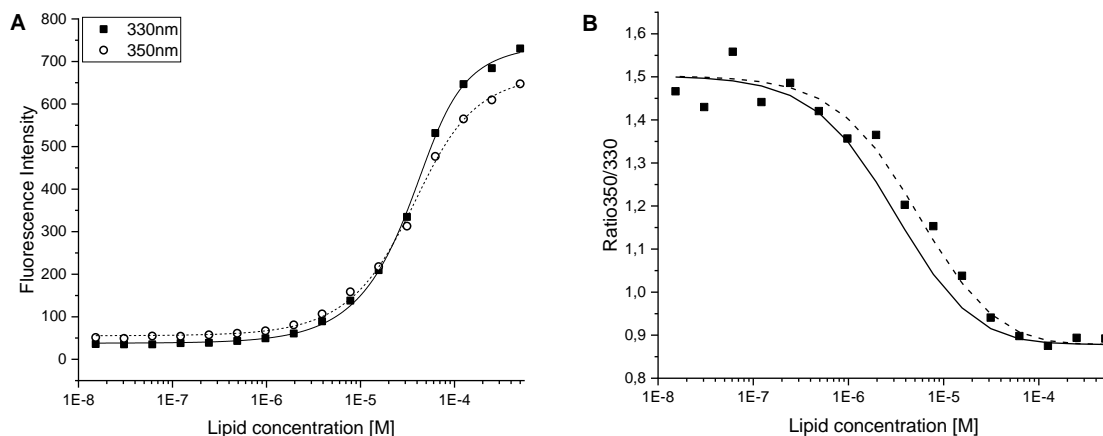


Figure V-12: A) Raw fluorescence curves at 330nm and 350nm of titrations of 5 μ M exenatide with liposomes composed of POPC/POPG 7:3 along with fit curves of a global fit representing $K_d = 1.4 \mu\text{M}$, $n = 9.2 \mu\text{M}$, $F_{330}(0) = 38$, $F_{330}(1) = 730$, $F_{350}(0) = 57$, $F_{350}(1) = 650$ according to eq. (V-8) with (V-9) and (V-10). B) Ratio 350 nm/330 nm of the data presented in panel A, along with a solid curve calculated on the basis of the fit parameters (K_d and n) obtained in panel A and a dashed curve fitted to the data shown here according to eq. (V-12), yielding $K_d = 1.2 \mu\text{M}$ and $n = 9.2$. For a compilation of these parameters and those for the other lipid mixtures (fits not shown), see Table V-4, "Fluorescence" section.

V.2.2.3 Comparison of binding events detected by ITC, fluorescence measurements and MST

In order to compare all of the above described methods used to study binding between exenatide and phospholipids, data obtained from MST had to be re-evaluated with the same fit-function (law of mass action with open stoichiometry n , equation (V-7)) used for ITC and fluorescence data. By taking into account the possibility of several phospholipids binding to one exenatide molecule ($n = L/P$), new binding parameters were obtained (see Table V-4).

The system at hand is much more complex than a simple ligand-to-receptor binding in solution. In line with the finding of a significant self-association of the peptide in the low micromolar concentration range (Figure V-10B), we have found that also membrane binding proceeds from a primary binding of the peptide to a number of lipids to the subsequent, secondary binding of peptide to pre-bound peptide layers. As different methods focus on different aspects of this complex behaviour, they may yield apparently contradictory results unless their different readouts are put into proper perspective.

Table V-4: Summary of K_d -values [μM] and Stoichiometry (n = lipid per peptide) derived from the different methods with which interactions were evaluated. Additionally, for ITC-experiments the reaction enthalpy ΔH [kcal/mol] is shown. All experiments were performed at pH 4.5 in 50 mM sodium acetate buffer.

Lipid composition	ITC (primary binding only)			MST				Fluorescence			
				Initial fluorescence		MST-signal		Fluorescence intensity		Ratio 350/330	
	K_d [μM]	n (L/P)	ΔH [kcal/mol]	K_d [μM]	n (L/P)						
POPC	No interaction detected										
POPC/POPG 7:3	5.8	26	-0.57	1.7	6.7	2.3	2.9	1.4	9.2	1.2	9.2
POPC/POPG 1:1	2.9	19	-0.77	0.5	5.0	2.4	3.1	0.3	4.4	4.2	4.4
POPG	0.6	8.9	-1.18	2.1	5.5	0.9	27	0.3	2.5	1.2	2.5

ITC seems uniquely suited to distinguish primary and secondary effects given that both types of binding contribute to liposome mass equally, to changes in water accessibility of Trp in the peptide similarly, but to the ITC signal with different signs. Both, strongly exothermic primary binding and weakly endothermic, secondary binding can be detected by ITC and primary binding can, to a good approximation, be fitted separately. The average number of lipids per primary binding site is 9, 20, and 26 lipids per site for membranes with 100%, 50%, and 30% POPG, respectively. Expressed per POPG only, which would be responsible for electrostatic binding, we obtain a common average of 9.5 ± 0.5 POPG molecules per site. Given that ITC detects binding within a few minutes after injection only, it is very likely that it includes little or no binding to the inner membrane surface, so that half of the lipid is inaccessible and the “contact site” would involve only patches of 4.8 POPG, along with 0 – 8 POPC molecules. Taking into account that a compact, spherical protein of 5 kDa would have a cross sectional area of about 6 lipid molecules and an alpha helix that of 2-3 lipids, it seems that a pure POPG membrane is virtually completely covered by peptide upon primary saturation. In membranes of lower POPG concentration, surface coverage could be weaker, with each peptide still clustering about 4 -5 PG molecules to its site so that the capacity is not significantly increased.

Secondary binding is qualitatively detected by ITC but it was not attempted to quantify it this way. A much more straightforward method to determine complete, i.e., primary and

secondary, binding is MST, which reports on size or mass changes of the liposome including all bound peptide molecules equally. MST of POPC/POPG mixtures suggested n values of about 3 lipids per site, which corresponds to 0.9 – 1.5 POPG for inside and outside and 0.4 – 0.8 POPG per site for outside only binding. These values provide further support to the secondary binding mechanism, given that they seem to require more than one layer of bound peptide covering the membrane surface. This is a rather clear result but the scatter of the fit parameters obtained by MST is somewhat larger.

A third method of characterizing binding is based on Trp fluorescence responding in intensity and wavelength to the polarity and water accessibility of the molecular environment of the Trp residue. Intensities were measured in the MST system and, at two wavelengths, in a fluorescence spectrometer. Intensities and spectral shapes were fitted separately, yielding consistent fits within experimental error (see Table V-4). Binding sites obtained by the two types of fits to the spectrometer data require 2.4 ± 0.4 POPG plus 0 – 6 POPC for full lipid accessibility or half as much for outside only binding to the liposomes. A priori, it is not clear whether primarily and secondarily bound peptides show virtually identical fluorescence properties. However, the fact that we obtained quite good fits of all intensities at 330 and 350 nm by a two-state model and the general consistence of the parameters with those obtained by MST suggests that this is essentially the case. Overall, the fit parameters should give a good idea of primary and secondary binding together.

The scheme (Figure V-13) illustrates the concentration ranges covered by the different experiments and the resulting ranges where primary and secondary binding proceed. Interestingly, MST is found primarily sensitive to secondary binding. Secondary binding may have a particularly strong effect on the hydrodynamic size due to surface roughness and/ or beginning, transient liposome association phenomena (see DLS data in Figure V-10), it also involves considerably more peptide molecules than primary binding.

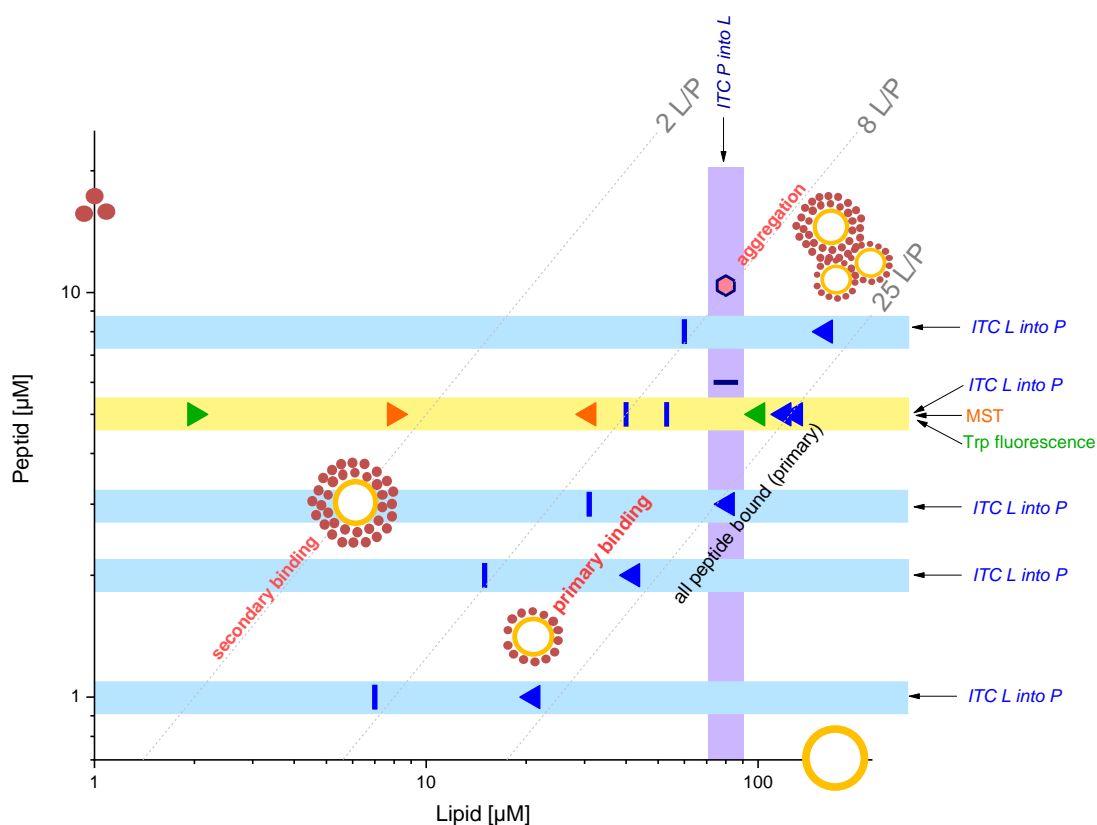


Figure V-13: Scheme describing the concentration ranges covered by the different experiments and the transition ranges revealed by them. Triangles indicate the approximate beginning and completion of transition ranges (blue: ITC; orange: MST; green: Trp fluorescence) and vertical bars are separators between secondary and primary (at lower lipid) and primary only (at higher lipid) binding. Grey grid lines illustrate specific total mole ratios of lipid-to-peptide. Concentration ranges covered by different experiments are illustrated by colored areas.

All dissociation constants are, within error, of the order $1 \mu\text{M}$. The fact that ITC reports primary and secondary binding as sequential effects implies that primary binding shows a higher affinity but this difference seems to be rather weak and could not be resolved. A possible decrease of K_d with increasing POPG concentration could be explained, for example, by the entropic “costs” of clustering POPG from a mixed membrane. A detailed and rigorous discussion of these subtle differences is, however, not warranted and outside the scope of this study.

Binding to zwitterionic POPC is at least 2 orders of magnitude weaker. Such a K_d may still suffice for binding all peptide in a lipid gel with its far higher concentration but the weaker binding energy would still allow for a faster off rate and, hence, release kinetics from the surface to the bulk solution.

V.2.2.4 Insertion of exenatide into phospholipid monolayers

The interactions between the phospholipid and the encapsulated exenatide as determined by MST, ITC and fluorescence measurements, could not explain the differences in release behavior as described in section V.1.4.2 for the differently composed VPGs. Thus, we wanted to investigate if the permeation behavior of exenatide through the phospholipid layers in the VPGs may explain the differences in release behavior.

In order to assess if exenatide permeates through the phospholipid layers, insertion of exenatide into lipid monolayers was investigated using a Langmuir trough. It is expected that after some time (few days of the release studies) pH of the inner phase of the VPG aligns to the pH of the release medium (20 mM PBS pH 7.4). Hence, experiments were performed at the more relevant pH of 7.4 only.

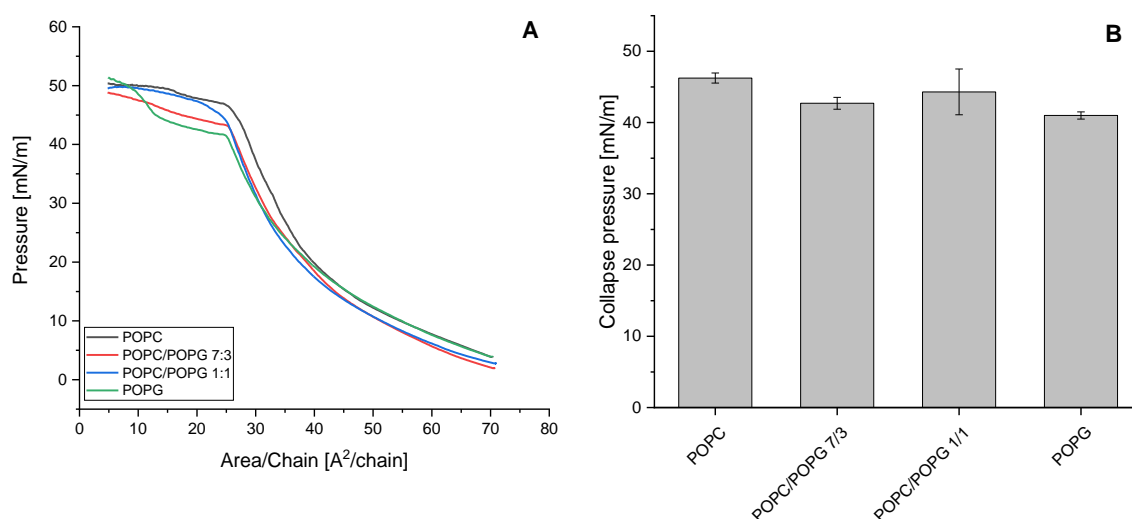


Figure V-14: Stability of phospholipid monolayers on 20 mM PBS pH 7.4. (A) Compression isotherms of lipid monolayers. (B) Collapse pressure obtained from compression isotherms.

By carefully dropping lipid-solutions on the surface of aqueous buffers, extremely thin lipid monolayers are formed [49]. First, the stability of the different lipid monolayers was tested by isothermal compression tests. Representative compression isotherms of the phospholipids are shown in Figure V-14A. All phospholipids and mixtures thereof form stable lipid monolayers at the surface. Collapse pressure ($\pi \approx 40\text{--}45$ mN/m) and the correlating area per molecule are similar for all tested phospholipids (Figure V-14B) and both are in the range of previous observed values for phospholipid monolayers [50].

With the aim to understand interactions of exenatide with lipid monolayers formed on a buffer subphase, the propensity of exenatide to localize at the air/water interface was determined by measuring the surface pressure with increasing exenatide concentration. The ability of α -helical peptides like exenatide to interact with membranes is usually associated with high surface activity [51]. This surface activity can be evaluated by observing the behavior of peptides at an air/water interface. The adsorption of exenatide to the surface results in a maximum surface pressure of $\pi_{\max} = 15.5 \text{ mN/m} \pm 1.6 \text{ mN/m}$. From this value the exenatide sub-phase concentration for the insertion studies of exenatide into the phospholipid monolayers is calculated. The obtained concentration ($2.5 \text{ }\mu\text{M}$) is a constant which represents the drug concentration at $0.5 \pi_{\max}$ [50].

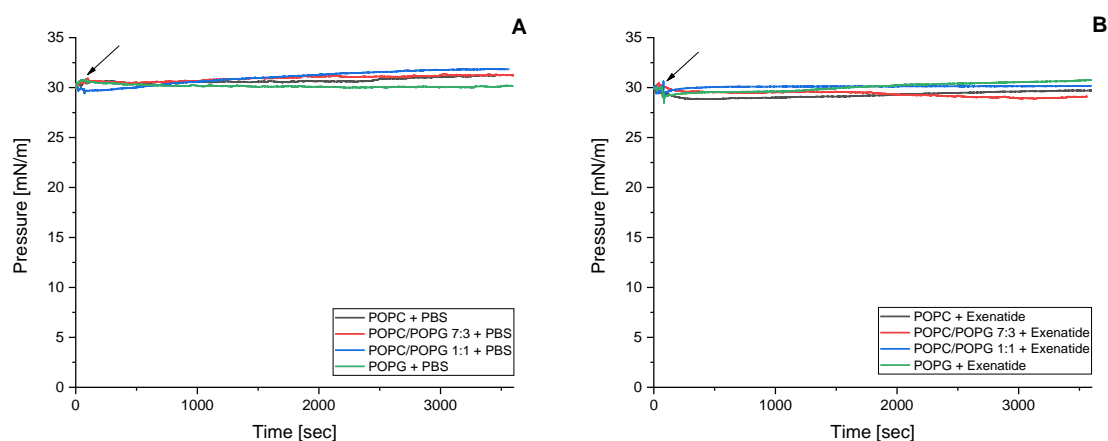


Figure V-15: Insertion of exenatide into phospholipid monolayers. A) Time course of surface pressure after injection of buffer in the subphase (20 mM PBS pH 7.4). **B)** Time course of surface pressure after injection of exenatide beneath the monolayer at a subphase concentration of $2.5 \text{ }\mu\text{M}$. Monolayers were formed from POPC, POPG and mixtures of both lipids (7:3 and 1:1). Arrow indicates the time of injection.

To characterize the peptide-lipid interactions between exenatide and the different phospholipids, a constant area approach was chosen. Exenatide was injected underneath a phospholipid monolayer with a surface pressure of 30 mN/m at a constant area. Then changes in surface pressure were monitored over 60 minutes. Peptide molecules, interacting only with the lipid head groups induce minimal surface pressure changes of less than 3 mN/m , while surface pressure changes of up to 10 mN/m are generally a result of the insertion of the peptide into the monolayer [51].

When exenatide is injected underneath phospholipid monolayers (Figure V-15B), no substantial changes in surface pressure in comparison to the “blank” injection of buffer

(Figure V-15A) was observed over 60 minutes, independently of the type of phospholipids in the monolayer.

In general, different mechanisms for the binding of water-soluble substrates like exenatide are thinkable. Non-charged and partially hydrophobic molecules intercalate into the hydrophobic regions of the fatty acyl chains of the lipid monolayer as a result of hydrophobic interactions, while charged molecules remain on the outside and may interact electrostatically with the polar head groups of the lipids [37]. Exenatide is negatively charged at pH 7.4 (as shown in section V.1.4.1). Hence, an insertion of the peptide into the lipid monolayer is very unlikely. The monolayer experiments in the presence of exenatide demonstrate that exenatide rather interacts with the polar head groups of the phospholipids (changes of $\pi \leq 3$ mN/m), than intercalates between the fatty acyl chains. This result is paralleled by the binding studies described above, which showed electrostatically interactions of the peptide at pH 4.5.

V.3 Conclusion

The release behavior of protein and peptide drugs from vesicular phospholipid gels is difficult to describe. A complex mixture of mechanisms affects the release behavior from VPGs and results in characteristic release curves depending on the type of phospholipids, phospholipid concentration, encapsulated protein, pH-value and buffer composition. In this chapter, the effect of protein-phospholipid interactions on the release from VPGs was investigated.

In vitro release tests of exenatide from VPGs with different phospholipid composition showed differences in the release kinetics of the peptide. While slow release was observed for VPGs composed of POPC, faster release was recorded when POPG was present in the formulation. At the same time an increase in viscosity was observed when the lipid mixture contained POPG. These observations are inconsistent with the expectation that VPGs with high viscosity show a slow release of the encapsulated drug. In order to show if the release rates were in fact an effect of interactions between the phospholipids and the encapsulated peptide, different methods (MST, ITC, fluorescence measurements) were chosen to investigate the binding of the two molecules.

For VPGs containing POPG the release of exenatide showed half-lives of several days in comparison to several weeks from VPGs composed of POPC. These differences were obviously a result of the erosion of the phospholipid matrix. MST, ITC and fluorescence measurements showed a strong binding of exenatide to POPG containing vesicles with high affinity at pH 4.5, while binding was not detectable at pH 7.4 with all methods. The fact that both gels (encapsulation pH 4.5 and 7.4) showed similar release rates, may be explained by a rapid alignment of the pH in the VPG to the surrounding buffer phase (pH 7.4). All obtained binding parameters ($K_d \approx 1 \mu\text{M}$) are comparable between the three techniques after fitting the data to the law of mass action with an open stoichiometry. However, different binding events, which are not registered by all methods with the same sensitivity, have to be distinguished. A significant self-association of the peptide occurs at low concentrations. Further, membrane binding of exenatide involves primary binding of the peptide to the phospholipids and secondary binding to pre-bound exenatide. While ITC seems to distinguish between primary and secondary effects, MST and fluorescence measurements are able to determine complete binding (primary and secondary binding).

VPGs composed of POPC showed much slower half-lives of several weeks, which could neither be attributed to the erosion of the VPG nor to interactions between the peptide and phospholipids. Thus, other mechanisms like stability and permeability of phospholipid membranes for drug compounds may be responsible for the sustained release from VPGs. In order to assess the permeability of exenatide through the phospholipid bilayers composed of POPC, POPG and mixtures of both, monolayer experiments at the air/water interface were conducted. Surface pressure measurements at a starting value of 30 mN/m and a constant area showed, that exenatide did not intercalate into the phospholipid monolayer, independently of the lipid composition. These findings suggest a very weak permeability of exenatide across the lipid membranes in the VPG.

In conclusion, interactions between the encapsulated protein and the phospholipid occur and are measurable with the commonly used techniques for the investigation of binding. However, binding is not the major or at least not the strongest factor influencing release behavior of proteins from VPGs. Depending on the lipid type and the encapsulated protein, erosion of the lipid matrix and permeability of the protein through the lipid layers are suggested to be the most powerful parameters controlling the release from VPGs *in vitro*. Though, it has to be taken into account, that erosion is expected to be different *in vivo* compared to the *in vitro* situation. In the present study, it was shown that VPGs composed of POPG or phospholipid mixtures containing POPG disintegrate faster in comparison to VPGs composed of POPC only. Since, for exenatide release from VPGs membrane permeability was found to be a minor factor, erosion of the VPGs is rate limiting for release kinetics in this specific case. However, it has to be kept in mind, that membrane permeability strongly depends on the encapsulated protein or peptide and the lipid composition. Further, encapsulation of proteins may also influence the erosion behavior of the VPGs, which has to be considered for each VPG formulation individually.

V.4 References

- [1] M. Brandl, M. Drechsler, D. Bachmann, and K. H. Bauer, "Morphology of semisolid aqueous phosphatidylcholine dispersions, a freeze fracture electron microscopy study," *Chem. Phys. Lipids*, vol. 87, pp. 65–72, 1997.
- [2] M. Brandl, "Vesicular Phospholipid Gels: A Technology Platform," *J. Liposome Res.*, vol. 17, no. 1, pp. 15–26, 2007.
- [3] W. Tian, S. Schulze, M. Brandl, and G. Winter, "Vesicular phospholipid gel-based depot formulations for pharmaceutical proteins: Development and in vitro evaluation," *J. Control. Release*, vol. 142, no. 3, pp. 319–325, 2010.
- [4] G. Winter, M. Brandl, S. Schulze, and W. Tian, "Vesikuläre Phospholipid-Gele mit proteinösen Substanzen," EP2210589, 2009.
- [5] C. Tardi, M. Brandl, and R. Schubert, "Erosion and controlled release properties of semisolid vesicular phospholipid dispersions," *J. Control. Release*, vol. 55, no. 2–3, pp. 261–270, 1998.
- [6] U. Massing, S. Cicko, and V. Ziroli, "Dual asymmetric centrifugation (DAC)-A new technique for liposome preparation," *J. Control. Release*, vol. 125, no. 1, pp. 16–24, 2008.
- [7] H. Grohganz, I. Tho, and M. Brandl, "Development and in vitro evaluation of a liposome based implant formulation for the decapeptide cetorelix," *Eur. J. Pharm. Biopharm.*, vol. 59, no. 3, pp. 439–448, 2005.
- [8] N. Qi *et al.*, "Sustained delivery of cytarabine-loaded vesicular phospholipid gels for treatment of xenografted glioma," *Int. J. Pharm.*, vol. 472, no. 1–2, pp. 48–55, 2014.
- [9] Y. Zhong *et al.*, "Vesicular phospholipid gels using low concentrations of phospholipids for the sustained release of thymopentin : pharmacokinetics and pharmacodynamics," *Pharmazie*, vol. 68, pp. 811–815, 2013.
- [10] G. Balsevich *et al.*, "Stress-responsive FKBP51 regulates AKT2-AS160 signaling and metabolic function," *Nat. Commun.*, vol. 8:1725, pp. 1–12, 2017.
- [11] M. Maiarù *et al.*, "The Stress Regulator Fkbp51: A Novel and Promising Druggable Target for the Treatment of Persistent Pain States Across Sexes," *Pain*, vol. 159, pp. 1224–1234, 2018.
- [12] M. L. Pöhlmann *et al.*, "Pharmacological Modulation of the Psychiatric Risk Factor FKBP51 Alters Efficiency of Common Antidepressant Drugs," *Front. Behav. Neurosci.*, vol. 12:262, pp. 1–8, 2018.
- [13] M. Breitsamer and G. Winter, "Needle-Free Injection of Vesicular Phospholipid Gels - A Novel Approach to Overcome an Administration Hurdle for Semisolid Depot Systems," *J. Pharm. Sci.*, vol. 106, no. 4, pp. 968–972, 2017.
- [14] C. Neuhofer, "Development of lipid based depot formulations using interferon-beta-1b as a model protein," Dissertation, Ludwig-Maximilians-Universität München, 2015.
- [15] W. Tian, "The Development of Sustained Release Formulation for Pharmaceutical

- Proteins based on Vesicular Phospholipid Gels,” Dissertation, Ludwig-Maximilians-Universität München, 2010.
- [16] M.-P. Even, “Twin-Screw Extruded Lipid Implants for Vaccine Delivery,” Dissertation, Ludwig-Maximilians-Universität München, 2015.
- [17] Y. Zhang *et al.*, “In vitro and in vivo sustained release of exenatide from vesicular phospholipid gels for type II diabetes,” *Drug Dev. Ind. Pharm.*, vol. 42, no. 7, pp. 1042–1049, 2015.
- [18] A.-E. Saliba, I. Vonkova, and A.-C. Gavin, “The systematic analysis of protein-lipid interactions comes of age,” *Nat. Rev. Mol. Cell Biol.*, vol. 16, no. 12, pp. 753–61, 2015.
- [19] F. Ruggeri, F. Zhang, T. Lind, E. D. Bruce, B. L. T. Lau, and M. Cárdenas, “Non-specific interactions between soluble proteins and lipids induce irreversible changes in the properties of lipid bilayers,” *Soft Matter*, vol. 9, no. 16, pp. 4219–4226, 2013.
- [20] S. T. Henriques and M. A. R. B. Castanho, “Environmental factors that enhance the action of the cell penetrating peptide pep-1: A spectroscopic study using lipidic vesicles,” *Biochim. Biophys. Acta - Biomembr.*, vol. 1669, no. 2, pp. 75–86, 2005.
- [21] J. E. Hare, S. C. Goodchild, S. N. Breit, P. M. G. Curmi, and L. J. Brown, “Interaction of Human Chloride Intracellular Channel Protein 1 (CLIC1) with Lipid Bilayers: A Fluorescence Study,” *Biochemistry*, vol. 55, no. 27, pp. 3825–3833, 2016.
- [22] M. Vollrath, “Extruded lipid implants for intravitreal use - protein stability, release kinetics and process design,” Dissertation, Ludwig-Maximilians-Universität München, 2017.
- [23] M. Takayama, S. Itoh, I. Nagasaki, and I. Tanimizu, “A new enzymatic method for determination of serum choline-containing phospholipids,” *Clin. Chim. Acta*, vol. 79, no. 1, pp. 93–98, 1977.
- [24] R. Tejera-Garcia, L. Connell, W. A. Shaw, and P. K. J. Kinnunen, “Gravimetric determination of phospholipid concentration,” *Chem. Phys. Lipids*, vol. 165, no. 6, pp. 689–695, 2012.
- [25] F. Tong, “Preparation of exenatide-loaded linear poly(ethylene glycol)-brush poly(l-lysine) block copolymer: Potential implications on diabetic nephropathy,” *Int. J. Nanomedicine*, vol. 12, pp. 4663–4678, 2017.
- [26] R. Liang *et al.*, “Effect of water on exenatide acylation in poly(lactide-co-glycolide) microspheres,” *Int. J. Pharm.*, vol. 454, no. 1, pp. 344–353, 2013.
- [27] S. A. I. Seidel *et al.*, “Microscale thermophoresis quantifies biomolecular interactions under previously challenging conditions,” *Methods*, vol. 59, no. 3, pp. 301–315, 2013.
- [28] S. A. I. Seidel *et al.*, “Label-free microscale thermophoresis discriminates sites and affinity of protein-ligand binding,” *Angew. Chemie - Int. Ed.*, vol. 51, no. 42, pp. 10656–10659, 2012.
- [29] M. Jerabek-Willemsen, C. J. Wienken, D. Braun, P. Baaske, and S. Duhr, “Molecular interaction studies using microscale thermophoresis,” *Assay Drug Dev. Technol.*,

- vol. 9, no. 4, pp. 342–353, 2011.
- [30] P. Linke *et al.*, “An Automated Microscale Thermophoresis Screening Approach for Fragment-Based Lead Discovery,” *J. Biomol. Screen.*, vol. 21, no. 4, pp. 414–421, 2016.
- [31] M. H. Moon, T. Hilimire, A. M. Sanders, and J. S. Schneekloth, Jr., “Measuring RNA-Ligand Interactions with Microscale Thermophoresis,” *Biochemistry*, vol. 57, no. 31, pp. 4638–4643, 2018.
- [32] A. Paavola, J. Yliruusi, Y. Kajimoto, E. Kalso, T. Wahlström, and P. Rosenberg, “Controlled Release of Lidocaine from Injectable Gels and Efficacy in Rat Sciatic Nerve Block,” *Pharmaceutical Research*, vol. 12, no. 12, pp. 1997–2002, 1995.
- [33] R. P. Rand and V. A. Parsegian, “Hydration forces between phospholipid bilayers,” *Biochim. Biophys. Acta - Rev. Biomembr.*, vol. 988, no. 3, pp. 351–376, 1989.
- [34] G. R. Bartlett, “Phosphorus Assay in Column Chromatography,” *J. Biol. Chem.*, vol. 243, pp. 466–468, 1959.
- [35] A. S. Ladokhin, S. Jayasinghe, and S. H. White, “How to Measure and Analyze Tryptophan Fluorescence in Membranes Properly, and Why Bother?,” *Anal. Biochem.*, vol. 285, no. 2, pp. 235–245, 2000.
- [36] A. Blume and A. Kerth, “Peptide and protein binding to lipid monolayers studied by FT-IRRA spectroscopy,” *Biochim. Biophys. Acta - Biomembr.*, vol. 1828, no. 10, pp. 2294–2305, 2013.
- [37] A. Seelig, “Local anesthetics and pressure: a comparison of dibucaine binding to lipid monolayers and bilayers,” *Biochim. Biophys. Acta*, vol. 899, pp. 196–204, 1987.
- [38] K. A. Burke, K. J. Kauffman, C. S. Umbaugh, S. L. Frey, and J. Legleiter, “The interaction of polyglutamine peptides with lipid membranes is regulated by flanking sequences associated with huntingtin,” *J. Biol. Chem.*, vol. 288, no. 21, pp. 14993–15005, 2013.
- [39] N. J. Buurma and I. Haq, “Calorimetric and Spectroscopic Studies of Hoechst 33258: Self-association and Binding to Non-cognate DNA,” *J. Mol. Biol.*, vol. 381, no. 3, pp. 607–621, Sep. 2008.
- [40] H. Y. Fan, G. Raval, A. Shalviri, S. May, X. Y. Wu, and H. Heerklotz, “Coupled equilibria of a self-associating drug loaded into polymeric nanoparticles,” *Methods*, vol. 76, pp. 162–170, Apr. 2015.
- [41] A. Cooper, “Microcalorimetry of Protein–Protein Interactions,” in *Protein Targeting Protocols*, New Jersey: Humana Press, 1998, pp. 11–22.
- [42] P. Wassmann *et al.*, “Structure of BeF₃–Modified Response Regulator PleD: Implications for Diguanylate Cyclase Activation, Catalysis, and Feedback Inhibition,” *Structure*, vol. 15, no. 8, pp. 915–927, 2007.
- [43] P. M. Matos, H. G. Franquelim, M. A. R. B. Castanho, and N. C. Santos, “Quantitative assessment of peptide-lipid interactions. Ubiquitous fluorescence methodologies,” *Biochim. Biophys. Acta - Biomembr.*, vol. 1798, no. 11, pp. 1999–2012, 2010.
- [44] T. Imoto, L. S. Forster, J. a Rupley, and F. Tanaka, “Fluorescence of lysozyme:

- emissions from tryptophan residues 62 and 108 and energy migration.,” *Proc. Natl. Acad. Sci. U. S. A.*, vol. 69, no. 5, pp. 1151–1155, 1972.
- [45] J. Dufourcq and J. F. Faucon, “Intrinsic fluorescence study of lipid-protein interactions in membrane models. Binding of melittin, an amphipathic peptide, to phospholipid vesicles,” *BBA - Biomembr.*, vol. 467, no. 1, pp. 1–11, 1977.
- [46] J. R. Lakowicz, *Principles of Fluorescence Spectroscopy Principles of Fluorescence Spectroscopy*, 3rd ed. New York: Springer, 2006.
- [47] F. Stauffer *et al.*, “Interaction between dengue virus fusion peptide and lipid bilayers depends on peptide clustering,” *Mol. Membr. Biol.*, vol. 25, no. 2, pp. 128–138, 2008.
- [48] G. Kemmer and S. Keller, “Nonlinear least-squares data fitting in Excel spreadsheets,” *Nat. Protoc.*, vol. 5, no. 2, pp. 267–281, 2010.
- [49] I. Langmuir and K. B. Blodgett, “Über einige neue Methoden zur Untersuchung von monomolekularen Filmen,” *Kolloid-Zeitschrift*, vol. 3, no. 73, pp. 257–263, 1935.
- [50] A. Casadó *et al.*, “Langmuir monolayers and Differential Scanning Calorimetry for the study of the interactions between camptothecin drugs and biomembrane models,” *Biochim. Biophys. Acta - Biomembr.*, vol. 1858, no. 2, pp. 422–433, 2016.
- [51] S. R. Dennison, F. Harris, and D. A. Phoenix, “A Langmuir approach on monolayer interactions to investigate surface active peptides.,” *Protein Pept. Lett.*, vol. 17, no. 11, pp. 1363–1375, 2010.

Chapter VI

APPLICATION OF VESICULAR PHOSPHOLIPID GELS AS DEPOT SYSTEM FOR SMALL HYDROPHOBIC DRUGS

Parts of this chapter have been published in the following original research papers:

- G. Balsevich, A.S. Häusl, C.W. Meyer, S. Karamihalev, X. Feng, M.L. Pöhlmann, C. Dournes, A. Uribe-Marino, S. Santarelli, C. Labermaier, K. Hafner, T. Mao, M. Breitsamer, M. Theodoropoulou, C. Namendorf, M. Uhr, M. Paez-Pereda, G. Winter, F. Hausch, A. Chen, M.H. Tschöp, T. Rein, N.C. Gassen, M.V. Schmidt, Stress-responsive FKBP51 regulates AKT2-AS160 signaling and metabolic function, *Nat. Commun.* 8:1725 (2017). (section VI.4.1)
- M. Maiarù, O.B. Morgan, T. Mao, M. Breitsamer, H. Bamber, M. Pöhlmann, M. V. Schmidt, G. Winter, F. Hausch, S.M. Géranton, The Stress Regulator Fkbp51: A Novel and Promising Druggable Target for the Treatment of Persistent Pain States Across Sexes, *Pain.* 159, 1224-1234 (2018). (section VI.4.2)
- M.L. Pöhlmann, A.S. Häusl, D. Harbich, G. Balsevich, C. Engelhardt, X. Feng, M. Breitsamer, F. Hausch, G. Winter, M. V. Schmidt, Pharmacological Modulation of the Psychiatric Risk Factor FKBP51 Alters Efficiency of Common Antidepressant Drugs, *Front. Behav. Neurosci.* 12:262 (2018). (section VI.4.3)

This work was conducted in close cooperation with the Max-Planck-Institute of Psychiatry in Munich and the University College of London. The personal contribution covers the development of SAFit2-VPG and #41-VPG and characterization of the *in vitro* release behavior as well as the preparation of SAFit2-VPG and #41-VPG for all *in vivo* studies. The *in vitro* release behavior of SAFit2-VPG was studied together with Weiwei Liu. Pharmacokinetic calculations were done by Weiwei Liu (LMU, Munich), Dr. Jilong Wang and Prof. Xiaojiao Du (Institutes for Life Sciences and School of Medicine, South China University of Technology, Guangzhou, China).

VI.1 Introduction

Within the last years, sustained release of small molecular weight drugs (MW < 1000 Da), as well as proteins and peptides from VPGs has received more and more attention. To date, several pharmaceutically relevant substances like cetorelix, thymopentin, cytarabine and exenatide have been successfully encapsulated in VPGs and sustained release from the depot matrix was demonstrated [1]–[5]. Since all of these molecules were soluble in aqueous buffers, direct entrapment was easily feasible by DAC, HPH or magnetic stirring. To this end, phospholipids and the aqueous drug solution were weighed accurately and homogenized with the method of choice. Other molecules like vincristine and gemcitabine have been encapsulated by passive loading [6]–[8].

The encapsulation of lipophilic compounds, which are insoluble in water, has been described in theory before [9], [10]. Within the present work, a depot formulation for two lipophilic drug candidates (SAFit2 and #41) was developed, using a direct incorporation method for lipophilic compounds. Furthermore, *in vitro* release behavior of the newly developed VPG formulations was investigated and correlated to *in vivo* plasma concentrations. Additionally, the performance of the depot was tested *in vivo* in different applications which will be summarized in the following [11]–[13].

VI.1.1 SAFit2

SAFit2 is a novel selective antagonist of FK506 binding protein 51 (FKBP51) by induced fit [14]. FKBP51 is best known as a regulator of the responsiveness of steroid hormone receptors, due to its classification as a co-chaperone for heat shock protein 90 (Hsp90) [15]. Thus, FKBP51 is a regulator of the hypothalamic-pituitary-adrenal axis (HPA-axis) and thereby a common target in recent research. However, it is structurally closely related to FKBP52, which antagonizes its effect. More specifically, while FKBP52 enhances glucocorticoid receptor (GR) activity, FKBP51 inhibits GR activity [14], [16]. Hence, selective inhibitors are needed to avoid FKBP52 inhibition which may be associated with severe side-effects [14].

The mechanism of action of SAFit2 is illustrated schematically in Figure VI-1. Stressful stimuli, corticotropin-releasing hormone (CRH) is released from the hypothalamus, which induces the release of adrenocorticotrophic hormone (ACTH) from the pituitary gland,

which in turn promotes the release of glucocorticoids (cortisol) from the adrenal glands. Subsequently, glucocorticoids activate the GR, which is chaperoned by Hsp90 and FKBP51. Upon glucocorticoid binding the GR-Hsp90 complex exchanges FKBP51 for FKBP52, which is able to interact with dynein and induces internalization of the receptor into the cell core. Subsequent FKBP5 gene transcription leads to secretion of new FKBP51. FKBP51 inhibits the negative feedback of glucocorticoids on the HPA-axis and hence leads to a hyperactivity of the HPA-axis [17].

It is known that single nucleotide polymorphisms (SNPs) in the FKBP5 gene (coding for FKBP51), which are associated with increased FKBP5 expression and thus increased FKBP51 levels, have a hand in stress-related and psychiatric disorders [11], [18]. In this context, SAFit2 antagonizes the effect of FKBP51 on the HPA-axis and hence has an impact on stress-related pathophysiologies.

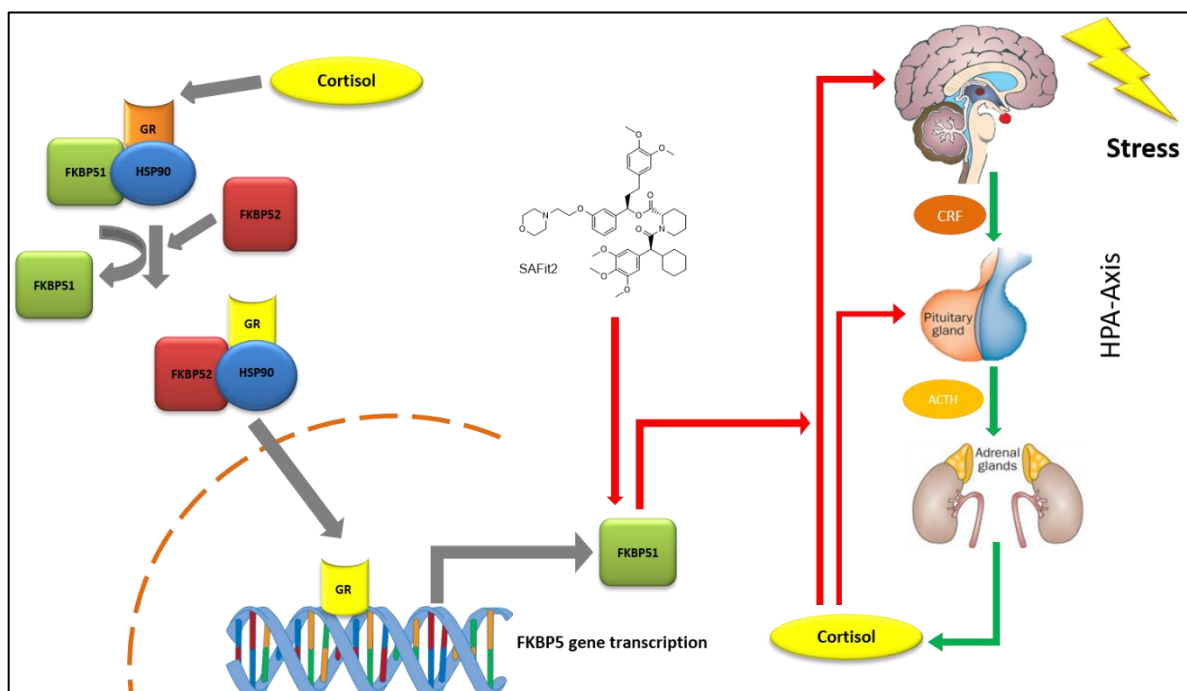


Figure VI-1: Schematic mechanism of action of SAFit2. SAFit2 inhibits the effect of FKBP51 and hence promotes the negative feedback of cortisol on the HPA-axis.

Thus, SAFit2 is a potential drug candidate in the treatment of several diseases like depression, cancer and diseases related to the energy metabolism [15].

Yet, the applicability of this new drug candidate is limited, due to its poor solubility in aqueous buffers and short plasma half-life [14]. A novel drug formulation with prolonged release kinetics is needed to facilitate its versatile application.

VI.1.2 Novel drug candidate #41

#41 is a novel drug candidate for psychiatric disorders. So far, little is known about #41 as a new drug candidate and the exact mechanism of action is not resolved yet. However, first tests *in vivo* show promising results. Yet, the applicability of the #41 is limited, due to its short plasma half-life (1.5 h) and poor solubility in aqueous buffers. As for SAFit2, a drug formulation is needed, which prolongs plasma half-life for #41 substantially.

VI.2 Material and Methods

VI.2.1 Material

Egg lecithin (Lipoid E80), containing at least 80% (m/m) phosphatidylcholine (PC), was purchased from Lipoid GmbH (Ludwigshafen a. Rhein, Germany). SAFit2 was obtained from the Max-Planck-Institute for Psychiatry (Munich, Germany). Tween 80 and propylene glycol were purchased from Sigma Aldrich GmbH (Steinheim, Germany) and PEG 400 was obtained from Merck KGaA (Darmstadt, Germany). Bovine serum albumin (BSA) was acquired by VWR International GmbH (Darmstadt, Germany). #41 was supplied by Lead Discovery Center (Dortmund, Germany) and Max-Planck-Institute of Psychiatry (Munich, Germany).

VI.2.2 Methods

VI.2.2.1 Preparation of VPG encapsulating SAFit2 or #41

Both substances were encapsulated into the VPG following the protocol by Brandl for the incorporation of drugs which are poorly soluble in aqueous medium [9].

To this end, Lipoid E80 was accurately weighed and solved in ethanol (conc. 500 mg/ml). Stock solutions with a final drug-concentration of 20 mg/ml of the two substances were prepared in ethanol (SAFit2) or acetone (#41). Then, the desired amount of the respective stock solution was added to the desired amount of the phospholipid solution and mixed by repeated pipetting or gentle shaking. To obtain a solid mixture of the two components, the organic solvent was subsequently evaporated in a vacuum drying oven at a temperature of 25 °C and a pressure of 10 mbar for at least 72 hours. After that, the phospholipid-drug-mixture was hydrated with 20 mM PBS pH 7.4 and homogenized with a Speedmixer™ DAC 150FVZ (Hauschild GmbH & Co KG, Hamm, Germany) for 45 minutes at 3500 rpm. Using this procedure SAFit2-VPG with 30 or 50% (m/m) Lipoid E80 and a drug-load of 10 mg/g and #41-VPG with 50% (m/m) Lipoid E80 and a drug-load of 10 mg/g or 20 mg/g was prepared. Additionally, #41-VPG with 50% (m/m) Lipoid E80 and a drug-load of 10 mg/g was prepared by TSC extrusion using a ZE-5 Mini-Extruder (ThreeTec GmbH & Co KG, Seon, Switzerland).

VI.2.2.2 Preparation of a SAFit2-solution as control for *in vivo* study

A nonretarded SAFit2 solution in 40% (m/m) propylene glycol, 20% (m/m) ethanol, 5% (m/m) Tween 80 and 5% (m/m) polyethylene glycol 400 in 0.9% (m/m) saline was prepared by solving SAFit2 in ethanol and carefully adding the other components to the solution. The final concentration of SAFit2 in the solution was 10 mg/ml. Using this solution, a comparison of the application of SAFit2-VPG to the injection of a nonretarded solution with the exact same dose and injection volume was possible.

VI.2.2.3 *In vitro* release studies

In vitro release behavior of SAFit2 or #41 from VPG was characterized using flow-through cells (FTC) as previously described by Tardi et al. [19]. To this end, approximately 0.5 g VPG was accurately weighed into the donor compartment of the custom-made release cells. As acceptor medium 20 mM PBS pH 7.4 or 20 mM PBS pH 7.4 containing 4% (m/v) bovine serum albumin (BSA) was used. Release buffer was supplied by a syringe pump (LA-160, Landgraf Laborsysteme HLL GmbH, Langenhagen, Germany) with a flow rate of 0.5 ml/h. Released fractions were collected at predetermined time points.

VI.2.2.3.1 Quantification of SAFit2 by RP-HPLC

SAFit2 concentration in the released fractions were quantified by RP-HPLC. Samples were prepared by dilution with ethanol (1:2), subsequent mixing using a vortexer and centrifugation for 10 minutes at 4 °C and 10 000 rpm. The clear supernatant was taken for analysis. By this extraction method an extraction efficiency of $100.2 \pm 1.6\%$ was achieved. A YMC-Triart C18 3 μm column (YMC Europe GmbH, Dinslaken, Germany) was used in combination with a UltiMate™ 3000 system (Thermo Fisher Scientific, Waltham, MA, USA) equipped with a UltiMate™ FLD 3100 fluorescence detector. Mobile phase A was composed of 0.1% (m/m) TFA and 10% (m/m) acetonitrile in HPW, while mobile phase B was composed of 0.1% (m/m) TFA in acetonitrile and a multi-step gradient (0-15 min: 20-100% mobile phase B; 15-17 min: 100% mobile phase B; 17-18 min: 100-20% mobile phase B; 18-21 min: 20% mobile phase B) with a flow of 0.5 ml/min was used for quantification. SAFit2 was detected at $\lambda_{\text{em}} = 310 \text{ nm}$ ($\lambda_{\text{ex}} = 280 \text{ nm}$) with a retention time of approximately 14 min. The method was qualified using samples with known

concentrations of SAFit2, BSA, phospholipids or mixtures of them after using the extraction protocol described above.

VI.2.2.3.2 Quantification of #41

Released fractions were quantified using LC-MS/MS. Quantification of the released samples was conducted by the Max-Planck-Institute of Psychiatry in Munich or by the Lead Discovery Center in Dortmund.

VI.2.2.3.3 Quantification of phosphatidylcholine

PC in the released fractions was quantified using a phospholipid assay (LabAssay™ Phospholipid, FUJIFILM Wako Chemicals Europe GmbH, Neuss, Germany) as described in section IV.2.5.3 .

VI.2.2.4 *In vivo* release studies

The *in vivo* study was performed in accordance with the European Communities' Council Directive 2010/63/EU by the Max-Planck-Institute of Psychiatry, Munich, Germany.

8 to 12-week-old male mice (C57BL/6N) were used for this experiment. Testing was carried out in the animal facilities of the Max-Planck-Institute of Psychiatry. Animal housing and conditions are described in detail by Pöhlmann et al. [12].

VI.2.2.4.1 SAFit2-VPG

SAFit2-VPG (30 and 50% (m/m) phospholipid concentration) and SAFit2-solution, as control for a fast releasing formulation, was tested *in vivo* after a single s.c. injection of the formulation in C57BL/6-mice (number of parallels = 6-7). All formulations were injected subcutaneously with a dose of 10 mg/kg body weight. Blood samples were taken at predetermined time-points and plasma concentration was analyzed by LC-MS/MS by the Max-Planck-Institute of Psychiatry (Munich, Germany) as described in detail by Gaali et al. [14].

VI.2.2.4.2 #41-VPG

#41-VPG with a phospholipid concentration of 50% (m/m) and a drug-load of 10 mg/g or 20 mg/g, prepared by different techniques (DAC or TSC extrusion) was tested *in vivo* after a single s.c. injection of the formulation (80 mg/kg or 160 mg/kg) in C57BL/6-mice (number of parallels = 5). Blood samples were taken at predetermined time-points and

plasma concentrations was determined by LC-MS/MS by the Max-Planck-Institute of Psychiatry (Munich, Germany) or the Lead Discovery Center (Dortmund, Germany).

VI.3 Development of SAFit2-VPG

SAFit2 is a hydrophobic drug candidate with a relatively short plasma half-life of only 9.7 hours after intra peritoneal injection [14]. Due to its application as an antidepressant drug or against chronic pain states, repeated application is needed to maintain therapeutic drug plasma levels for a longer period of time. Subsequently, for further development of the drug candidate, a depot formulation is needed to facilitate clinical applications.

By a simple direct incorporation method similar to the one described by Brandl, it was possible to encapsulate SAFit2 into VPGs [10]. The release behavior of SAFit2 from the obtained VPG was characterized *in vitro* and *in vivo*. SAFit2-VPG was tolerated well by the animals after s.c. injection.

VI.3.1.1 *In vitro* release behavior of SAFit2 from VPG

A sustained release profile was observed for SAFit2-VPG containing 30% (m/m) or 50% (m/m) of Lipoid E80 (see Figure VI-2). While SAFit2-VPG 30% (m/m) releases the drug substance continuously with a low release rate, a biphasic behavior was observed for SAFit2-VPG 50% (m/m). Release is very slow during the first 7 days, then release rate increases significantly.

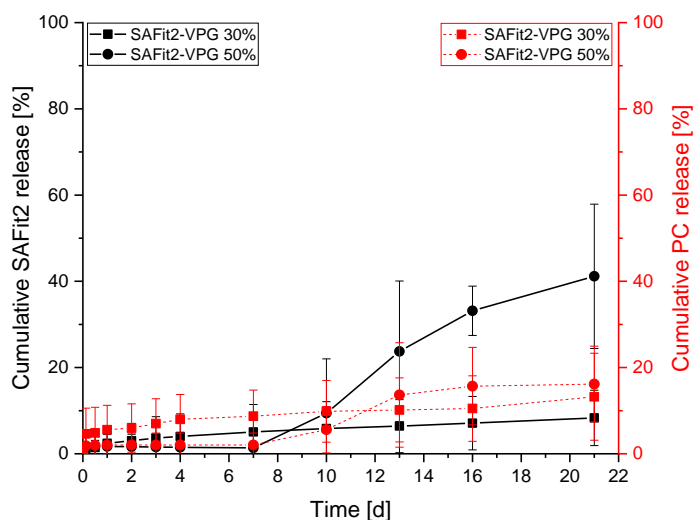


Figure VI-2: *In vitro* release behavior of SAFit2 from VPG. Left axis and black curves show cumulative release of SAFit2 in %, while right axis and grey curves show cumulative release of PC in %.

In both cases, release behavior for SAFit2 can be correlated to release of PC and thus erosion of the phospholipid matrix of the VPG. This close correlation was to be expected

due to the high hydrophobicity of SAFit2 and its insolubility in aqueous solution. Hence, simultaneous release of SAFit2 and PC is a result of the erosion of the VPG, releasing SAFit2 mainly in phospholipid vesicles or particles. Only a very low concentration of SAFit2 may be released as free drug by diffusion through the VPG.

VI.3.1.2 Pharmacokinetic study of SAFit2-VPG

Next to the *in vitro* characterization of SAFit2-VPG, both VPG formulations were also tested *in vivo*. Additionally, an aqueous SAFit2-solution was developed to be able to compare the s.c. VPG applications, with a s.c. application of nonretarded SAFit2 with the same injection volume and dose as used in VPG applications.

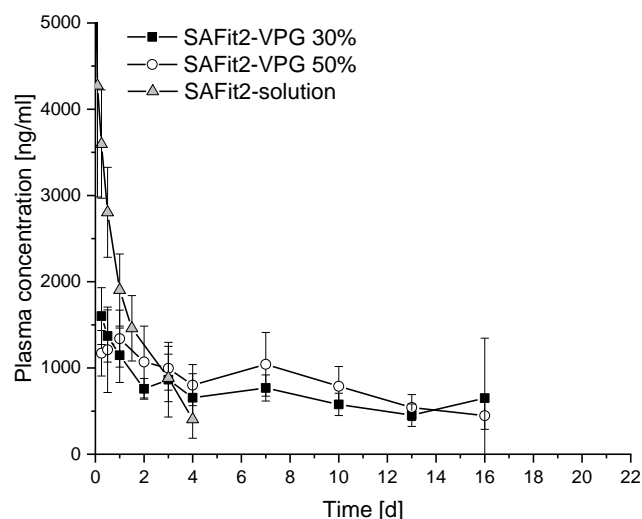


Figure VI-3: Blood plasma concentration of SAFit2 after a single s.c. injection of SAFit2-VPG 30% (m/m) (filled squares), SAFit2-VPG 50% (m/m) (open circles) and SAFit2-solution (grey triangles).

Both VPG formulations show sustained release of SAFit2, while the SAFit2-solution shows fast release with a burst phase in the first few hours. Pharmacokinetic parameters (see Table VI-1) were estimated from the plasma concentration curves, which are shown in Figure VI-3. Calculations were done by Weiwei Liu (Pharm. Technology and Biopharmaceutics, LMU, Munich), Dr. Jilong Wang and Prof. XiaoJiao Du (Institutes for Life Sciences and School of Medicine, South China University of Technology, Guangzhou, China) using a non-compartmental model.

As expected SAFit2 concentration reaches its maximum concentration (c_{max}) only few hours after s.c. injection of the solution. This result is in good accordance with the values found by Gaali et al. for i.p. administration [14]. The encapsulation of SAFit2 in VPG as a

depot, results in lower c_{max} -values and increased t_{max} . Pharmacokinetic behavior during the first few days after application, strongly depends on the phospholipid concentration of the formulation. While SAFit2-VPG 30% (m/m) leads to a t_{max} of approximately 6 hours, SAFit2-VPG 50% (m/m) results in an increased t_{max} 36 hours after administration. Hence, the encapsulation of SAFit2 into VPGs as drug delivery device, leads to a prolonged release over several days.

Table VI-1: Summary of PK parameters for SAFit2-VPG. (Non-compartmental model, calculated by Dr. Jilong Wang and Prof. XiaoJiao Du)

	SAFit2- solution	SAFit2-VPG 30%	SAFit2-VPG 50%
$t_{1/2}$ [h]	30.73	215.72	146.17
t_{max} [h]	2.3	6	36
c_{max} [$\mu\text{g/ml}$]	5692.32	1520.11	1473.34
AUC_{0-t} [$\text{h}\cdot\mu\text{g/ml}$]	135857.40	264254.83	327500.32
$AUC_{t-\infty}$ [$\text{h}\cdot\mu\text{g/ml}$]	164585.26	406632.98	431084.84
Cl/F [l/h/kg]	0.067	0.027	0.025

Both, *in vitro* and *in vivo* data showed that SAFit2-VPGs achieved sustained release of the drug candidate for several days without significant initial burst release. However, *in vitro* and *in vivo* release profiles show differences, which may be a result of the release model and drug used in this study. Different release models (e.g. dialysis bag model by Zhang et al., micro-centrifugation tube model by Even) have been described in literature amongst which the FTC model is the most investigated *in vitro* [3], [19], [20]. However, all current models do have drawbacks and none of them has been properly correlated to *in vivo* data since most of the *in vivo* studies concentrate on the pharmacodynamic effect of the encapsulated drug after release from VPG.

Additionally to the *in vitro* release model, drug properties, which may have an influence on the release behavior, have to be taken into account. A drug with high hydrophobicity, like in the case of SAFit2, limits the choice of release models to those, which not only show diffusion-controlled release as it is the case in the dialysis bag model mentioned above. A high partition coefficient and hence high hydrophobicity of a drug result in slower diffusion. Thus, release from VPG is rather erosion controlled since the drug is released in

lipid vesicles or particles rather than as free drug and the release model should take this into account.

In a similar way *in vitro* release is influenced by the acceptor medium, which is in our case an aqueous salt solution (20mM PBS pH 7.4) with albumin (BSA). For a good *in vitro-in vivo* correlation it is important to simulate the physiological conditions as good as possible. Thus, BSA was added to the acceptor medium as it was described before [21].

Improved *in vitro* release models for semisolid drug formulations like VPGs and more *in vivo* data on different drug compounds are needed to find a good *in vitro-in vivo* correlation.

VI.4 *In vivo* applications of SAFit2-VPG

In the last years, SAFit2-VPG has been used for different applications *in vivo*. Since a complete reproduction of this data is beyond the scope of this work, focus was set on formulation relevant data. Thus, in this section the relevant data from publications, which we have contributed to in the course of this thesis, is summarized shortly.

VI.4.1 Balsevich et al., Stress-responsive FKBP51 regulates AKT2-AS160 signaling and metabolic function, *Nature Communications* (2017)

High-fat diet (HFD) or other exposure to nutrient overload, is known to be a stress factor and leads to increases in the FKBP51 levels [22], [23]. Nevertheless, the role of FKBP51 in whole body glucose metabolism has not been elucidated so far. In this study, Balsevich et al. investigated the role of FKBP51 in energy and glucose homeostasis.

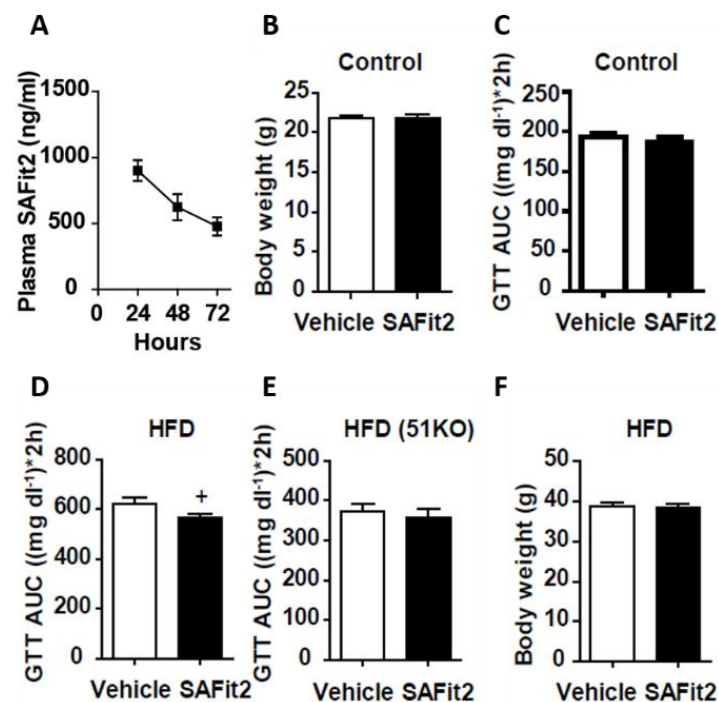


Figure VI-4: Metabolic effects of SAFit2 treatment. A) High SAFit2 plasma levels were observed for 72 hours after a single s.c. injection of SAFit2. B) Body weight under control diet conditions. C) Glucose tolerance under control diet conditions. SAFit2 has no effect on glucose tolerance. D) Glucose tolerance under HFD conditions. SAFit2 significantly improves glucose tolerance. E) Effect of SAFit2 was not present in 51KO-mice under HFD conditions. F) Body weight under HFD conditions. (Figure was adapted from Balsevich et al. [11].)

In the course of the presented work, SAFit2 was used to antagonize the effect of FKBP51 as a possible treatment for metabolic stress-related disorders like type 2 diabetes. To this end, SAFit2 was encapsulated into VPG to achieve high plasma concentrations for a prolonged time. It was shown that a single injection of SAFit2 resulted in elevated plasma levels of the drug for 72 hours post-injection (Figure VI-4A). Although, SAFit2-VPG did not show any effect in chow fed mice 48 hours after injection (Figure VI-4B and Figure VI-4C), glucose tolerance was significantly improved in HFD-fed mice (Figure VI-4D). This effect was found to be specific to FKBP51 inhibition, since no effect on 51KO-mice was observed (Figure VI-4E). Further, body weight was not affected by the SAFit2 treatment (Figure VI-4F).

The encapsulation of SAFit2 in VPG facilitated its application in this study and prolonged SAFit2 effect to over 3 days after application. The pharmacological antagonization of FKBP51 by SAFit2 improves glucose tolerance and thus may be a treatment opportunity for type 2 diabetes.

VI.4.2 Maiarù et al., The stress regulator FKBP51: a novel and promising druggable target for the treatment of persistent pain states across sexes, Pain (2018)

Traumatic events are powerful stress-factors, which induce HPA-axis activation. Recently it was demonstrated that FKBP51 plays a key role in the development and maintenance of chronic joint inflammatory pain [24], [25]. In this context, Maiarù et al. explored the potential of FKBP51 as a new pharmacological target for the treatment of chronic pain across the sexes.

A single i.p. injection of a nonretarded SAFit2 solution (solution A: in 4% (m/m) ethanol, 5% (m/m) PEG 400 and 5% (m/m) Tween 80 in 0.9% (m/m) saline, conc.: 2 mg/ml) was able to reduce the injury-induced mechanical hypersensitivity after full development of the pain state i.e. 3 days after complete Freund's adjuvant (CFA) injection in the ankle joint (Figure VI-5A) or 5 days after spared nerve injury (SNI) surgery (Figure VI-5B). However, the effect of this single i.p. injection lasted no longer than 8 hours in both models. Repeated injection (twice daily over 4 days) resulted in a significant reduction of the injury-induced hypersensitivity for up to 4 days in both pain models (Figure VI-5C and

Figure VI-5D). Finally, to improve animal stress and the efficacy of the drug treatment, VPGs were used as a sustained drug delivery device for SAFit2. A single s.c. injection of SAFit2-VPG 5 days after SNI surgery reduced injury-induced hypersensitivity for at least 7 days after injection (Figure VI-5E).

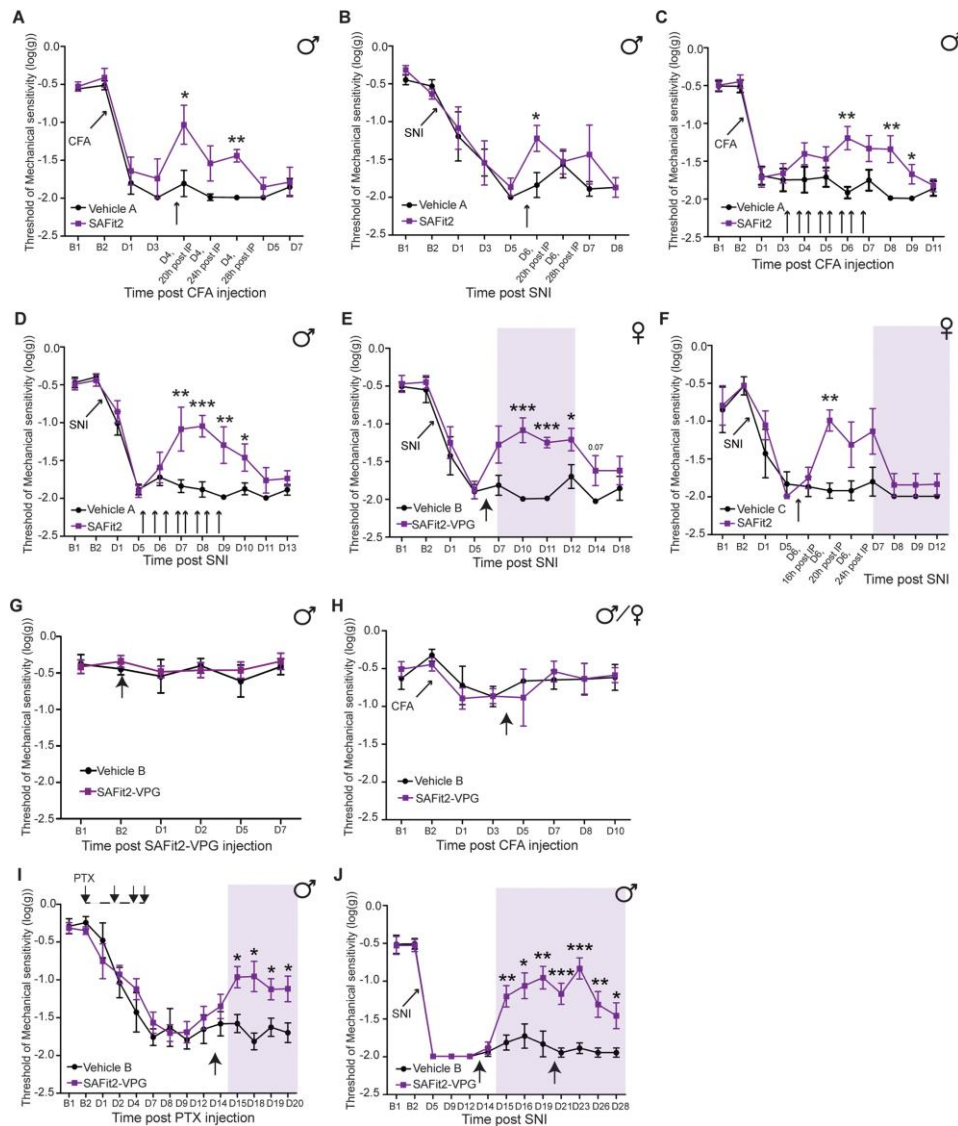


Figure VI-5: Pharmacological blockade of FKBP51 reduces the mechanical hypersensitivity seen in long-term pain states across sexes. A) Single i.p. injection of SAFit2-solution A 3 days after CFA injection. B) Single i.p. injection of SAFit2-solution A 5 days after SNI surgery. C) Repeated i.p. injection of SAFit2-solution A 3 days after CFA injection. D) Repeated i.p. injection of SAFit2-solution A 5 days after SNI surgery. E) Single s.c. injection of SAFit2-VPG 5 days after SNI surgery. F) Single s.c. injection of SAFit2-solution B 5 days after SNI surgery. G) SAFit2-VPG had no effect in naïve mice. H) SAFit2-VPG had no effect in CFA-injected FKBP5 KO mice. I) Single s.c. injection of SAFit2-VPG, 12 days after the first PTX injection. J) Delayed (12 days) and repeated administration of SAFit2-VPG after SNI surgery. (Figure was adapted from Maiarù et al. [13])

The depot effect of the VPG was confirmed by the injection of a SAFit2-solution (solution B: in 20% (m/m) ethanol, 40% (m/m) propylene glycol, 5% (m/m) PEG 400 and 5% (m/m)

Tween 80 in 0.9% (m/m) saline, conc.: 10 mg/ml) with the same dose (100 mg/kg) and injection volume as used for the VPG (Figure VI-5F). Further, the effect of SAFit2 on paclitaxel (PTX) treatment was investigated. As expected, SAFit2-VPG was able to reduce the mechanical hypersensitivity for at least 5 days after injection (12 days after the first PTX injection) (Figure VI-5I). Additionally, it was shown, that SAFit2-VPG could improve long-term pain states that have been established for at least one week and repeated SAFit2-VPG administration (7 days after the first application) maintains the improvement of the pain state (Figure VI-5J).

Altogether, the presented data suggests, that FKBP51 is a promising target for the treatment of chronic-pain and SAFit2 is a potent antagonist of FKBP51. The administration of SAFit2 encapsulated in VPG, resulted in an effect of the drug candidate over at least 5 days after a single injection and 10 days after repeated injection. Hence, SAFit2-VPG has a high potential for chronic treatment of injury-induced mechanical hypersensitivity.

VI.4.3 Pöhlmann et al., Pharmacological Modulation of the Psychiatric Risk Factor FKBP51 Alters Efficiency of Common Antidepressant Drugs, *Frontiers in Behavioral Neurosciences* (2018)

Since pharmacological treatment of mental disorders (i.e. depression or anxiety disorders) with a single drug is often rather ineffective, co-medication with functional diverse antidepressants are often needed. For further development of SAFit2 as a new drug candidate, it is important to know if FKBP51 inhibition interferes with the effect of other antidepressants and anxiolytics. In this work, Pöhlmann et al. investigated the combination of SAFit2 with the commonly prescribed selective serotonin reuptake inhibitor (SSRI) escitalopram.

The focus of this study was on the pharmacological effects only, while VPG was only used as a drug delivery vehicle. Although the depot effect of VPGs was not addressed, for the sake of completeness a short description of the results obtained with SAFit2-VPG is given in the following.

SAFit2-VPG already showed beneficial release behavior and efficacy of SAFit2 treatment during both above described *in vivo* studies. Thus, VPG was used in the current study as a drug delivery device for SAFit2, while escitalopram was injected as aqueous solution.

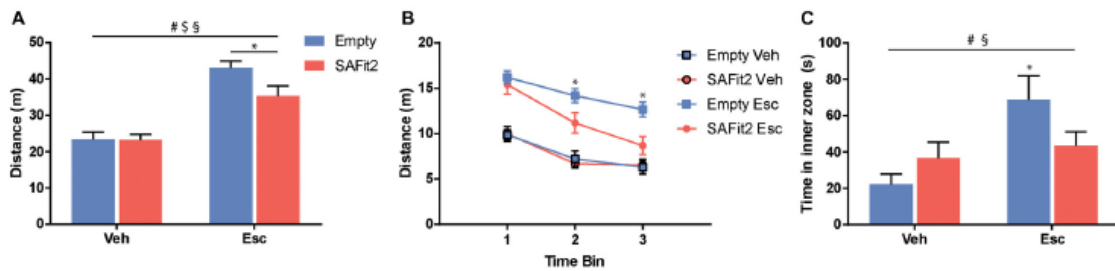


Figure VI-6: Treatment with SAFit2 and escitalopram (Esc) affected behavior in open field test (anxiety-test). A) Distance traveled during the test. B) When splitting the test in three time-bins of 5 min each, no differences were observed between the two escitalopram groups in the first five minutes but significant differences in time-bin 2 and 3. C) Exploration time of the inner zone. (Figure was adapted from Pöhlmann et al. [12])

Interestingly, escitalopram efficacy in anxiety-related tests was lowered by combining it with SAFit2 (Figure VI-6), while stress coping behavior was improved by the combination of both drugs (Figure VI-7).

The study shows, that combination of SAFit2 with SSRIs could be beneficial in anxiety disorders and depression, more prone to stress.

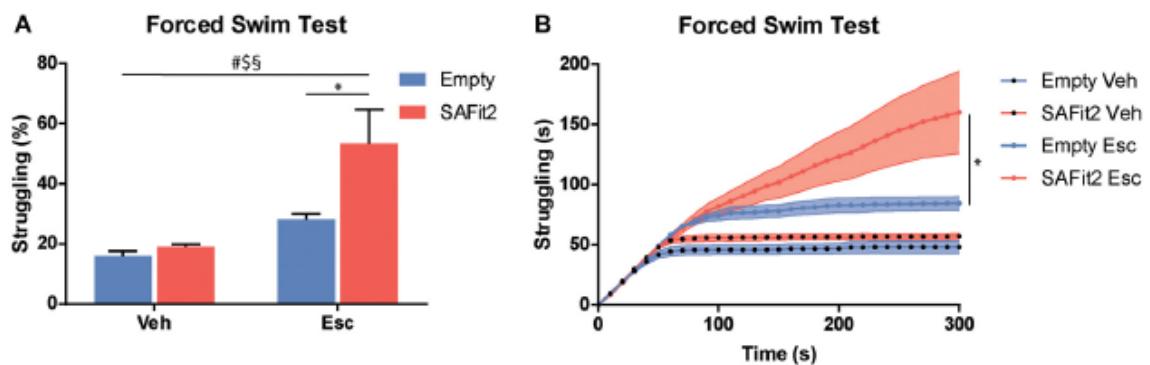


Figure VI-7: Treatment with SAFit2 and escitalopram (Esc) affected behavior in forced swim test (stress-coping test). A) Struggling time was significantly increased by combination of SAFit2 with escitalopram. B) Time course of the forced swim test shows that animals with SAFit2 treatment struggle significantly more in the last 3 minutes. (Figure was adapted from Pöhlmann et al. [12])

VI.5 Development of a VPG formulation for the delivery of #41

#41 is a highly hydrophobic molecule and thus shows poor solubility in aqueous buffers. To encapsulate such molecules in relevant concentrations in VPG, a homogenous mixture of the substance and the phospholipids is needed. To this end, the drug substance and the phospholipids are brought into solution by organic solvents and mixed in the desired quantities in solution. Then the organic solvent is removed, the mixture is re-hydrated with aqueous buffer and homogenized with one of the before mentioned methods. Hence, solubility of #41 in different solvents was tested and data is summarized in Table VI-2.

Table VI-2: Summary of the solubility study for #41.

Solvent	Concentration [mg/ml]
<i>Ethanol</i>	not soluble
<i>2-Propanol</i>	not soluble
<i>Acetone</i>	28.0
<i>Methanol</i>	50.0

Even though the organic solvent is evaporated in a vacuum drying oven for several hours, the presence of residual solvent is likely and cannot be ruled out. ICH guideline ICH Q3C(R5) defines the toxicological acceptable limits for residual solvents and classifies organic solvents according to their toxicity [26]. Following this guideline, the use of methanol as a solvent should be limited (class 2 solvent) in pharmaceutical products. Thus, despite of the superior solubility of #41 in methanol, acetone (class 3 solvent = solvent with low toxic potential) was preferred for the preparation of #41-VPG.

By solving #41 in acetone and subsequent mixing with a phospholipid solution in ethanol, a homogenous mixture was achieved. After evaporation of the solvent mixture, the mixture was re-hydrated with 20 mM PBS pH 7.4 and VPGs were prepared either by DAC or by TSC extrusion. In both cases, a macroscopically homogenous VPG was obtained.

Residual acetone or ethanol in the VPG was not determined in this first, basic study and #41-VPG was tolerated well by the animals during the *in vivo* study. However, residual

solvent concentrations should be determined during further development of the preparation process of #41-VPGs.

VI.5.1 *In vitro* release behavior of #41 from VPG

As shown in Figure VI-8, #41 is released (acceptor medium: 20mM PBS pH 7.4) from VPG slowly with an almost linear release profile over more than 18 days. Differences between the formulations and preparation techniques are observable. First, release is slower (0.7% per day) when the VPG is prepared by TSC extrusion. In comparison to that, VPG prepared by DAC releases #41 with a release rate of 1.8% per day. Furthermore, an increase of the drug-load from 1% (10 mg/g) to 2% (20 mg/g) does not result in significant changes in the release rate.

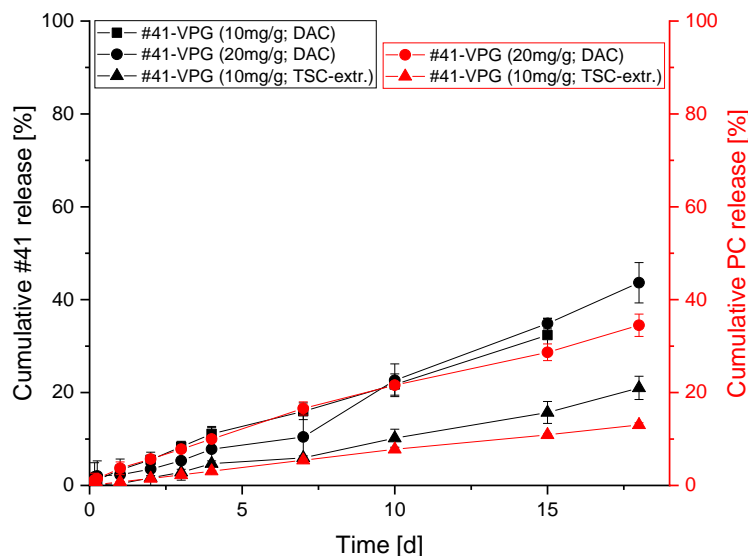


Figure VI-8: *In vitro* release characterization for #41-VPG. Black curves show cumulative release of #41 from VPG prepared by DAC or TSC-extrusion with different drug load (20 mg/g). Red curves show simultaneous PC release.

When looking at the erosion behavior of the phospholipid matrix, differences were observable for the different preparation methods. VPG prepared by extrusion disintegrates more slowly in comparison to VPG prepared by DAC. Additionally, erosion of the lipid matrix and release of #41 are in good accordance, which is an expected consequence of the high hydrophobicity of the drug candidate.

Overall, #41 is released *in vitro* over more than 18 days since release curves show an incomplete, still increasing cumulative concentration at the end of the testing period.

VI.5.2 *In vivo* performance of #41-VPG

Results of the first *in vivo* study are inconclusive and thus not shown here. So far, only few things can be concluded from the first study.

Plasma concentrations of #41 after administration of the drug candidate in VPGs show sustained release of the substance over several hours. First, rough estimations of the plasma half-life show that encapsulation of #41 into VPGs prolongs the plasma half-life to 25 – 45 hours, in comparison to 1 - 2 hours after a single i.p. injection of #41-solution in DMSO/PEG 400/PBS (20/40/40).

After sacrificing the animals at 120 or 168 hours, the VPG is still visible at the injection site. Thus, in contrast to a mainly erosion driven process *in vitro* release kinetics *in vivo* may be influenced by other factors as well.

VI.6 Conclusion

Within this chapter, VPGs were applied as depot drug delivery system for two small molecular weight, hydrophobic drugs.

Both drug candidates were encapsulated successfully into VPGs by a direct incorporation process. A similar encapsulation process has been described in theory before by Brandl et al. and was modulated to fit the special requirements (i.e. solubility in specific solvents) of the two substances.

In vitro release studies showed a sustained release of SAFit2 from VPG composed of 30% (m/m) or 50% (m/m) egg lecithin over several days, which was dominated by the erosion of the phospholipid matrix. A pharmacokinetic study *in vivo* showed faster release in comparison to *in vitro*, but still a significant prolongation of plasma half-life in comparison to a non-retarded formulation.

The pharmacological effect of SAFit2 was shown after application of the substance encapsulated in VPGs. SAFit2 improves glucose tolerance in mice, reduces injury-induced mechanical hypersensitivity in chronic pain treatment and shows promising results in combination with SSRIs in anxiety disorders and depression. Hence, the encapsulation of SAFit2 into VPGs prolongs the duration of the pharmacological effect *in vivo* up to 5 days (or 10 days after repeated administration) and facilitates the versatile application of the novel drug candidate. Additionally, all *in vivo* studies showed that VPGs were tolerated well, since no adverse reactions were observed at the injection site.

Next to the application of VPGs for SAFit2, #41 was encapsulated into VPGs. #41-VPG showed sustained release *in vitro*, which was obviously controlled by erosion of the VPG. Release rates were different, when different manufacturing techniques were chosen for #41-VPG. Slow release was achieved when #41-VPG was prepared by extrusion using a TSC extruder, while faster release rates occurred after preparation of the #41-VPG by DAC. It is hypothesized that larger vesicles, which are obtained after preparation of the VPGs by extrusion result in a slower erosion process *in vitro* and thus also slower release of the hydrophobic drug.

In vivo a substantial prolongation of plasma half-life was observed, when #41 was encapsulated into VPGs. However, due to the inconclusiveness of the *in vivo* data, further studies are needed to characterize depot effect of VPGs for #41.

In conclusion, our study confirms the excellent biocompatibility of VPGs in general and demonstrates their application as drug delivery device for hydrophobic substances. The preparation of VPGs by extrusion does not only lead to superior sustained release behavior, but may also facilitate the direct entrapment of hydrophobic substances by co-extrusion with the phospholipids, rendering the use of organic solvents unnecessary.

VI.7 References

- [1] H. Grohganz, I. Tho, and M. Brandl, "Development and in vitro evaluation of a liposome based implant formulation for the decapeptide cetorelix," *Eur. J. Pharm. Biopharm.*, vol. 59, no. 3, pp. 439–448, 2005.
- [2] Y. Zhong *et al.*, "Vesicular phospholipid gels using low concentrations of phospholipids for the sustained release of thymopentin : pharmacokinetics and pharmacodynamics," *Pharmazie*, vol. 68, pp. 811–815, 2013.
- [3] Y. Zhang *et al.*, "In vitro and in vivo sustained release of exenatide from vesicular phospholipid gels for type II diabetes," *Drug Dev. Ind. Pharm.*, vol. 42, no. 7, pp. 1042–1049, 2015.
- [4] N. Qi *et al.*, "Sterilization stability of vesicular phospholipid gels loaded with cytarabine for brain implant," *Int. J. Pharm.*, vol. 427, pp. 234–241, 2012.
- [5] N. Qi *et al.*, "Sustained delivery of cytarabine-loaded vesicular phospholipid gels for treatment of xenografted glioma," *Int. J. Pharm.*, vol. 472, no. 1–2, pp. 48–55, 2014.
- [6] R. Moog *et al.*, "Change in pharmacokinetic and pharmacodynamic behavior of gemcitabine in human tumor xenografts upon entrapment in vesicular phospholipid gels," *Cancer Chemother. Pharmacol.*, vol. 49, pp. 356–366, 2002.
- [7] R. Moog, "Einschluß von Gemcitabin (dFdC) in vesikulare Phospholipidgele : in vivo und in vitro - Untersuchungen zur Stabilität , Pharmakokinetik und antitumoralen Wirksamkeit," Dissertation, Albert-Ludwigs-Universität Freiburg, 1998.
- [8] F. Güthlein *et al.*, "Pharmacokinetics and antitumor activity of vincristine entrapped in vesicular phospholipid gels," *Anticancer. Drugs*, vol. 13, no. 8, pp. 797–805, 2002.
- [9] M. Brandl, "Vesicular Phospholipid Gels: A Technology Platform," *J. Liposome Res.*, vol. 17, no. 1, pp. 15–26, 2007.
- [10] M. Brandl, "Vesicular phospholipid gels," in *Liposomes - Methods and Protocols*, vol. 1, V. Weissing, Ed. New York: Humana Press, 2003, pp. 205–212.
- [11] G. Balsevich *et al.*, "Stress-responsive FKBP51 regulates AKT2-AS160 signaling and metabolic function," *Nat. Commun.*, vol. 8:1725, pp. 1–12, 2017.
- [12] M. L. Pöhlmann *et al.*, "Pharmacological Modulation of the Psychiatric Risk Factor FKBP51 Alters Efficiency of Common Antidepressant Drugs," *Front. Behav. Neurosci.*, vol. 12:262, pp. 1–8, 2018.
- [13] M. Maiarù *et al.*, "The Stress Regulator Fkbp51: A Novel and Promising Druggable Target for the Treatment of Persistent Pain States Across Sexes," *Pain*, vol. 159, pp. 1224–1234, 2018.
- [14] S. Gaali *et al.*, "Selective inhibitors of the FK506-binding protein 51 by induced fit," *Nat. Chem. Biol.*, vol. 11, no. 1, pp. 33–37, 2014.
- [15] M. V Schmidt, M. Paez-Pereda, F. Holsboer, and F. Hausch, "The Prospect of FKBP51 as a Drug Target," *ChemMedChem*, vol. 7, no. 8, pp. 1351–1359, 2012.
- [16] E. R. Sanchez, "Chaperoning steroidal physiology: Lessons from mouse genetic

- models of Hsp90 and its cochaperones," *Biochim. Biophys. Acta*, vol. 1823, pp. 722–729, 2012.
- [17] C. L. Storer, C. A. Dickey, M. D. Galigniana, T. Rein, and M. B. Cox, "FKBP51 and FKBP52 in Signaling and Disease," *Trends Endocrinol Metab*, vol. 22, no. 12, pp. 481–490, 2011.
- [18] A. S. Zannas, T. Wiechmann, N. C. Gassen, and E. B. Binder, "Gene–Stress–Epigenetic Regulation of FKBP5: Clinical and Translational Implications," *Neuropsychopharmacology*, vol. 41, no. 1, pp. 261–274, 2016.
- [19] C. Tardi, M. Brandl, and R. Schubert, "Erosion and controlled release properties of semisolid vesicular phospholipid dispersions," *J. Control. Release*, vol. 55, no. 2–3, pp. 261–270, 1998.
- [20] M.-P. Even, "Twin-Screw Extruded Lipid Implants for Vaccine Delivery.," Dissertation, Ludwig-Maximilians-Universität München, 2015.
- [21] M. J. Blanco-Prieto *et al.*, "Importance of the test medium for the release kinetics of a somatostatin analogue from poly(D,L-lactide-co-glycolide) microspheres," *Int. J. Pharm.*, vol. 184, no. 2, pp. 243–250, 1999.
- [22] K. P. Karalis, P. Giannogonas, E. Kodela, Y. Koutmani, M. Zoumakis, and T. Teli, "Mechanisms of obesity and related pathology: linking immune responses to metabolic stress.," *FEBS J.*, vol. 276, no. 20, pp. 5747–5754, 2009.
- [23] G. Balsevich *et al.*, "The interplay between diet-induced obesity and chronic stress in mice: potential role of {FKBP}51," *J. Endocrinol.*, no. 1479-6805 (Electronic), 2014.
- [24] S. M. Géranton, C. Morenilla-Palao, and S. P. Hunt, "A Role for Transcriptional Repressor Methyl-CpG-Binding Protein 2 and Plasticity-Related Gene Serum-and Glucocorticoid-Inducible Kinase 1 in the Induction of Inflammatory Pain States," *J. Neurosci.*, vol. 27, no. 23, pp. 6163–6173, 2007.
- [25] M. Maiarù *et al.*, "The stress regulator FKBP51 drives chronic pain by modulating spinal glucocorticoid signaling," *Sci. Transl. Med.*, vol. 8, no. 325, pp. 1–11, 2016.
- [26] International Conference on Harmonisation of Technical Requirements for Registration of Pharmaceuticals for Human Use, "Impurities: Guideline for Residual Solvents Q3C(R5)," London, UK, 2011.

Chapter VII

SUMMARY AND OUTLOOK

Parenteral depot systems for the sustained release of drugs were intensively researched over the last years. Amongst a variety of different starting materials for depot formulations, lipids have proven to be versatile due to their biodegradability and biocompatibility. Besides solid lipid nanoparticles (SLNs), solid lipid implants (SLIs), liposomes for sustained delivery and other systems, vesicular phospholipid gels (VPGs) were successfully investigated for their potential as drug delivery system with sustained release kinetics for macromolecules, such as proteins, and small molecular weight substances.

The work presented in this thesis focused on the optimization of different aspects of VPGs as depot formulation: their manufacturing, administration and application. Moreover, interactions between the encapsulated protein and the phospholipids were investigated in an attempt to understand the release mechanisms of proteins and peptides from these systems.

Chapter I contains the general introduction of the thesis. The state of the art of VPGs with special focus on the delivery of proteins and peptides is reviewed. Manufacturing techniques, which have developed over the years, as well as different encapsulation procedures are discussed. Furthermore, *in vitro* models for release testing of substances from VPGs are introduced and theories on the release mechanism are explained. Additionally, different applications of VPGs in the last years, as storage form for liposomes or depot formulation for different types of molecules are summarized.

In **Chapter II** the aims of the thesis are explained.

The administration of highly viscous drug formulations is a challenge for drug formulation development, especially for semisolid systems like VPGs. Formulations with high viscosity cannot be administered conventionally by using needle and syringe. In this context, **Chapter III** focuses on the optimization of the administration process, by using needle-free injection (NFI) technology. Establishing and qualifying a simple and more elegant administration technique, compared to injection with needle and syringe or alternatively implantation during surgery, is demonstrated. By using the (FDA approved) Biojector 2000 it was possible to inject VPGs with a phospholipid concentration of up to 50% (m/m) into pig skin post mortem with two types of single-use syringes with different orifice diameter. Beyond that, the limits of injectability were tested and post mortem injections were supported by measurements of the pressure of the ejected jet stream. It was shown that NFI is very robust against changes in phospholipid concentration, temperature and injection volume. However, NFI of VPGs is limited at an injection volume of 1 ml since the pressure of the jet stream drops below a critical value of 8 MPa at this volume and wet shots occur more often.

NFI opens the possibility for further development and clinical applications of VPGs, since it facilitates pain-free administration of the system.

Besides challenges in the administration of the semisolid VPGs, manufacturing of these systems e.g. by dual asymmetric centrifugation (DAC) or high-pressure homogenization (HPH) underlies several drawbacks. In **Chapter IV** twin-screw (TSC) extrusion is suggested as continuous manufacturing method for the preparation of VPGs. This chapter focuses on the optimization of the manufacturing process by TSC extrusion with regards to process parameters and how changing these parameters resulted in changes in viscosity and vesicle size.

In vitro release behavior was characterized with FITC-Dextran and a monoclonal antibody (mAb) and similar or even superior release kinetics were found for VPGs prepared by extrusion in comparison to the established DAC method. The differences in release behavior were explained to some extent by differences in vesicle size. VPGs composed of larger vesicles (e.g. after preparation by TSC) erode slower in comparison to VPGs with very small vesicles (e.g. prepared by DAC). Viscosity of the formulation is only a minor indicator for release behavior.

Moreover, the stability of proteins (mAb and EPO) during encapsulation into VPGs by extrusion was demonstrated. After 3 months of storage both proteins were stable in the formulation and no aggregation or degradation was observed. Besides the stability of the encapsulated proteins or peptides, the physical stability of the VPG was tested over a storage time of three months at 2 - 4 °C and 25 °C. Stable VPG were achieved, using the HAAKE MiniLab® Micro Rheology Compounder and ZE-5 Mini- Extruder.

A first attempt at up-scaling the process to a larger Leistritz Micro 27 GL-28D extruder, resulted in VPG with decreased mixing quality and stability and revealed room for future process optimization. Longer residence time of the phospholipid buffer mixture, in combination with a different screw design and die size, may achieve a compromise between an easy process, good up-scalability and a sufficient VPG stability, as well as preferred sustained release kinetics.

TSC extrusion is the first method described for continuous and fast production of VPG with easy controllability of temperature and shearing forces. The parameters during extrusion and procedure itself are flexible and, in theory, may also facilitate the direct entrapment of lipophilic substances by co-extrusion with the phospholipids.

However, more effort has to be put into process optimization with different extruders to achieve robust, stable products. Furthermore, chemical stability of the phospholipids during extrusion has to be evaluated, since metal abrasion from the moving parts of the extruder may make the lipids more vulnerable to chemical degradation. Different strategies, like the addition of antioxidants or chelators, as well as coated extruders or extruders made from ceramic are proposed to overcome these challenges in the future.

Release from VPG is a result of a complex mixture of mechanisms like erosion, diffusion, membrane permeability and interactions. Additionally, composition and physical parameters of the VPG, like viscosity of the formulation, influence release kinetics.

Chapter V deals with interactions between encapsulated protein and phospholipids and their effect on release behavior from VPG. High affinity ($K_d \approx 1 \mu\text{M}$) of exenatide to liposomes composed of POPG (anionic phospholipid) at pH 4.5, where exenatide is slightly positively charged, was shown by MST, ITC and fluorescence measurements, while no interactions were measurable for liposomes containing POPC, a globally neutral phospholipid or at pH 7.4, where the peptide is negatively charged. Two different binding

events, which are not registered by all three methods, were distinguished. Primary binding of exenatide to the phospholipids and secondary binding of the peptide to pre-bound peptide are involved in the complete membrane binding process of exenatide. While ITC is able to distinguish both processes, MST and fluorescence measurements only determine complete binding.

After all, the faster release from POPG-containing VPGs, with half-lives of several days in comparison to several weeks from VPGs composed of 100% POPC, could not be correlated with interactions. It was demonstrated that release from VPGs containing POPG is rather erosion controlled. A mechanism based on poor membrane permeability of exenatide is proposed for VPGs composed of POPC only. Investigations of exenatide interactions with lipid monolayers (composed of POPC, POPG, and mixtures of both) at the air/water interface showed no intercalation of the peptide into the membrane, independently of the phospholipid composition. Since these findings suggest a very weak permeability of exenatide across the phospholipid membranes, erosion is proposed to be the rate limiting factor for exenatide release from VPG.

These results highlight that release from VPGs is a multifactorial process. Erosion of the VPG and barrier permeability contribute majorly to release behavior and depend on the composition of the VPG as well as on the encapsulated protein, while interactions between the encapsulated protein and the phospholipid only have a minor impact to overall release. Still, the transferability of this study to other proteins and peptides, as well as other phospholipids is limited. Stronger interactions between the protein and phospholipid may result in a stronger effect on the release behavior. Even if this study brought deeper insight into the mechanism behind the release of proteins and peptides from VPGs, the contribution of interactions to the release kinetics has to be assessed in case to case studies taking into account the encapsulated drug, the phospholipid as well as surrounding conditions.

In the past, VPGs have been mainly used for the encapsulation and sustained release of hydrophilic drugs. Within **Chapter VI** two hydrophobic drug candidates, SAFit2 and #41, were encapsulated into VPGs and used for different applications. Both substances were successfully encapsulated by a direct incorporation process, using ethanol or acetone as organic solvents. *In vitro* release studies demonstrated sustained release of SAFit2 and

#41 and a correlation between erosion of the VPG matrix and release of the drug candidates was observed. Pharmacokinetic studies *in vivo* showed a substantial increase in plasma half-life after release from VPGs for both substances. For SAFit2-VPG 50% (m/m) a plasma half-life of 36 hours was determined, in comparison to only two hours after administration of a non-retarded SAFit2 solution. *In vivo* data for #41 was inconclusive, allowing only a rough estimation of plasma half-lives. Nevertheless, again a up to ten-fold prolongation of plasma half-life was achieved by encapsulation of the drug into VPGs.

Besides the described *in vitro* and *in vivo* characterization of the VPG formulations, three *in vivo* studies on pharmacological effect of SAFit2 after release from VPGs were successfully conducted. Due to encapsulation of SAFit2 into VPGs, pharmacologic effect was successfully prolonged to 5 to 10 days after administration. Additionally, SAFit2 showed beneficial effects in the treatment of chronic pain states, metabolic disorders and mental disorders like anxiety and depression.

Based of the very promising results of the *in vivo* studies, VPGs encapsulating SAFit2 and #41 should be developed further in the future. First steps into this direction have already been taken in this work, showing a slower *in vitro* release of #41 and erosion of the phospholipid matrix after preparation of the VPG by TSC. On the basis of this the development of a direct encapsulation technique for #41, as well as for SAFit2, in a one-step, solvent-free process by co-extrusion is thinkable. By that, release kinetics could be further improved and manufacturing process could be simplified significantly.

In the course of this thesis it was possible to improve, optimize and overcome some of the challenges arising from VPGs as novel drug delivery systems. A step towards an explanation of the release behavior was taken and possibilities for further applications were evaluated. In general, further research on this topic should focus on the development of more sophisticated *in vitro* release models for VPGs and the construction of a reliable *in vitro* – *in vivo* correlation.

Chapter VIII

APPENDIX

VIII.1 List of Figures

Figure I-1: Graphical abstract.	3
Figure I-2: Schematic drawing of a dual asymmetric centrifuge (left) from the side in comparison to a dual centrifuge from the top (middle) and from the side (right).	13
Figure I-3: Schematic drawing of the flow through release cell described by Tardi et al. (1998).	15
Figure I-4: Overview of applications for VPGs.	17
Figure III-1: (A) Visual appearance of the injected depot from the side (MB-VPG 35% (m/m)); (B), (C) and (D) injection site from above after the injection of formulations with (B) 25% (m/m), (C) 35% (m/m) and (D) 55% (m/m) phospholipid content.	39
Figure III-2: NFI into pig skin post mortem. (1A) Injection site from above after injection of a formulation containing 40% (m/m) phospholipids. (1B) Cut through the injection site for the visualization of the penetration depth. (2A) Intradermal injection (SRB-VPG 50% (m/m)) without residues of the VPG on the surface. Pink color of the dyed VPG is visible through the upper skin layers. (2B) Cut through the injection site.	40
Figure III-3: Injection depth of VPG formulations into (●) gelatin blocks and (▼) pig skin post mortem with increasing phospholipid amount. Data is plotted as mean ± SD (n=2 or 3).	41
Figure III-4: Cumulative release of EPO from VPG with a phospholipid content of 45% (m/m). EPO-VPG was either filled into the eppendorf tubes with a conventional needle and syringe  or ejected with the Biojector 2000  previous to release testing. Data is plotted as mean ± SD (n=3).	42
Figure III-5: Schematic drawing of the Texture Analyzer for measurement of injection force.	47
Figure III-6: Experimental setup of the jet force measurement.	49
Figure III-7: Viscosity (at shearing rate 32.9 s ⁻¹) and gel strength of VPGs with increasing phospholipid concentration in % (m/m). VPGs were composed of Lipoid E80 and 20 mM PBS pH 7.4. (n=3, Mean ± SD)	50
Figure III-8: Injection force of VPGs with different phospholipid concentration during injection with needle and syringe - comparison of different injection conditions. Dashed line shows injection force of 25 N.	52
Figure III-9: NFI into pig skin post mortem. Injection site from above after injection of SRB-VPGs containing 40% (m/m) (A) or 50% (m/m) (B) phospholipids using a No3 single use syringe for injection. Lower row shows cuts through the injection site: 40% (m/m) SRB-VPG (C) and 50% (m/m) SRB-VPG (D).	53

Figure III-10: Injection depth of VPG formulations composed of E80 as phospholipid and 20mM PBS pH 7.4 as aqueous phase. VPGs with phospholipid concentrations between 30 and 50% (m/m) were injected into pig skin post mortem with No2 (white squares) and No3 (black dots) single use syringes.	54
Figure III-11: Needle-free injection of 0.25 ml, 0.5 ml and 1.0 ml (from left to right) of VPGs (composed of 45% (m/m) Lipoid E80 and Sulforhodamin B solution in 20 mM PBS pH 7.4) using the Biojector 2000 device with No2 syringes. Top row shows injection site from above directly after administration. Bottom row shows trans-sectional cuts through the injection site.	55
Figure III-12: Exemplary force profiles of VPGs after ejection of 0.25 ml with a Biojector 2000 and No2 syringe. Phospholipid concentration was increased from 25% (m/m) to 45% (m/m).	57
Figure III-13: Initial force (A) and injection duration (B) of the ejection of VPGs with increasing phospholipid concentration with different single-use syringes (No2 and No3). VPGs were composed of Lipoid E80 (25 -50% (m/m)) and 20mM PBS pH 7.4. Graphs show mean (n=3) \pm SD.	57
Figure III-14: Exemplary force profiles of the ejection of 0.25 ml of 40% (m/m) VPGs composed of Lipoid E80 an 20mM PBS pH 7.4 with No2 (black curve) and No3 (red curve) syringe.	58
Figure III-15: Initial pressure (A) and drop-off pressure (B) of the jet stream of VPGs with increasing phospholipid concentration. Red bars in (B) show viscosity of the formulation. Viscosity was compared at a shearing rate of 32.9 s ⁻¹ . VPGs were composed of Lipoid E80 (25 - 50% (m/m)) and 20mM PBS pH 7.4. Graphs show mean (n=3) \pm SD.	59
Figure III-16: Initial pressure (A) and drop-off pressure (B) of 40% (m/m) VPG composed of Lipoid E80 and 20 mM PBS pH 7.4 after injection of 0.25 ml. Red bars in (B) show viscosity of the formulation at different temperatures. Viscosity was compared at a shearing rate of 32.9 s ⁻¹ . Graphs show mean (n=3) \pm SD.	60
Figure III-17: Initial pressure (A), injection duration (B) and drop-off pressure (C) of VPG composed of 40% (m/m) Lipoid E80 and 20 mM PBS pH 7.4 for different injection volumes (0.25 ml, 0.5 ml and 1.0 ml). Graphs show mean (n=3) \pm SD. Red line indicates critical drop-off pressure at 8 MPa.	61
Figure IV-1: Schematic drawing of the barrel of a twin-screw extruder with co-rotating screws.	68
Figure IV-2: A) ZE-5 Mini-Extruder with barrel and drive unit. B) Detailed image of the barrel with three heating elements and the die. C) Parallel, conveying screws used during extrusion with the ZE-5 Mini-Extruder.	72
Figure IV-3: A) MiniLab® Micro Rheology Compounder. B) Detailed view of the open barrel with the two conical, conveying screws and the automatic bypass.	73
Figure IV-4: A) Leistritz Micro 27GL extruder. B) Schematic drawing of the screw design used for the mixing screw.	73
Figure IV-5: Schematic reaction of the phosphatidylcholine quantification [29].	78
Figure IV-6: Effects of different parameters during extrusion on viscosity (bar plot) and vesicle size (scatter plot) after dilution of the VPG. A) Variation of the screw rotation speed. B) Variation of re-cycling duration. C) Variation of the barrel temperature. D) Comparison of different preparation methods.	

- E) Variation of the die diameter. White symbols or bars represent samples prepared by extrusion, grey symbols or bars represent samples prepared by magnetic stirring and black symbols or bars represent samples prepared by dual asymmetric centrifugation. (Mean \pm SD; n=3)85
- Figure IV-7: Effect of increasing phospholipid concentration on viscosity (bar plot) and vesicle size (scatter plot) after dilution of the VPG after preparation by different methods. White symbols or bars represent samples prepared by extrusion, grey symbols or bars represent samples prepared by magnetic stirring and black symbols or bars represent samples prepared by dual asymmetric centrifugation. (Mean \pm SD; n=3)86
- Figure IV-8: Effects of different parameters during extrusion on viscosity (bar plot) and vesicle size (scatter plot) after dilution of the VPG. A) Variation of the screw rotation speed. B) Variation of the barrel temperature. C) Comparison of different preparation methods. D) Variation of the die diameter. E) Comparison of different phospholipid concentrations. White symbols or bars represent samples prepared by extrusion, grey symbols or bars represent samples prepared by magnetic stirring and black symbols or bars represent samples prepared by dual asymmetric centrifugation. (Mean \pm SD; n=3)88
- Figure IV-9: Effects of different parameters during extrusion on viscosity (bar plot) and vesicle size (scatter plot) after dilution of the VPG. A) Variation of the screw rotation speed. B) Variation of the barrel temperature. C) Comparison of different preparation methods. D) Variation of the die diameter. E) Comparison of different phospholipid concentrations. F) Comparison of the effect of different die lengths (short: 0.2 mm, long: 2.0 mm). White symbols or bars represent samples prepared by extrusion, grey symbols or bars represent samples prepared by magnetic stirring and black symbols or bars represent samples prepared by dual asymmetric centrifugation. (Mean \pm SD; n=3)92
- Figure IV-10: Macroscopic appearance of the VPG during preparation process by extrusion. A) Untreated phospholipids with methylene blue solution. B) Pre-mixture of phospholipids and methylene blue solution after 3 minutes of magnetic stirring. C) VPG after a single extrusion process of the pre-mixture.93
- Figure IV-11: Effect of screw design and speed on A) viscosity, B) Size and C) PDI of VPGs after dilution. VPGs with a phospholipid concentration of 40% (m/m) and 45% (m/m) were prepared.95
- Figure IV-12: Comparison of viscosity of VPGs prepared by different methods, with increasing phospholipid concentration.95
- Figure IV-13: Characterization of *in vitro* release behavior of the model compound FITC-Dextran (70 kDa) from 45% (m/m) VPG. VPG were prepared by dual asymmetric centrifugation (DAC), magnetic stirring (MAG) or extrusion using the ThreeTec ZE-5 Mini-Extruder (TTE) or the HAAKE MiniLab® Rheology Compounder (HE). A) Viscosity at shearing rate of 32.9 s⁻¹. B) Cumulative release of FITC-Dextran (70 kDa). C) Cumulative release of phosphatidylcholine for characterization of the erosion process. (Mean \pm SD, n=3)96
- Figure IV-14: Characterization of the released fractions. A) Vesicle sizes determined in the released fractions. B) PDI of the released fractions. Black lines show mean, boxes show 25-75% range and

- error bars show standard deviation. All values were calculated from measured data of all released fractions (n = 25 in triplicates). 97
- Figure IV-15: FTIR spectra of OVA. A) OVA-solution; B) OVA-VPG (red) and placebo VPG (blue) directly on the ATR-crystal; C) OVA-VPG after dilution and chloroform extraction (red) and OVA-solution after extraction treatment (green). 98
- Figure IV-16: Chromatograph of IFN β -1b incorporated in VPG directly after dilution (solid line) or after centrifugation (dotted line). 99
- Figure IV-17: Investigation of EPO stability in VPG evaluated by SDS-PAGE. A) Directly after preparation of the VPG by the different techniques. B) After one month storage of the VPG prepared by different techniques. C) After three months storage of the VPG. Line 1: Molecular weight standard; Line 2: EPO-stock solution; Line 3: EPO-VPG prepared by DAC; Line 4: EPO-VPG prepared by magnetic stirring; Line 5: EPO-VPG prepared with ThreeTec extruder; Line 6: EPO-VPG prepared by HAAKE-extruder..... 100
- Figure IV-18: Investigation of mAb stability in VPG evaluated by SDS-PAGE. A) Directly after preparation of the VPG by the different techniques. B) After one month storage of the VPG prepared by different techniques. C) After three months storage of the VPG. Line 1: Molecular weight standard; Line 2: mAb-VPG prepared by DAC; Line 3: mAb- VPG prepared by magnetic stirring; Line 4: mAb-VPG prepared with ThreeTec extruder; Line 5: mAb-VPG prepared by Leistritz-extruder; Line 6: mAb-stock solution. 101
- Figure IV-19: Characterization of *in vitro* release behavior of mAb from VPG (large symbols, solid lines, left axis) in comparison to cumulative release of phosphatidylcholine (small symbols, dashed lines, right axis). mAb-VPG (10 mg/g) was prepared by dual asymmetric centrifugation (DAC) or extrusion using the ThreeTec ZE-5 Mini-Extruder (TTE) or the Leistritz Micro 27 GL (LEI). (n=3, Mean \pm SD). 102
- Figure IV-20: Amplitude sweep for VPGs (40% (m/m) Lipoid E80, 20mM PBS pH 7.4) prepared by A) DAC, B) HAAKE MiniLab[®] extruder (HE), C) Leistritz extruder (LEI), D) ThreeTec ZE-5 Mini-Extruder (TTE) or E) magnetic stirring (MAG). LVE-region is marked in grey..... 106
- Figure IV-21: Characterization of VPG composed of 40% (m/m) Lipoid E80 and 20mM PBS pH 7.4 over storage time of three months. VPGs are prepared by dual asymmetric centrifugation (DAC), magnetic stirring (MAG), or extrusion with the ThreeTec ZE-5 (TTE), HAAKE MiniLab[®] (HE) or Leistritz extruder (LEI). Viscosity of the samples stored at A) 4°C or B) 25 °C is compared at 32.9 s⁻¹. Z-Average of the vesicles obtained after dilution of the VPG after storage at C) 4°C or D) 25 °C..... 109
- Figure IV-22: Macroscopic appearance of VPG 40% (m/m) prepared with Leistritz extruder. A) VPG directly after preparation is homogenous in appearance without visible phase separation. B) VPG after three months of storage at 25 °C shows phase separation. Red arrow indicates separated aqueous phase in the VPG..... 110

Figure IV-23: Representative microscopic images of the differently prepared VPGs directly after preparation (left) and after three months of storage at 2-4 °C (right). Pictures are taken with 100-fold magnification.....	111
Figure V-1: Graphical abstract.....	121
Figure V-2: Zeta potential of exenatide with increasing pH value. (Mean \pm SD, n=3).....	128
Figure V-3: FTIR spectra of exenatide solution with increasing pH value.....	128
Figure V-4: Viscosity of VPG with a total phospholipid concentration of 40% (m/m) loaded with exenatide (0.5 mg/g). VPG was prepared with different phospholipid compositions. For comparison the viscosity at a shearing rate of 32.9 s ⁻¹ was taken. (Mean \pm SD, n=3).....	129
Figure V-5: <i>In vitro</i> release of exenatide from VPG and erosion behavior of VPG during release. A) Cumulative exenatide release from VPG. Exenatide was encapsulated at pH 4.5 in all formulations. (Release medium: 20 mM PBS pH 7.4). Dashed lines show fit with equation (V-1). B) Cumulative exenatide release from VPG. Exenatide was encapsulated at pH 7.4 in all formulations. (Release medium: 20 mM PBS pH 7.4). C) Cumulative optical density of the released fractions obtained from <i>in vitro</i> release of exenatide. D) Cumulative PC concentration obtained from phospholipid assay for all formulations containing POPC is shown in percentage of total PC in the VPG formulation. (Mean \pm SD; n = 3).....	131
Figure V-6: Raw MST-traces of the titration of exenatide (5 μ M) with liposomes composed of a mixture of POPC and POPG 7:3 at pH 4.5. Liposome concentration increases from dark green (30.5 nM) over yellow (7.8 – 31.25 μ M) to dark red (1.0 mM) as arrow indicates.	133
Figure V-7: A) Raw fluorescence spectra: Initial Fluorescence change with increasing amount of POPC/POPG 1:1 liposomes in exenatide solution (pH 4.5). Liposome concentration decreases from capillary position 1 (0.5 mM) to capillary position 16 (15.3 μ M). B) Fitting function of the initial fluorescence signal of POPC/POPG 1:1 liposomes to exenatide at pH 4.5. (Mean \pm Kd Confidence, n = 3).....	134
Figure V-8: Comparison of Dose Response determined by MST-Signals of the titration of exenatide (5 μ M) with liposomes at A) pH 4.5 and B) pH 7.4 (n=3). Fit functions for the two POPC/POPG mixtures and the pure POPG liposomes are shown for pH 4.5.....	135
Figure V-9: A dilution experiment (“blank”, black crosses) performed by diluting aliquots of exenatide (100 μ M) into matching acetate buffer at pH 4.5 indicates that exenatide assembles at high concentrations. Titration of exenatide aliquots (100 μ M) into the cell filled with POPC vesicles (red triangles) (80 μ M lipid) yields practically identical heats. Data are shown as a function of exenatide concentration.	147
Figure V-10: A) ITC of POPC (red triangles) and POPC/POPG 1:1 (blue dots) vesicles (80 μ M lipid) titrated with exenatide (100 μ M) at pH 4.5. Data is shown as a function of exenatide/lipid ratio. The solid line represents a simulation with the same fitting parameters found by the fit in panel C. B) DLS measurements of exenatide-into-lipid titration. 8 μ L aliquots of an exenatide solution (100 μ M) were titrated into a cuvette containing 1.4 mL POPC/POPG 1:1 vesicles (80 μ M lipid) every 5	

minutes. C) ITC curve of exenatide (3 μM) titrated with lipid vesicles (800 μM) composed of POPC (red triangles) and POPC/POPG 1:1 (blue dots). Data is shown as a function of lipid/exenatide ratio. As in panel A, no interaction of exenatide with pure POPC could be observed under the chosen conditions. The model 'one set of sites' was used to fit POPC/POPG 1:1 data (solid line). Injections at the beginning of the titration at low lipid/exenatide ratio were excluded. D) DLS measurements of lipid-into-exenatide titration. 8 μL aliquots of POPC/POPG 1:1 vesicles (800 μM lipid) were titrated into a cuvette containing 1.4 mL exenatide solution (3 μM) every 5 minutes. 148

Figure V-11: Normalized fluorescence spectra of the titration of exenatide (5 μM) with A) POPG-liposomes (0.5 mM - 1.5×10^{-5} mM) and B) POPC-liposomes (0.5 mM - 1.5×10^{-5} mM). 151

Figure V-12: A) Raw fluorescence curves at 330nm and 350nm of titrations of 5 μM exenatide with liposomes composed of POPC/POPG 7:3 along with fit curves of a global fit representing $K_d = 1.4 \mu\text{M}$, $n = 9.2 \mu\text{M}$, $F_{330}(0) = 38$, $F_{330}(1) = 730$, $F_{350}(0) = 57$, $F_{350}(1) = 650$ according to eq. (V-8) with (V-9) and (V-10). B) Ratio 350 nm/330 nm of the data presented in panel A, along with a solid curve calculated on the basis of the fit parameters (K_d and n) obtained in panel A and a dashed curve fitted to the data shown here according to eq. (V-12), yielding $K_d = 1.2 \mu\text{M}$ and $n = 9.2$. For a compilation of these parameters and those for the other lipid mixtures (fits not shown), see Table V-4, "Fluorescence" section. 153

Figure V-13: Scheme describing the concentration ranges covered by the different experiments and the transition ranges revealed by them. Triangles indicate the approximate beginning and completion of transition ranges (blue: ITC; orange: MST; green: Trp fluorescence) and vertical bars are separators between secondary and primary (at lower lipid) and primary only (at higher lipid) binding. Grey grid lines illustrate specific total mole ratios of lipid-to-peptide. Concentration ranges covered by different experiments are illustrated by colored areas. 156

Figure V-14: Stability of phospholipid monolayers on 20 mM PBS pH 7.4. (A) Compression isotherms of lipid monolayers. (B) Collapse pressure obtained from compression isotherms. 157

Figure V-15: Insertion of exenatide into phospholipid monolayers. A) Time course of surface pressure after injection of buffer in the subphase (20 mM PBS pH 7.4). B) Time course of surface pressure after injection of exenatide beneath the monolayer at a subphase concentration of 2.5 μM . Monolayers were formed from POPC, POPG and mixtures of both lipids (7:3 and 1:1). Arrow indicates the time of injection. 158

Figure VI-1: Schematic mechanism of action of SAFit2. SAFit2 inhibits the effect of FKBP51 and hence promotes the negative feedback of cortisol on the HPA-axis. 169

Figure VI-2: *In vitro* release behavior of SAFit2 from VPG. Left axis and black curves show cumulative release of SAFit2 in %, while right axis and grey curves show cumulative release of PC in %. 175

Figure VI-3: Blood plasma concentration of SAFit2 after a single s.c. injection of SAFit2-VPG 30% (m/m) (filled squares), SAFit2-VPG 50% (m/m) (open circles) and SAFit2-solution (grey triangles). 176

Figure VI-4: Metabolic effects of SAFit2 treatment. A) High SAFit2 plasma levels were observed for 72 hours after a single s.c. injection of SAFit2. B) Body weight under control diet conditions. C) Glucose

tolerance under control diet conditions. SAFit2 has no effect on glucose tolerance. D) Glucose tolerance under HFD conditions. SAFit2 significantly improves glucose tolerance. E) Effect of SAFit2 was not present in 51KO-mice under HFD conditions. F) Body weight under HFD conditions. (Figure was adapted from Balsevich et al. [11].)	179
Figure VI-5: Pharmacological blockade of FKBP51 reduces the mechanical hypersensitivity seen in long-term pain states across sexes. A) Single i.p. injection of SAFit2-solution A 3 days after CFA injection. B) Single i.p. injection of SAFit2-solution A 5 days after SNI surgery. C) Repeated i.p. injection of SAFit2-solution A 3 days after CFA injection. D) Repeated i.p. injection of SAFit2-solution A 5 days after SNI surgery. E) Single s.c. injection of SAFit2-VPG 5 days after SNI surgery. F) Single s.c. injection of SAFit2-solution B 5 days after SNI surgery. G) SAFit2-VPG had no effect in naïve mice. H) SAFit2-VPG had no effect in CFA-injected FKBP5 KO mice. I) Single s.c. injection of SAFit2-VPG, 12 days after the first PTX injection. J) Delayed (12 days) and repeated administration of SAFit2-VPG after SNI surgery. (Figure was adapted from Maiarù et al. [13])	181
Figure VI-6: Treatment with SAFit2 and escitalopram (Esc) affected behavior in open field test (anxiety-test). A) Distance traveled during the test. B) When splitting the test in three time-bins of 5 min each, no differences were observed between the two escitalopram groups in the first five minutes but significant differences in time-bin 2 and 3. C) Exploration time of the inner zone. (Figure was adapted from Pöhlmann et al. [12])	183
Figure VI-7: Treatment with SAFit2 and escitalopram (Esc) affected behavior in forced swim test (stress-coping test). A) Struggling time was significantly increased by combination of SAFit2 with escitalopram. B) Time course of the forced swim test shows that animals with SAFit2 treatment struggle significantly more in the last 3 minutes. (Figure was adapted from Pöhlmann et al. [12])	183
Figure VI-8: <i>In vitro</i> release characterization for #41-VPG. Black curves show cumulative release of #41 from VPG prepared by DAC or TSC-extrusion with different drug load (20 mg/g). Red curves show simultaneous PC release.	185

VIII.2 List of Tables

Table I-1: Chronologic summary of VPG formulations with encapsulated drugs which were investigated over the last years.	18
Table III-1: Summary of the physical properties of VPGs. Viscosity was determined with a rotational rheometer (PP25 with Physica MCR 100, Anton Paar, Ostfildern, Germany) with a plate/plate geometry. Gel strength and injection forces were determined with a Texture Analyzer (TA.XT plus, Stable Micro Systems, UK) in compression mode.....	45
Table IV-1: List of chemicals and salts, which were used.....	71
Table IV-2: Summary of protein preparation prior to encapsulation into VPGs.....	75
Table IV-3: Overview of settings changed during method development using the re-cycling function. (Varied parameters are emphasized for each experiment in bold letters.)	82
Table IV-4: Overview of settings changed during method development with the HAAKE MiniLab® extruder. (Varied parameters are emphasized for each experiment in bold letters.)	87
Table IV-5: Comparison of product temperature of the VPGs after extrusion and the set barrel temperature during continuous run. (n = 3; Mean ± SD)	87
Table IV-6: Overview of settings changed during method development with the ThreeTec ZE-5. (Varied parameters are emphasized for each experiment in bold letters.).....	90
Table IV-7: Overview on process parameters during preparation by extrusion.	105
Table IV-8: Parameters derived from rheologic measurements.	107
Table V-1: Zeta potential of the liposomes used for interaction studies. (Mean ± SD, n = 3)	132
Table V-2: Summary of K _d -values [μM] derived from the MST measurements. All experiments were performed at pH 4.5 in 50 mM sodium acetate buffer.	136
Table V-3: Multi-step-gradient elution used during RP-HPLC quantification of exenatide.....	142
Table V-4: Summary of K _d -values [μM] and Stoichiometry (n = lipid per peptide) derived from the different methods with which interactions were evaluated. Additionally, for ITC-experiments the reaction enthalpy ΔH [kcal/mol] is shown. All experiments were performed at pH 4.5 in 50 mM sodium acetate buffer.	154
Table VI-1: Summary of PK parameters for SAFit2-VPG. (Non-compartmental model, calculated by Dr. Jilong Wang and Prof. Xiaojiao Du)	177
Table VI-2: Summary of the solubility study for #41.....	184

VIII.3 List of Abbreviations

ACTH	adrenocorticotrophic hormone
BSA	bovine serum albumin
CFA	complete Freund's adjuvant
C_{max}	maximum plasma concentration
CRH	corticotropin-releasing-hormone
DAC	dual asymmetric centrifugation
DAOS	N-Ethyl-N-(2-hydroxy-3-sulfopropyl)-3,5-dimethoxyaniline, sodium salt
DC	dual centrifugation
DLS	dynamic light scattering
DNA	deoxyribonucleic acid
E80	Lipoid E80, egg lecithin
EDTA	ethylenediaminetetraacetic acid
EPO	erythropoietin
Esc	escitalopram
FDA	food and drug administration
FF-TEM	freeze fracture transmission electron microscopy
FITC	fluorescein isothiocyanate
FKBP5	FK506 binding protein 5
FTC	flow-through cell
FT-IR	Fourier-transform infrared spectroscopy
G'	storage modulus
G''	loss modulus
G-CSF	granulocyte-colony stimulating factor
GR	glucocorticoid receptor
HE	HAAKE MiniLab® Micro Rheology Compounder
HFD	high fat diet
HME	hot melt extrusion
HPA-axis	hypothalamic-pituitary-adrenal-axis
HPH	high pressure homogenization
HPLC	high performance liquid chromatography
HPW	highly purified water
Hsp90	heat shock protein 90
i.m.	intra muscular
i.p.	intra peritoneal
i.v.	intra venous
IFN	interferon

IgG	immunoglobulin G
ITC	isothermal titration calorimetry
LC-MS/MS	liquid chromatography–mass spectrometry
LEI	Leistritz Micro 27GL-28D
LVE-region	linear viscoelastic region
mAb	monoclonal antibody
MAG	magnetic stirring
MB	methylene blue
MCT	medium chain triglyceride
MES	2-(N-morpholino) ethanesulfonic acid
MLV	multilamellar vesicles
MSD	mean square distance
MST	microscale thermophoresis
MVL	multivesicular liposomes
MW	molecular weight
MWCO	molecular weight cut off
NFI	needle-free injection
OD	optical density
OVA	ovalbumin
PAMPA	parallel artificial membrane permeability assay
PBS	phosphate buffered saline
PC	phosphatidylcholine
PDI	polydispersity index
PEG	polyethylene glycol
PK	pharmacokinetic
PLA	polylactide
PLGA	poly(lactic-co-glycolic acid)
POPC	1-palmitoyl-2-oleoyl-sn-glycero-3-phosphocholine
POPG	1-palmitoyl-2-oleoyl-sn-glycero-3-phospho-(1'-rac-glycerol)
PPSG	phospholipid-based phase separation gel
PTX	paclitaxel
QCM	quartz crystal microbalance
RES	reticulo-endothelial system
RMSD	root mean square distance
RNA	ribonucleic acid
RP	reverse phase
s.c.	subcutaneous
S100	Lipoid S100, soy lecithin

SAFit2	selective antagonist of FKBP51 by induced fit 2
SD	standard deviation
SDS	sodium dodecyl sulfate
SDS-PAGE	sodium dodecyl sulfate–polyacrylamide gel electrophoresis
SLI	solid lipid implant
SLN	solid lipid nanoparticle
SNI	spared nerve injury
SNP	single nucleotide polymorphism
SPR	surface plasmon resonance
SRB	sulforhodamine B
SSRI	selective serotonin reuptake inhibitor
SUV	small unilamellar vesicles
TFA	trifluoroacetic acid
T _m	phase transition temperature
t _{max}	time at which maximum plasma concentration is reached
Tris	tris(hydroxymethyl)aminomethane
TRP2	tyrosinase related protein 2
TSC	twin-screw
TTE	ThreeTec ZE-5 Mini-Extruder
VPG	vesicular phospholipid gel

VIII.4 Publications arising from this thesis

M. Breitsamer, G. Winter

Needle-free injection of vesicular phospholipid gels - a novel approach to overcome an administration hurdle for semisolid depot systems. Journal of Pharmaceutical Sciences (2017)

DOI: 10.1016/j.xphs.2016.12.020, PMID: 28041969

G. Balsevich, A.S. Häusl, C.W. Meyer, S. Karamihalev, X. Feng, M.L. Pöhlmann, C. Dournes, A. Uribe-Marino, S. Santarelli, C. Labermaier, K. Hafner, T. Mao, M. Breitsamer, M. Theodoropoulou, C. Namendorf, M. Uhr, M. Paez-Pereda, G. Winter, F. Hausch, A. Chen, M.H. Tschöp, T. Rein, N.C. Gassen, M.V. Schmidt

Stress-responsive FKBP51 regulates AKT2-AS160 signaling and metabolic function, Nature Communications (2017)

DOI:10.1038/s41467-017-01783-y

M. Maiarù, O.B. Morgan, T. Mao, M. Breitsamer, H. Bamber, M. Pöhlmann, M. V. Schmidt, G. Winter, F. Hausch, S.M. Géranton

The Stress Regulator Fkbp51: A Novel and Promising Druggable Target for the Treatment of Persistent Pain States Across Sexes, Pain (2018)

DOI:10.1097/j.pain.0000000000000445

M.L. Pöhlmann, A.S. Häusl, D. Harbich, G. Balsevich, C. Engelhardt, X. Feng, M. Breitsamer, F. Hausch, G. Winter, M. V. Schmidt

Pharmacological Modulation of the Psychiatric Risk Factor FKBP51 Alters Efficiency of Common Antidepressant Drugs, Frontiers in Behavioral Neurosciences (2018)

DOI:10.3389/fnbeh.2018.00262.

M. Breitsamer, G. Winter

Vesicular phospholipid gels as drug delivery systems for small molecular weight drugs, peptides and proteins: state of the art review. International Journal of Pharmaceutics (2018)

DOI: 10.1016/j.ijpharm.2018.12.030.

M. Breitsamer, A. Stulz, H. Heerklotz, G. Winter

Do interactions between Protein and Phospholipids influence the release behavior from lipid-based exenatide depot systems?; Submitted for publication to European Journal of Pharmaceutics and Biopharmaceutics in January 2019.

A. Stulz, M. Breitsamer, G. Winter, H. Heerklotz

Different aspects of a complex protein-lipid binding equilibrium as seen by ITC, Fluorescence, and MST.

Manuscript in preparation.

VIII.5 Patent

M.Breitsamer, N. Deiringer, G. Winter

“Herstellung von VPG mittels Schnecken-Extrusion”

Application number: DE 10 2018 010 063.5

Date of application: 17.03.2018

VIII.6 Poster presentations

M. Breitsamer, N. Deiringer, G. Winter

Preparation of Vesicular Phospholipid Gels by Twin-Screw Extrusion
BioVaria, Munich, Germany 8th-9th of May 2019

M. Breitsamer, G. Winter

Needle-free injection of Vesicular Phospholipid Gels – a robust technology
11th World Meeting on Pharmaceutics, Biopharmaceutics and Pharmaceutical
Technology, Granada, Spain 19th-22th of March 2018

M. Breitsamer, N. Deiringer, G. Winter

Preparation of Vesicular Phospholipid Gels by Twin-Screw Extrusion
11th World Meeting on Pharmaceutics, Biopharmaceutics and Pharmaceutical
Technology, Granada, Spain 19th-22th of March 2018

**M.L. Pöhlmann, A.S. Häusl, J. Hartmann, D. Harbich, B. Schmid, N. Dedic, X. Feng, M.
Breitsamer, M. Vollrath, A. Mederer, G. Balsevich, C. Engelhardt, F. Hausch, J.M.
Deussing, G. Winter, A. Chen, M.V. Schmidt**

Unraveling the functional contribution of FKBP51 in relevant brain areas to stress
vulnerability;

ECNP Workshop for Junior Scientists in Europe, Nice, France, 9-12th March 2017

M. Breitsamer, G. Winter

Needle-free injection of vesicular phospholipid gels

Annual Meeting of the German Pharmaceutical Society, Munich, Germany, 4-7th October
2016